Function and dysfunction in neuronal endosomal transport and sorting

Dissertation

Zur Erlangung des akademischen Grades

des Doktors der Naturwissenschaften (*Dr. rer nat.*)

Des Fachbereichs Biologie der Fakultät für Mathematik,

Informatik und Naturwissenschaften

der Universität Hamburg

Vorgelegt von

Marcel Klein

Hamburg, 2022

Datum der Disputation: 24.04.2023

Erster Gutachter: PD Dr. Guido Hermey

Zweiter Gutachter: Prof. Dr. Christian Lohr

Summary

The nervous system is formed by a complex network of neurons and glia cells and exerts distinct functions upon various cue stimuli. Cellular functionality highly depends on correct intracellular protein sorting and trafficking as this defines the subcellular compartmentalization of organelles. In neurons this compartmentalization is in particular challenging because these are polarized cells with stimuli receiving somatodendritic and stimuli transmitting axonal compartments. Thus, the protein composition of the different polarized regions in neurons is essential for accurate functionality. Their polarity and also their postmitotic state make neurons highly vulnerable to dysregulations underlying impaired protein trafficking and make them less adaptable to a resulting imbalanced energy metabolism. In several neurodegenerative and psychiatric diseases neuronal endosomal protein trafficking is impaired. This includes malfunction of the autophagy-endolysosome system in monogenetic lysosomal storage disorders such as Neuronal Ceroid Lipofuscinoses. In this dissertation, I describe the converging links of CLN3 protein, which is mutated in juvenile Neuronal Ceroid Lipofuscinosis, and the γ-secretase subunit Pen2 in the autophagy-endolysosome system. CLN3 and Pen2 have earlier been described to interact and I demonstrate their co-localization in late endosomes and endolysosomes. I further show that a knockout of either CLN3 or Pen2 in HeLa cells leads to decreased lysosomal proteolytic processing, a decreased number of lysosomes, a partially impaired compartmentalization between late endosomes and lysosomes, and an increased autophagy induction with a functioning autophagic flux as shown by the elevated number of autophagosomes and autolysosomes before and after nutrient deprivation. As impairments of Pen2 functionality and other γ-secretase subunits are common risk factors for Alzheimer's disease, I subsequently compare converging links between the different Neuronal Ceroid Lipofuscinoses subtypes and Alzheimer's disease. I refer that amyloid β accumulation, a hallmark of Alzheimer's disease, was also identified in some cases of Neuronal Ceroid Lipofuscinoses and that lysosomal inclusions which were previously thought specific for Neuronal Ceroid Lipofuscinoses have been observed in patients with canonical Alzheimer's disease gene mutations. In accordance with previous investigations linking the Alzheimer's disease hallmarks, neurofibrillary tangles and senile plaques, to impairments in the autophagy-lysosome system, and my observations of Pen2 involvement in the autophagy-lysosome system, I propose that the primary cause of Alzheimer's disease, like for Neuronal Ceroid

Lipofuscinosis, are impairments of protein trafficking and function in the autophagy-endolysosome system. My colleagues and I further investigate the novel interaction between another Alzheimer's disease risk factor SorLA and the scaffold protein PICK1. We demonstrate that PICK1 interacts with the last three amino acids of the cytoplasmic C-terminus of SorLA, and I show their colocalization in neuronal vesicular structures, and that SorLA internalization is independent of its interaction with PICK1 in SH-SY5Y neuroblastoma cells. SorLA is a member of the Vps10p-D receptor family that seems to be involved in different distinct intracellular sorting mechanisms. The Vps10p-D receptor family consist in mammals of Sortilin, SorLA, SorCS1, SorCS2 and SorCS3. Dysfunction of the Vps10p-D receptors has been linked to several neurodegenerative and psychiatric diseases including Alzheimer's disease. Decoding the dynamic intracellular itineraries of Vps10p-D receptors is crucial to understand their role in physiological and cytopathological processes. The direct observation of their interactions at spatial and temporal levels to examine local dynamics by live imaging has been challenging as terminal fluorophore tagging presumably impedes a large number of their protein interactions and functions. Therefore, I aimed to generate functional fluorophore tagged versions of either Vps10p-D receptor by accurate internal tag insertion. Internal tag positioning had to be chosen carefully to not interfere with any of the structures of the different domains of the receptors. Here, I present the functionality of the different domains in the designed internal fluorophore tagged Vps10p-D receptors. I demonstrate their correct folding by computational applications and accordingly their exit of the ER using immunocytochemistry. I identify the detailed subcellular localizations of all tagged Vps10p-D receptors which are in accordance with the so far known and published localizations. Successful dimerization experiments with fluorophore tagged SorCS2 show the functionality of the leucine rich domain in the tagged SorCS subfamily. I also demonstrate for the first time that all Vps10p-D receptors can internalize brain-derived neurotrophic factor independent of tropomyosin receptor kinase B. These results introduce the tagged Vps10p-D receptors as novel powerful tools for live analysis of protein trafficking and sorting mechanisms.

Zusammenfassung

Das Nervensystem besteht aus einem komplexen Netzwerk von Neuronen und Gliazellen und übt spezifische Funktionen bei verschiedenen Reizen aus. Zelluläre Funktionen hängen stark von korrekter intrazellulärer Sortierung und Transport von Proteinen ab, da dadurch die subzelluläre Kompartimentierung von Organellen definiert wird. In Neuronen stellt diese Kompartimentierung eine besondere Herausforderung dar, da sie polarisierte Zellen mit somatodendritischen Kompartimenten für den Empfang von Reizen und axonalen Kompartimenten für die Übertragung von Reizen sind. Deshalb ist die Proteinzusammensetzung der verschiedenen polarisierten Regionen in Neuronen für deren korrekte Funktionalität entscheidend. Ihre Polarität und auch ihr postmitotischer Zustand machen Neurone sehr anfällig für Dysregulationen aufgrund eines gestörten Proteintransports, und weniger anpassungsfähig an einen daraus resultierenden unausgeglichenen Energiestoffwechsel. Der neuronale und endosomale Transport von Proteinen ist bei verschiedenen neurodegenerativen und psychiatrischen Erkrankungen gestört. Dazu gehören Fehlfunktionen des Autophagie-Endolysosomen-Systems bei monogenetischen lysosomalen Speicherkrankheiten wie den Neuronalen Ceroid-Lipofuszinosen. In dieser Dissertation beschreibe ich die konvergierenden Verbindungen zwischen dem Protein CLN3, das bei juveniler Neuronaler Ceroid-Lipofuszinose mutiert ist, und der γ-Sekretase-Untereinheit Pen2 im Autophagie-Endolysosomen-System. CLN3 und Pen2 interagieren miteinander, und ich zeige ihre gemeinsame Lokalisation in späten Endosomen und Endolysosomen. Außerdem zeige ich, dass ein Knockout von CLN3 oder Pen2 in HeLa-Zellen zu einer verringerten lysosomalen proteolytischen Prozessierung, einer verringerten Anzahl von Lysosomen, einer teilweise gestörten Kompartimentierung zwischen späten Endosomen und Lysosomen und einer erhöhten Autophagie-Induktion mit funktionierendem autophagischen Flux führt, wie die erhöhte Anzahl von Autophagosomen und Autolysosomen vor und nach Nährstoffentzug der Zellen zeigt. Da Beeinträchtigungen der Pen2-Funktionalität und anderer γ-Sekretase-Untereinheiten häufige Risikofaktoren für Morbus Alzheimer sind, vergleiche ich anschließend übereinstimmende Verbindungen zwischen den verschiedenen Untertypen Neuronaler Ceroid-Lipofuszinose und Morbus Alzheimer. Ich verweise darauf, dass die Anhäufung von Amyloid β, ein typisches Merkmal von Morbus Alzheimer, auch in einigen Fällen von Neuronalen Ceroid-Lipofuszinosen festgestellt wurde und dass lysosomale Einschlüsse, von denen man bisher annahm, sie seien spezifisch

für Neuronale Ceroid-Lipofuszinosen, auch bei Patienten mit kanonischen Alzheimer-Genmutationen beobachtet wurden. Passend zu früheren Untersuchungen, die die typischen Merkmale von Morbus Alzheimer, Alzheimer-Fibrillen und senile Plaques, mit Beeinträchtigungen des Autophagie-Lysosomensystems in Verbindung bringen, und meinen Beobachtungen der Mitwirkung von Pen2 am Autophagie-Lysosomensystem, nehme ich an, dass die Hauptursache von sowohl Morbus Alzheimer, als auch der Neuronalen Ceroid-Lipofuszinose Beeinträchtigungen des Proteintransports und der Funktion des Autophagie-Lysosomensystems sind. Meine Kollegen und ich untersuchen außerdem die neu identifizierte Interaktion zwischen einem weiteren Alzheimer-Risikofaktor SorLA und dem Gerüstprotein PICK1. Wir zeigen, dass PICK1 mit den letzten drei Aminosäuren des zytoplasmatischen C-Terminus von SorLA interagiert. Ich zeige außerdem ihre Colokalisierung in neuronalen vesikulären Strukturen, und dass die Internalisierung von SorLA in SH-SY5Y-Neuroblastomzellen unabhängig von seiner Interaktion mit PICK1 ist. SorLA ist ein Mitglied der Vps10p-D-Rezeptorfamilie, die an unterschiedlichen intrazellulären Sortierungsmechanismen beteiligt zu sein scheint. Die Vps10p-D-Rezeptorfamilie besteht bei Säugetieren aus Sortilin, SorLA, SorCS1, SorCS2 und SorCS3. Funktionsstörungen der Vps10p-D-Rezeptoren werden mit verschiedenen neurodegenerativen und psychiatrischen Erkrankungen in Verbindung gebracht, darunter auch Morbus Alzheimer. Das Verstehen der dynamischen intrazellulären Wege der Vps10p-D-Rezeptoren ist daher entscheidend für das Verständnis ihrer Rolle bei physiologischen und zytopathologischen Prozessen. Die direkte Beobachtung ihrer Interaktionen auf räumlicher und zeitlicher Ebene zur Untersuchung ihrer lokalen Dynamik durch Lebendzellbeobachtungen stellte sich bisher als schwierig heraus, da die terminale Markierung mit Fluorophoren vermutlich eine große Anzahl ihrer Proteininteraktionen und -funktionen verhindert. Um dies zu umgehen, habe ich funktionelle, intern mit Fluorophoren markierte Versionen aller Vps10p-D-Rezeptoren erzeugt. Die Position der internen Markierungen musste sorgfältig gewählt werden, um die Strukturen der verschiedenen Domänen der Rezeptoren nicht zu beeinträchtigen. Ich demonstriere hier die Funktionalität der unterschiedlichen Domänen in den entworfenen, mit internen Fluorophoren markierten Vps10p-D-Rezeptoren. Ich zeige ihre korrekte Faltung mit Hilfe von Computersimulationen und ihren Austritt aus dem ER mit Hilfe der Immunzytochemie. Ich beschreibe die detaillierten subzellulären Lokalisationen aller markierten Vps10p-D-Rezeptoren, die mit den bisher bekannten und veröffentlichten Lokalisationen übereinstimmen. Erfolgreiche

Dimerisierungsexperimente mit Fluorophor-markiertem SorCS2 zeigen die Funktionalität der leucinreichen Domäne in der fluorophor markierten SorCS-Unterfamilie. Außerdem konnte ich zum ersten Mal zeigen, dass alle Vps10p-D-Rezeptoren den Wachstumsfaktor BDNF unabhängig von Tropomysoinkinase-Rezeptoren internalisieren können. Diese Ergebnisse zeigen, dass die markierten Vps10p-D-Rezeptoren neuartige, leistungsstarke Werkzeuge für die Live-Analyse von Protein-Transport und Sortierungsmechanismen sind.

Abbreviations

AMPK	AMP-activated protein kinase
AD	Alzheimer's disease
ADHD	attention deficit hyperactivity disorder
AICD	APP intracellular domain
ALS	amyotrophic lateral sclerosis
AMPAR	α-amino-3-hydroxy-5-methyl-4-isoxazolepropionic acid receptor
AP	adaptor protein complex
APH-1	anterior pharynx-defective 1
APOE	apolipoprotein E
APP	amyloid precursor protein
ASIC2a	acid sensing ion-channel 2a
ATP13A2	ATPase 13A2
ATP5MC	ATP synthase membrane subunit c
Aβ	amyloid β
BACE1	β-secretase
BAR	Bin-Amphiphysin-Rvs
BDNF	brain-derived neurotrophic factor
BECN-1	Beclin-1
BIN1	bridging interactor 1
CAMKI	Ca^{2+}/calmodulin-dependent protein kinase I
CbCLN3Δ$^{exon7/8}$	cerebellar neuronal precursor cells with *CLN3Δ$^{exon7/8}$* mutation
CD2AP	CD2-associated protein
CGN	*cis*-Golgi network
CLN	ceroid-lipofuscinosis neuronal
CNS	central nervous system
COP	coat protein complex
CRL	cullin-RING ligase
CRL3	cullin-RING ligase 3
CTFα	α-carboxyl terminal fragment of APP containing 83 amino acids
CTFβ	β-carboxyl terminal fragment of APP containing 99 amino acids
CTS	cathepsin
DAT	dopamine transporter
DNAJC5	DnaJ heat shock protein family Hsp40 member C5
EAAT3	excitatory amino acid transporter 3
EE	early endosome
EOAD	early onset Alzheimer's disease
ER	endoplasmic reticulum
ERBB2	erb-b2 receptor tyrosine kinase 2
ERGIC	endoplasmic reticulum-Golgi-intermediate compartment
ESCRT	endosomal sorting complexes required for transport
fAD	familial Alzheimer's disease
FLIM	fluorescence lifetime microscopy

GFP	green fluorescent protein
GGA	Golgi-localized γ ear-containing Arf-binding protein
Glut4	glucose transporter type 4
GRN	granulin
GTP	guanosine triphosphate
HAP1	huntingtin associated protein 1
HCS70	heat-shock cognate protein of 70 kDa
HTT	huntingtin
KCTD7	potassium channel tetramerization domain-containing protein 7
LAMP2A	lysosome-associated membrane protein type 2A
LC3-I	microtubule-associated protein 1A/1B light chain 3-I
LC3-II	microtubule-associated protein 1A/1B light chain 3-II
LE	late endosome
LIMP2	lysosomal integral protein 2
LOAD	late onset Alzheimer's disease
LRP1	low-density receptor-related protein 1
LTD	long-term depression
LTP	long-term potentiation
M6P	mannose-6-phosphate
mBDNF	mature form of brain derived neurotrophic factor
MFSD8	major facilitator superfamily domain containing 8
mHTT	mutant huntingtin
mNGF	mature nerve growth factor
mNT	mature neurotrophic factor
MPR	mannose-6-phosphate receptor
mRNA	messenger ribonucleic acid
mTOR	mammalian target of rapamycin
mTORC1	mammalian target of rapamycin complex 1
NCL	neuronal ceroid lipofuscinosis
NFT	neurofibrillary tangle
NGF	nerve growth factor
NMDAR	*N*-methyl-D-aspartate receptor
NT	neurotrophic factor
NT3	neurotrophin 3
Nuc	nucleus
OST	oligosaccharyltransferase
$p75^{NTR}$	p75 neurotrophin receptor
PACS-1	phosphofurin acidic cluster sorting protein 1
PD	Parkinson's disease
PDGF-BB	platelet derived growth factor BB
PDZ proteins	PDZ domain containing proteins
Pen2	presenilin enhancer 2
PGRN	progranulin
PICALM	phosphatidylinositol binding clathrin assembly protein
PICK1	protein interacting with C Kinase 1

PKD	polycystic kidney disease
PNS	peripheral nervous system
PPT1	palmitoyl protein thioesterase 1
proBDNF	unprocessed form of brain derived neurotrophic factor
proNGF	unprocessed form of nerve growth factor
proNT	unprocessed form of neurotrophic factor
PSD95	postsynaptic density protein 95
PSEN1	presenilin-1
PSEN2	presenilin-2
Rab	Ras-related G-protein
RAB11FIP4	Rab11 family interacting protein 5
RAP	receptor associated protein
RE	recycling endosome
RFP	red fluorescent protein
SAP	sphingolipid activator proteins
SAP97	synapse-associated protein 97
sAPPα	soluble APP fragment α
sAPPβ	soluble APP fragment β
SNAP25	synaptosomal-associated protein 25
SNARE	soluble *N*-ethylmaleimide sensitive factor attachment receptor
SOD1	superoxide dismutase 1
SorCS	Sortilin related VPS10 domain containing receptor
SorCS subgroup	SorCS1, SorCS2 and SorCS3
SPC	sequence peptidase complex
SV	Secretory vesicle
TARP	transmembrane AMPAR regulatory protein
TDP43	TAR DNA-binding protein 43
TFEB	transcription factor EB
TGN	*trans*-Golgi network
TPP1	tripeptidyl peptidase 1
Trk	tropomyosin receptor kinase
ULK1	UNC-51 like kinase 1
Vps10p-D	vacuolar protein sorting defective 10 protein domain

Table of Content

1. Introduction

The general role of the nervous system is to detect intrinsic and extrinsic cue stimuli and to transmit them between the brain and the rest of the organism. For this transmission neurons play a key role as they generate electric action potentials from said stimuli and pass them on from one to another to finally activate consequential actions. Neurons are polarized cells that stereotypically consist of a stellate cell body or soma that branches out several long dendritic processes at one pole and a single long axon with strong distal arborization at the other pole (Deiters, 1865; von Waldeyer, 1891). Despite this universal appearance, neurons have been recognized to have a huge morphological heterogeneity with different specified functionalities underlying discrete molecular mechanisms and therefore form a highly complex network (Ramón y Cajal, 1906; Zeng et al., 2018).

Different types of glia cells that mainly execute supportive functions to maintain the nervous system accompany neurons. Microglia have immunological functions and are usually sitting in a resting state during which they scan their local territorial domain in the brain. Upon disease or injury, they proliferate and transform into active brain macrophages to phagocyte cells or cellular compartments (del Río-Hortega, 1919; Kettenmann et al., 2011). The axon of a neuron is isolated by myelin sheaths produced by oligodendrocytes in the central nervous system (CNS) or myelinating Schwann cells in the peripheral nervous system (PNS) to enable its rapid saltatory conduction (del Río-Hortega, 1921; del Río-Hortega, 1922; Stadelmann et al., 2019). Astrocytes, the most abundant glia cell type in the CNS, interact with endothelia cells which tightly enclose blood vessels in the brain. Together these cells form the blood brain barrier to avoid entering of toxins, pathogens or other substances circulating in the blood into the brain. Through specific transporters, however, astrocytes can surpass this barrier to provide neurons with nutrients from the blood. Astrocytes also have homeostatic properties like the buffering of K^+ and neurotransmitter recycling by interacting at synaptic sites (Lee et al., 2022). In the PNS homeostasis is controlled predominantly by satellite glia cells (Hanani and Verkhratsky, 2021).

Signal transduction between neurons occurs at synapses, which consist of presynaptic nerve endings, postsynaptic dendritic spines, and a synaptic cleft between these sites. Neurons receive chemical signals at the postsynaptic site which can de- or hyperpolarize the cell. This polarization is processed in the soma and can generate electric action potentials at the axon hillock which are

sent through the axon to the presynaptic sites. In the presynapse this signal is transformed into a chemical signal i.e., neurotransmitter release into the synaptic cleft which is then detected by neurotransmitter receptors on the postsynaptic dendritic spines of the next neuron (Dale, 1935; Eccles, 1976). To maintain this complex signal transmission the transcription and translation of the involved proteins as well as their correct targeting to the appropriate subcellular localizations is of crucial importance as malfunction of this machinery easily leads to a dysregulated system and subsequent neurological or neuropsychological diseases. During neurogenesis neurons emigrate from the (sub-)ventricular zone and afterwards no longer undergo mitosis. They become differentiated postmitotic cells. They achieve this state by constantly controlling their cell cycle and failure of this vigilance reinitiates the cell cycle and puts them into an altered state often leading to neuronal death (Herrup and Yang, 2007). Together, the postmitotic state and the complex molecular structure of neurons make them especially vulnerable as their functionality requires precise orchestration and organization of the involved cellular and molecular processes.

1.1. Endosomal protein trafficking in neurons

New proteins are synthesized at cytosolic ribosomes through the translation of messenger ribonucleic acid (mRNA) into an amino acid sequence (Palade, 1958; Pardee, 1954). Proteins that traffic through the endosomal pathway and transmembrane proteins contain a terminal signal peptide, which is recognized by a signal peptide recognition particle that conveys translocation of the emerging protein and ribosomes to the endoplasmic reticulum (ER) membrane (Fig. 1). Then, the emerging protein is co-translationally transported into the ER lumen through the signal peptide binding translocon complex. In the ER proteins undergo several co- and post-translational modifications including cleavage of their amino terminal signal peptide sequence by the signal sequence peptidase complex (SPC) (Braakman and Hebert, 2013; Rapoport, 2007). Moreover, proteins fold into their tertiary structure. Protein folding is realized through different chaperones, proteins arresting the unfolded protein in the ER to facilitate structural modifications like disulfide bonds through their interactions with protein disulfide isomerases or proline isomerization through interaction with prolyl peptidyl *cis-trans* isomerases. Cytosolic domains of transmembrane proteins as well as cytosolic proteins undergo folding through specific cytosolic chaperone complexes. Most proteins receive Asn(N)-linked glycosylation in the ER through the oligosaccharyltransferase (OST). The OST transfers a preassembled carbohydrate

consisting of two *N*-acetyl glucosamines, nine mannoses, and three glucoses to the Asn (Nilsson and von Heijne, 1993). The glucoses are identified by different carbohydrate-binding chaperones and only after cleaving all three glucose residues by glucosidases and one mannose residue by ER α-mannosidase I the protein can exit the ER (Braakman and Hebert, 2013).

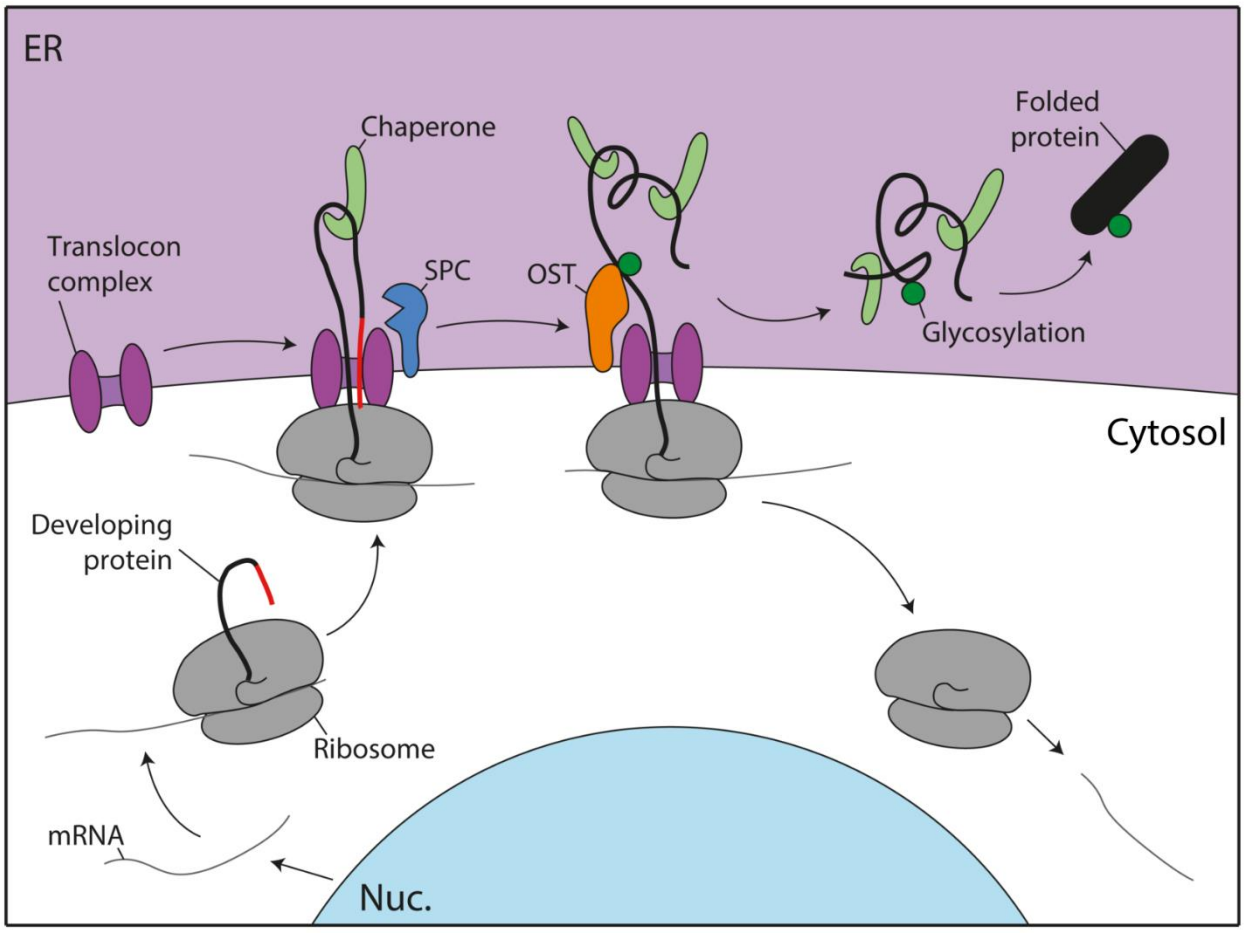

Fig. 1 Co- and post-translational protein modifications in the ER. The messenger RNA (mRNA) is transported from the nucleus (Nuc.) to the cytosol and is translated into a protein at the ribosome. A developing protein containing a signal peptide (red) interacts co-translationally with the translocon complex in the endoplasmic reticulum (ER) membrane. The translocon complex translocates the developing protein into the ER lumen. The signal peptide is cleaved off by the sequence peptidase complex (SPC) and the developing protein is glycosylated by the oligosaccharyltransferase (OST). Chaperones mediate protein folding of the developing protein co-and post-translationally until it is folded correctly and released into its respective pathway. After the protein translation ribosome and mRNA dissociate from the ER membrane.

The proteins that are processed in the ER and non-ER resident then actively traffic to the *cis*-Golgi network (CGN) and are subsequently sorted between the Golgi complex, the plasma membrane, and endosomes. Between the different compartments, proteins get transported through tubular or vesicular intermediates that bud from one compartment to another. This vesicle budding forms through the interaction of transmembrane cargo proteins with specific adaptor and scaffold proteins that recruit accessory proteins and vesicular coating complexes, which induce membrane curvature and scission (Fig. 2). After vesicle formation the outer coating of the vesicles

disassembles, and the vesicle can be transported to its target membrane through cytoskeletal motor proteins (Bonifacino and Glick, 2004; Wang et al., 2020). The intermediate vesicles then fuse to the target membrane by the interaction of the residing soluble *N*-ethylmaleimide sensitive factor attachment receptors (SNAREs) at both membranes and therefore form the SNARE-complex. Additionally, endosomal identity and intermediate compartments are defined by specific Ras-related G-proteins (Rab proteins), which bind guanosine triphosphate (GTP) upon activation and therefore anchor into the vesicle membrane. Endosomal target membranes carry Rab effector proteins which bind to the active Rab proteins and enable SNARE-complex formation. After vesicle fusion Rab proteins get deactivated by GTP hydrolysis to GDP to detach them from the membrane into the cytoplasm (Barr and Lambright, 2010; Martinez and Goud, 1998). Anterograde transport from the ER to the CGN along the tubular ER-Golgi-intermediate compartment (ERGIC) is facilitated by Rab1 and the coat protein complex (COP) II. ER resident proteins that are mistarget to the ERGIC and Golgi complex or involved in ER to Golgi sorting contain a C-terminal KDEL (KKXX) sequence and are retrogradely transported to the ER, which is facilitated by Rab2 and vesicle coating through COPI (Wang et al., 2020).

In the Golgi complex, the proteins are further modified and prepared for their distinct sorting. One key regulation in the Golgi complex is the processing of the carbohydrate portions of glycosylated proteins. The N-linked glycosylation, that proteins receive in the ER, follows a specific sequence of reactions depending on their sorting destination. Proteins following the secretory pathway i.e., proteins destined for secretion or the plasma membrane, acquire a specific set of different oligosaccharides while migrating from the CGN to the *trans*-Golgi network (TGN) (Fleischer, 1983; Stanley, 2011). Secretion and targeting to the plasma membrane is then mediated by the formation of Rab8 positive secretory vesicles (SV) from the TGN that finally fuse to the plasma membrane (Martinez and Goud, 1998). Here we differentiate between the default constitutive secretory pathway and the regulated secretory pathway, in which exocytosis must be activated by external factors binding to specific receptors in the plasma membrane (Chavez et al., 1996).

To maintain neuronal functions the correct distribution of proteins to either somatodendritic compartments or the axon of neurons is essential. This compartmentalization of proteins also determines the identity of these polarized regions of neurons. Specific adaptor proteins can support distinct protein transport pathways. Thus, proteins targeted towards axons and synaptic

vesicles rely on neuronal adaptor protein complex 3-b2 mediated vesicle formation from endosomal compartments and the TGN (Newell-Liwa et al., 2007). Additionally, neurons partially rely on local protein secretion from the ER at distal regions. Therefore, ER, ERGIC and ER exit-site are distributed also in distal dendrites and axons. Golgi and Golgi-like structures, however, have only been observed in the soma. Instead, small Golgi outposts, also called Golgi satellites, have been observed in dendrites, which facilitate local processing of proteins following the secretory pathway. Yet, their exact mechanisms are still poorly understood (Mikhaylova et al., 2016; Pierce et al., 2001; Wang et al., 2020).

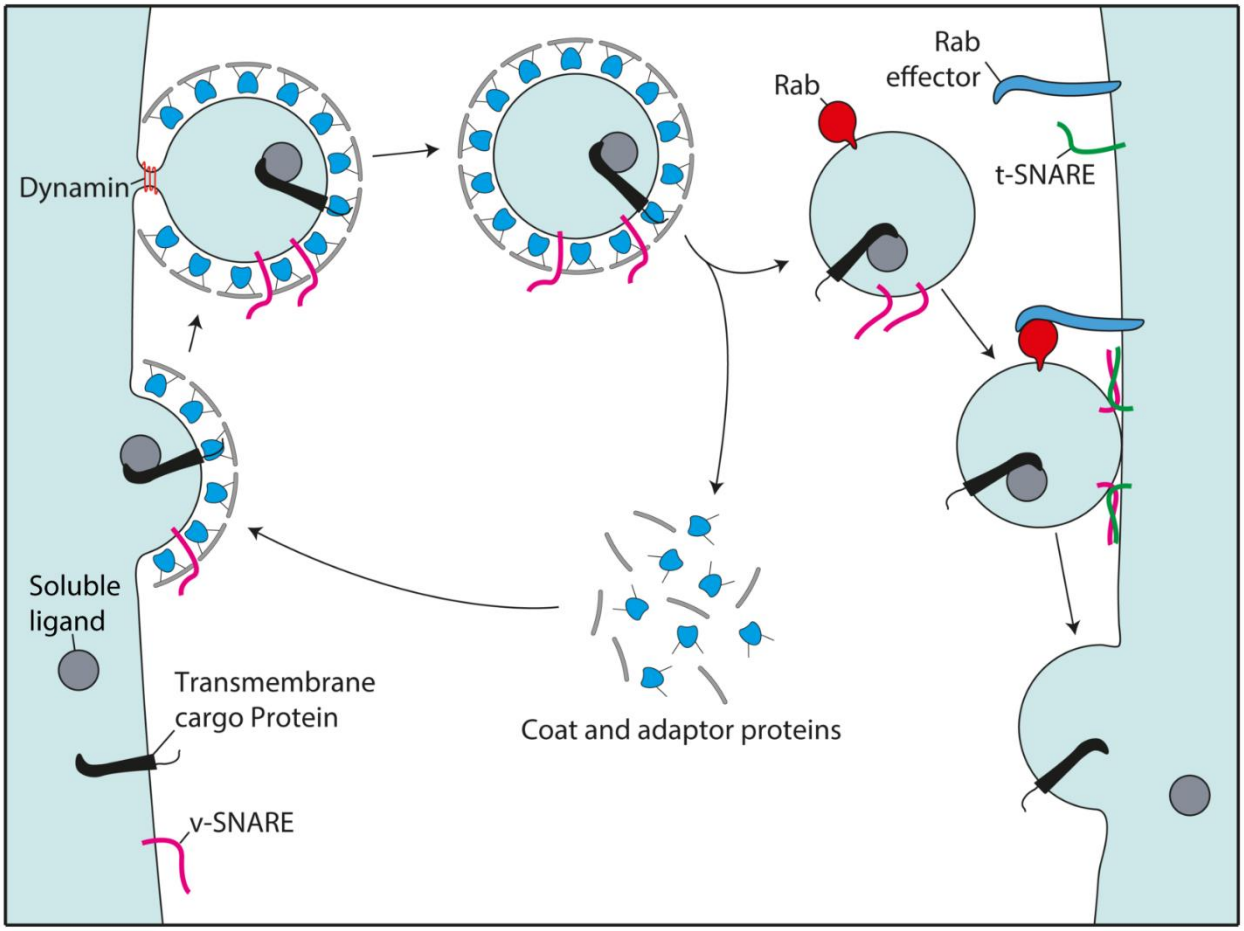

Fig. 2 Vesicle budding between cellular compartments. Transmembrane cargo proteins (black) interact with soluble ligands (grey) with their extracellular moiety and bind cytosolic adaptor proteins (blue) with their cytoplasmic tail. Adaptor proteins recruit coat proteins (grey) which induce curvature of the membrane. v-SNARE proteins (pink) localize to the forming vesicle. Dynamin facilitates scission of the vesicle from the compartment. The vesicle gets uncoated by dissociation of the bound coat and adaptor protein and travels toward its destined compartment. Compartment specific Rab proteins (red) in the vesicle membrane interact with Rab effectors in the target membrane. v-SNARE proteins in the vesicle membrane interact with t-SNARE proteins (green) in the target membrane and pull the vesicle closer to the vesicle until it fuses with the target membrane. The soluble ligand dissociates from the transmembrane cargo protein.

After their targeting to the plasma membrane, transmembrane proteins can be again endocytosed constitutively or upon ligand interaction in a clathrin-dependent or -independent manner (Fig. 3,①). For a clathrin-dependent internalization of free or ligand bound

transmembrane proteins their cytoplasmic domains feature internalization motifs that convey interactions with adaptor protein complex 2 (AP-2) (Pearse et al., 2000). All adaptor protein complexes interact with cytoplasmic domains of transmembrane proteins and recruit clathrin coatings to facilitates vesicle formation. The newly derived early endosomes (EE) carry activated Rab5 and segregate into different trafficking pathways. In EEs the internalized transmembrane proteins can dissociate from their ligands and subsequentially get recycled to the plasma membrane through Rab4 mediated fast or Rab11 mediated slow recycling endosomes (RE). From EEs proteins can also be sorted to late endosomes (LE) which are the pre-stage to endolysosomes where enzymatic degradation occurs. Rab7 mediates transport from EEs to LEs and Rab9 from LEs to the TGN and towards endo-lysosomal compartments (Kucera et al., 2016; Martinez and Goud, 1998). Some proteins however traffic from EEs and LEs towards the TGN through interaction with the five-subunit retromer complex (Seaman, 2012). Adaptor protein complex 1 (AP-1) facilitates the formation of most intermediates between the TGN and LEs but also of recycling endosomes (Bonifacino and Rojas, 2006; Tan and Gleeson, 2019). Other intermediates between the TGN and LEs but also between LEs and endolysosomes are formed by cargo interaction with the ubiquitous adaptor protein complex 3 (AP-3). Additional clathrin adaptors that play an important role in vesicle formation to transport proteins from the TGN to LEs or endolysosomes are the monomeric Golgi-localized γ ear-containing Arf-binding proteins 1-3 (GGA1-3) (Tan and Gleeson, 2019).

For most soluble glycosylated proteins that are destined for lysosomes their glycosylation gets phosphorylated in the CGN to produce a mannose-6-phosphate residue, which in the TGN can be recognized by mannose-6-phosphate receptors (MPR) (Fig. 3,②) (Campbell et al., 1983). These MPRs directly interact with AP-1 to transport the lysosomal proteins into LEs (Klumperman et al., 1998). Due to the lower pH in the LEs (pH ~5.5 – ~6.0) the lysosomal proteins dissociate from the MPRs to finally be transported to the even more acidic lysosomes (pH ~4.5 – ~5.5) (Hu et al., 2015). Lysosomal proteins without a mannose-6-phosphate residue are transported towards LEs in an MPR-independent manner. They specifically bind to sorting receptors like the lysosomal integral membrane protein 2 (LIMP2) or Sortilin which again bind with their cytoplasmic domains AP-1 or AP-3 (Braulke and Bonifacino, 2009; Fujita et al., 1999; Honing, 1998; Malik and Willnow, 2020).

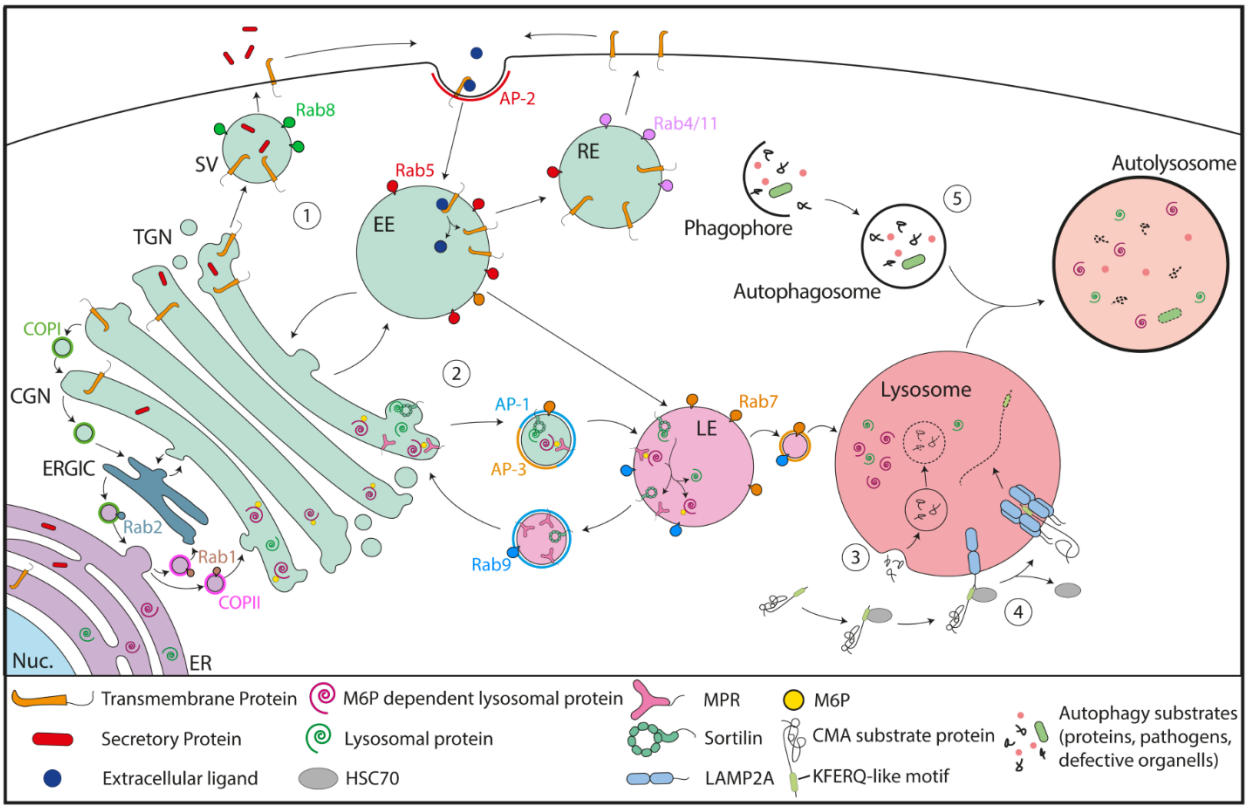

Fig. 3 Endosomal sorting and the lysosome-autophagosome system. After protein translation and folding in the endoplasmic reticulum (ER), transmembrane, secretory and lysosomal proteins are sorted to the cis-Golgi network (CGN) through COPII coated vesicles by traversing the ER-Golgi intermediate compartment (ERGIC). From the CGN they are sorted to the trans-Golgi network (TGN). Proteins involved in this sorting process and ER resident proteins that are missorted to the Golgi are retrogradely transported from the Golgi apparatus to the ER through COPI coated vesicles. (1) Transmembrane and secretory proteins are sorted towards the plasma membrane through secretory vesicles (SV). Secretory vesicles are secreted into the extracellular space and transmembrane proteins can interact with extracellular ligands and be internalized into early endosomes (EE) by interacting with adaptor protein 2 (AP-2). In endosomes the ligands dissociate from the transmembrane proteins. From EEs transmembrane proteins are either recycled back to the plasma membrane through recycling endosomes (RE) or retrogradely transported to late endosomes (LE) or the TGN. (2) Lysosomal proteins with a mannose-6-phosphate (M6P) modification (pink coil) are sorted by the M6P receptor (MPR) and other lysosomal proteins (green coil) can be sorted by Sortilin e.g.. MPR and Sortilin both interact with adaptor protein 1 (AP-1) but some lysosomal proteins are sorted to LEs via transmembrane proteins interacting with adaptor protein 3 (AP-3). At LEs the lysosomal proteins dissociate from their sorting receptors and are transported towards lysosomes. MPR and Sortilin are retrogradely transported from LEs to the TGN. (3) Microautophagy. Bulk of proteins can be taken up by invaginations and are then degraded in endolysosomal compartments. (4) Chaperone-mediated autophagy. Substrate proteins with a KFERQ-like amino acid motif bind to the chaperone heat-shock cognate protein of 70 kDa (HSC70), which guides them to the lysosomal protein lysosome-associated membrane protein type 2A (LAMP2A). The substrate protein unfolds its structure and is translocated by LAMP2 tetramers to the lysosomal lumen for degradation. (5) Macroautophagy. Proteins, protein aggregates, pathogens and defective organelles are enclosed by phagophores and form autophagosomes. Autophagosomes then fuse with lysosomes to form autolysosomes for degradation of the autophagy substrate. The different compartments harbor specific Rab proteins (Rab1/2/4/5/7/8/9/11) in their membranes for distinct compartmentalization.

In lysosomes intracellular and exogenous substrates are degraded through enzymatic activity. Degradation of pathogens, defective organelles, cytosolic proteins, or protein aggregates is primarily rendered by autophagy. The three main types of autophagy known are microautophagy (Fig. 3,③), chaperone mediated autophagy (Fig. 3,④) and macroautophagy (Fig. 3,⑤) (Fleming et al., 2022). During chaperone mediated autophagy the cytosolic chaperone heat-shock cognate protein 70 kDa (HSC70) interacts with KFERQ-like motifs of substrate proteins and directs them

together with several co-chaperones to the lysosome-associated membrane protein type 2A (LAMP2A). The substrate protein unfolds through its chaperone interaction and LAMP2A forms a homotetramer to translocate it into the lysosomal lumen for subsequential degradation (Kaushik and Cuervo, 2018). For macroautophagy (Fig. 4) a phagophore is generated, that encloses degradation substrates like pathogens, defective organelles, proteins, or protein aggregates to form an autophagosome (Andres-Alonso et al., 2021). The microtubule-associated protein 1A/1B light chain 3-II (LC3-II) translocates to the evolving phagophore membrane and plays an important role in autophagosome formation. LC3-II is the lipidated form of its cytosolic precursor LC3-I (Heckmann and Green, 2019). Protein aggregates destined for degradation are ubiquitinated and recruited to phagophores by the ubiquitin receptor p62 through its interaction with LC3 (Chen et al., 2020). The generation of phagophores is stress-induced and initiated by AMP-activated protein kinase (AMPK) activation and inhibition of the mammalian target of

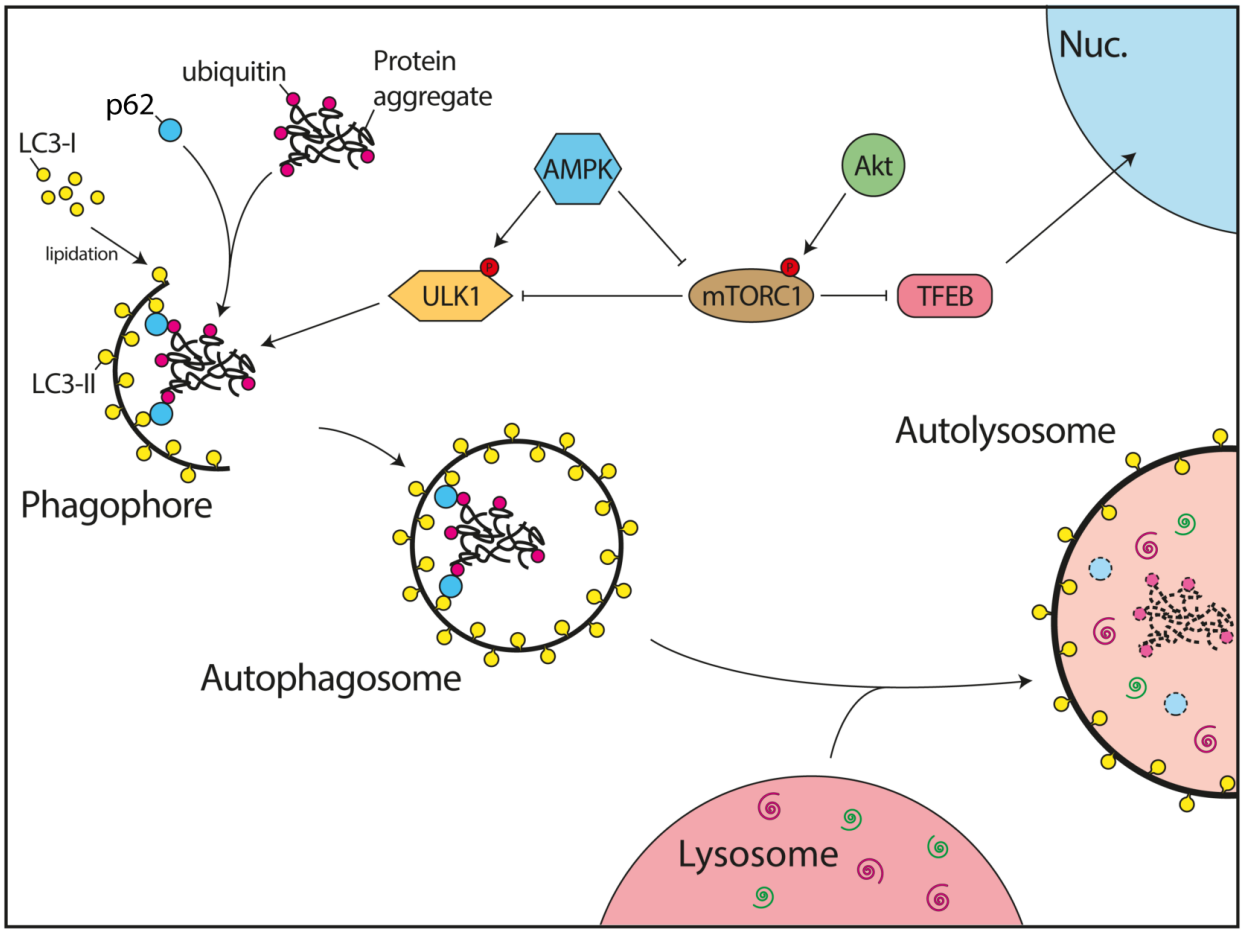

Fig. 4 Macroautophagy. Macroautophagy is initiated by ULK1 phosphorylation by AMPK. AMPK also inhibits the mTOR complex 1 (mTORC1), which is an inhibitor for ULK1 phosphorylation and transcription factor EB (TFEB) translocation to the nucleus (Nuc.). mTORC1 is activated by phosphorylation through Akt kinase. TFEB translocation to the Nuc. facilitates transcription of autophagy related genes. Upon autophagy initiation LC3-I is lipidated to LC3-II and binds to a developing phagophore with a double membrane. Poly-ubiquitinated protein aggregates that are targeted for macroautophagy by the interaction of ubiquitin with p62. p62 recruits the aggregates to phagophores by interacting with LC3-II. Upon the growth of the phagophore it eventually forms an isolated autophagosome that finally fuses with a lysosome for substrate degradation.

rapamycin (mTOR) or the serine/threonine-protein kinase named Akt kinase. AMPK phosphorylates and thereby activates the core autophagy machinery which includes the serine/threonine protein kinase UNC-51 like kinase 1 (ULK1) complex (Kim et al., 2011). ULK1 activation gets inhibited by the mTORC1 pathway, which is activated through the Akt kinase. The mTOR pathway also modulates the activity of transcription factor EB (TFEB), which predominantly regulates autophagy and lysosomal biogenesis (di Malta et al., 2019). Autophagosomes fuse with lysosomes to form degradative autolysosomes. This autophagic flux is highly regulated by the endosomal sorting complexes required for transport (ESCRT) proteins (Habib et al., 2021). Microautophagy is characterized by invaginations of cytoplasmic components into the endo-lysosomal system. This fast process seems to be independent from the core autophagy machinery but requires involvement of ESCTR-III and VPS4 (Schuck, 2020).
The misregulation of the lysosome-autophagy system and the resulting impairments of intracellular degradation processes are often causative for different neuronal diseases like the lysosomal storage disorder Neuronal Ceroid Lipofuscinosis.

1.2. Neuronal Ceroid Lipofuscinoses

Neuronal Ceroid Lipofuscinoses (NCL) are a group of 12 autosomal recessive and one autosomal dominant monogenetic rare neurodegenerative lysosomal storage disorders that are commonly known as Batten disease. They mainly affect children and are considered the most common early life onset neurodegenerative diseases. The exact manifestation of the disease differs among the NCL subtypes and ranges from neonatal to early adulthood (Butz et al., 2020). All NCL subtypes are characterized by the intracellular accumulation of autofluorescent lysosomal storage material, so called lipofuscin. Depending on the subtype, the storage material is either predominantly composed of ATP synthase membrane subunit c (ATP5MC) or the sphingolipid activator proteins A and D (Cotman and Staropoli, 2012; Kim et al., 2022). These accumulations are believed to underly misregulations in the autophagy-endolysosome system. The resulting gradual neurodegeneration in patients suffering from NCL is manifested by progressive loss of vision and subsequential or simultaneous motor disabilities, epileptic seizures, loss of cognitive functions and premature death (Schulz et al., 2013). Among the most active phagocytic cells in the human body are retinal pigment epithelium cells (Mazzoni et al., 2014). This likely explains the observed initial onset symptoms of NCLs in the retina leading to vision loss and probably relates their origin to dysregulated autophagic functions rather than to a consequence of storage

material accumulation. The following rapid neurodegeneration observed in other parts of the brain is maybe due to the high vulnerability of neurons as previously described. The NCL subtypes are named ceroid-lipofuscinosis neuronal (CLN) 1-8 and 10-14 and are differentiated by mutations in specific genes which all function in the transport of components or in degradative pathways of the autophagy-endolysosome system (Butz et al., 2020). These genes can be divided into genes encoding soluble proteins and genes encoding transmembrane proteins (Fig. 5). The following two sections summarize the known functions of these proteins based on investigations of the respective human or murine proteins as well as of homologous proteins in other model organisms.

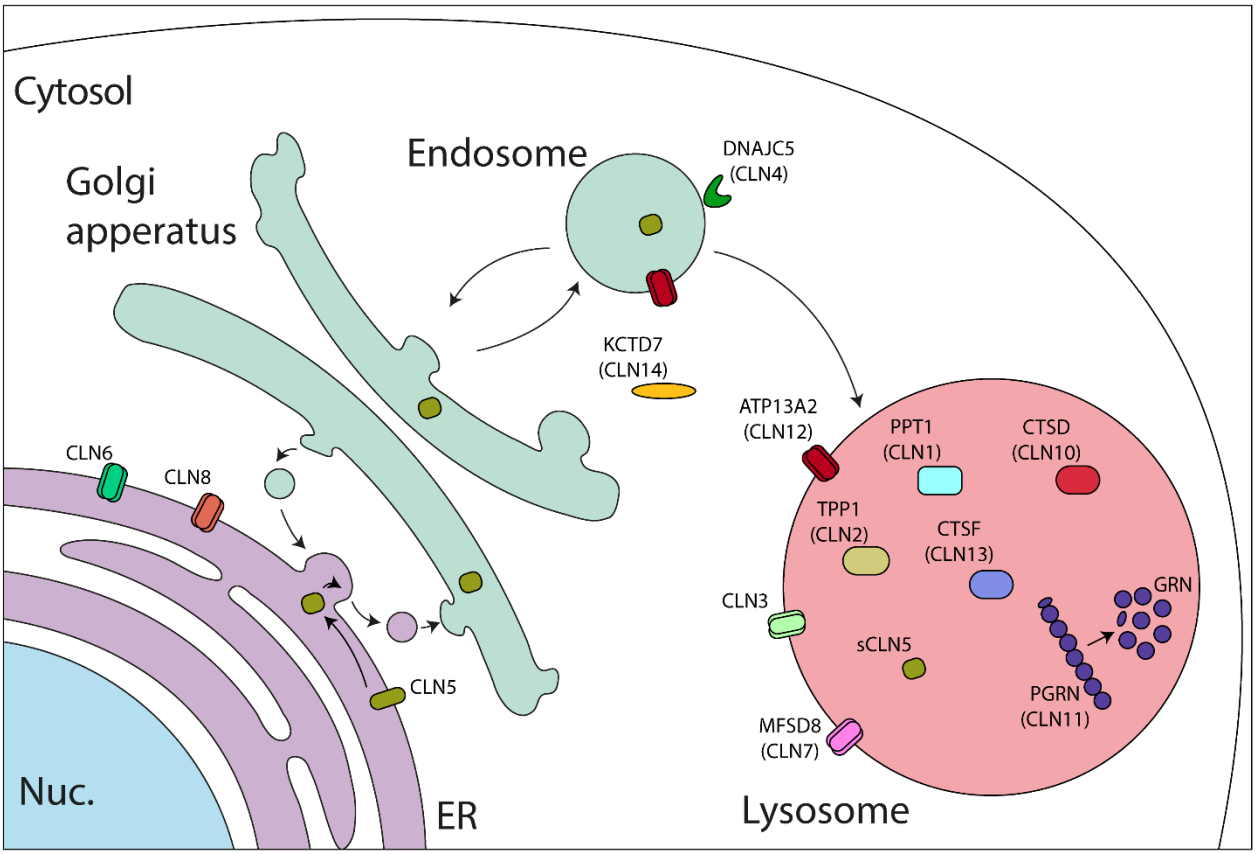

Fig. 5 Subcellular localization of the CLN proteins. The CLN1 protein PPT1, the CLN2 protein TPP1, the CLN10 protein CTSD, the CLN11 protein PGRN and the CLN13 protein CTSF are soluble proteins that are localized in lysosomes. PGRN is processed to GRN in lysosomes. The CLN14 protein KCTD7 and the CLN4 protein DNAJC5 are soluble proteins in the cytosol. DNAJC5 associates to endosomal membranes. CLN3 and the CLN7 protein MFSD8 are transmembrane proteins that are localized in lysosome membranes. The CLN12 protein ATP13A2 is a transmembrane protein that is localized in lysosome and endosome membranes. CLN5, CLN6 and CLN8 are endoplasmic reticulum (ER) resident transmembrane proteins. CLN5 can be processed in the ER to soluble CLN5 (sCLN5) that can be sorted into lysosomes. Nuc. Nucleus

1.2.1. Soluble CLN proteins

The NCL subtypes with mutations in genes encoding soluble proteins include CLN1, CLN2, CLN4, CLN10, CLN11, CLN13 and CLN14. In CLN1 disease the *PPT1* gene encoding the palmitoyl protein thioesterase 1 (PPT1) is mutated. CLN1 onset usually occurs between 6 and 24 months of age. PPT1 cleaves S-acetylated palmitate from substrates in lysosomes but localizes also to synaptosomes, synaptic vesicles, axons, and the extracellular space (Camp and Hofmann, 1993; Vesa et al., 1995). It has been involved in the metabolism of lipids like cholesterol, exocytosis, endocytosis, apoptosis, and synaptic recycling in neurons (Ahtiainen et al., 2003, 2006; Cho and Dawson, 2000; Kim et al., 2008; Lyly et al., 2008). PPT1 is also important in autophagic cargo degradation by altering the mTOR pathway. *PPT1*-deficiency has been shown to decrease mTOR complex 1 (mTORC1) and thereby increases TFEB activity (Yun et al., 2020). Loss of *PPT1* leads to an increased number of autophagosomes and impairs the autophagic flux (Bagh et al., 2017; Rebecca et al., 2019; Sarkar et al., 2020; Yun et al., 2020). PPT1 also seems to play an important role for Rab7 localization (Sarkar et al., 2020).

CLN2 disease onset usually occurs during the late infantile stage between two and four years and derives from mutations in the *TPP1* gene encoding tripeptidyl peptidase 1 (TPP1), which is a serine protease that cleaves N-terminal tripeptides from proteins (Lin et al., 2001). TPP1 localizes to lysosomes and the extracellular space and is a regulator of apoptosis, endocytosis, and autophagy (Junaid et al., 2000; Smith et al., 2019; Vines and Warburton, 1998). Deficiency of TPP1 has been shown to modulate expression of different autophagy related proteins like Rab7b (Domowicz et al., 2019). TPP1 seems to have modulating functions in the Akt-mTOR pathway as TPP1-deficiency showed elevated levels of phosphorylated Akt and other Akt-mTOR pathway modulators (Smith et al., 2019; Vidal-Donet et al., 2013). These effects lead to the activation of mTORC1 and consequentially to the inhibition of autophagy as shown in CLN2 patients (Vidal-Donet et al., 2013).

CLN4 disease, also known as adult Kufs disease or Parry disease, is the only autosomal dominant NCL. It is an adult-onset disease in which the *DNAJC5* gene expressing the cytosolic vesicle-associated co-chaperone DnaJ heat shock protein family Hsp40 member C5 (DNAJC5) is mutated (Mole and Cotman, 2015; Schulz et al., 2013). DNAJC5 associates to several membranes within endosomal and endo-lysosomal trafficking pathways where it regulates vesicle fusion and

separation by interacting with synaptosomal-associated protein 25 (SNAP25) of the SNARE complex and Dynamin-1 and thereby assisting with their folding (Chandra et al., 2005; Rozas et al., 2012; Sharma et al., 2012; Zhang et al., 2012). The loss of DNAJC5 leads to automatic degradation of unfolded SNAP25 by the proteasome and consequently impairs SNARE complex formation leading to neurodegeneration (Cadieux-Dion et al., 2013; Chandra et al., 2005; Tobaben et al., 2001; Tobaben et al., 2003). DNAJC5 also regulates trafficking and final secretion of misfolded proteins through non-lysosomal association, as well as lysosomal enzyme activity and Rab7 levels (Benitez and Sands, 2017; Lee et al., 2022). When associated to endolysosomes it acts as a co-chaperone of HSP70 (Fontaine et al., 2016). As this process is dependent on the ESCRT-VPS4 complex DNAJC5 is consequently believed to promote microautophagy (Lee et al., 2022; Sahu et al., 2011).

CLN10 disease is caused by different mutations in the *CTSD* gene encoding cathepsin (CTS) D (CTSD). CLN10 disease is mostly congenital but can also onset up to an adult age. CTSD is an aspartyl endopeptidase with enzymatic functions in lysosomes and has been linked to autophagic and apoptotic processes (Kim et al., 2022). It undergoes proteolytic processing from pro-CTSD to mature CTSD and this maturation is often affected through *CTSD* mutations (Bunk et al., 2021). Such mutations can also cause poor localization of CTSD and other enzymes to lysosomes as well as increased levels of the autophagosome cargo binding protein p62 and other polyubiquitinated proteins resulting in increased lysosomal substrate accumulation (Bae et al., 2015). Moreover, loss of CTSD increases autophagosome but decreases autolysosome formation, as shown by the accumulation of autophagosome proteins in non-autolysosomal compartments (Bae et al., 2015; Hah et al., 2012; Marques et al., 2020; Zheng et al., 2020).

CLN11 disease onset occurs during early adulthood and is caused by mutations in the *GRN* gene encoding progranulin (PGRN). PGRN is proteolytically processed to granulin (GRN) by cathepsins within endolysosomes (Kim et al., 2022). Apart from CLN11, heterozygous *GRN* mutations can also cause frontotemporal lobar dementia (Smith et al., 2012). GRN has been linked to cell migration, inflammation, cancer progression, and autophagy but its distinct function remains still unclear. PGRN is known to associate with Rab2A, which facilitates autolysosome fusion and seems to regulate the AMPK-mTOR pathway (Zhao et al., 2021). Upon PGRN deficiency phosphorylation of AMPKα and Ca^{2+}/calmodulin-dependent protein kinase I (CAMKI) are reduced resulting in decreased autophagy and autophagosome accumulation (Zhao et al., 2021; Zhou et

al., 2019). Additionally, several proteins involved in trafficking, fusion and maturation of vesicles related to the autophagy-lysosome pathway are differentially expressed through the loss of GRN. This includes the sorting receptor Sortilin, which sorts CTSD and CTSH and other lysosomal proteins towards lysosomes (Braulke and Bonifacino, 2009b; Canuel, et al., 2008; Elia et al., 2019), and TPP1, CTSD, CTSZ and TFEB (Huang et al., 2020; Tanaka et al., 2014). GRN also regulates the phosphorylation of Akt kinase and ULK1 (Liu et al., 2015; Zhou et al., 2019). Overall, these findings demonstrate that GRN initiates autophagosome formation, influences protein production and consequentially participates in autophagic degradation.

CLN13 disease or Kufs disease type B is an early adult-onset NCL characterized by mutations in the *CTSF* gene encoding the cysteine protease CTSF (Wang et al., 1998). CTSF localizes to lysosomes but truncated mutant versions form perinuclear aggregates enclosed in p62 positive aggresomes which are degraded by autophagy via interactions with LC3 (Jerič et al., 2013). CTSF has enzymatic functions within lysosomes and autophagic involvement has been suggested (Kim et al., 2022).

CLN14 disease has an infantile to late infantile onset between eight and nine months of age and carries mutations in the *KCTD7* gene encoding the potassium channel tetramerization domain-containing protein 7 (KCTD7). CLN14 patients have earlier been diagnosed with progressive myoclonic epilepsy type 3 (Kousi et al., 2012; Krabichler et al., 2012; van Bogaert et al., 2007). In 2012, Staropoli et al. linked *KCTD7* mutations to NCLs by identifying ceroid/lipofuscin in peripheral blood and skin biopsy of patients (Staropoli et al., 2012). KCTD7 is a cytosolic adaptor protein which is part of the Cullin-RING ligase (CRL) 3 (CRL3) complex. CRL complexes ubiquitinate substrates, which in CRL3 are recruited by KCTD7, for subsequential degradation (Fouad et al., 2019). CRL3-KCTD7 substrates have long been elusive but most recently, lysosomal and autophagic functions have been reported by identifying its interaction and recruitment of the transmembrane CLN protein CLN5. Thus, deficiency of KCTD7 causes CLN5 accumulation resulting in impaired trafficking of lysosomal enzymes and therefore lysosomal dysfunction (Wang et al., 2022).

1.2.2. Transmembrane CLN proteins

The NCL subtypes with mutations in genes encoding transmembrane proteins include CLN3, CLN5, CLN6, CLN7, CLN8 and CLN12. CLN3 disease has a juvenile onset between four and ten years and

is the most common form of NCL. It underlies mutations in the *CLN3* gene encoding the CLN3 protein, of which the function remains yet elusive (Cotman and Lefrancois, 2021). CLN3 is a multispanning transmembrane protein. It harbors a lysosomal target motif, through which it predominantly localizes to late endosomes and lysosomes (Oetjen et al., 2016; Storch et al., 2004). Because CLN3 interacts with Rab7A (Uusi-Rauva et al., 2012; Yasa et al., 2020) and CLN3 deficiency revealed several defects in endocytosis, autophagy, and lysosomal functions it is thought play a role in the endosomal and the autophagy-lysosome system but also in protein secretion and mitophagy (Kim et al., 2022). This assumption is based on altered lysosomal transport, lysosomal acidification, defects in MPR targeting as well as altered expression, activity, and secretion of various lysosomal enzymes after CLN3 depletion (Fossale et al., 2004; Lojewski et al., 2014; Ramirez-Montealegre and Pearce, 2005; Schmidtke et al., 2019). The most common mutation in CLN3 patients is a deletion of exon 7 and 8, $CLN3\Delta^{exon7/8}$. It encodes a truncated version of CLN3 which is retained in the ER (Oetjen et al., 2016). In a knock-in model of $CLN3\Delta^{exon7/8}$ accumulation of autophagosomal and autolysosomal proteins was observed (Cao et al., 2006).

CLN5 disease is a late-infantile onset NCL. It is caused by mutations in the *CLN5* gene encoding a cysteine-based S-depalmitoylase (Luebben et al., 2022). The CLN5 protein is expressed as a type-II transmembrane protein which is proteolytically processed and converted to a soluble form by signal peptidase and homologous signal peptidase-like proteases (Jules et al., 2017). Glycosylated soluble CLN5 can traffic towards the lysosome in an MPR- and Sortilin-independent manner. It is, however, believed to modulate Rab7 and retromer functions and thereby regulates endosome-to-TGN retrieval of the retromer interactor Sortilin (Mamo et al., 2012; Schmiedt et al., 2010). It's exact role in the autophagic flux is still a matter of debate as there have been contradictory findings in different disease models. Most models suggest decreased autophagy by a lack of autophagosome-lysosome fusion when CLN5 is ablated (Basak et al., 2021; Best et al., 2017; Leinonen et al., 2017; Nakamura and Yoshimori, 2017; Yasa et al., 2021). In other models knock-down of CLN5, however, demonstrates decreased levels of phosphorylated Akt and mTOR, efficient autophagic flux and even increased autophagic degradation (Adams et al., 2019; J. Xing et al., 2021). Nonetheless, decreased autophagy fits to the findings of decreased lysosomal enzyme effects, movement, and acidity as well as increased levels of autophagosomal proteins and substrates upon CLN5-deficiency (Kim et al., 2022).

CLN6 disease has a late infantile onset and underlies mutations in the *CLN6* gene which encodes an uncharacterized ER-residing transmembrane protein also called CLN6. It is believed to facilitate trafficking of lysosomal enzymes from the ER to the Golgi complex. CLN6-deficiency leads to reduced levels of TPP1, PPT1 and CTSD (Bajaj et al., 2020). Number and size of autophagic compartments, as well as autophagic markers and substrate proteins are increased upon CLN6 disease or deficiency. Accordingly, CLN6 regulates lysosome pH and autophagic degradation (Best et al., 2017; Cannelli et al., 2009; Thelen et al., 2012; von Eisenhart-Rothe et al., 2018).

In the late infantile onset CLN7 disease the *MFSD8* gene encoding the endo-lysosomal chloride channel major facilitator superfamily domain containing 8 (MFSD8) is mutated (Wang et al., 2021). Several studies observed autophagic dysregulations upon MFSD8 deficiency, like impairments in the mTOR pathway, the accumulation of ubiquitin-positive proteins and p62 levels, and altered lysosomal activities (Brandenstein et al., 2016; Connolly et al., 2019; Danyukova et al., 2018). Patient derived tissue showed an increase in autophagosome and lysosome number and a decrease in lysosomal size (Geier et al., 2019) which has been explained recently by the modulation of chloride currents in endolysosomes through MFSD8 in a Ca^{2+}/calmodulin dependent way (Wang et al., 2021).

The late infantile onset of CLN8 disease is caused by mutations in the *CLN8* gene which encodes an ER to Golgi cargo receptor. This CLN8 protein facilitates the anterograde transport from the ER to the CGN of various proteins by interacting with COPII (Bajaj et al., 2020; di Ronza et al., 2018; Lonka et al., 2000). Among these, it interacts with several lysosomal proteins like the CLN proteins PPT1, TPP1 and CTSD, but also proteins involved in membrane trafficking, mitophagy and lipid synthesis and transport (di Ronza et al., 2018; Lonka et al., 2000; Passantino et al., 2013; Vance et al., 1997). CLN8-deficency leads to defective phospholipid synthesis and therefore altered lipid compositions of mitochondria-associated membranes (Vance et al., 1997), as well as a reduction in lysosomal activity and biogenesis (di Ronza et al., 2018) and thus affects autophagy.

Mutated forms of the *ATP13A2* gene encoding the polyamine-transporting ATPase 13A2 (ATP13A2) can cause the juvenile onset CLN12 disease but also a juvenile onset form of Parkinson's disease called Kufor Rakeb Syndrome (Mole and Cotman, 2015; Schulz et al., 2013). Interestingly, increased expression of *ATP13A2* is also identified as a prognostic biomarker for colon cancer (Chen et al., 2020). ATP13A2 seems to regulate the active transport of inorganic

cations like irons in endosomes, lysosomes and multivesicular bodies and its mutations therefore results in iron toxicity-induced neurodegeneration (Rajagopalan et al., 2016; Ramonet et al., 2012; Tsunemi et al., 2014). ATP13A2 deficiency has been linked to accumulation of ceroid lipofuscin and ubiquitin-positive proteins (Gusdon et al., 2012; Kett et al., 2015), to alterations in intracellular trafficking, decreased lysosomal acidification and enzyme maturation. This ultimately reduces the clearance of autolysosomes (Dehay, Martinez-Vicente, et al., 2012; Dehay et al., 2012; Matsui et al., 2013; Nyuzuki et al., 2020; Usenovic et al., 2012).

Several studies demonstrate an etiologic and genetic overlap between NCLs and Alzheimer's disease (AD). This includes a genetic linkage of several CLN genes to AD as their mutations or ablations can cause typical AD phenotypes (Bagh et al., 2017; Cataldo et al., 1991; Cheng et al., 2018; Ehling et al., 2013; Fenoglio et al., 2009; Lee et al., 2011; Qureshi et al., 2018; Riemenschneider et al., 2006; Sheng et al., 2014; Sleat et al., 2022; Solé-Domènech et al., 2018; Viswanathan et al., 2009; Xu et al., 2017).

1.3. Endolysosomal trafficking defects underlying Alzheimer's disease

Alzheimer's disease (AD) is the most prevalent progressive adult-onset neurodegenerative disease. Late onset AD (LOAD) which comprises around 95% of all AD cases occurs after the age of 65. In around 5% of AD patients, the disease manifests earlier than at the age of 65 which is considered as early onset AD (EOAD). 1-2% of AD progressions are dominantly inherited as familial AD (fAD), whereas sporadic AD is multifactorial and associated with several risk factors. These risk factors include aging, additional inherited genetic dispositions, environmental factors, and epigenetic factors (Breijyeh and Karaman, 2020; DeTure and Dickson, 2019). AD manifests itself through profound cognitive decline, progressive memory loss, and retrograde and anterograde amnesia (Bai et al., 2021). AD pathology is characterized by severe histopathological changes, such as degeneration of the hippocampus and subsequent loss of cortical matter. These changes are accompanied by senile plaques composed out of extracellular amyloid β (Aβ) accumulations, neurofibrillary tangles (NFT) from intra- and extra-cellular accumulations of hyperphosphorylated tau protein, and synaptic loss, which can already be observed in early AD stages (Alzheimer, 1907; Brion et al., 1985; Glenner and Wong, 1984; Grundke-Iqbal, Iqbal, Quinlan, et al., 1986; Grundke-Iqbal, Iqbal, Tung, et al., 1986; Nukina and Ihara, 1986). Aβ monomers derive from proteolytic processing of the amyloid precursor protein (APP), oligomerize and finally form neurotoxic amyloid plaques that can stimulate immune responses

through astrocytes and microglia and damage neuronal axons and dendrites. According to the amyloid hypothesis, senile plaques resulting from Aβ secretion are considered the primary cause of AD (Breijyeh and Karaman, 2020). This hypothesis, however, does not take the cytopathological misregulations into account that might underly plaque formation. Moreover, it is still unclear whether extracellular Aβ aggregates are the result of neuronal secretion or the remains after neuronal death, caused by intracellular misregulation. Tau protein is a major microtubule-associated protein that impacts the assembly and stabilization of microtubules. Abnormal hyperphosphorylation of tau causes its dissociation from microtubules which disrupts the microtubule structure (Yuksel and Tacal, 2019). NFTs accumulate first in somatodendritic compartments, then displace the nucleus to the somatic periphery and finally form partially proteolysis resistant extracellular tangles after neural loss. Senile plaque deposition and NFT formation, however, is also caused by aging alone, which can be challenging for AD identification (Bai et al., 2021). Interestingly, Aβ formation induces pathways that trigger tau hyperphosphorylation and tau also pathologically regulates Aβ formation (Bloom, 2014). However, APP processing deficits seem to have an even higher impact on intracellular tau aggregation than Aβ itself (Kametani and Hasegawa, 2018).

Major genetic dispositions have been identified to cause AD initiation. These underly mutations in the *APP* gene or in genes encoding proteins that are involved in APP proteolytic processing or trafficking (Bai et al., 2021; Goate et al., 1991; Szabo et al., 2022). APP is a transmembrane protein that can be processed in an amyloidogenic and a non-amyloidogenic pathway (Fig. 6). This is highly dependent on its post-translational modifications which alter its protein interactions and intracellular trafficking (Yuksel and Tacal, 2019). Through interaction with AP-4, APP is sorted from the TGN to the cellular surface (Burgos et al., 2010) where it can undergo non-amyloidogenic processing facilitated by α-secretase, which cleaves APP into the soluble APP fragment α (sAPPα) and a carboxyl terminal fragment containing 83 amino acids (CTFα/C83). α-secretase processing prevents Aβ formation (Sisodia, 1992) and is promoted by specific post-translational glycosylations of APP (Jacobsen and Iverfeldt, 2011). Contrary to Aβ, neuroprotective abilities that promote neurite outgrowth, cell adhesion and synaptogenesis have been reported for sAPPα (Chasseigneaux and Allinquant, 2012). CTFα can be internalized and is further processed by the γ-secretase complex to the 3 kDa peptide p3 and the APP intracellular domain (AICD). Unprocessed APP can be internalized via interactions with AP-2 (Poulsen et al., 2015), which can be modulated by low-density receptor-related protein 1 (LRP1),

Sortilin or calsyntenin-1 (Yuksel and Tacal, 2019), and transported along the endo-lysosomal system through its interaction with AP-3 (Tam et al., 2016). AP-2 and AP-3 binding motifs can be inhibited by specific phosphorylations. APP can also traffic retrogradely from endosomes to the TGN through interaction with the retromer interacting protein SorLA (Andersen et al., 2005; Andersen et al., 2006; Vieira et al., 2010). By this, SorLA targets APP to a non-amyloidogenic pathway. Notably, the SorLA encoding gene *SORL1* is associated with fAD (Nicolas et al., 2015; Rogaeva et al., 2007). Internalized APP can be recycled either back to the plasma membrane or undergo amyloidogenic processing in endosomal compartments by its proteolytic cleavage through β-secretase (BACE1) (Caporaso et al., 1994; Nordstedt et al., 1993). BACE1 processing results in the soluble APP fragment β (sAPPβ) and the membrane-anchored β-carboxyl terminal fragment (CTFβ/C99) and can be decreased through specific APP glycosylations

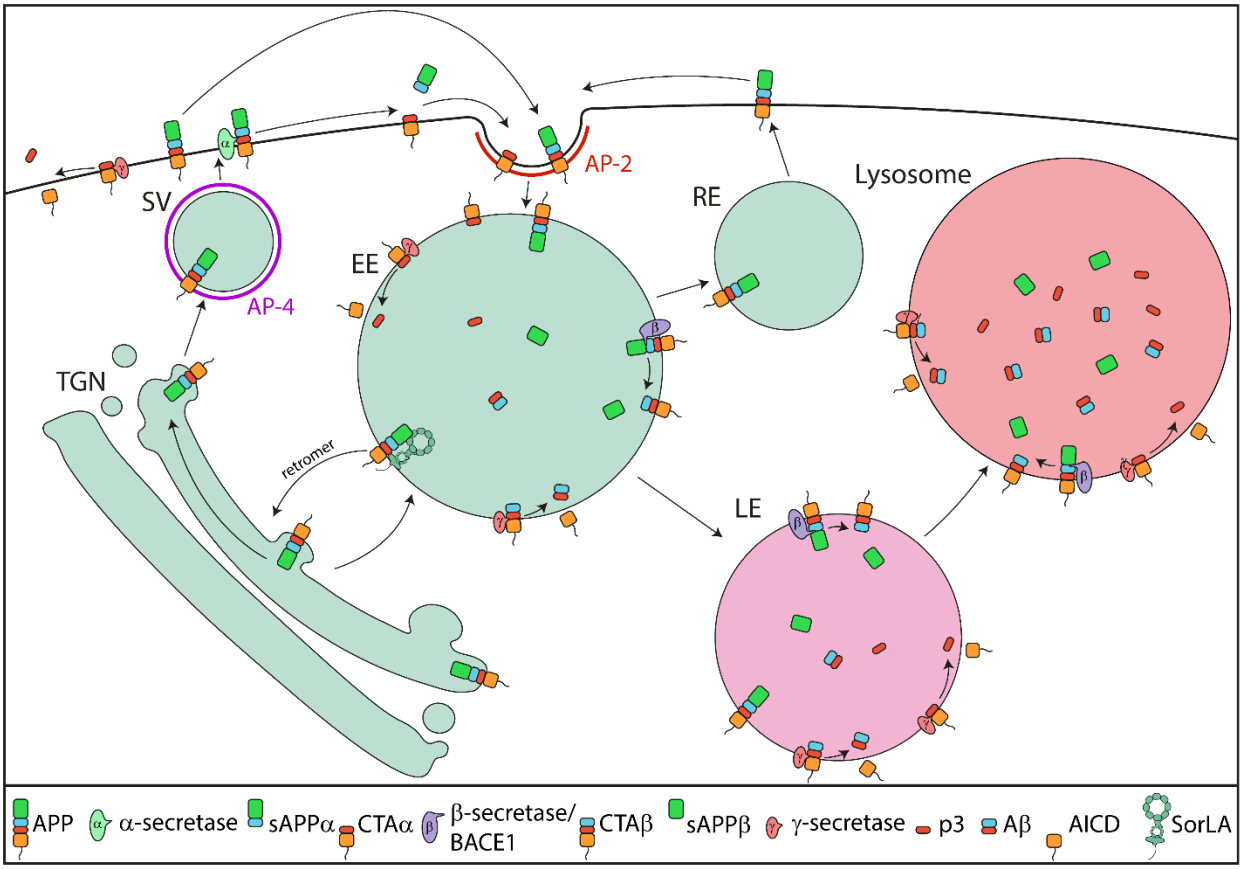

Fig. 6 Trafficking and processing of APP. Secretory vesicles (SV) transport the amyloid precursor protein (APP) from the trans-Golgi network (TGN) to the plasma membrane through its cytoplasmic interaction with AP-4. At the plasma membrane APP can be processed by α-secretase to CTAα and sAPPα. sAPPα is released into the extracellular space and CTAα can further be processed by γ-secretase to p3 and APP intracellular domain (AICD). Unprocessed APP and CTAα can alternatively be internalized into early endosomes (EEs) through their cytoplasmic interaction with AP-2. In endosomes APP can be processed by β-secretase to CTAβ and sAPPβ. CTAβ is further processed by γ-secretase to AICD and Aβ. Alternatively, APP in EEs can be sorted either back to the plasma membrane through recycling endosomes (RE), retrogradely to the TGN in a retromer-dependent way through its interaction with SorLA or to late endosomes (LE). In the TGN APP is again sorted into secretory vesicles. All endosomal APP products and unprocessed endosomal APP in LEs are finally transported to lysosomes for β- and γ-secretase processing and degradation.

(Nakamura and Kurosaka, 2019). In endosomes or lysosomes, the γ-secretase complex further processes CTFβ to AICD and Aβ (Takami et al., 2009). Whether Aβ is subsequently secreted or released to the extracellular space through apoptotic demise of neurons is currently a matter of debate. The γ-secretase complex is composed of presenilin enhancer 2 (Pen2/PSENEN2), anterior pharynx-defective 1 (APH-1), nicastrin and their catalytic core of either presenilin-1 (PSEN1) or presenilin-2 (PSEN2) (de Strooper, 2003; Takasugi et al., 2003). PSEN1-containing complexes are broadly distributed in endosomes whereas PSEN2-containing complexes are mainly targeted to late endosomes and lysosomes (Meckler and Checler, 2016; Sannerud et al., 2016). All members of the γ-secretase complex are well-known AD risk factors and mutations in PSEN1 or PSEN2 are especially frequent (Kim, 2019; Levy-Lahad et al., 1995; Sherrington et al., 1995). AD related mutations cause an increased formation of Aβ and its accumulation in senile plaques (Gandy, 2005; Xia, 2000).

Various additional risk factors for AD functionally involved in intracellular trafficking or the endosome-autophagy system in neurons and glia cells have been identified (Szabo et al., 2022). In accordance, different studies report pathological enlargement of EEs, lysosomes and autophagic vesicles as well as an accumulation of lysosomal hydrolases like CTSD, gradual loss of chaperone mediated autophagy, and disrupted lysosomal proteolysis (Bourdenx et al., 2021; Cataldo et al., 1991; Lee et al., 2022c; Nixon, 2017; Whyte et al., 2017). One of the strongest genetic risk factors for AD is the apolipoprotein E (APOE) isoform APOE4 (Corder et al., 1993; Strittmatter et al., 1993), a glycoprotein which is a receptor-mediated endocytic ligand for lipoprotein particles like cholesterol in astrocytes and microglia. This uptake is also an essential key feature for myelin production in the CNS (Breijyeh and Karaman, 2020). In astrocytes APOE interacts with the phosphatidylinositol binding clathrin assembly protein (PICALM), another AD risk factor, to control internalization of cell surface ligands (Narayan et al., 2020). PICALM is a clathrin binding protein mediating endocytosis and trafficking between TGN and endosomes (Tebar et al., 1999). The second most prevalent risk factor after APOE4 in LOAD is the adaptor protein bridging interactor 1 (BIN1) which induces membrane curvature during endocytosis through its falcate Bin-Amphiphysin-Rvs (BAR) domain, recruits clathrin and interacts with dynamin, that facilitates vesicle scission during endosome budding events (Sottejeau et al., 2015; Sweitzer and Hinshaw, 1998). BIN1 has also been proposed to modulate Aβ production and NFT pathology (Andrew et al., 2019; Holler et al., 2014). Another AD risk factor, the CD2-associated protein (CD2AP) modulates endosome morphology and recycling and acts as an adaptor protein

for protein trafficking towards lysosomes (Cormont et al., 2003; Furusawa et al., 2019). Overexpression of CD2AP stimulates APP degradation and its deficiency causes APP accumulation in early endosomes (Furusawa et al., 2019; Ubelmann et al., 2017).

The earlier mentioned transmembrane protein SorLA that interacts with APP belongs to the Vps10p-D sorting receptor family, of which two other members, named Sortilin and Sortilin related VPS10 domain containing receptor 1 (SorCS1), also regulate APP sorting and are genetically linked as risk factors to AD (Gustafsen et al., 2013; Hermey et al., 2015; Reitz et al., 2011). SorLA facilitates the retrograde transport of APP to the TGN and its redirection to the plasma membrane, Sortilin promotes non-amyloidogenic processing of APP and its sorting to lysosomes as well as its degradation, and SorCS1 reduces the anterograde transport of APP and increases the number of stationary APP vesicles (Coulson and Andersen, 2015; Gustafsen et al., 2013; Hermey et al., 2015). In conclusion, a number of AD risk factors have been identified. Of these several are involved in molecular sorting mechanisms and likely play a major role in APP processing, Aβ formation and AD progression.

1.4. The Vps10p-Domain receptor family

In mammals the vacuolar protein sorting defective 10 protein domain (Vps10p-D) receptor family comprises the five type-I transmembrane proteins Sortilin, SorLA, SorCS1, SorCS2 and SorCS3 that all regulate intracellular trafficking of several ligands (Hermey, 2009; Malik and Willnow, 2020). All family members are predominantly expressed in the developing and adult nervous system with specific spatiotemporal expression patterns (Hermans-Borgmeyer et al., 1999; Hermey et al., 2001a; Oetjen et al., 2014; Rezgaoui et al., 2001; Sarret et al., 2003) and all but SorCS3 are also expressed in varying peripheral tissue (Boggild et al., 2016; Hermans-Borgmeyer et al., 1998; Hermey et al., 1999; Jacobsen et al., 1996; Petersen et al., 1997). They are all genetically linked risk factors for LOAD as well as for several other neurological, neuropsychological, but also metabolic diseases (Andersen et al., 2005; Baum et al., 2008; Beecham et al., 2009; Bellenguez et al., 2022; Chaves et al., 2019; Christoforou et al., 2011; Clee et al., 2006; Dodson et al., 2008; Goodarzi et al., 2007; Hermey et al., 2015, 2019; Hu et al., 2010; Kathiresan et al., 2007; Lane et al., 2010; Lionel et al., 2011; Ma et al., 2017; Mitok et al., 2022; Offe et al., 2006; Olsen et al., 2019; Parks et al., 2013; Paterson et al., 2010; Philtjens et al., 2018; Reitz et al., 2011; Rogaeva et al., 2007; Shade et al., 2022; Smith et al., 2018; Wang et al., 2012; Wu et al., 2020; Xu et al., 2013).

In the extracellular/luminal moiety of all Vps10p-D receptors, their structural hallmark is a Vps10p-D forming a 10 bladed β-propeller that resembles a conical funnel with binding sites for diverse ligands (Kitago et al., 2015; Quistgaard et al., 2009). This Vps10p-D has first been described in the yeast sorting protein Vps10p (Marcusson et al., 1994). Additionally, Vps10p-D receptors also share a Vps10p-D preceding N-terminal propeptide. The propeptides of all family members are cleaved by the proprotein convertase furin within the TGN. This proteolytical step activates Sortilin and SorLA for ligand binding (Petersen et al., 1999; Westergaard et al., 2005). Further domains in their luminal moiety differ among the Vps10p-D receptors. The transmembrane domains are followed by a short cytoplasmic tail, containing interaction sites for various adaptor and scaffold proteins, that direct the proteins to their destined compartments to exert their functions. These domains and interaction sites, however, also differ among the receptors (Hermey, 2009; Malik and Willnow, 2020). They are all sorted to the plasma membrane through the secretory pathway and can be internalized by canonical endocytic signals (Nielsen et al., 2001; Nielsen et al., 2007; Nielsen et al., 2008; Oetjen et al., 2014).

1.4.1. Sortilin

In contrast to other Vps10p-D receptors the Sortilin luminal/extracellular moiety comprises only the Vps10p-D. From the ER Sortilin is most likely released to the CGN by dissociation from the ER residing chaperone receptor associated protein (RAP) (Petersen et al., 1997; Petersen et al., 1999). Sortilin facilitates trafficking of various internalized ligands to lysosomes and transport of cargo from the Golgi complex to endosomes through its cytosolic interactions with AP-1, AP-2, GGAs and the retromer subunit VPS35 (Canuel et al., 2008a; Hermey, 2009; Kim et al., 2010; Nielsen et al., 2001). Specific phosphorylation of the Sortilin cytoplasmic tail negatively regulate the interactions with AP-1 and GGAs (Pallesen et al., 2020).

Besides its earlier described interactions with APP, Sortilin has been identified to interact with and to modulate trafficking of the neuropeptide neurotensin (Mazella et al., 1998; Petersen et al., 1999), the lipoprotein lipase (Nielsen et al., 1999), different apolipoproteins (Carlo, 2013), and the lysosomal cofactors sphingolipid activator proteins (SAPs) for degradation (Chen et al., 2005). Sortilin further interacts with the unprocessed forms of neurotrophins (proNTs), specifically nerve growth factor (proNGF), brain-derived neurotrophic factor (proBDNF) and neurotrophin 3 (proNT3) (Chen et al., 2005; Nykjaer et al., 2004; Tauris et al., 2011; Teng et al.,

2005) but also with the mature form of NGF (mNGF) with low affinity (Leloup et al., 2017; Nykjaer et al., 2004). Sortilin builds a complex by interacting with proNTs and the p75 neurotrophin receptor ($p75^{NTR}$) which regulates synaptic plasticity and trigger apoptotic signalling (Jansen et al., 2007; Nykjaer and Willnow, 2012; Nykjaer et al., 2004). Sortilin also interacts with the receptors of mature neurotrophic factors (mNTs), the tropomyosin receptor kinase A-C (TrkA-C), and promotes their cell and synaptic surface expression (Vaegter et al., 2011). Additionally, complex formation of proBDNF, Sortilin and huntingtin associated protein 1 (HAP1) sorts proBDNF to secretory granules for activity dependent release (Nykjaer and Willnow, 2012). The Sortilin Vps10p-D also interacts with the glucose transporter type 4 (Glut4) and facilitates its retromer regulated retrograde transport to the TGN (Pan et al., 2017). Homodimerization of Sortilin through its β-propeller can trigger the pH dependent release of several Vps10p-D ligands, like in the acidic milieu of late endosomes and lysosomes (Januliene et al., 2017a; Leloup et al., 2017). In disease Sortilin is considered a risk factor for LOAD (Gustafsen et al., 2013), frontotemporal dementia (Hu et al., 2010; Philtjens et al., 2018), Huntington's disease (Chaves et al., 2019), and also cardiovascular and other metabolic diseases(Mitok et al., 2022).

1.4.2. SorLA

In SorLA the luminal/extracellular moiety is followed by an YWTD repeat shaped as a β-propeller, an EGF precursor type repeat, LDLR class A repeats and fibronectin-type III repeats (Gent and Braakman, 2004; Hermey, 2009; Kitago et al., 2015; Yamazaki et al., 1996). Similar to Sortilin, SorLA release from the ER to the CGN is most likely initiated through its dissociation from RAP (Petersen et al., 1999) and it conveys sorting of various ligands including APP (see 1.4 Trafficking in Alzheimer's Disease) between endosomes and Golgi compartments through its cytosolic interaction with GGAs, the retromer subunit VPS26, AP-1 but also AP-2 and the cytosolic phosphofurin acidic cluster sorting protein 1 (PACS-1) (Andersen et al., 2005; Burgert et al., 2013; Coulson and Andersen, 2015; Dumanis et al., 2015; Jacobsen et al., 2002; Knight et al., 2016; Nielsen et al., 2007; Offe et al., 2006; Rogaeva et al., 2007; Schmidt et al., 2007). Expression of SorLA can be induced as a neuronal response to mature BDNF (mBDNF) (Rohe et al., 2009).

Like Sortilin, SorLA has been reported to interact with neurotensin and lipoprotein lipase (Jacobsen et al., 2001). Through its interaction with TrkB it enhances TrkB surface expression and therefore the response to mBDNF (Rohe et al., 2013). SorLA also interacts with the platelet

derived growth factor BB (PDGF-BB) (Gliemann et al., 2004). Apart from regulating APP trafficking, SorLA also interacts with Aβ itself (Kitago et al., 2015) and enables binding and release of the AD risk factor APOE (Jacobsen et al., 2001; Kitago et al., 2015; Yamazaki et al., 1996). Recently, SorLA-deficiency has also been shown to cause elevated Aβ and tau CSF levels (Andersen et al., 2022), APP-dependent defects in the endolysosome-autophagy network (Hung et al., 2021), EE enlargement in neurons independently from APP processing (Knupp et al., 2020) and impaired trafficking of TrkB and the AMPAR subunit GluA1 (Mishra et al., 2022). As a risk factor SorLA has been genetically linked to EOAD and LOAD (Andersen et al., 2005; Dodson et al., 2008; Offe et al., 2006; Rogaeva et al., 2007), but also to hypercholesterolemia (Kathiresan et al., 2007), and obesity (Parks et al., 2013).

1.4.3. The SorCS subfamily

The SorCS subfamily of the Vps10p-D receptor family was identified in 1999 by Hermey et al. and includes the receptors SorCS1, SorCS2 and SorCS3 (Hermey et al., 1999). Their hallmark characteristic is a so-called leucine rich domain which is located between the Vps10p-D and the transmembrane domain. It contains imperfect leucine-rich repeats, but also regions with homology to polycystic kidney disease (PKD) domains and is thought to allow receptor dimerization (Hermey et al., 1999; Januliene et al., 2017b; Leloup et al., 2018). In contrast to Sortilin and SorLA, the respective propeptides of the SorCS subfamily are not interacting with their own Vps10p-Ds and thus not inhibiting Vps10-D ligand binding. The SorCS subgroup receptors are all suggested to convey internalization of extracellular ligands through their AP-2 interaction motif in their respective cytoplasmic tail and seem less engaged in Golgi-late endosome trafficking (Hermey, 2009; Malik and Willnow, 2020; Nielsen et al., 2008). Expression of the SorCS subfamily is most abundant during the developing brain and in the adult brain, they display an almost complementary expression pattern (Hermey et al., 2004).

1.4.3.1. SorCS1

SorCS1 is expressed as seven different splice variants with alternative cytoplasmic domains (Hermey et al., 2003). The most conserved splice variants between mice and men are SorCS1b, SorCS1c-α, SorCS1c-β, SorCS1c-δ and SorCS1e (Hermey, 2009). Notably, SorCS1b and SorCS1e lack functional internalization motifs in their cytoplasmic domains and SorCS1b is localized predominantly to the cell surface (Hermey et al., 2003). In contrast, all other SorCS1 splice

variants are targeted to the Golgi complex and to somatodendritic endosomal compartments like EEs and REs (Hermey et al., 2003; Savas et al., 2015). SorCS1 expression is found in excitatory and inhibitory neurons (Savas et al., 2015) and can be induced by chemically provoked seizures (Hermey et al., 2004).

SorCS1 controls trafficking of the neuronal adhesion protein neurexin from EEs to REs and their transport to the axon. This has been demonstrated through its interactions with the Rab11 family interacting protein 5 (RAB11FIP5) that regulates intracellular neurexin 1α transport (Ribeiro et al., 2019; Savas et al., 2015). Knockout of SorCS1 downregulates the surface expression of another neuronal adhesion protein neuroligin, the neuron-glia cell adhesion molecule (L1/NgCAM), APP, and α-amino-3-hydroxy-5-methyl-4-isoxazolepropionic acid receptors (AMPAR) and therefore suggest SorCS1 involvement in their internalization (Ribeiro et al., 2019; Savas et al., 2015). Earlier studies already described the interactions of SorCS1 with APP (Hermey et al., 2015; Lane et al., 2010) and overexpression experiments showed reduced γ-secretase activity and Aβ levels (Reitz et al., 2011). SorCS1 also interacts with TrkB and inhibits its surface activity (Subkhangulova et al., 2018). Like SorLA, SorCS1 also interacts with PDGF-BB (Hermey et al., 2006). SorCS1 has been identified as a genetic risk factor for LOAD (Hermey et al., 2015; Lane et al., 2010; Reitz et al., 2011; Wang et al., 2012; Xu et al., 2013), attention deficit hyperactivity disorder (ADHD) (Lionel et al., 2011), type 1 (Paterson et al., 2010) and type 2 diabetes (Clee et al., 2006; Goodarzi et al., 2007), and brain arteriolosclerosis (Shade et al., 2022).

1.4.3.2. SorCS2

SorCS2 expression is not affected by kainic acid induced seizures (Hermey et al., 2004). It is expressed in neuronal somatodendritic vesicles and Schwann cells of the CNS but not in the axon of neurons (Glerup et al., 2016). In the hippocampus it presents a predominant expression in the CA2 region, and besides other areas, it is also expressed in dopaminergic midbrain nuclei and the dorsal thalamus (Hermey et al., 2004; Rezgaoui et al., 2001).

Knockout of SorCS2 in mice demonstrates the absence of hippocampal long-term potentiation (LTP), reduced dopamine levels and metabolism, decreased dopaminergic hyperinnervation of the frontal cortex, decreased alcohol preference, decreased levels of *N*-methyl-D-aspartate receptor (NMDAR) subunits, and oxidative brain damage along with enhanced neuronal cell death and increased mortality during epilepsy (Glerup et al., 2014; Malik et al.,

2019; Olsen et al., 2019; Yang et al., 2021). SorSC2 sustains LTP through its targeting of TrkB to the postsynaptic density which might also control memory processing in the amygdala (Glerup et al., 2016; Olsen et al., 2019). Like Sortilin, SorCS2 builds a complex with proNGF or proBDNF and $p75^{NTR}$ to regulate trophic and apoptotic signalling, but it also interacts with mNGF with low affinity (Glerup et al., 2014; Leloup et al., 2018). SorCS2 mediates axonal growth cone retraction (Deinhardt et al., 2011) but also induces NMDAR-dependent long-term depression (LTD) in the CA1 region of the hippocampus (Glerup et al., 2016; Yang et al., 2021). SorCS2 mediates trafficking of the NMDA receptor subunit NR2A in the dopaminergic system and is required for social memory (Ma et al., 2017; Yang et al., 2021). In Huntington's disease patients SorCS2 also interacts with mutant huntingtin (mtHTT) which results in mislocalized SorCS2 expression (Ma et al., 2017). Accordingly, SorCS2 has been recognized as a genetic risk factor in Huntington's disease (Ma et al., 2017), alcohol use disorder (Olsen et al., 2019; Smith et al., 2018), epilepsy (Malik et al., 2019), but also bipolar disorder (Baum et al., 2008; Christoforou et al., 2011), schizophrenia (Christoforou et al., 2011) and LOAD (Beecham et al., 2009).

1.4.3.3. SorCS3

The *SorCS3* gene shares around 75% identity with *SorCS1* (Hermey et al., 2004). In contrast to all other Vps10p-D receptor genes that are dispersed throughout the genome, the *SorCS1* and *SorCS3* genes locate in different species adjacent to each other on one chromosome. This indicates that one gene might originate from the other by gene duplication (Hermey, 2009).The expression of SorCS3 is highly activity regulated and induced by kainic acid provoked seizures (Hermey et al., 2004), LTP (Maag et al., 2015), fear conditioning (Rao-Ruiz et al., 2019), and visual stimulation (Cho et al., 2016). In embryonic and early postnatal stages, SorCS3 is mainly expressed in thalamic nuclei. During postnatal development and in the adult, forebrain structures like the hippocampus, especially its CA1 region, and the cerebral cortex are predominantly marked by SorCS3 expression (Hermey et al., 2004). On the cellular level, SorCS3 is localized to somatodendritic vesicles, the cell surface, and the Golgi complex (Oetjen et al., 2014).

SorCS3 interacts with proNGF, mNGF and PDGF-BB (Hermey et al., 2006; Westergaard et al., 2005). Like SorCS1 it inhibits TrkB surface activity through its interaction with TrkB (Subkhangulova et al., 2018). Knockout of SorCS3 in mice displays deficits in LTD, synaptic transmission, spatial learning and memory, and increased fear extinction (Breiderhoff et al., 2013; Christiansen et al., 2017) suggesting a contribution of SorCS3 in the formation of synaptic

plasticity. The interaction of the SorCS3 cytoplasmic domain with the scaffold proteins protein interacting with C Kinase 1 (PICK1) and postsynaptic density protein 95 (PSD95) eventually promotes synaptic efficacy through retaining surface expression of AMPAR (Malik and Willnow, 2020; Wu et al., 2020). The diseases, in which SorCS3 is considered a genetic risk factor include ADHD (Lionel et al., 2011; Wu et al., 2020), schizophrenia, bipolar disorder, autism spectrum disorder, depression (Wu et al., 2020), LOAD (Beecham et al., 2009) and brain arteriolosclerosis (Shade et al., 2022).

1.5. Objectives

Functional intracellular trafficking in neurons is essential for the viability of the nervous system. Neurological degradation often underlies the intra- or extracellular accumulation of different aggregates from neural cells. Such histopathological hallmarks can be traced back to impaired trafficking of proteins or smaller peptides. Close literature research demonstrates conspicuous overlaps and shared deficits in different molecular sorting components between various neurological diseases. This includes misregulation in protein trafficking and the autophagy-lysosome system in NCLs and AD. In this dissertation, I investigate intracellular sorting mechanisms in models for healthy and diseased cells. These give rise to alterations in intracellular trafficking and in the endolysosome-autophagy system as possible primary causes of NCLs and AD. In addition, I illuminate functions of different sorting receptors, by studying novel interactions and presenting novel tools to investigate these receptors in live cell analysis. The following sections demonstrate the converging roles of the NCL gene *CLN3* and the AD risk factor *PEN2* in the autophagy-lysosome system (section 2) and review further impacts of shared genetic predispositions affecting both NCL and AD progression (section 3). Moreover, the next sections demonstrate how the AD disease risk factor SorLA, a Vps10p-D receptor which facilitates trafficking between endo-lysosomal compartments, interacts with the scaffold protein PICK1, which is involved in protein sorting and endosome formation (section 4). Finally, I introduce novel functional internally tagged Vps10p-D receptors as powerful tools to investigate protein sorting and demonstrate their interaction and internalization capacities for the neurotrophic factor BDNF (section 5).

2.

Converging roles of PSENEN/PEN2 and CLN3 in the autophagy-lysosome system

Marcel Klein, Abuzar Kaleem, Sandra Oetjen, Daniela Wünkhaus, LarsBinkle, Sandra Schilling, Milena Gjorgjieva, Ralf Scholz, Doris Gruber-Schoffnegger, Stephan Storch, Stefan Kins, Gerard Drewes, Sabine Hoffmeister-Ullerich, Dietmar Kuhl and Guido Hermey

Research-Article

Autophagy. 2022 Sept; 18(9), 2068-2085.
Epub ahead of print Dec. 2021.
DOI: 10.1080/15548627.2021.2016232

Personal contribution

Experiment planning, execution and analysis of Fig. 1 J-M, Fig. 3 C, Fig. 4, Fig. 5 A+F, Fig. S1 B, Fig. S4 B, Fig. S5, Fig. S6 and Fig. S7 were performed by Marcel Klein. Description of the respective experiments in the manuscript was performed by Marcel Klein and PD Dr. Guido Hermey. Additional experiments during the review process were performed by Marcel Klein. Editorial work of the manuscript during the review process was performed by Marcel Klein and PD Dr. Guido Hermey.

21.12.2022 Hamburg

Date and City

Signature supervisor

PD Dr. Guido Hermey

AUTOPHAGY
2022, VOL. 18, NO. 9, 2068–2085
https://doi.org/10.1080/15548627.2021.2016232

Taylor & Francis
Taylor & Francis Group

RESEARCH PAPER

Converging roles of PSENEN/PEN2 and CLN3 in the autophagy-lysosome system

Marcel Klein[a,1], Abuzar Kaleem[a,1], Sandra Oetjen[a,1], Daniela Wünkhaus[b], Lars Binkle[c], Sandra Schilling[d], Milena Gjorgjieva[a], Ralf Scholz[a], Doris Gruber-Schoffnegger[b], Stephan Storch[e], Stefan Kins[d], Gerard Drewes[f], Sabine Hoffmeister-Ullerich[g], Dietmar Kuhl[a], and Guido Hermey [a]

[a]Institute for Molecular and Cellular Cognition, Center for Molecular Neurobiology Hamburg, University Medical Center Hamburg-Eppendorf, Hamburg, Germany; [b]Evotec SE, Manfred Eigen Campus, Hamburg, Germany; [c]Institute of Neuroimmunology and Multiple Sclerosis, Center for Molecular Neurobiology Hamburg, University Medical Center Hamburg-Eppendorf, Hamburg, Germany; [d]Division of Human Biology and Human Genetics, University of Kaiserslautern, Kaiserslautern, Germany; [e]Department of Pediatrics, University Medical Center Hamburg-Eppendorf, Hamburg, Germany; [f]Cellzome, Functional Genomics Research and Development, Heidelberg, Germany; [g]Bioanalytics, Center for Molecular Neurobiology Hamburg, University Medical Center Hamburg-Eppendorf, Hamburg, Germany

ABSTRACT

PSENEN/PEN2 is the smallest subunit of the γ-secretase complex, an intramembrane protease that cleaves proteins within their transmembrane domains. Mutations in components of the γ-secretase underlie familial Alzheimer disease. In addition to its proteolytic activity, supplementary, γ-secretase independent, functions in the macroautophagy/autophagy-lysosome system have been proposed. Here, we screened for PSENEN-interacting proteins and identified CLN3. Mutations in *CLN3* are causative for juvenile neuronal ceroid lipofuscinosis, a rare lysosomal storage disorder considered the most common neurodegenerative disease in children. As mutations in the *PSENEN* and *CLN3* genes cause different neurodegenerative diseases, understanding shared cellular functions of both proteins might be pertinent for understanding general cellular mechanisms underlying neurodegeneration. We hypothesized that CLN3 modulates γ-secretase activity and that PSENEN and CLN3 play associated roles in the autophagy-lysosome system. We applied CRISPR gene-editing and obtained independent isogenic HeLa knockout cell lines for *PSENEN* and *CLN3*. Following previous studies, we demonstrate that PSENEN is essential for forming a functional γ-secretase complex and is indispensable for γ-secretase activity. In contrast, CLN3 does not modulate γ-secretase activity to a significant degree. We observed in *PSENEN*- and *CLN3*-knockout cells corresponding alterations in the autophagy-lysosome system. These include reduced activity of lysosomal enzymes and lysosome number, an increased number of autophagosomes, increased lysosome-autophagosome fusion, and elevated levels of TFEB (transcription factor EB). Our study strongly suggests converging roles of PSENEN and CLN3 in the autophagy-lysosome system in a γ-secretase activity-independent manner, supporting the idea of common cytopathological processes underlying different neurodegenerative diseases.

Abbreviations: Aβ, amyloid-beta; AD, Alzheimer disease; APP, amyloid precursor protein; ATP5MC, ATP synthase membrane subunit c; DQ-BSA, dye-quenched bovine serum albumin; ER, endoplasmic reticulum; GFP, green fluorescent protein; ICC, immunocytochemistry; ICD, intracellular domain; JNCL, juvenile neuronal ceroid lipofuscinosis; KO, knockout; LC3, microtubule associated protein 1 light chain 3; NCL, neuronal ceroid lipofuscinoses; PSEN, presenilin; PSENEN/PEN2: presenilin enhancer, gamma-secretase subunit; TAP, tandem affinity purification; TEV, tobacco etch virus; TF, transferrin; WB, Western blot; WT, wild type.

ARTICLE HISTORY
Received 14 June 2021
Revised 3 December 2021
Accepted 6 December 2021

KEYWORDS
Alzheimer disease; cln3 disease; γ-secretase; knockout cells; neuronal ceroid lipofuscinosis; transcription factor eb

Introduction

PSENEN/PEN2 (presenilin enhancer, gamma-secretase subunit) is the smallest subunit of the γ-secretase complex, an intramembrane protease that cleaves type-I transmembrane proteins within their transmembrane domains. γ-secretase is composed of four subunits, PSENEN, NCSTN (nicastrin), a variant of APH1 (aph-1 homolog, gamma-secretase subunit) and PSEN1 (presenilin 1) or PSEN2 (presenilin 2), which harbor the catalytic site [1–3]. All subunits of the γ-secretase complex are transmembrane proteins translated at the endoplasmic reticulum (ER), where the complex assembles [1]. PSENEN is the last subunit that joins the γ-secretase complex. It binds PSEN and facilitates its endoproteolysis, thereby conferring γ-secretase activity [2,3].

A large number of type-I transmembrane proteins serve as γ-secretase substrates, such as NOTCH1 and APP (amyloid precursor protein). Following sequential cleavage of APP by α- or BACE/β-secretase and γ-secretase, the proteolytic products – including amyloid-beta (Aβ) and the APP intracellular domain – are released extracellularly and intracellularly, respectively [4–6]. Mutations in components of the γ-secretase complex cause familial Alzheimer disease (AD) [7]. Most of these mutations result in an increase in the production of Aβ, which can accumulate in the brain and is thought as a primary cause of AD. Apart from the mutations

CONTACT Guido Hermey guido.hermey@zmnh.uni-hamburg.de Institute for Molecular and Cellular Cognition, Center for Molecular Neurobiology Hamburg, University Medical Center Hamburg-Eppendorf, 20251 Hamburg, Germany
[1]These authors contributed equally

causing AD, other mutations in *PSENEN, PSEN1* and *NCSTN* have been reported to cause *acne inversa*, a chronic inflammatory disease of hair follicles [8]. It has been suggested that the molecular pathogenesis implicates the γ-secretase-NOTCH pathway [8]. Upon cleavage by γ-secretase the NOTCH1 intracellular domain translocates to the nucleus, acts as a transcriptional activator and regulates cell fate [9]. Aside from APP and NOTCH1, γ-secretase cleaves a large number of other physiologically relevant substrates such as CDH1 (cadherin 1), the receptor tyrosine kinase ERBB4 and NGFR/p75NTR (nerve growth factor receptor), and signaling of these multiple proteolytic substrates are likely to be modulated by γ-secretase [10].

In addition to its proteolytic function, supplementary, γ-secretase independent, functions of PSENs in the autophagy-lysosome system have been proposed [11–14]. Cells co-express differing γ-secretase complexes, including either PSEN1 or PSEN2. PSEN1-containing complexes are broadly distributed in the cell, and several partially controversial studies suggest that PSEN1 regulates lysosomal function [11,15–19]. In contrast, PSEN2 harbors a lysosomal targeting signal and is targeted to late endosomes and lysosomes, but its lysosomal function is poorly described [20,21]. Moreover, lysosomal dysfunction has been implicated as a driver of increased amyloidogenic processing or incomplete Aβ degradation and may be one mechanism underlying sporadic AD [12,18]. Yet, PSENEN has not been studied in the context of macroautophagy (hereafter referred to as autophagy) and lysosomal function.

Here, we performed a tandem-affinity-purification (TAP)-tag screen to identify additional PSENEN interacting proteins. We found CLN3, a protein with six predicted transmembrane domains and the N and C termini facing the cytoplasm [22,23]. Mutations in CLN3 are causative for juvenile neuronal ceroid lipofuscinosis (JNCL) or CLN3 disease [24]. The disease belongs to the neuronal ceroid lipofuscinoses (NCLs), a group of rare lysosomal storage disorders considered the most common neurodegenerative disease in children characterized by gradual neurodegeneration. The age of disease onset differs between defined subtypes caused by mutations in different genes (*CLN1* to *CLN8; CLN10* to *CLN14*) [25,26]. The pathological hallmark is the intracellular accumulation of lysosomal autofluorescent storage material, so-called lipofuscin. These deposits are found in neurons and are as well abundant in non-neuronal cells outside the nervous system. Depending on the subtype, the storage material is either predominantly composed of ATP5MC (ATP synthase membrane subunit c) or the sphingolipid activator proteins A and D [23]. Further, the storage material can comprise to a different degree additional components such as the lysosomal proteins PPT1 (palmitoyl-protein thioesterase 1), TPP1 (tripeptidyl peptidase 1), and CTSD (cathepsin D) [27], and strikingly, accumulation of Aβ has been reported in some cases [28–30]. More recently, the examination of unexplained AD cases identified a genomic region directly upstream of the *CLN3* gene using genetic linkage analysis [31] and a missense variant in *CLN5* by whole-exome sequencing [32].

The classical juvenile form of NCL, JNCL or CLN3 disease, manifests mostly at the age of about six years in affected children with normal early development [25,26]. Clinical symptoms include progressive blindness, cognitive decline frequently accompanied by epileptic seizures, loss of motor function and a significantly reduced lifespan. JNCL is inherited in an autosomal recessive manner and about 60 different mutations in *CLN3* have been identified in affected individuals to date. The most frequent mutation, found in about 80% of disease chromosomes, is a 1.02 kb genomic deletion comprising exons 7 and 8, resulting in a frameshift in the coding sequence and a premature stop codon [23,33]. In mammals, CLN3 is ubiquitously expressed at a low level [24,34]. The low expression level, its hydrophobic nature and the unavailability of highly specific antibodies restricted analysis of CLN3 and so far, its function remains elusive. However, the protein presents a canonical functional lysosomal targeting motif, and prominent lysosomal localization seems most likely [34–39]. Studies from a CLN3 disease knock-in mouse model and from a resultant cell line suggest alterations in the endosomal and autophagy-lysosome system [40–42]. Other cellular studies support endosomal-lysosomal associated functions of CLN3 [43,44], altered lysosomal arginine transport in patient-derived lymphoblasts [45], and defects in Mannose-6-Phosphate receptor targeting after *CLN3* knockdown [46].

Here, we identified an interaction of PSENEN and CLN3 and demonstrated a co-distribution of transcripts as well as colocalization and cotransport of the proteins. We hypothesized that CLN3 modulates γ-secretase activity and that PSENEN and CLN3 play associated roles in the autophagy-lysosome system. To address these hypotheses, we generated isogenic *PSENEN*- and *CLN3*-deficient HeLa cell lines and confirmed impaired γ-secretase activity in the *PSENEN* knockout (KO) cells. In contrast, *CLN3* ablation did not alter γ-secretase activity to a significant degree. Additional phenotypic characterization revealed shared alterations in the autophagy-lysosome system of both KO cell lines.

Results

To identify PSENEN interaction partners, we performed a directed proteomic survey employing the tandem affinity purification (TAP) – tandem mass spectrometry methodology [47]. PSENEN was expressed with a C-terminal TAP-Tag in SK-N-BE neuroblastoma cells and subjected to tandem affinity purification, a procedure consisting of two specific binding and two specific elution steps under mild conditions, which preserve the integrity of protein-protein interactions. Affinity-purified complexes were resolved on SDS-PAGE, Coomassie-stained and co-purified proteins identified by peptide sequencing using tandem mass spectrometry. We identified CLN3 as an interaction partner and validated the interaction by co-immunoprecipitation (Figure 1A). We transfected HeLa cells with GFP-PSENEN and HA-CLN3 or GFP and HA-CLN3 and precipitated proteins with anti-GFP nanobodies. GFP-PSENEN co-precipitated HA-CLN3 whereas GFP alone was unproductive in this assay

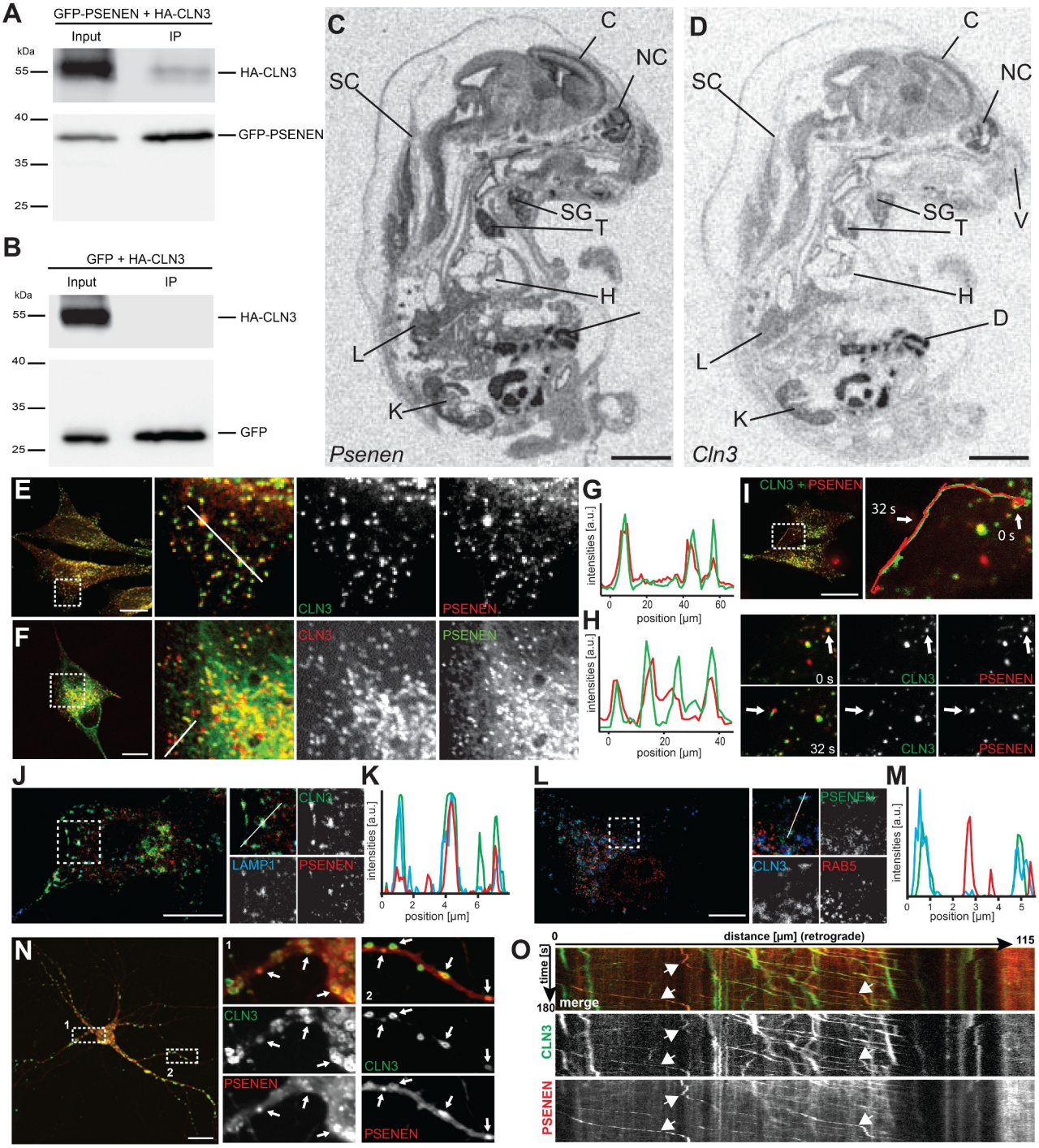

Figure 1. Interaction, co-expression and colocalization of PSENEN and CLN3. (A, B) Co-immunoprecipitation of GFP-PSENEN and HA-CLN3. GFP-PSENEN (A) or GFP (B) were co-expressed with HA-CLN3 in HeLa cells and immunoprecipitated with an anti-GFP antibody. HA-CLN3 was co-precipitated with GFP-PSENEN (**A**), but not with GFP alone (**B**). (C, D) Autoradiograms of parasagittal sections through embryonic mice at E16 hybridized with specific radiolabeled probes for *Psenen* (C) and *Cln3* (D) reveal similar expression patterns. (E, F) HeLa cells co-transfected with GFP-CLN3 (green) and tdTomato-PSENEN (red) (E) or with mCherry-CLN3 (red) and GFP-PSENEN (green) (F), were immunostained using respective antibodies and analyzed by confocal microscopy. Dotted boxes in the left panels indicate magnified areas shown in the right panels. Line plots (G, H) correspond to the white lines indicated in the merged zoom-ins in (**E**) and (**F**). (I) Tracking of GFP-CLN3- and tdTomato-PSENEN-positive endosomes in HeLa cells by time-lapse analysis using confocal spinning disk microscopy. The dotted box in the overview indicates the magnified area in which co-trafficking was analyzed. Single images below show initial position (0 s) and after tracking (32 s) of an endosome (arrows). (J, L) HeLa cells co-transfected with GFP-CLN3 and mCherry-PSENEN and immunostained using respective antibodies and an anti-LAMP1 antibody (J) or transfected with GFP-PSENEN and HA-CLN3 and immunostained using respective antibodies and an anti-RAB5 antibody (L). Dotted boxes in the left panels indicate magnified areas shown to the right. Line plots (K, M) correspond to the white lines indicated in the merged zoom-ins in (**J**) and (**L**). (N) Dissociated hippocampal neurons transfected with GFP-CLN3 (green) and tdTomato-PSENEN (red) immunostained at DIV10. Magnifications of a somatic (dotted box 1) and of a neuritic area (dotted box 2) are shown. Arrows point at areas of colocalization. (O) Time-lapse video microscopy analysis of dissociated hippocampal neurons (DIV 6) transfected with GFP-CLN3 (green) and tdTomato-PSENEN (red) imaged over 180 s. Kymographs show predominant retrograde movement of GFP-CLN3- and tdTomato-PSENEN-positive endosomes. Scale bars in (**C**) and (**D**): 2 mm; in (**E, F, I, J, L, N**): 20 µm. C, cerebral cortex; D, duodenum; H, heart; K, kidney; L, lung; NC, nasal cavity; SC, spinal cord; SG submandibular gland; T, thymus; V, vibrissae.

(Figure 1A, B). Next, we analyzed tissue expression of both genes and the subcellular localization and transport of the proteins to estimate the relevance of the observed interaction. An almost ubiquitous expression was detected in embryonic mice for *Psenen* and *Cln3* mRNA by *in situ* hybridization (Figure 1C, D). Both genes share the highest transcript levels in the gastrointestinal tract, kidney, liver, heart, thymus, and the central nervous system with prominent signals in the cerebral cortex and thalamic area. We expressed fluorophore-tagged versions of PSENEN and CLN3 in HeLa cells and in dissociated primary murine hippocampal neurons. In HeLa cells, both CLN3 and PSENEN localized to endosomal structures (Figure 1E-H). Furthermore, PSENEN and CLN3 colocalized to identical vesicles, and time-lapse video microscopy analysis demonstrated vesicular cotransport (Figure 1I and S1A). PSENEN- and CLN3-positive endosomes were to a large extend also positive for the late endosome-lysosome marker proteins LAMP1 and RAB7A, but only to a minor extend for the early endosomal marker protein RAB5A (Figure 1J-M and S1B). In neurites, PSENEN and CLN3 also colocalized to identical vesicles and the majority of PSENEN- and CLN3-positive vesicles showed a retrograde movement (Figure 1N, O). The interaction, co-expression, colocalization, and cotransport suggested an association of PSENEN and CLN3. We hypothesized that CLN3 modulates the proteolytic function of γ-secretase, because PSENEN is a subunit of the γ-secretase complex. In addition, we considered an associated role of PSENEN and CLN3 in the autophagy-lysosome system in which CLN3 is thought to play a role and PSENEN has not been studied yet.

In order to test these hypotheses, we generated *PSENEN*- as well as *CLN3*-deficient isogenic HeLa cell lines. Toward this end, we applied the CRISPR gene-editing approach and obtained independent isogenic HeLa knockout (KO) cell lines for *PSENEN* and *CLN3*. The introduced indel mutations resulted in frameshifts shortly after the start codons, leading to premature stop codons and the encoded truncated PSENEN and CLN3 proteins are most likely nonfunctional (Figure S2). We observed an unaltered morphology of the KO cells as compared to wild type cells. Proliferation of *CLN3* KO and *PSENEN* KO cells was moderately but significantly increased as compared to wild types (Figure S3).

It has been demonstrated before that PSENEN ablation impedes PSEN endoproteolytic activation, γ-secretase complex formation, and trafficking from the ER to the Golgi [2,48–50]. We analyzed the effect of PSENEN and CLN3 ablation on the intracellular localization of PSEN2 (Figure 2A). For immunocytochemical localization, we used an antibody that specifically detects the PSEN2 C-terminal fragment of proteolytically activated PSEN2 (PSEN2-CTF). In HeLa wild type and *CLN3* KO cells PSEN2-CTF is localized to endosomal structures, which are to a large extent positive for the late endosome-lysosome marker LAMP2. In contrast, employing the same PSEN2 antibody on *PSENEN* KO cells resulted in a weaker and diffuse staining (Figure 2A). We assessed the endoproteolytic processing of PSEN1 and PSEN2 by immunoblotting using C-terminal fragment specific antibodies. In wild type and *CLN3* KO cell lysates, the respective endoproteolytically-derived C-terminal fragments were detected (Figure 2B). These were absent in cell lysates from *PSENEN* KO cells suggesting a strong reduction or the complete loss of PSEN endoproteolytic activation (Figure 2B). Next, we generated tagged γ-secretase substrates to test if *CLN3* ablation impedes or alters γ-secretase activity. We transfected cells with a Notch-ΔE HA-tagged construct that serves as a substrate for γ-secretase without prior processing by α-secretase or BACE/β-secretase [51] (Figure 2C). In alternative experiments, we used a construct encoding full-length APP (APP-FL) with a C-terminal GFP-tag (Figure 2D). The APP-FL-GFP is first cleaved by α- or BACE/β-secretase. Subsequently, γ-secretase cleavage releases the C-terminal APP-intracellular domain (APP-ICD) into the cytosol (Figure 2D). Both constructs, NOTCH-ΔE-HA and APP-FL-GFP, were processed in wild type and *CLN3* KO cells by γ-secretase, because we detected in immunoblots tagged fragments corresponding in their size to the respective intracellular domains (ICDs) (Figure 2E, G). In lysates of *PSENEN* KO cells, these fragments were absent (Figure 2E, G). In addition, immunoblot analysis of APP-FL-GFP transfected cells revealed increased levels of a larger fragment corresponding to the expected size of the transmembrane stub in *PSENEN* KO cell lysates (Figure 2G). These results demonstrate, as expected, impaired γ-secretase activity in *PSENEN* KO cells. In rescue experiments, γ-secretase activity was restored in *PSENEN* KO cells by expression of GFP-PSENEN (Figure 2F) or expression of HA-PSENEN (Figure 2H). In view of these results obtained by overexpressing γ-secretase substrates, we next assessed the processing of endogenous APP. Endogenous sAPP-α levels were almost identical between the cell lines. We measured endogenous Aβ40 and Aβ42 levels in cell culture media of wild type and knockout cells. As expected, Aβ levels were markedly reduced in *PSENEN* KO cells, whereas in *CLN3* KO cells, total Aβ levels were not significantly altered as compared to wild type cells (Figure 2I). Taken together, these experiments substantiate highly reduced or absent PSEN endoproteolytic processing and γ-secretase activity in *PSENEN* KO cells and corroborate studies by others demonstrating that PSENEN is indispensable for γ-secretase activity. In addition, the rescue experiments confirm the specificity of the *PSENEN* KO. Conversely, PSEN endoproteolytic processing and γ-secretase activity were not altered in *CLN3* KO cells strongly suggesting that CLN3 is dispensable for γ-secretase function and does not modulate its activity to a significant degree.

We reasoned that both proteins might play cooperative or converging roles in the autophagy-lysosome system. To assess lysosomal function, we compared the lysosomal-proteolytic activity of the KO cells and wild types. First, the activity of the lysosomal enzyme HEXA/β-hexosaminidase A was determined in whole cell lysates. Equal amounts of total protein from each lysate were incubated with the artificial HEXA substrate 4-nitrophenyl-N-acetyl-β-D-glucosaminide and the yield of substrate conversion to 4-nitrophenol was analyzed by spectrophotometry. As compared to wild types HEXA activity was significantly reduced in *CLN3* KO and *PSENEN* KO cells (Figure 3A). Next, we loaded cells with fluorescently labeled self-quenched polymeric bovine serum albumin (dye-quenched BSA, DQ-BSA). Upon uptake by endocytosis DQ-

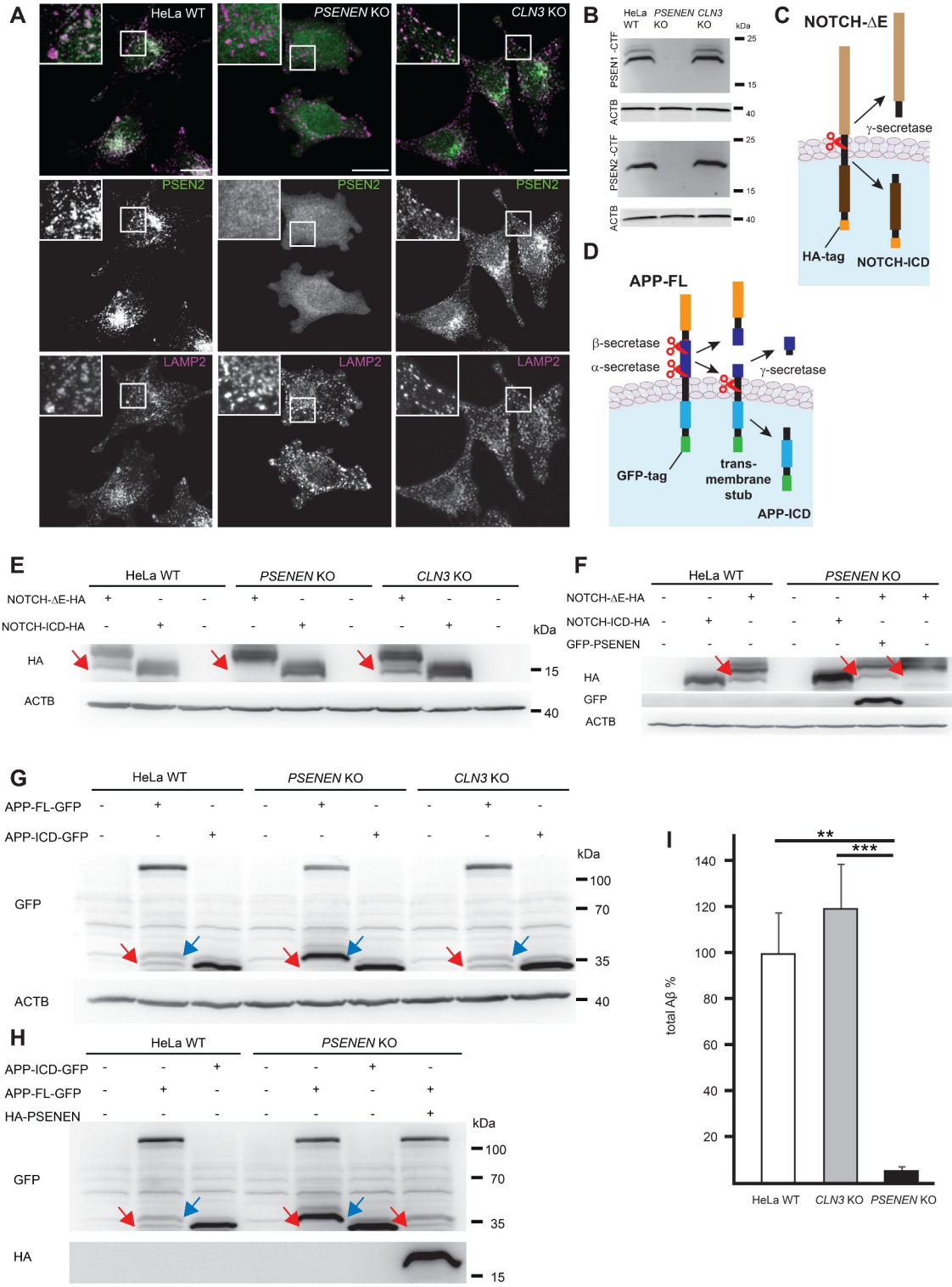

Figure 2. Impeded γ-secretase processing in *PSENEN* KO cells, but not in *CLN3* KO cells. (A) Immunocytochemical localization of PSEN2 using an antibody specific for the processed C-terminal fragment (CTF) of PSEN2 (green) and an antibody against LAMP2 (magenta) in HeLa wild type (WT), *PSENEN* KO and *CLN3* KO cells. Scale bars: 20 µm. (B) Detection of processed PSEN1 and PSEN2 in cell lysates using CTF specific antibodies. The CTFs are not detectable on immunoblots of *PSENEN* KO cell lysates indicating that PSENs are not processed. ACTB/β-actin immunoblotting was performed to control equal loading. (C) Illustration of the HA-tagged NOTCH-ΔE construct which serves as a substrate for γ-secretase without prior processing by other secretases. (D) Illustration of the GFP-tagged APP-full length (APP-FL) construct processed by α- or BACE/β-secretase before the remaining transmembrane stub is cleaved by γ-secretase and the intracellular domain (ICD) is released. (E) Analysis of cleavage products by immunoblotting. NOTCH-ICD-HA was transfected to estimate the size of the cleaved ICD. The NOTCH-ICD band is absent in *PSENEN* KO cell lysates expressing NOTCH-ΔE, but present in both WT and *CLN3* KO cell lysates (red arrows). (F) Expression of GFP-PSENEN restores γ-secretase activity in *PSENEN* KO cells. Note the presence of the NOTCH-ICD band (red arrows) in GFP-PSENEN transfectants. (G) Immunoblot analysis of APP-FL-GFP transfected cells. The band corresponding to the APP-ICD-GFP fragment is present in WT and *CLN3* KO cell lysates (red arrow). In contrast, this band is absent in *PSENEN* KO cell lysates, but levels of a larger fragment corresponding to the expected size of the transmembrane stub (blue arrows) are increased. (H) Expression of HA-PSENEN restores γ-secretase activity in *PSENEN* KO cells. Note, the presence of the APP-ICD-GFP band (red arrows) and the reduction of the band corresponding to the transmembrane stub (blue arrows) in HA-PSENEN transfectants. (I) Quantification of secreted total Aβ (Aβ40 and Aβ42) by ELISA. Aβ levels were normalized to sAPP-α levels. Data represent mean ± standard deviation (SD), one-way ANOVA p-values, **$p < 0.001$; ***$p < 0.0001$.

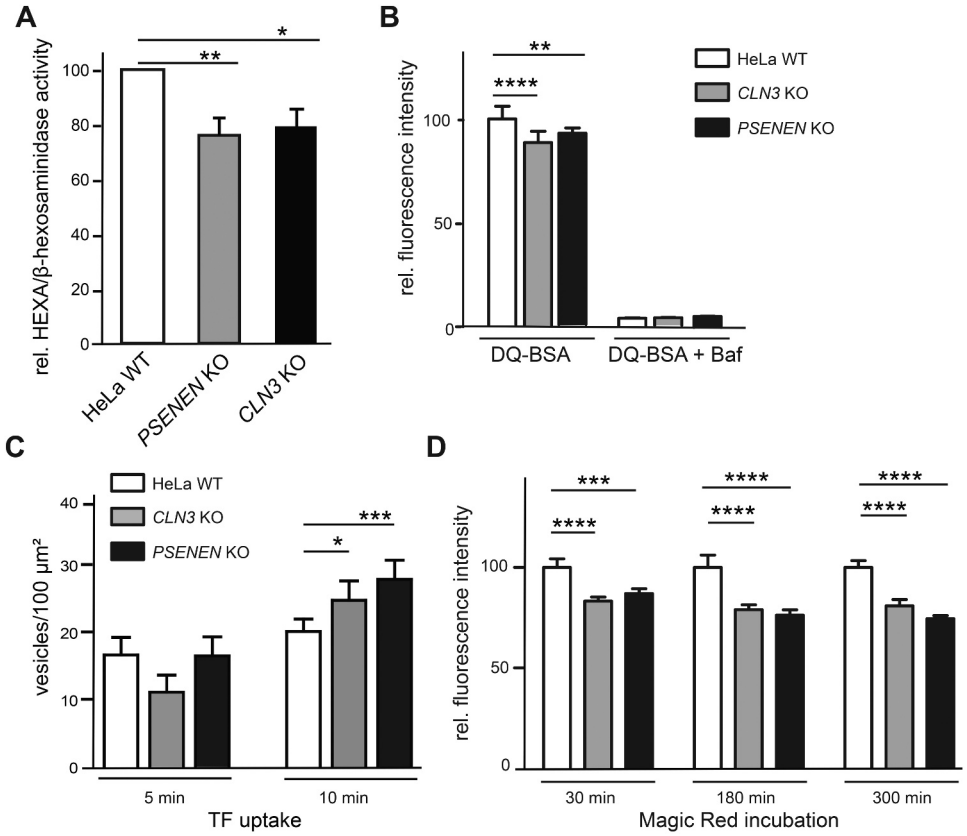

Figure 3. Ablation of *PSENEN* and *CLN3* reduces lysosomal proteolytic activity. (A) Relative activity of HEXA/β-hexosaminidase A in extracts of HeLa WT, *PSENEN* KO, *CLN3* KO cells. Data represent mean ± SD, one-way ANOVA p-values, *p < 0.05; **p < 0.001. (B) Decreased lysosomal capacity assessed through the DQ-BSA assay. Relative fluorescence intensity after 6 h incubation, with and without 100 nM bafilomycin A_1 (Baf) is shown. Data represent mean ± SD; two-way ANOVA p-values, **p < 0.001; ***p < 0.0001. (C) Quantification of TF uptake. Plots represent TF-Alexa Fluor 555-positive vesicles per 100 μm^2 after 5 and 10 min uptake. Data represent mean ± SD; two-way ANOVA p-values, *p < 0.05; ***p < 0.0001. (D) Lysosomal CTSB enzyme activity in HeLa WT, *PSENEN* KO, *CLN3* KO cells. Plots represent fluorescence intensity after 30 min, 180 min and 300 min of Magic Red incubation. Data represent mean ± SD; two-way ANOVA p-values, ***p < 0.0001; ****p < 0.00001.

BSA accumulates in lysosomes. As DQ-BSA enters these acidic compartments, proteases cleave the polypeptide and generate fluorescent peptide fragments. The rate of the released fluorescence increases proportionally to the activity of the lysosomal proteases. A lower rate of DQ-BSA hydrolysis suggests a decrease in the activity of lysosomal proteases *in situ*. Fluorescence intensity was monitored and compared in the presence or absence of bafilomycin A_1. Bafilomycin A_1 is inhibiting vacuolar-type H^+-ATPase (V-ATPase)-dependent acidification of lysosomes. A significant reduction of fluorescence intensity was detected in *CLN3* KO and *PSENEN* KO cells as compared to WT cells (Figure 3B and S4A). Pre-incubation with bafilomycin A_1 resulted in a distinct decrease of fluorescence signals in all investigated cell lines. To exclude that the DQ-BSA results were obscured by differential endocytic uptake by the KO versus wild type cells, we performed a TF (transferrin)-uptake experiment. Cells were labeled on ice with TF conjugated to a fluorescent dye. After washing, cells were incubated at 37°C for different time points and fluorescent vesicles were determined. TF uptake was comparable after 5 minutes and slightly increased after 10 min in the two KO cell lines as compared to wild types confirming that endocytic uptake rates were not a limiting factor (Figure 3C and S4B). In addition, we engaged the Magic Red Cathepsin B assay. This fluorescence based live cell assay employs a cell membrane permeant substrate and, therefore, cannot be affected by possible differential endocytosis rates. The substrate is cleaved upon cathepsin enzyme activity in lysosomes and results in a fluorescent signal. Fluorescence intensity was monitored and compared at three time points, after 30 min, 180 min and 300 min substrate incubation. *CLN3* KO and *PSENEN* KO cells showed significantly lower fluorescence intensities as compared to isogenic wild types for all three incubation times (Figure 3D and S4C). Taken together, three assays independently confirmed a decreased lysosomal activity in both KO cell lines.

To further investigate the impact of *PSENEN* or *CLN3* ablation on the endosomal-lysosomal system, we assessed changes in the subcellular localization of endosomal markers in KO and wild type cells. To this end, we analyzed the relative overlap of the late endosomal/lysosomal proteins LAMP1 and LAMP2 with the early endosomal marker protein RAB5 and the retromer subunit VPS35 which is crucial for retrieval and recycling from early endosomes to the trans Golgi network or the plasma membrane. In all cell types, RAB5 or VPS35 displayed no enhanced localization to LAMP1- or LAMP2-positive structures under control conditions or after starvation (Figure 4A and S5). RAB9 has been involved in retrograde transport from late endosomes to

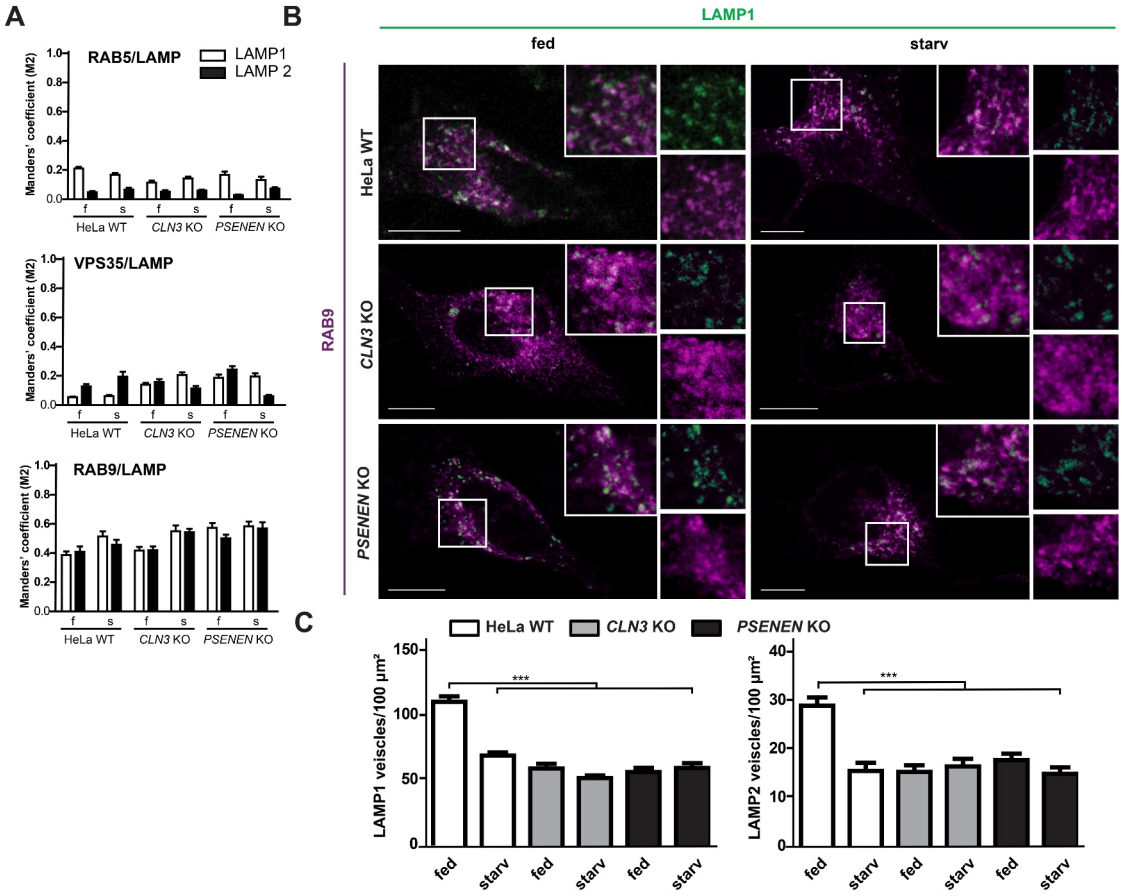

Figure 4. Ablation of *PSENEN* and *CLN3* reduces the number of lysosomes. (A) Plots show the Manders' coefficient of LAMP1 or LAMP2 immunocytochemical co-localization with RAB5, VPS35 and RAB9 in fed HeLa WT, *CLN3* KO, *PSENEN* KO cells and after 6 h starvation (S). Values are means ± SD of n = 50 cells pooled from three different experiments. (B) Representative confocal images of LAMP1 (green) and RAB9 (magenta) immunocytochemical localization in fed HeLa WT, *CLN3* KO, *PSENEN* KO cells and after 6 h starvation (starv). Scale bars: 10 µm. (C) Plots represent LAMP1- and LAMP2-positive vesicles per 100 µm^2. Values are means ± SD of n = 50 cells pooled from three different experiments; one-way ANOVA p-values, ***p < 0.0001.

lysosomes, in the targeting of lysosomal enzymes and mannose-6-phosphate receptors and is suggested to play a role in autophagosome biogenesis [52]. In fed wild type cells we observed colocalization of RAB9 with LAMP1 and LAMP2. This was slightly increased in starved cells. In *PSENEN* KO cells and in *CLN3* KO cells, localization of RAB9 to LAMP1- and LAMP2-positive vesicles was further increased after starvation, suggesting minor alterations in Golgi to late endosome-lysosome compartmentalization (Figure 4A, B). Quantification of LAMP1- and LAMP2-stained vesicles revealed a significantly reduced number in starved wild type cells as compared to fed cells (Figure 4C). We observed already in fed *PSENEN* KO and *CLN3* KO cells a reduction of LAMP1- and LAMP2-positive vesicles to the same degree as shown in starved wild type cells (Figure 4C). After starvation, the number of LAMP1- and LAMP2-stained endosomes was not further decreased in the KO cells (Figure 4C). Taken together, these experiments demonstrate reduced lysosomal proteolytic activity and a reduced number of late endosomes-lysosomes in both KO cell lines.

We assessed as well the localization of the autophagosome marker LC3 to LAMP1- and LAMP2-positive structures. In all 3 cell lines we observed only minor localization of LC3 to LAMP1- and LAMP2-positive vesicles under control (fed) conditions (Figure 5A and S6). Starvation moderately expanded the localization of LC3 to these structures. This was even more evident after treatment with the lysosomotropic chemical ammonium chloride (NH_4Cl) that neutralizes lysosomal pH, prevents the fusion of autophagosomes with lysosomes and promotes aggregation of autophagosomes (Figure 5A and S6). However, these immunocytochemical analyses did not reveal obvious differences between the cell lines. Subsequently, we employed immunoblotting to monitor LC3 levels. LC3 is a microtubule-associated protein playing an important role in autophagosome formation. After initial synthesis, LC3 is proteolytically processed, named LC3-I, and finally lipidated, named LC3-II. The latter is associated with autophagosomal membranes and detectable by immunoblotting [53]. To assess alterations of LC3-II levels in the isogenic cell lines, we quantified these in immunoblots of cell lysates. Control cells were compared with cells treated with NH_4Cl alone or together with lysosomal inhibitors. We already observed a small increase of the LC3-II:ACTB/β-actin ratio in *PSENEN* KO and *CLN3* KO cells as compared to wild types under control conditions (Figure 5B,C). This difference was more pronounced after the addition of NH_4Cl alone or in combination with the lysosomal protease inhibitors E64d and pepstatin A (Figure 5B,C). In independent experiments, we

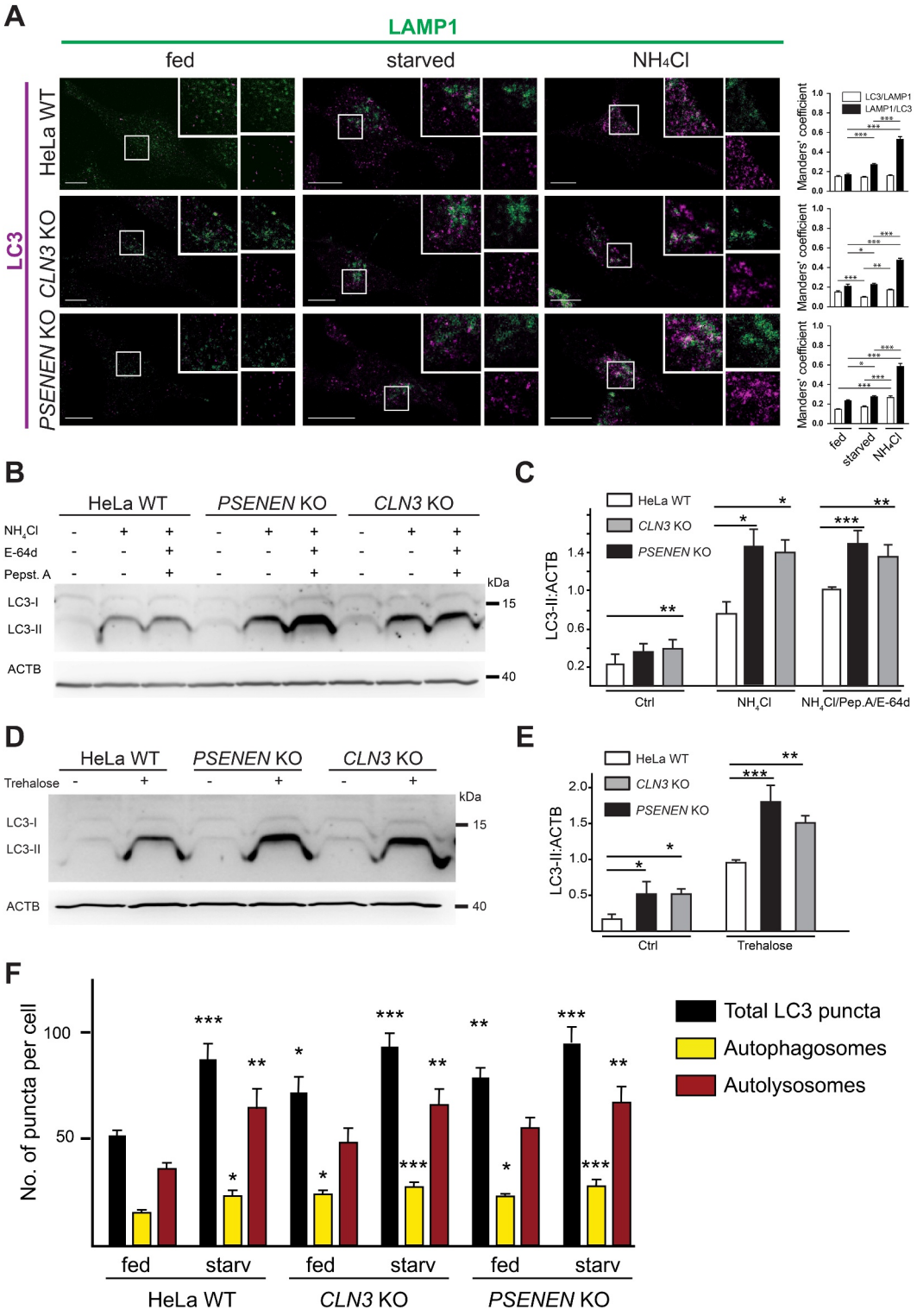

Figure 5. Altered LC3-II levels and autophagy induction in *PSENEN* KO and *CLN3* KO cells. (A) Representative confocal images of LAMP1 (green) and LC3 (magenta) immunocytochemical localization in fed HeLa WT, *CLN3* KO, *PSENEN* KO cells, 6 h after starvation or 6 h after NH_4Cl treatment. Scale bars: 10 µm. Plots on the right show respective Manders' coefficient of LAMP1 and LC3 co-localization. Values are means ± SD of n = 50 cells pooled from three different experiments. (B) Representative immunoblot analysis of endogenous LC3 (LC3-I and -II) and ACTB under control conditions or after NH_4Cl alone or together with lysosomal inhibitor treatment for 6 h. (C) Densiometric analysis of LC3-II band intensity normalized to ACTB. Values are means ± SD of n = 10 independent experiments; one-way ANOVA with Dunnett's post hoc test. (D) Representative immunoblot analysis of endogenous LC3 (LC3-I and -II) and ACTB under control conditions or 24 h after trehalose treatment. (E) Densiometric analysis of LC3-II band intensity normalized to ACTB. Values are means ± SD of n = 7 independent experiments; one-way ANOVA with a Dunnett's post hoc test. (F) HeLa WT, *CLN3* KO or *PSENEN* KO cells were transfected with a mCherry-GFP-LC3 construct, cultured under control conditions (fed) or starved for 6 h in EBSS (starv) and analyzed by live confocal microscopy. The plots show the quantification of total LC3-positive puncta (black), the number of autophagosomes (spots positive for GFP and positive for mCherry) (yellow) and number of autolysosomes (spots negative for GFP and positive for mCherry) (red). Values are means ± SD of n = 3 independent experiments. Total numbers of LC3 puncta per cell, autophagosomes per cell and autolysosomes per cell in starved WT cells and in fed or starved KO cells were compared to the respective numbers in fed WT cells. p-Values were calculated using one-way ANOVA with a post hoc Tukey test, *p < 0.05; **p < 0.001; ***p < 0.0001.

applied trehalose, which is regarded as a mTORC1-independent autophagy enhancer [53]. Consistently, we also observed under control conditions a small increase of the LC3-II:ACTB ratio in *PSENEN* KO and *CLN3* KO cells. Trehalose treatment further increased the LC3-II:ACTB ratio (Figure 5D,E). Collectively these data suggested increased autophagosome levels in the KO cells. These could be caused by a block of the autophagic flux due to hampered lysosome-autophagosome fusion or by enhanced autophagosome biogenesis.

To assess the autophagosome-lysosome fusion, cells were transfected with a tandem fluorophore-tagged LC3 expression construct and analyzed by confocal live microscopy. LC3-II fused to both GFP and mCherry is detectable as green and red puncta at the autophagosome membrane. Upon fusion of autophagosomes with acidic lysosomes, the acid sensitive fluorescent GFP signal is quenched by low pH, whereas the acid insensitive mCherry signal is still detectable until final degradation in autolysosomes. This change in fluorescence allows visualization of the autophagic flux. The total number of LC3-II-positive puncta significantly increased in wild types after starvation (Figure 5F). In both knockout cells, the total number of LC3-II-positive puncta was already increased to a similar degree under fed conditions and further raised by starvation (Figure 5F). The increased total LC3-II puncta, which corresponds to increased LC3-II levels, observed after expression of the tandem fluorophore-tagged LC3 construct in the KO cells compared to wild types is in accordance with the elevated endogenous LC3-II levels detected in immunoblots (Figure 5B-E). As compared to fed cells, wild type cells exhibited increased levels of autophagosomes (yellow, overlay of red, mCherry, and green, GFP, puncta) and autolysosomes (red puncta) after 6 h starvation (Figure 5F and S7). Already in fed KO cells, the number of autophagosomes and autolysosomes was elevated compared to wild type cells and further increased by starvation (Figure 5F). In all three cell types, the number of autolysosomes was higher than the number of autophagosomes and both increased after starvation. This strongly suggests a functional fusion of autophagosomes and lysosomes in all cell types.

In summary, these observations demonstrate an increased number of autophagosomes and an increased fusion of autophagosomes and lysosomes in the KO cells. This prompted us to investigate altered lysosome and autophagosome biogenesis on the transcriptional level. The expression of lysosomal and autophagic genes in response to pathways sensing lysosomal stress and nutritional conditions is coordinated to a large extent by TFEB (transcription factor EB) [54]. To assess the altered transcription of lysosomal/autophagy genes by TFEB, we monitored the expression of a number of TFEB target genes and genes encoding lysosomal proteins under control conditions and 2 h, 4 h, 6 h, or 8 h after starvation by quantitative real-time PCR (RT-qPCR) (Figure 6). In this expression analysis, we included the knocked-out genes *CLN3* and *PSENEN*. In the knockout cells, the non-coding transcripts of the respective knocked-out genes (Figure S2) were detected, but their expression was markedly reduced (Figure 6). In *CLN3* KO cells, *PSENEN* transcript levels were almost unchanged, but slightly induced 2 and 4 h after starvation. In *PSENEN*-KO cells, *CLN3* expression was moderately but constantly upregulated at all analyzed time points. *PSEN2* expression was increased in *PSENEN* KO cells with strongest induction after 4 h starvation. TFEB expression was upregulated in fed and starved *CLN3* KO cells with maximal expression 4 h after starvation. This expression peak was shared by *PSENEN* KO cells. Transcript levels of other lysosomal proteins such as CTSB (cathepsin B) and CTSD (cathepsin B), GLB1/β-galactosidase (galactosidase beta 1), PSAP (prosaposin), and TPP1, as well as SESN2 (sestrin 2) were upregulated in fed and starved *PSENEN* KO cells. In *CLN3* KO cells these transcript levels were not always altered, but in most cases upregulated after 4 h starvation. These results demonstrate an overall increased expression of TFEB targets (*CTSB, CTSD, GLB1, PSAP, TPP1*) and of *TFEB* itself in fed and starved *PSENEN* KO. Notably, expression of *SESN2*, which is not regarded as a TFEB target [55], was induced similarly and suggested the involvement of additional factors. In fed and starved *CLN3* KO cells, however, *TFEB* expression was upregulated and transcript levels of some lysosomal genes were increased after 4 h starvation. Since both knockouts affected expression of *TFEB* or TFEB regulated target genes, we investigated TFEB in more detail. TFEB localizes to the cytosol. Upon activation, it translocates to the nucleus and initiates gene expression. Next, we assessed altered nuclear versus cytosolic localization of TFEB by immunocytochemistry. Nuclear localization was slightly increased in fed KO cells as compared to wild types and this difference was more pronounced after 2 h and 4 h starvation (Figure 7). However, after 6 h starvation a comparable nuclear localization of TFEB was observed in wild type and KO cells (Figure 7 and S8). Finally, we analyzed TFEB protein levels by immunoblotting and observed increased TFEB levels in both KO cell lines (Figure 8A). Starvation induces dephosphorylation of TFEB, which corresponds to a reduced molecular weight observed in immunoblots (Figure 8A). Stable expression of GFP-PSENEN in *PSENEN* KO cells and of CLN3 in *CLN3* KO cells, respectively, reversed the increased TFEB levels (Figure 8B,C). Taken together, these analyses demonstrate increased TFEB levels following *PSENEN* as well as *CLN3* ablation and strongly suggest altered activity of TFEB in the analyzed *PSENEN* KO and *CLN3* KO HeLa cell lines.

Discussion

We identified an interaction of PSENEN and CLN3 and demonstrated co-expression, colocalization, and endosomal cotransport of both proteins. Mutations in the respective genes are causative for different neurodegenerative diseases, AD and CLN3 disease. Therefore, understanding the shared cellular function of both proteins might be pertinent for understanding general cellular mechanisms underlying neurodegenerative diseases. To investigate the relation of PSENEN and CLN3 on a cellular level, we generated isogenic knockout HeLa cell lines.

PSENEN is a subunit of the γ-secretase complex. Accordingly, we hypothesized that CLN3 might alter γ-secretase function and studied γ-secretase mediated processing in the KO cells. In accordance with previous

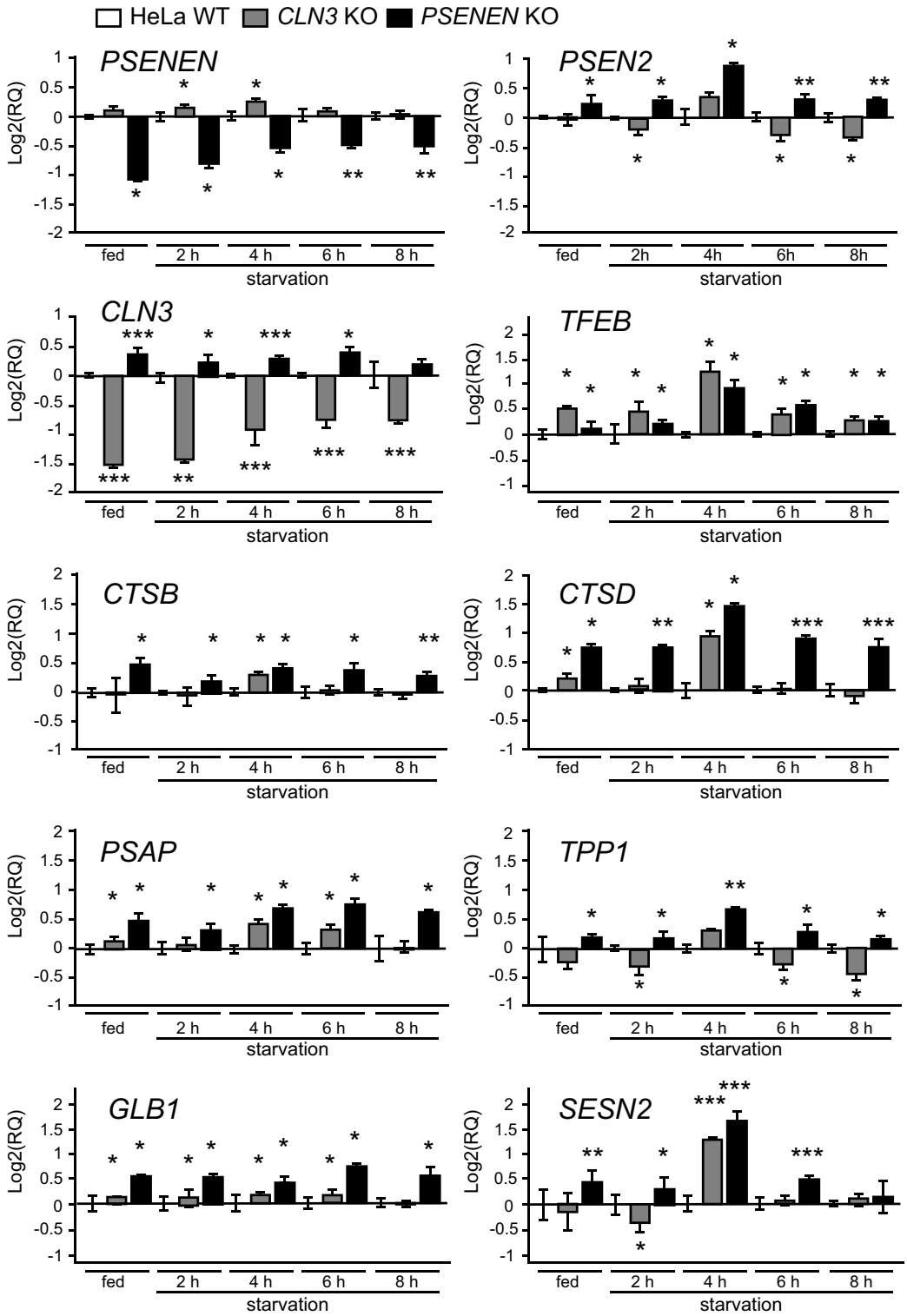

Figure 6. Gene expression analysis of *PSENEN* KO and *CLN3* KO cells. *APRT*-normalized mRNA changes under control conditions (fed) and 2 h, 4 h, 6 h and 8 h after starvation analyzed by real-time qPCR. Changes were normalized to wild type cells. The experiment was repeated with *HPRT*-normalization and similar results obtained. RQ, mean expression level; mean ± SD. p-Values were calculated using REST©-software, *p < 0.05; **p < 0.001; ***p < 0.0001.

studies, we demonstrate that PSENEN is essential for forming a functional γ-secretase complex and is indispensable for γ-secretase activity. Whereas the knockout of *Psenen* in mice results in an embryonic lethal phenotype [50], its ablation appears not per se mortal on a cellular level. This corroborates the notion that inhibition or knockout of γ-secretase does not generally lead to toxicity in cell culture, suggesting that general removal of protein stubs is not essential or that other means of removal exist [7].

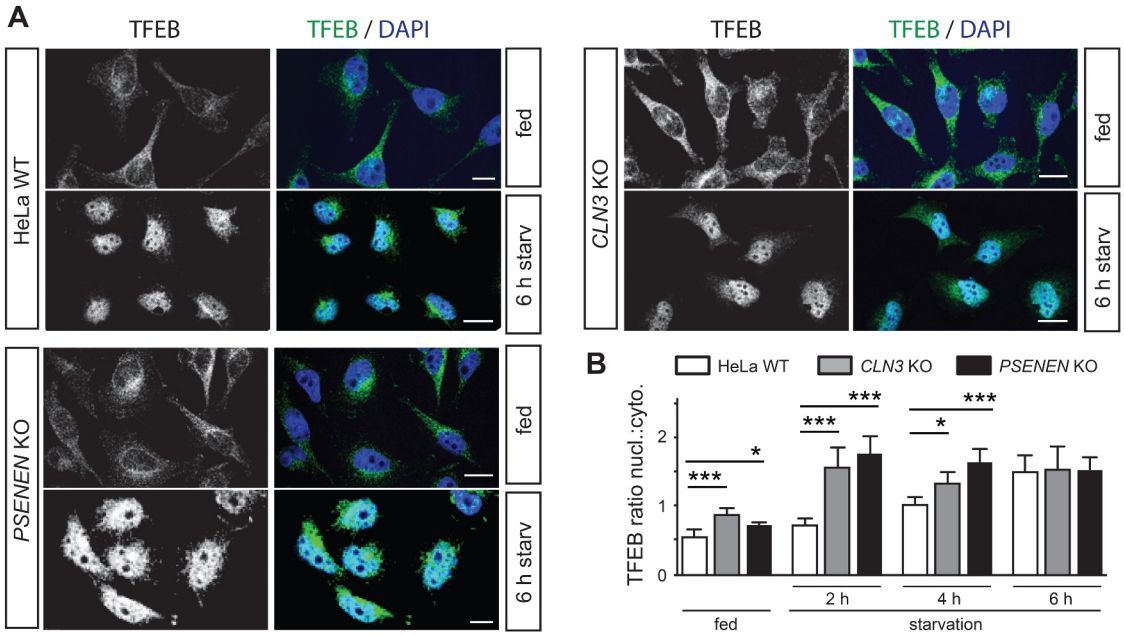

Figure 7. Accelerated TFEB nuclear translocation in *PSENEN* KO and *CLN3* KO cells. (A) Images of TFEB (green) immunolocalization in HeLa WT, *CLN3* KO and *PSENEN* KO cells under control conditions (fed) and 6 h after starvation (6 h starv). DAPI (blue) was used to label nuclei. Scale bars: 10 µm. (B) Plots show the TFEB nuclear to cytosolic ratio under control conditions and 2 h, 4 h and 6 h after starvation. Values are means ± SD of n = 20 cells pooled from three independent experiments, one-way ANOVA with a post hoc Tukey test *p < 0.05; ***p < 0.0001.

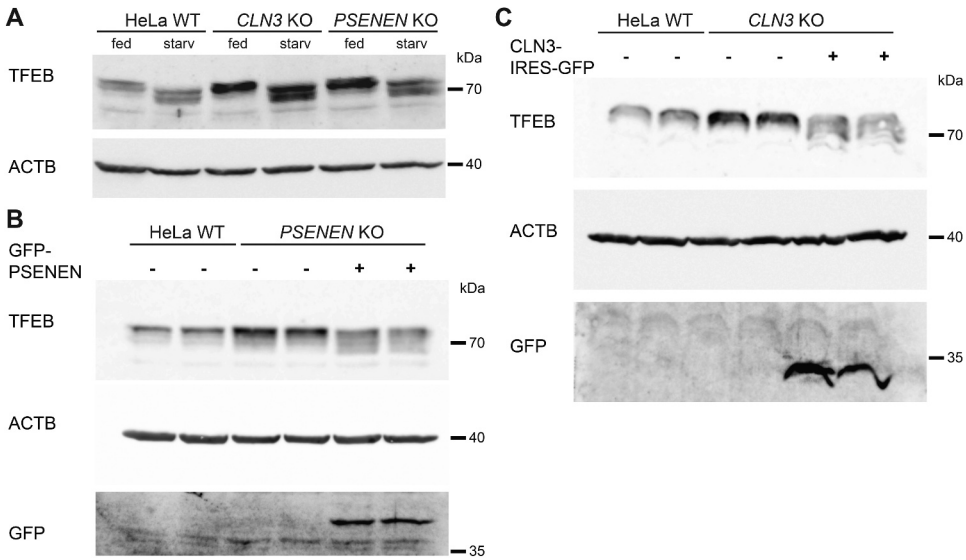

Figure 8. Increased TFEB levels in *PSENEN* KO and *CLN3* KO cells. (A) Immunoblot analysis of TFEB in HeLa wild type (WT), *CLN3* KO and *PSENEN* KO cells under control conditions (fed) and after 3 h starvation (starv). ACTB levels are shown as loading controls. (B) Elevated TFEB levels under control conditions in *PSENEN* KO cells were reduced to wild type levels when stably transfected with GFP-PSENEN. Stable GFP-PSENEN expression was confirmed using anti-GFP antibody. Two independent cell clones were analyzed. (C) Elevated TFEB levels under control conditions in *CLN3* KO cells were reduced to wild type levels when stably transfected with CLN3. Stable expression of the CLN3-IRES-GFP construct was confirmed by anti-GFP antibody and by sequencing of RT-PCR-amplified *CLN3* transcripts. Two independent cell clones were analyzed.

We provide strong evidence that, in contrast to PSENEN, CLN3 is dispensable for γ-secretase function and does not modulate its activity to a significant degree. This implies that some of the previously described similarities in AD and CLN3 disease pathology, such as the accumulation of Aβ, are not a direct consequence of *CLN3* ablation. We cannot exclude a dominant negative role of CLN3 mutants in altering γ-secretase function. This seems, however, unlikely as the most prevalent mutation found in CLN3 disease is regarded as a functional ablation of the CLN3 protein that, if expressed at all, is retained in the ER [34,56–58].

In agreement with its role in a lysosomal storage disease and its assumed subcellular localization, previous studies demonstrated alterations in the autophagy-lysosome system upon *CLN3* ablation. A recent study employed siRNA-mediated knock down of CLN3 and observed enhanced autophagosome biogenesis and autophagic flux [59]. In accordance with our results, this study suggests functional

lysosome and autophagosome fusion in *CLN3* ablated cells and not its impairment as described for a number of lysosomal storage diseases. Moreover, the authors proposed an enhancement of the autophagy-lysosome system as a compensatory stress response to impaired energy metabolism upon *CLN3* deficiency [59]. The upregulation of *TFEB* transcripts and an increase of *CTSB, CTSD, PSAP, TPP1* expression observed here after starvation in *CLN3* KO HeLa cells also suggests a compensatory mechanism to cope with a metabolic deficit caused by the absence of CLN3 in lysosomes.

To investigate CLN3 function, three different knockout and knock-in mouse models have been generated [60–62]. All three models resemble a number of phenotypic and histopathological abnormalities of the human CLN3 disease, including the accumulation of storage material predominantly composed of ATP5MC/subunit c of the mitochondrial ATP synthase. Therefore, a *CLN3* knockout is regarded as a disease model.

The so far most frequently used cellular model for CLN3 disease is a cerebellar neuronal precursor cell line (CbCln3 delta ex7/8 cells) derived from a CLN3 disease knock-in mouse [62]. These cells accumulate storage material, ATP5MC, in enlarged lysosomes [41,42]. This occurred in confluent cells, but not under sub-confluent conditions [42]. Moreover, under sub-confluent conditions the number of lysosomes was reduced [63], whereas the number of autophagosomes was increased [64]. The observations in sub-confluent cells corroborate our results in HeLa *CLN3* KO cells, reduced number of lysosomes and increased numbers of autophagosomes. Notably, we failed to observe the accumulation of storage material in HeLa *CLN3* KO cells when we analyzed ATP5MC levels at steady state and after cell cycle arrest. Thus, it is tempting to speculate that the here generated HeLa *CLN3* KO cells correspond to cells that are still capable adapting to several of the gene ablation-initiated defects before developing disease-like cytopathology. The observed increased TFEB levels might counteract disease-like progression, such as the accumulation of storage material.

TFEB coordinates the expression of lysosomal and autophagic genes in response to pathways sensing lysosomal stress and nutritional conditions. Thus, the identified increased autophagosome and autolysosome levels are in accordance with increased TFEB levels. In line with these assumptions, increased TFEB levels have been shown to induce lysosomal exocytosis and to rescue pathologic intracellular storage [65]. A pharmacological activation of TFEB reversed some of the phenotypes in CLN3 disease mouse models [66]. Notably, TFEB activation has been suggested as a possible strategy to counteract disease progression in a broader range of neurodegenerative diseases [54] and mice with neuronal-targeted TFEB are characterized by reduced levels of amyloid-β peptides and amyloid plaques [67].

It is conceivable, that the here studied HeLa cells are less prone to accumulate storage material. Therefore, further studies employing more differentiated cells that possess a highly active lysosomal compartment or non-dividing cells which might more likely accumulate storage material should be used to substantiate to what extend increased TFEB levels and other factors ameliorate pathological phenotypes on a cellular level.

A structure-based prediction in combination with additional functional clues supports the here identified interaction of PSENEN and CLN3 [68] and was specified in the integrated interactions database [69]. CLN3 has been shown to play a role in the lysosome-autophagy system before. Therefore, and irrespective of the nature of the PSENEN and CLN3 interaction, which may be transient or part of a larger complex, we speculated that PSENEN plays also a role in the lysosome-autophagy system and ablation of both proteins might result in concordant cellular phenotypes.

To the best of our knowledge, this is the first study considering PSENEN function in the endosomal-lysosomal-autophagy system, and the observed consequences of *PSENEN* ablation have not been described before. In contrast to the difference in γ-secretase function, *PSENEN* KO and *CLN3* KO cells presented indeed to a large extend corresponding alterations in our analyses. We observed in both KO cells a reduced activity of lysosomal enzymes, a reduced number of late endosomes and lysosomes, an increased number of autophagosomes and autolysosomes, and increased TFEB levels.

The autophagic flux includes autophagosome-lysosome fusion and (auto-) lysosomal degradation. Our data suggest functional and increased autophagosome-lysosome fusion in *PSENEN* KO and *CLN3* KO cells, whereas the lysosomal degradation appears reduced. The observed increased autophagosome-lysosome fusion might consume a large number of lysosomes. Along with a shortage of lysosomal degradation, lysosome recycling, or biogenesis, this might be causative for the reduced number of late endosomes and lysosomes in the KO cells.

CLN3 transcript levels were increased in *PSENEN* KO cells. This finding supports a possible compensatory upregulation of transcripts following the ablation of an interaction partner. However, *PSENEN* KO cells demonstrated increased expression of several lysosomal genes and *CLN3* induction might also be part of a general induction of lysosomal genes in *PSENEN* KO cells.

Taken together, on the cellular level the *PSENEN* KO resembles to a large extend the cellular phenotype of a knockout of the lysosomal storage disease gene *CLN3*. Autophagy impairment is commonly implicated in the pathological characteristics of AD [12]. PSENEN is a subunit of the γ-secretase complex. PSEN2 harbors a lysosomal targeting signal [21], and γ-secretase complexes including PSEN2 are targeted to lysosomes [20,21]. So far, functions in the autophagy-lysosome system have been proposed particularly for PSEN1, but how PSEN1 regulates lysosomal function remains controversial [11,15–19]. However, pharmacological γ-secretase inhibition did not alter lysosome-autophagy functions to a similar degree, suggesting that these alterations are independent of γ-secretase activity [11]. The here studied *PSENEN* knockout impairs the formation of all γ-secretase complexes, similar to a double knockout of *PSEN1* and *PSEN2* (*PSEN* dKO). Therefore, a phenotypic overlap between *PSENEN* KO and *PSEN* dKO cells is expected. Phenotypic differences might point to γ-secretase complex independent

functions of PSENEN or of PSENs. Analyses of *psen* dKO embryonic stem cells and *psen* dKO mice derived embryonic fibroblasts demonstrated increased and decreased LC3-II levels [11,19,70]. Moreover, increased TFEB protein levels, reduced nuclear translocation of TFEB after starvation and a reduced expression of TFEB target genes have been described [70]. Although some of these observations are inconsistent, a partial phenotypic overlap, such as increased LC3-II and TFEB levels, in *PSENEN* KO and *PSEN* dKO cells seems likely. However, clarification of a putative function of γ-secretase in the autophagy-lysosome system, that is independent of substrate cleavage, clearly requires additional studies on the individual γ-secretase components.

In summary, the identical alterations observed in the isogenic *PSENEN* KO and *CLN3* KO cells support γ-secretase independent function of PSENEN in the autophagy-lysosome system and our results point to dysfunctions in the autophagy-lysosome system that might in general be causative for different neurodegenerative diseases.

Materials and methods

Antibodies

The following primary antibodies were used: ACTB/β-actin (Sigma, A5441; Western blot [WB] 1:100.000); DS-red (Clontech, 632,496; immunocytochemistry [ICC], 1:500); GFP (Abcam, ab13970; ICC 1:5000, WB 1:10.000); HA-epitope-tag (Covance, MMS-101 R; WB 1:1000); LAMP1 (BD Bioscience, 555,798; ICC, 1:3000); LAMP2 (BD Bioscience, 555,803; ICC 1:3000); LC3B (Novus, NB100-2220; WB 1:1000); LC3B (clone EPR18709, Abcam, ab192890; ICC 1:3000); PSEN1 (clone EP2000Y, Abcam, ab76083; WB 1:1000); PSEN2 (clone EP1515Y, Abcam, ab51249; WB 1:1000, ICC 1:3000); RAB5 (Abcam, ab18211; ICC 1:1000); RAB9 (Cell Signaling, 5118; ICC, 1:1000); TFEB (Cell Signaling, 37,785; ICC 1:1000); TFEB (Cell Signaling, 4240; WB 1:1000); VPS35 (Abcam, ab10099; ICC 1:500). Fluorescent Alexa Fluor conjugated (Invitrogen, A11001, A11008, A11039, A21428 or A21422) or horseradish peroxidase (HRP)-conjugated (Dianova, 49,988 or 49,533) secondary antibodies were used.

DNA constructs

PSENEN-TAP was generated by site-specific recombination of a PCR-amplified ORF of PSENEN into a modified TAP-tagged version of the Moloney murine leukemia virus-based vector pZome1 (Cellzome). The TAP-tag was built of a protein A and a CALM (calmodulin)-binding site separated by a tobacco etch virus (TEV) cleavage site. Human *PSENEN* cDNA was PCR-amplified, cloned into the pENTR/D-TOPO cDNA vector (Thermo Fisher Scientific, K240020), and transferred by LR recombination using Gateway LR Clonase (Thermo Fisher Scientific, 11,791,019) into the L21 vector. L21 is available in different versions encoding N-terminal protein tags (HA, GFP, tdTomato), added in frame to the insert cloned into the Gateway cassette [34]. A corresponding portfolio of tagged CLN3 constructs has been generated by us before [34]. In addition, human *CLN3* was PCR-amplified and cloned into pIRES2-EGFP (BD Bioscience, PT3267-5), and the CLN3-IRES2-EGFP cassette was finally transferred into pcDNA3.1/Zeo (Invitrogen, V86020). pCS2 NOTCH1 ΔEMV-6MT was a gift from Raphael Kopan and Jeffrey Nye (Addgene, 41,737) [51] and used as a template for PCR-amplification and cloning of the full-length insert or of a fragment encoding the intracellular domain respectively into pENTR/D-TOPO and subsequently into L21 to generate HA-tagged constructs. Full-length APP_{695} in pcDNA3.1 [71] was used as a template for PCR-amplified cloning of the full-length insert or of a fragment encoding the intracellular domain respectively into pENTR/D-TOPO and subsequently into L21 to generate GFP-tagged constructs. pBABE-puro mCherry-EGFP-LC3B was a gift from Jayanta Debnath (Addgene, 22,418) [72] and used for subcloning of mCherry-EGFP-LC3B into L21. tdTomato-RAB5A and tdTomato-RAB7A were cloned into L21 tdTomato from GFP-RAB5A and GFP-RAB7A [71] by LR recombination. pLAMP1-mCherry was a gift from Amy Palmer (Addgene, 45,147) [73].

Tandem affinity purification

Tandem affinity purification was performed as described before [47]. In brief, SK-N-BE (2) neuroblastoma cells expressing PSENEN with a C-terminal TAP-Tag were generated by retroviral gene transfer. Cell lysates were incubated with 200 µl of IgG-agarose beads (Sigma, A0919) for 2 h at 4°C. Beads were collected, washed and incubated with cleavage buffer (10 mM Tris, pH 7.5, 100 mM NaCl, 1 mM DTT, 0.1% Igepal [Sigma, I-3021], 0.5 mM EDTA) and 100 units of TEV protease (Invitrogen, 12,575,023) for 1 h at 16°C. The eluate was transferred into a column containing 200 µl of calmodulin-agarose (Stratagene, 214,303) in 10 mM Tris, pH 7.5, 100 mM NaCl, 1 mM DTT, 0.1% Igepal, 2 mM $MgCl_2$, 2 mM imidazole (Roth, 3899.2), 4 mM $CaCl_2$ and after washing bound proteins were eluted with 10 mM Tris, pH 8.0, 5 mM EGTA at 37°C. Eluates were separated by SDS PAGE and stained with colloidal Coomassie Brilliant Blue (Bio-Rad, 1,610,436). Gels were sliced, cut bands reduced, alkylated, and digested as described previously [74] and peptides were sequenced by tandem mass spectrometry (Waters Cap LC and QTOF Ultima). Proteins were identified by using Mascot software (Matrix Science, UK).

Cultivation and transfection of cells

HeLa cells (DSMZ, ACC57) were cultured in Dulbecco's modified Eagle's medium (DMEM) (Gibco, 11,971–025) supplemented with 10% fetal calf serum (FCS, GIBCO, 10,109,163). Cells were transiently transfected using Lipofectamine 2000 (Invitrogen, 11,668,019) according to the manufacturer's instructions. Stable transfectants were selected and cultured in DMEM containing 150 µg/ml Zeocin (Invivogen, ant-zn) as described previously [75]. Positive cell clones with equal expression levels were identified by immunocytochemistry and immunoblot analysis. In addition, cells expressing the GFP-IRES-CLN3 construct were

analyzed for wild type CLN3 expression by RT-PCR and sequencing of respective PCR products.

For starvation, cells were cultured for indicated times in Earle's Balanced Salt Solution (EBSS; Gibco, 24,010). To challenge the autophagy pathway, cells were cultured for 6 h in DMEM supplemented with 10 mM NH_4Cl (Sigma, 213,330) alone or with the protease inhibitors E-64d (Sigma, E8640) or pepstatin A (Applichem, A2205) (each 10 μg/ml) or for 24 h in DMEM supplemented with 100 mM trehalose (Sigma, T9531).

Primary cultured hippocampal neurons were prepared as described before [76]. In brief, we used E17 embryos from timed-pregnant C57BL/6 J mice. Dissected hippocampi were collected in HANKS' medium without calcium and magnesium (Sigma, H-2387) supplemented with 20% FCS, washed in HANKS' medium, and treated with papain (Sigma, P4762) and DNAse (Invitrogen, 18,047–019) in digestion buffer (137 mM NaCl, 5 mM KCl, 7 mM $Na_2HPO_4(2xH_2O)$, 25 mM HEPES, pH 7.4) for 30 min at 37°C. Tissue was subsequently washed two times with HANKS' medium and resuspended in 2 ml dissociation buffer (HANKS' medium, 12 mM $MgSO_4(7xH_2O)$) supplemented with DNAse. Cells were dissociated by triturating and adding HANKS' medium plus 20% FCS stopped the dissociation reaction. Cells were sedimented and seeded in PNGM™-medium (Lonza, CC-4462) on poly-L-lysine (Sigma, P9155)-coated glass coverslips at a density of 40,000 cells/cm^2. At 3 days in vitro (DIV) cells were transfected using Lipofectamine LTX (Invitrogen, 15,338,100). Live cell imaging, fixation, staining and analysis followed at indicated DIV.

Immunocytochemistry, colocalization analysis, and live-cell imaging

For immunocytochemistry, cells were cultured on cover slips, washed in PBS (137 mM NaCl, 2.7 mM KCl, 8.1 mM Na_2HPO_2, 1.47 mM KH_2PO_4), fixed in PBS with 4% paraformaldehyde and 4% sucrose (or with 100% ice-cold methanol for LC3 staining), washed and permeabilized with PBS with 0.5% saponin (Sigma, S7900) or 0.05% Triton X-100 (Roth, 3051.2). Cells were incubated with antibodies in the presence of 10% serum (Gibco, 10,270–160) and 0.5% saponin and analyzed by confocal microscopy using a Leica TCS SP8 microscope. For colocalization analysis, laser power and gain were identical between images. Using the Fiji ImageJ plugin JaCoP (ImageJ software; US National Institutes of Health, Bethesda) the Mander's coefficients for colocalization M1 and M2 were calculated. Bar graphs were produced using Graph Pad Prism 5 and statistically analyzed by a one-way analysis of variance (ANOVA) with a post hoc Tukey test (IBM SPSS Statistics 25).

For time-lapse video microscopy, cells were transfected with constructs encoding fluorophore tagged CLN3 and PSENEN fusion proteins in glass bottom dishes. During live-cell imaging, transfected cells were temperature- (37°C) and CO_2-controlled (5%). Images were taken every 200–300 ms over indicated periods using a spinning disk confocal microscope (Visitron Systems). Kymographs were created using the Multiple-Kymograph plugin of Fiji ImageJ.

For autophagic flux analysis, cells were seeded in glass bottom dishes and transfected with the tandem mCherry-GFP-LC3 construct. After 24–48 h, live imaging analysis was performed under control conditions or 6 h after starvation and the mCherry and GFP signals were recorded in parallel with a Leica TCS SP8 confocal microscope. The number of cellular vesicles per channel was counted by transforming the recorded confocal z-stacks into binary images applying an equal threshold between images and subsequently using the Fiji ImageJ function "analyze particles". Spatially close vesicles were separated using the Fiji ImageJ function "watershed" and background signals were ruled out by excluding single pixel counts. Bar graphs were produced using Graph Pad Prism 5. After confirming normal distribution using a Kolmogorov-Smirnov test, statistical differences were confirmed by one-way ANOVA with a post hoc Tukey test in IBM SPSS Statistics 25.

Immunoprecipitation

HeLa cells were transfected with constructs encoding HA-CLN3 and GFP-PSENEN or with HA-CLN3 and GFP. Twenty-four h post transfection, cells were lysed in 100 mM NaCl, 50 mM Tris-HCl, 1 mM $CaCl_2$, 1 mM $MgCl_2$, 0.5% NP40 (Sigma, 21–3277), 1 mM PMSF (Roth, 6367.1), pH 7.5, cell debris sedimented for 10 min at 16,000 g and 10% of each supernatant were taken as an expression control (input) and immunoprecipitation was performed using anti-GFP nanobody coupled to magnetic beads (ChromoTek, gtma-20) for 30 min at 4°C. After washing with 100 mM NaCl, 50 mM Tris-HCl, 1 mM $CaCl_2$, 1 mM $MgCl_2$, 0.01% Triton X-100, 1 mM PMSF, pH 7.5 protein complexes were subjected to SDS-PAGE and immunoblotting.

Immunoblotting

Protein concentration was determined using the bicinchoninic acid (BCA) method (BCA Protein Assay; Pierce, 23,227). Equal amounts of protein samples were mixed with SDS sample buffer, boiled at 95°C for 5 min, subjected to reducing SDS-PAGE using 4–16% acrylamide gels and transferred to PVDF membranes. Subsequently the membranes were incubated with primary antibodies, HRP-conjugated secondary antibodies, and ECL-solution (SuperSignalWest Pico; Thermo-scientific, 34,580). Chemiluminescence signals were detected with a LAS4000Mini system (Fuji). For quantification and statistical analysis, 6–10 independent experiments were performed. Bands of immunoblots were quantified by using Multi Gauge V3.2 (Fuji), Fiji ImageJ and a one-way ANOVA with a post hoc Dunnett's test for statistical analysis.

In situ hybridization

In situ hybridization was performed as described before [77]. In brief, antisense RNA probes labeled with α-^{35}S-UTP were generated according to the manufacturer's instructions (Ambion, 1344). Cryosections (20 μm) from C57BL/6 J mice (embryonic day 16) were fixed, acetylated, dehydrated, and subjected to *in situ* hybridization at 55°C for 18 h, followed by

RNaseA (AppliChem, A3832) treatment for 30 min at 37°C, and a high-stringency wash was performed in 0.1 x saline sodium citrate buffer (15 mM NaCl, 1.5 mM sodium citrate, pH 7) at 55°C. Slides were exposed to X-ray films (Kodak Biomax MR, Amersham Biosciences, Z363030) for 72 h. The probe used for detection of *Cln3* transcripts comprised nucleotides 1–653 of the murine cDNA cloned in pBSK (Stratagene, 212,205), which was linearized with NotI for antisense transcription. A cDNA clone (IMAGp998J21802Q, Source Bioscience) comprising the entire open reading frame and 5′- and 3′-UTR sequence of murine *Psenen* served as a template to clone the probe used for detection of *Psenen* transcripts into pBSK and comprised 594 nucleotides. This was linearized with NotI for the antisense probe. Specificity of signals was verified by comparing antisense with sense controls.

Generation of knockout cells

In order to generate knockout cells, guide RNA (gRNA) corresponding to the first exon of *CLN3* (CACCGCGGCGCTTTTCGGATTCCGA) and to the first exon of *PSENEN* (CACCGCCTGGAGCGAGTGTCCAATG) was designed and cloned into pX330-U6 expressing a humanized Cas9 [78]. HeLa cells were co-transfected with pX330-U6-gRNA-CLN3 or pX330-U6-gRNA-*PSENEN* and pcDNA3.1/Zeo. Twenty-four h after transfection, cells were selected with zeocin (250 µg/ml) for 5 days to enrich transfected cells. Subsequently, cells were cultured for 2 weeks in DMEM with 10% FCS, single clones were isolated, genomic DNA extracted and genomic sequences surrounding *CLN3* and *PSENEN* genes amplified by PCR and sequenced. DNA sequencing identified different knockout cell clones carrying specific indel mutations. Two differently targeted and independent *CLN3* KO clones and two independent *PSENEN* KO clones with identical mutations (Figure S2) were expanded and analyzed in parallel to exclude clonal effects. Results showed similar phenotypes. KO cells were continuously genotyped by PCR using respective genomic DNA extracted from cells, the primer pairs (5′-TTGTTCTAATAGGGGCGTGG and 5′-CCTCCTCTGTGCTCTAGACT) for *PSENEN* KO cells and (5′-CCAGCCCCTCCCTTTTTCACG and 5′-TGGGGCAAACCAGTGGATTCAG) for *CLN3* KO cells and sequencing of gel-extracted PCR products.

Cell growth analysis

Cells were seeded in 24-well plates at a density of 5,000 cells per well. Images were captured at identical areas in a 4 h interval for 8 days and confluence was measured using the IncuCyte S3 live cell imaging system (Sartorius). Data of each image was normalized individually and averaged over 4 wells. To compensate for variations within individually measured time points by the confluence mask, a rolling average using a window of 6 time points was applied. The time point of maximal growth (maximum slope) was used to set an interval of 12 h before and 12 h after this time point for statistical analysis using two-sided Mann-Whitney U-tests.

Quantification of Aβ levels

Cell culture media (DMEM without FCS) was collected following conditioning for 24 h and cell debris removed by centrifugation. Secreted Aβ40 and Aβ42 peptides and sAPP-α were quantified by sandwich enzyme-linked immunosorbent assay according to the manufacturer's instructions (IBL, ELISA JP27729 human amyloid β and JP27734 human sAPP-α). All measurements were performed in triplicates. sAPP-α levels were almost identical between the cell lines. Aβ levels were normalized to sAPP-α levels. Statistical analysis was performed with GraphPad Prism using a one-way ANOVA with a post hoc Tukey test.

Lysosomal protease activity measurement

For the measurement of HEXA/β-hexosaminidase A activity, cells were lysed in 20 mM Tris-HCl, 150 mM NaCl, 10 mM EDTA, 1% Triton X-100, pH 8. Protein concentration was measured using the BCA method. From each cell lysate, 100 µg total protein was incubated with HEXA substrate (10 mM 4-nitrophenyl-N-acetyl-β-D-glucosaminide [Sigma, N9376], 100 mM sodium citrate, 0.2% Triton X-100, pH 4.6) for 30 min at 37°C. The reaction was stopped with 0.05 M glycine-NaOH, pH 10.4 and enzymatic activity determined as released 4-nitrophenol by measuring absorbance at 405 nm using a spectrophotometer (Amersham Biosciences). Statistical analysis was performed with GraphPad Prism using a one-way ANOVA with a post hoc Bonferroni test.

Lysosomal protease activity in cells was determined using DQ-red-BSA (Thermo Fisher Scientific, D12051) and CTSB activity was determined using Magic Red Cathepsin B (ImmunoChemistry Technologies, ICT-937). Cells were seeded at a density of 15,000 cells per well in poly-L-lysine coated 96-well plates. After 24 h, cells were incubated with 10 µg/µl DQ-red-BSA in DMEM with 1% FCS, 1% non-essential amino acids, 1% Glutamax (Invitrogen, 35,050–38), 1% HEPES for 1 h or 6 h. In parallel experiments, 100 nM bafilomycin A_1 (Biomol, cay11038-500) was added. To determine CTSB activity, cells were incubated with Magic Red staining solution diluted in DMEM with 1% FCS, 1% non-essential amino acids, 1% Glutamax, 1% HEPES to a 1-fold concentration at 37°C for 30 min, 180 min and 300 min respectively. After incubation, cells were washed once with PBS, stained with Hoechst (Thermo Fisher Scientific, H3570) for 5 min at 37°C and washed again three times with PBS. Fluorescence was measured using automated confocal microscopy (OPERA Phenix high content system, PerkinElmer) with a 20-fold magnification. Image analysis was performed with the Columbus and Spotfire software (PerkinElmer). Only living cells, distinguishable from dead cells via Hoechst staining, were used for analysis. Background from untreated wells was subtracted and fluorescence intensity was normalized to

the cell number. Statistical analysis was performed with GraphPad Prism using a two-way ANOVA and multiple comparison with a post hoc Tukey test which is using a single pooled variance for calculations.

TF uptake assay

Twenty-four h after transfection with GFP, cells were starved 1 h at 37°C in Opti-MEM (Gibco, 11,058,021) and labeled 1 h at 4°C with 50 µg/ml fluorescent transferrin-Alexa Fluor 555 (Thermo Fisher Scientific, T35352) in Opti-MEM. After washing, cells were incubated for different time intervals at 37°C. Cells were fixed with 4% paraformaldehyde and stained with primary anti-GFP and secondary Alexa Fluor 488 antibodies. The GFP signal (Alexa Fluor 488) was used to visualize cells. Fluorescent vesicles (Alexa Fluor 555) per cell were determined by confocal microscopy using identical laser power and gain between images and the "analyze particles" function of the Fiji ImageJ software. Bar graphs were produced using Graph Pad Prism 5. After confirming normal distribution using a Kolmogorov-Smirnov test, statistical differences were confirmed by one-way ANOVA with a post hoc Tukey test in IBM SPSS Statistics 25.

Gene expression analysis by quantitative real-time PCR

Cells were treated as indicated and total RNA extracted using Trizol (Thermo Fisher Scientific, 15,596,026). RNA integrity was assessed by inspection of *RNA18S* and *RNA28S* ribosomal RNA bands using agarose gel-electrophoresis and quantity was determined by optical density measurement using NanoDrop 2000 (Thermo Scientific).

We performed expression analysis as described before [79]. In brief, residual genomic DNA was removed and one µg total RNA per reaction was reverse transcribed to cDNA by using oligo dT primers as well as hexamer primers and SuperScript IV according to the manufacturer's instructions (VILO Mastermix with ezDNase, Thermo Fisher Scientific, 11,766,050). Gene expression levels were determined by quantitative real-time PCR performed in a QuantStudio 6 Flex Real-Time PCR System (Applied Biosystems). We used the following Fam labeled TaqMan Gene Expression Assays (Thermo Fisher Scientific) to detect expression of genes of interest: *CLN3*: Hs00164002_m1; *CTSB*: Hs00157194_m1; *CTSD*: Hs00157201_m1; *GLB1*: Hs01035168_m1; *PSENEN*: Hs01033961_g1; *PSAP*: Hs01551096_m1; *PSEN2*: Hs00240982_m1; *SESN2*: Hs00230241_m1; *TFEB*: Hs00292981_m1 and *TPP1*: Hs00166099_m1. All assays were exon-spanning with similar amplicon length. Prior to the determination of the relative differences in expression levels of the genes of interest, the three different Vic labeled TaqMan Gene Expression Assays *APRT*: Hs00356991_m1; *HPRT*: Hs02800695_m1 and *TBP*: Hs00427620_m1 were evaluated for their suitability as reference genes by analyzing their expression stability under the different conditions analyzed in this study. To this end, we used the RefFinder software, which combines the results of four different software packages for the stability of expression analysis [80]. Best performance was observed for *APRT* and *HPRT* and we chose *APRT* as reference for duplex assays, because its expression level was similar to that of our genes of interest. In control experiments, the complete RT-qPCR analysis of all cell lines was also performed with *HPRT* as a reference gene with a congruent outcome. We established duplex assays for the comparative analysis of expression of the genes of interest by determining the respective concentration of the transcript of interest and of the reference transcript by simultaneous detection in the same reaction. RT-qPCR was performed using TaqMan Gene Expression master mix (Thermo Fisher Scientific, 4,369,542) in a 384-well format, reaction volumes were 10 µl and the number of replicates per sample was three. We applied the following thermal cycling conditions: activation of hot-start Taq DNA Polymerase at 95°C for 10 min and two-step cycling with denaturation at 95°C for 15 s, annealing and extension at 60°C for 60 s and fluorescence data collection run in 40 cycles. Differential gene expression was calculated with the Relative Quantification app (Version 3.8, Thermo Fisher), using the individually determined efficiencies of the respective targets for the ΔΔ-Ct determinations. The REST software was utilized to evaluate the significance of the relative differences [81].

Statistical analysis

Statistical tests were performed using Graph-Pad Prism or IBM SPSS Statistics software and analyzed by a one-way analysis of variance (ANOVA) with a post hoc Tukey test or a post hoc Bonferroni test or two-way ANOVA and multiple comparison with a post hoc Tukey test. For gene expression analysis, the REST software was utilized to evaluate the significance of the relative differences.

Ethics approval

No experiments on living animals were conducted for this study. Housing and scarification of animals as well as use of animal material in this study were ethically reviewed and carried out in accordance with European Directive 2010/63/EEC and local policies on the care, welfare and treatment of animals.

Acknowledgments

We thank Barbara Merz and Andrea Zaisser for skilled technical assistance and the UKE microscopy imaging facility (umif) for providing confocal microscopes and support.

Disclosure statement

No potential conflict of interest was reported by the author(s).

Funding

This work was supported by the Deutsche Forschungsgemeinschaft [425373668, HE 3220/4-1] and the NCL Foundation.

ORCID

Guido Hermey http://orcid.org/0000-0003-4762-5262

References

[1] Takasugi N, Tomita T, Hayashi I, et al. The role of presenilin cofactors in the gamma-secretase complex. Nature. 2003 Mar 27;422(6930):438–441.

[2] Kaether C, Haass C, Steiner H. Assembly, trafficking and function of gamma-secretase. Neurodegener Dis. 2006;3(4–5):275–283.

[3] Cai T, Tomita T. Structure-activity relationship of presenilin in γ-secretase-mediated intramembrane cleavage. Semin Cell Dev Biol. 2020 Mar;105:102–109.

[4] De Strooper B. Aph-1, Pen-2, and Nicastrin with Presenilin generate an active gamma-Secretase complex. Neuron. 2003 Apr 10;38(1):9–12.

[5] Lichtenthaler SF, Haass C, Steiner H. Regulated intramembrane proteolysis–lessons from amyloid precursor protein processing. J Neurochem. 2011 Jun;117(5):779–796.

[6] Eggert S, Thomas C, Kins S, et al. Trafficking in alzheimer's disease: modulation of app transport and processing by the transmembrane proteins LRP1, SorLA, SorCS1c, Sortilin, and calsyntenin. Mol Neurobiol. 2018 Jul;55(7):5809–5829.

[7] Wolfe MS. Unraveling the complexity of γ-secretase. Semin Cell Dev Biol. 2020 Jan;105:3–11.

[8] Wang B, Yang W, Wen W, et al. Gamma-secretase gene mutations in familial acne inversa. Science. 2010 Nov 19;330 (6007):1065.

[9] Hori K, Sen A, Artavanis-Tsakonas S. Notch signaling at a glance. J Cell Sci. 2013 May;126(Pt 10):2135–2140.

[10] Güner G, Lichtenthaler SF. The substrate repertoire of γ-secretase /presenilin. Semin Cell Dev Biol. 2020 Jun;105:27–42.

[11] Neely KM, Green KN, LaFerla FM. Presenilin is necessary for efficient proteolysis through the autophagy-lysosome system in a gamma-secretase-independent manner. J Neurosci. 2011 Feb 23;31(8):2781–2791.

[12] Nixon RA, Yang DS. Autophagy failure in Alzheimer's disease–locating the primary defect. Neurobiol Dis. 2011 Jul;43(1):38–45.

[13] Wilson CA, Murphy DD, Giasson BI, et al. Degradative organelles containing mislocalized alpha-and beta-synuclein proliferate in presenilin-1 null neurons. J Cell Biol. 2004 May;165(3):335–346.

[14] Esselens C, Oorschot V, Baert V, et al. Presenilin 1 mediates the turnover of telencephalin in hippocampal neurons via an autophagic degradative pathway. J Cell Biol. 2004 Sep;166 (7):1041–1054.

[15] Coen K, Flannagan RS, Baron S, et al. Lysosomal calcium homeostasis defects, not proton pump defects, cause endo-lysosomal dysfunction in PSEN-deficient cells. J Cell Biol. 2012 Jul 9;198 (1):23–35.

[16] Lee JH, McBrayer MK, Wolfe DM, et al. Presenilin 1 maintains lysosomal Ca(2+) homeostasis via TRPML1 by Regulating vATPase-mediated lysosome acidification. Cell Rep. 2015 Sep 1;12(9):1430–1444.

[17] Lee JH, Yu WH, Kumar A, et al. Lysosomal proteolysis and autophagy require presenilin 1 and are disrupted by Alzheimer-related PS1 mutations. Cell. 2010 Jun 25;141 (7):1146–1158.

[18] Whyte LS, Lau AA, Hemsley KM, et al. Endo-lysosomal and autophagic dysfunction: a driving factor in Alzheimer's disease? J Neurochem. 2017 Mar;140(5):703–717.

[19] Zhang X, Garbett K, Veeraraghavalu K, et al. A role for presenilins in autophagy revisited: normal acidification of lysosomes in cells lacking PSEN1 and PSEN2. J Neurosci. 2012 Jun 20;32 (25):8633–8648.

[20] Meckler X, Checler F. Presenilin 1 and presenilin 2 target gamma-secretase complexes to distinct cellular compartments. J Biol Chem. 2016 Jun 10;291(24):12821–12837.

[21] Sannerud R, Esselens C, Ejsmont P, et al. Restricted location of PSEN2/gamma-secretase determines substrate specificity and generates an intracellular abeta pool. Cell. 2016 Jun 30;166 (1):193–208.

[22] Nugent T, Mole SE, Jones DT. The transmembrane topology of batten disease protein CLN3 determined by consensus computational prediction constrained by experimental data. FEBS Lett. 2008 Apr 2; 582(7):12821–12837.

[23] Cotman SL, Starpoli JF. The juvenile batten disease protein, CLN3, and its role in regulating anterograde and retrograde post-Golgi trafficking. Clin Lipidol. 2012;7(1):79–91.

[24] Lerner TJ, Boustany R-MN, Anderson JW, International-Batten-Disease-Consortium. Isolation of a novel gene underlying batten disease, CLN3. Cell. 1995;82(6):949–957.

[25] Kollmann K, Uusi-Rauva K, Scifo E, et al. Cell biology and function of neuronal ceroid lipofuscinosis-related proteins. Biochim Biophys Acta. 2013 Nov;1832(11):1866–1881.

[26] Butz ES, Chandrachud U, Mole SE, et al. Moving towards a new era of genomics in the neuronal ceroid lipofuscinoses. Biochim Biophys Acta Mol Basis Dis. 2020 Sep;1866(9):165571.

[27] Anderson GW, Goebel HH, Simonati A. Human pathology in NCL. Biochim Biophys Acta. 2013 Nov;1832(11):1807–1826.

[28] Herva R, Tyynela J, Hirvasniemi A, et al. Northern epilepsy: a novel form of neuronal ceroid-lipofuscinosis. Brain Pathol. 2000 Apr;10(2):215–222.

[29] Wisniewski KE, Kida E, Gordon-Majszak W, et al. Altered amyloid beta-protein precursor processing in brains of patients with neuronal ceroid lipofuscinosis. Neurosci Lett. 1990 Nov 27;120 (1):94–96.

[30] Wisniewski KE, Maslinska D, Kitaguchi T, et al. Topographic heterogeneity of amyloid B-protein epitopes in brains with various forms of neuronal ceroid lipofuscinoses suggesting defective processing of amyloid precursor protein. Acta Neuropathol. 1990;80(1):26–34.

[31] Cheng R, Tang M, Martinez I, et al. Linkage analysis of multiplex caribbean hispanic families loaded for unexplained early-onset cases identifies novel Alzheimer's disease loci. Alzheimers Dement (Amst). 2018;10:554–562.

[32] Qureshi YH, Patel VM, Berman DE, et al. An Alzheimer's disease-linked loss-of-function cln5 variant impairs cathepsin d maturation, consistent with a retromer trafficking defect. Mol Cell Biol. 2018 10;38(20). 10.1128/MCB.00011-18

[33] Kousi M, Lehesjoki AE, Mole SE. Update of the mutation spectrum and clinical correlations of over 360 mutations in eight genes that underlie the neuronal ceroid lipofuscinoses. Hum Mutat. 2012 Jan;33(1):42–63.

[34] Oetjen S, Kuhl D, Hermey G. Revisiting the neuronal localization and trafficking of CLN3 in juvenile neuronal ceroid lipofuscinosis. J Neurochem. 2016 Nov;139(3):456–470.

[35] Storch S, Pohl S, Braulke T. A dileucine motif and a cluster of acidic amino acids in the second cytoplasmic domain of the batten disease-related CLN3 protein are required for efficient lysosomal targeting. J Biol Chem. 2004 Dec 17;279 (51):53625–53634.

[36] Kyttala A, Ihrke G, Vesa J, et al. Two motifs target Batten disease protein CLN3 to lysosomes in transfected nonneuronal and neuronal cells. Mol Biol Cell. 2004 Mar;15(3):1313–1323.

[37] Kyttala A, Yliannala K, Schu P, et al. AP-1 and AP-3 facilitate lysosomal targeting of Batten disease protein CLN3 via its dileucine motif. J Biol Chem. 2005 Mar 18;280(11):10277–10283.

[38] Mao Q, Xia H, Davidson BL. Intracellular trafficking of CLN3, the protein underlying the childhood neurodegenerative disease, Batten disease. FEBS Lett. 2003 Dec 4;555(2):351–357.

[39] Schroder B, Wrocklage C, Pan C, et al. Integral and associated lysosomal membrane proteins. Traffic. 2007 Dec;8(12):1676–1686.

[40] Cao Y, Espinola JA, Fossale E, et al. Autophagy is disrupted in a knock-in mouse model of juvenile neuronal ceroid lipofuscinosis. J Biol Chem. 2006 Jul 21;281(29):20483–20493.

[41] Schmidtke C, Tiede S, Thelen M, et al. Lysosomal proteome analysis reveals that CLN3-defective cells have multiple enzyme deficiencies associated with changes in intracellular trafficking. J Biol Chem. 2019 06; 294(24): 9592–9604.

[42] Fossale E, Wolf P, Espinola JA, et al. Membrane trafficking and mitochondrial abnormalities precede subunit c deposition in a cerebellar cell model of juvenile neuronal ceroid lipofuscinosis. BMC Neurosci. 2004 Dec 10;5:57.

[43] Lojewski X, Staropoli JF, Biswas-Legrand S, et al. Human iPSC models of neuronal ceroid lipofuscinosis capture distinct effects of TPP1 and CLN3 mutations on the endocytic pathway. Hum Mol Genet. 2014 Apr;23(8):2005–2022.
[44] Yasa S, Modica G, Sauvageau E, et al. CLN3 regulates endosomal function by modulating Rab7A-effector interactions. J Cell Sci. 2020 Mar;133(6). 10.1242/jcs.234047.
[45] Ramirez-Montealegre D, Pearce DA. Defective lysosomal arginine transport in juvenile Batten disease. Hum Mol Genet. 2005 Dec;14 (23):3759–3773.
[46] Metcalf DJ, Calvi AA, Seaman M, et al. Loss of the Batten disease gene CLN3 prevents exit from the TGN of the mannose 6-phosphate receptor. Traffic. 2008 Nov;9(11):1905–1914.
[47] Brajenovic M, Joberty G, Kuster B, et al. Comprehensive proteomic analysis of human Par protein complexes reveals an interconnected protein network. J Biol Chem. 2004 Mar 26;279 (13):12804–12811.
[48] Holmes O, Paturi S, Selkoe DJ, et al. Pen-2 is essential for gamma-secretase complex stability and trafficking but partially dispensable for endoproteolysis. Biochemistry. 2014 Jul 15;53 (27):4393–4406.
[49] Prokop S, Shirotani K, Edbauer D, et al. Requirement of PEN-2 for stabilization of the presenilin N-/C-terminal fragment heterodimer within the gamma-secretase complex. J Biol Chem. 2004 May 28 279(22):23255–23261.
[50] Bammens L, Chávez-Gutiérrez L, Tolia A, et al. Functional and topological analysis of Pen-2, the fourth subunit of the gamma-secretase complex. J Biol Chem. 2011 Apr;286(14):779–796.
[51] Kopan R, Schroeter EH, Weintraub H, et al. Signal transduction by activated mNotch: importance of proteolytic processing and its regulation by the extracellular domain. Proc Natl Acad Sci U S A. 1996 Feb 20;93(4):1683–1688.
[52] Kucera A, Bakke O, Progida C. The multiple roles of Rab9 in the endolysosomal system. Commun Integr Biol. 2016 Jul-Aug;9(4): e1204498.
[53] Klionsky DJ, Abdel-Aziz AK, Abdelfatah S, et al. Guidelines for the use and interpretation of assays for monitoring autophagy. Autophagy. 2021Jan; 171: 1–382(4th edition)(1)
[54] Bajaj L, Lotfi P, Pal R, et al. Lysosome biogenesis in health and disease. J Neurochem. 2018 Aug 9;148:573–589.
[55] Sardiello M, Palmieri M, Di Ronza A, et al. A gene network regulating lysosomal biogenesis and function. Science. 2009 Jul 24;325(5939):473–477.
[56] Chan CH, Mitchison HM, Pearce DA. Transcript and in silico analysis of CLN3 in juvenile neuronal ceroid lipofuscinosis and associated mouse models. Hum Mol Genet. 2008 Nov 1;17(21):3332–3339.
[57] Kitzmuller C, Haines RL, Codlin S, et al. A function retained by the common mutant CLN3 protein is responsible for the late onset of juvenile neuronal ceroid lipofuscinosis. Hum Mol Genet. 2008 Jan 15;17(2):303–312.
[58] Jarvela I, Lehtovirta, M, Tikkanen, R, et al. Defective intracellular transport of CLN3 is the molecular basis of Batten disease (JNCL). Hum Mol Genet. 1999 Jun;8(6):1091–1098.
[59] Zhong Y, Mohan K, Liu J, et al. Loss of CLN3, the gene mutated in juvenile neuronal ceroid lipofuscinosis, leads to metabolic impairment and autophagy induction in retinal pigment epithelium. Biochim Biophys Acta Mol Basis Dis. 2020 Oct 1;1866(10):165883.
[60] Katz ML, Shibuya H, Liu PC, et al. A mouse gene knockout model for juvenile ceroid-lipofuscinosis (Batten disease). J Neurosci Res. 1999 Aug 15;57(4):551–556.
[61] Mitchison HM, Bernard DJ, Greene ND, et al. Targeted disruption of the Cln3 gene provides a mouse model for batten disease. the batten mouse model consortium [corrected]. Neurobiol Dis. 1999 Oct;6(5):321–334.
[62] Cotman SL, Vrbanac, V, Lebel, LA, et al. Cln3(Deltaex7/8) knock-in mice with the common JNCL mutation exhibit progressive neurologic disease that begins before birth. Hum Mol Genet. 2002 Oct 15;11(22):2709–2721.
[63] Cao Y, Staropoli JF, Biswas S, et al. Distinct early molecular responses to mutations causing vLINCL and JNCL presage ATP synthase subunit C accumulation in cerebellar cells. PLoS One. 2011 Feb 17;6(2):e17118.
[64] Chandrachud U, Walker MW, Simas AM, et al. Unbiased cell-based screening in a neuronal cell model of batten disease highlights an interaction between Ca2+ homeostasis, autophagy, and CLN3 protein function. J Biol Chem. 2015 Jun 5;290 (23):2709–2721.
[65] Medina DL, Fraldi A, Bouche V, et al. Transcriptional activation of lysosomal exocytosis promotes cellular clearance. Dev Cell. 2011 Sep 13;21(3):421–430.
[66] Palmieri M, Pal R, Nelvagal HR, et al. mTORC1-independent TFEB activation via Akt inhibition promotes cellular clearance in neurodegenerative storage diseases. Nat Commun. 2017 Feb 6;8:14338.
[67] Xiao Q, Yan P, Ma X, et al. Neuronal-Targeted TFEB accelerates lysosomal degradation of app, reducing abeta generation and amyloid plaque pathogenesis. J Neurosci. 2015 Sep 2;35 (35):12137–12151.
[68] Zhang QC, Petrey D, Deng L, et al. Structure-based prediction of protein-protein interactions on a genome-wide scale. Nature. 2012 Oct 25;490(7421):556–560.
[69] Kotlyar M, Pastrello C, Malik Z, et al. IID 2018 update: context-specific physical protein-protein interactions in human, model organisms and domesticated species. Nucleic Acids Res. 2019 Jan 8;47(D1):D581–D589.
[70] Reddy K, Cusack CL, Nnah IC, et al. Dysregulation of nutrient sensing and clearance in presenilin deficiency. Cell Rep. 2016 Mar 8;14(9):2166–2179.
[71] Hermey G, Schmidt N, Bluhm B, et al. SorCS1 variants and amyloid precursor protein (APP) are co-transported in neurons but only SorCS1c modulates anterograde APP transport. J Neurochem. 2015 Oct;135(1):60–75.
[72] N'Diaye EN, Kajihara KK, Hsieh I, et al. PLIC proteins or ubiquilins regulate autophagy-dependent cell survival during nutrient starvation. EMBO Rep. 2009 Feb;10(2):173–179.
[73] Van Engelenburg SB, Palmer AE. Imaging type-III secretion reveals dynamics and spatial segregation of Salmonella effectors. Nat Methods. 2010 Apr;7(4):325–330.
[74] Shevchenko A, Wilm M, Vorm O, et al. Mass spectrometric sequencing of proteins silver-stained polyacrylamide gels. Anal Chem. 1996 Mar 1;68(5):850–858.
[75] Nielsen MS, Keat SJ, Hamati JW, et al. Different motifs regulate trafficking of SorCS1 isoforms. Traffic. 2008 Jun;9(6):980–994.
[76] Oetjen S, Mahlke C, Hermans-Borgmeyer I, et al. Spatiotemporal expression analysis of the growth factor receptor SorCS3. J Comp Neurol. 2014 Oct 15;522(15):3386–3402.
[77] Denkena J, Zaisser A, Merz B, et al. Neuronal activity regulates alternative exon usage. Mol Brain. 2020 Nov 10;13(1):148.
[78] Cong L, Ran FA, Cox D, et al. Multiplex genome engineering using CRISPR/Cas systems. Science. 2013 Feb 15;339 (6121):819–823.
[79] Hermey G, Hoffmeister-Ullerich SA, Merz B, et al. Amyloidosis causes downregulation of SorLA, SorCS1 and SorCS3 expression in mice. Biol Chem. 2019 Aug 27;400(9):1181–1189.
[80] Xie F, Xiao P, Chen D, et al. miRDeepFinder: a miRNA analysis tool for deep sequencing of plant small RNAs. Plant Mol Biol. 2012 Jan;80 (1):75–84.
[81] Pfaffl MW. Relative expression software tool (REST) for group-wise comparison and statistical analysis of relative expression results in real-time PCR. Nucleic Acids Res. 2002 May;30(9):e36.

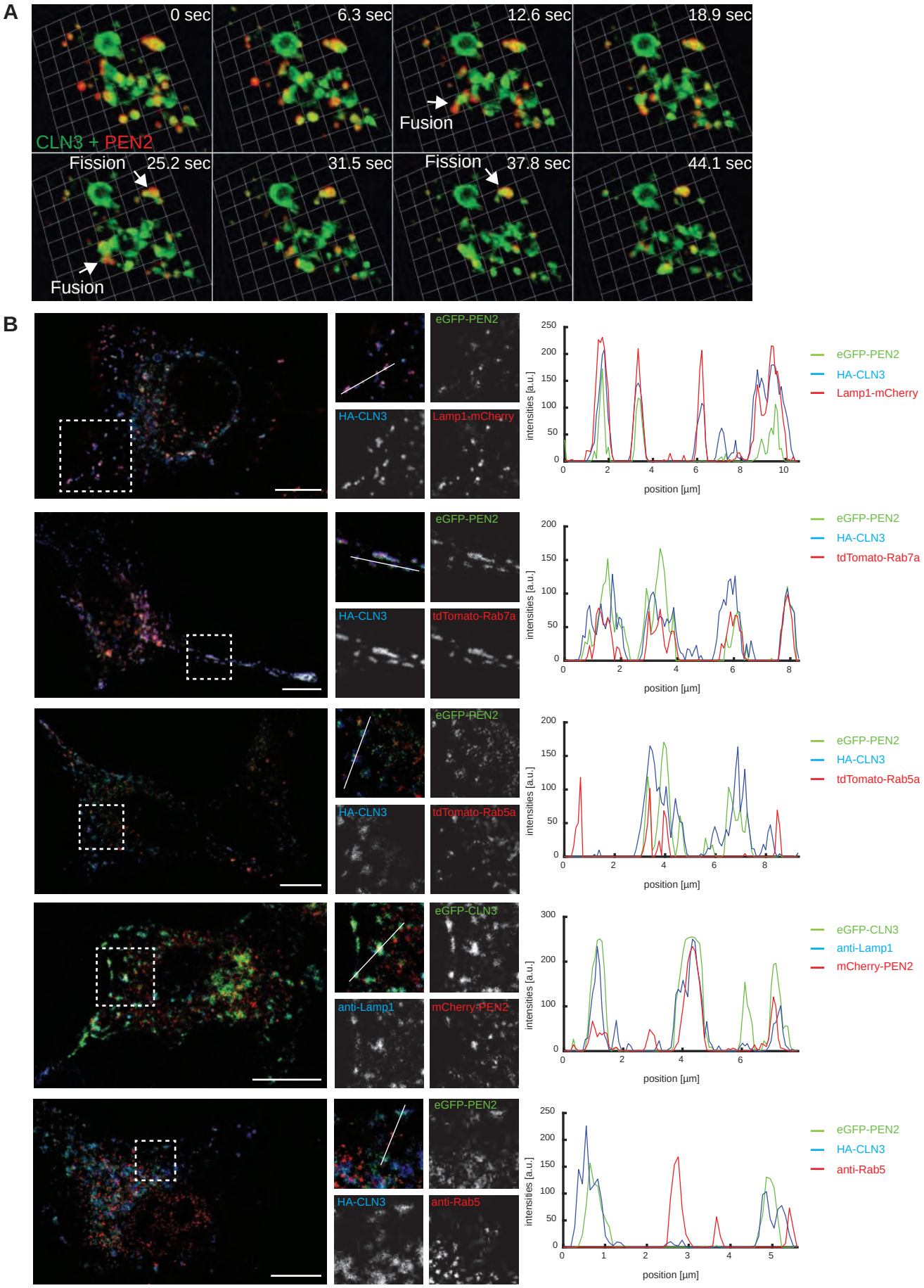

Figure S1. Imaging of CLN3 and PEN2 positive endosomes.
(A) HeLa cells were co-transfected with GFP-CLN3 (green) and tdTomato-PEN2 (red) and analyzed by spinning disk confocal microscopy. Shown is a 3D projection of a 1 min live-cell video microscopy of GFP-CLN3- and tdTomtao-PEN2-positive endosomes which show fusion and fission events (arrows). 1 Unit = 1.72µm. (B) HeLa cells were co-transfected with the indicated constructs, immunostained using respective and specified antibodies and analyzed by confocal microscopy. Scale bars: 20 µm. Dotted boxes in the left panels indicate magnified areas shown in the right panels. Line plots (right) correspond to the white lines indicated in the merged zoom-ins.

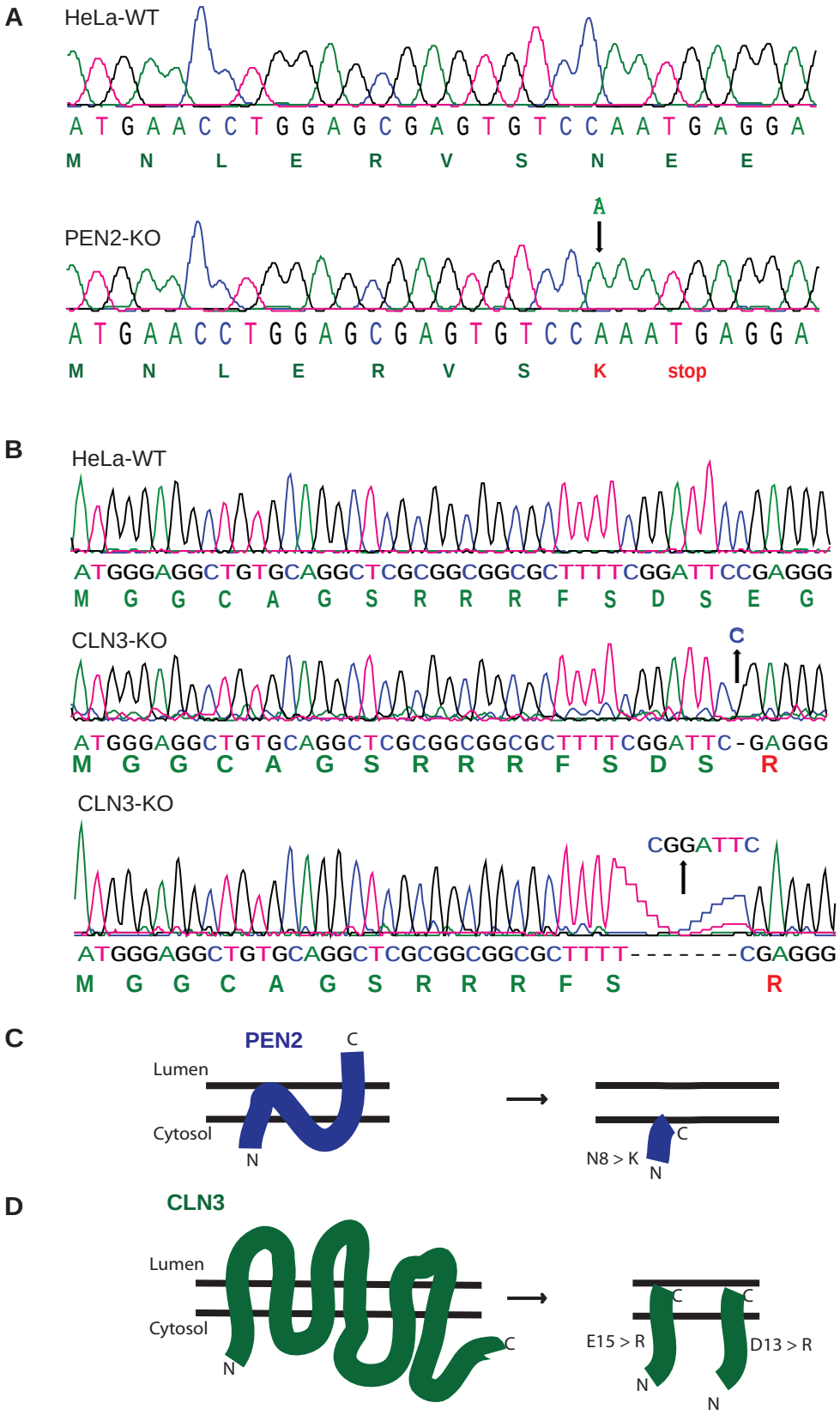

Figure S2. CRISPR-CAS9 mediated CLN3 and PEN2 knock out in HeLa cells

(A, B) Genomic DNA of HeLa wild type (WT) and HeLa knockout (KO) cells was amplified by PCR and sequenced. Sequencing traces of one PEN2 knockout line demonstrates an adenosine, A, insertion in the *PEN2* sequence (A) as compared to the wild type sequence (upper panel). Sequencing traces of two alternative CLN3 knockout lines demonstrate a cytosine, C, or a CGGATTC deletion in the *CLN3* gene (B). Arrows indicate indel mutations. The lower sequences correspond to the encoded amino acid sequence, beginning with the first methionine, M, indels lead to illustrated frame shifts (red letters) and premature stop codons. (C) The PEN2 protein has a cytosolic N-terminus, a luminal C-terminus and harbors three membrane-embedded domains, with the first two domains traversing only half of the lipid bilayer and the third passing through the membrane. The indel mutation in *PEN2* causes a frameshift after 7 amino acids, a premature stop codon after amino acid 8 and results in a truncated protein. (D) The CLN3 protein consists of 6 transmembrane domains in which N- and C-terminal ends are facing the cytosol. The indel mutations in *CLN3* cause a frame shift at amino acid E15 or D13, and a premature stop codon after 53 or 51 amino acids respectively and result in a truncated protein.

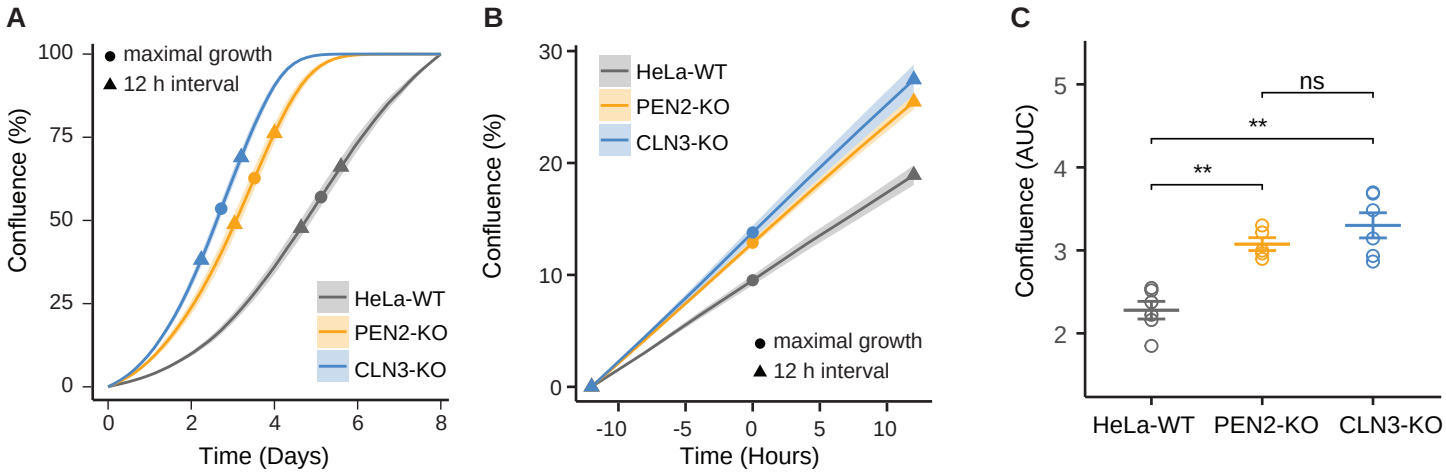

Figure S3. Comparison of cell growth of WT, CLN3-KO and PEN2-KO HeLa cells.
(A) Representative growth rate (confluence over time). (B) Plot of the confluence interval 12 h before and 12 h after maximal growth (average of 6 experiments). Time point -12 h was set to zero. (C) Area under the curve (AUC) from (B) was used for statistical analysis using two-sided Mann–Whitney U-tests, **p<0.001.

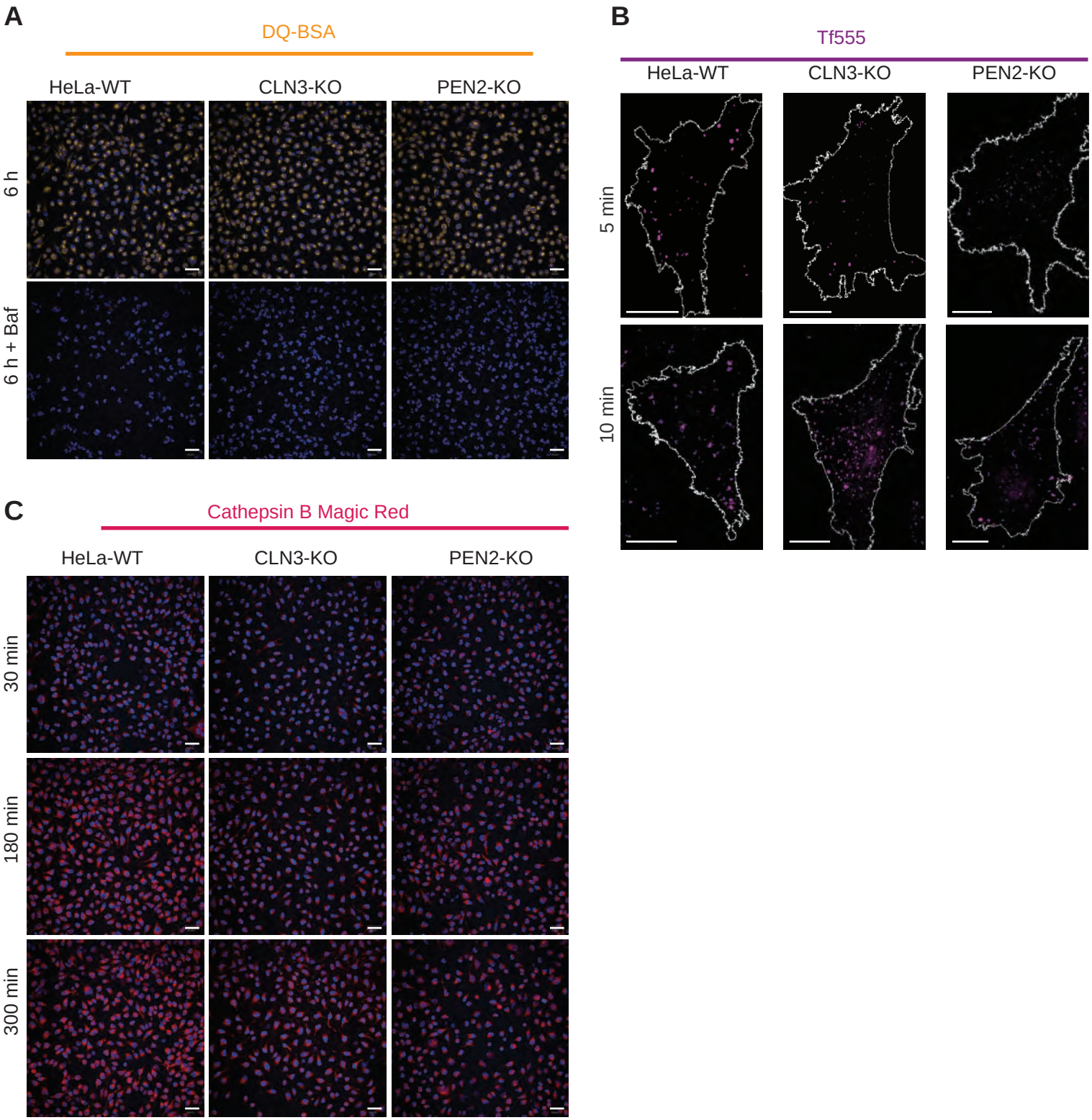

Figure S4. Representative confocal images of the DQ-BSA assay, the transferrin uptake assay and the magic red assay

(A) Representative confocal images of the DQ-BSA assay after 6 h incubation time, with and without 100nM Bafilomycin (Baf). Yellow, fluorescence released by DQ-BSA hydrolysis; blue, Hoechst staining. Scale bars: 50 µm. (B) Cells were transfected with eGFP to identify single cells. 24 h after transfection, cells were starved for 1 h, subsequently labelled for 1 h at 4°C with fluorescent transferrin-Alexa-555, washed and incubated for 5 or 10 min at 37°C. The GFP signal was used to visualize and to encircle (white lines) cells. Fluorescent vesicles (Alexa-555) per cell were determined by confocal microscopy. Scale bars: 10 µm. (C) Representative confocal images of the Cathepsin B – magic red assay after indicated incubation times. Red, fluorescence released by magic red hydrolysis; blue, Hoechst staining. Scale bars: 50 µm.

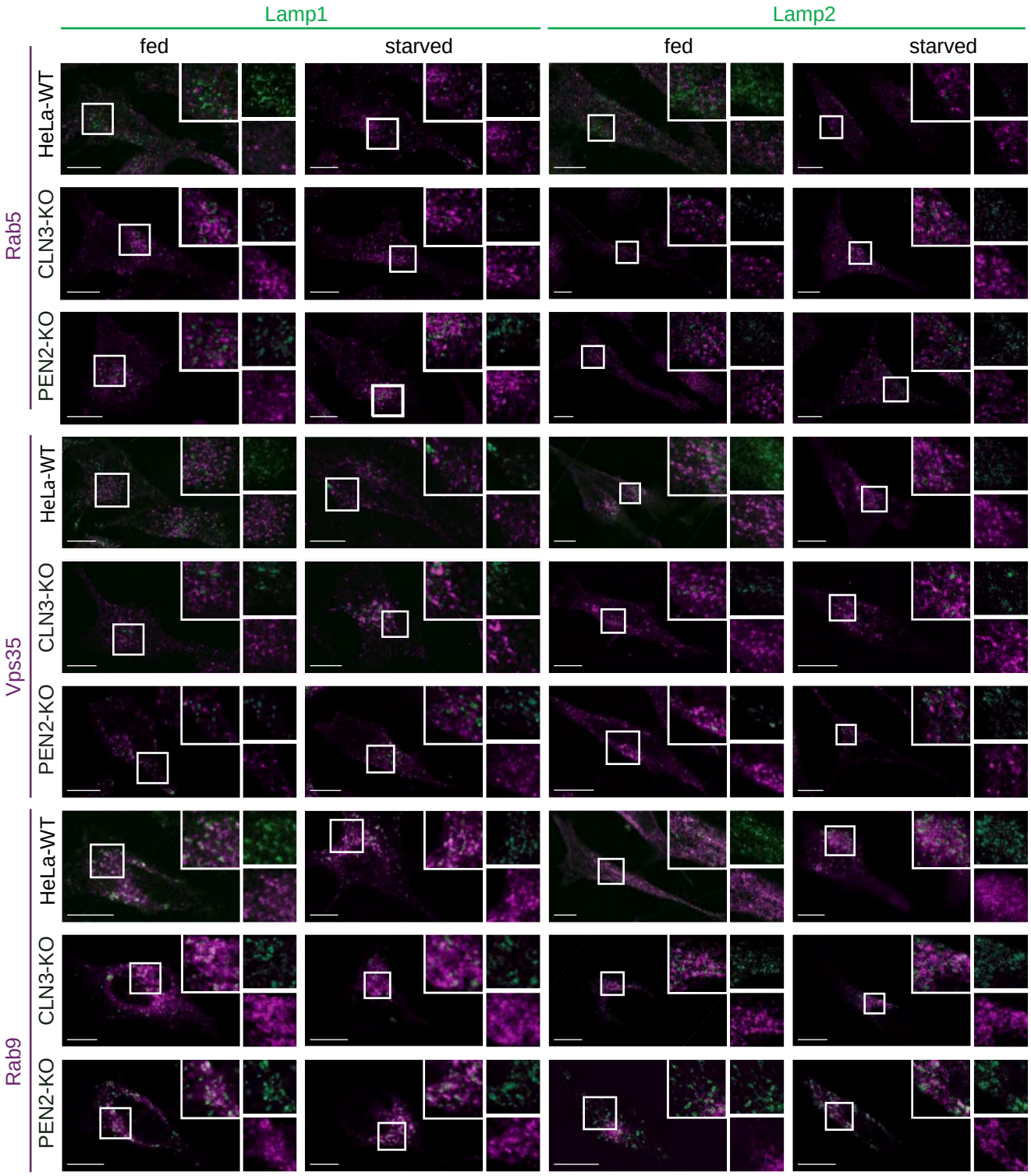

Figure S5. Representative images of Lamp1 and Lamp2 and Rab5, Rab9 and Vps35 localization. Representative confocal images of Lamp1 and Lamp2 (green) and Rab5, Rab9 and Vps35 (magenta) immunocytochemical localization in fed HeLa-WT, CLN3-KO, PEN2-KO cells and after 6 h starvation. Magnifications of selected areas (boxes) are shown as insets. Scale bars: 10 µm.

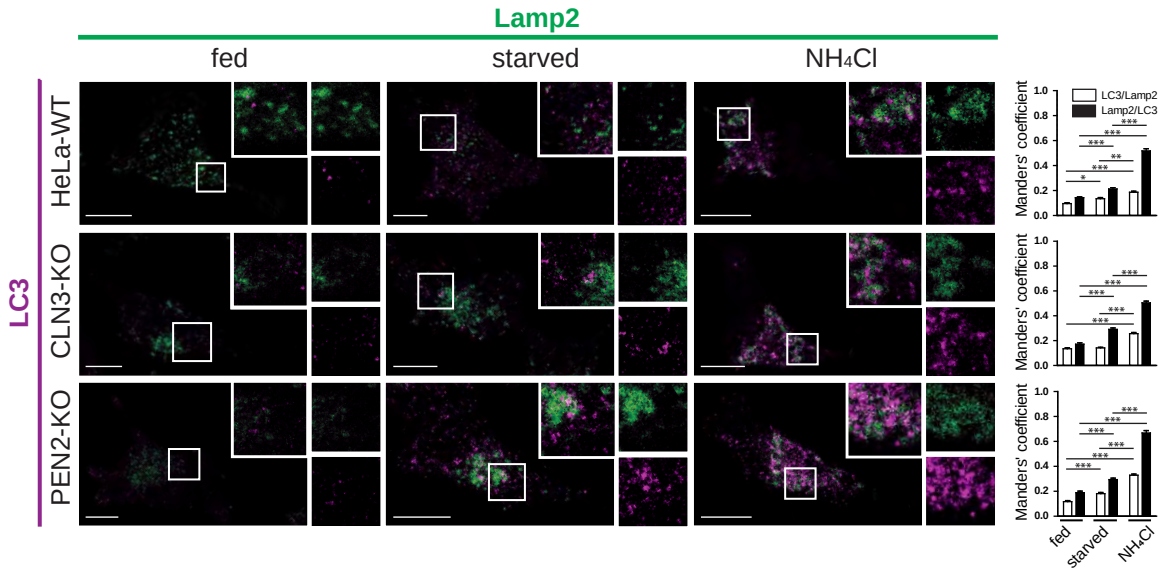

Figure S6. Representative images of Lamp2 and LC3 localization.
Representative confocal images of Lamp2 (green) and LC3 (magenta) immunocytochemical localization in fed HeLa-WT, CLN3-KO, PEN2-KO cells, 6h after starvation or 6 h after NH4Cl treatment. Scale bars: 10 µm. Plots on the right show respective Manders' coefficient of Lamp2 and LC3 co-localization. Values are means ± SD of n=50 cells pooled from three different experiments.

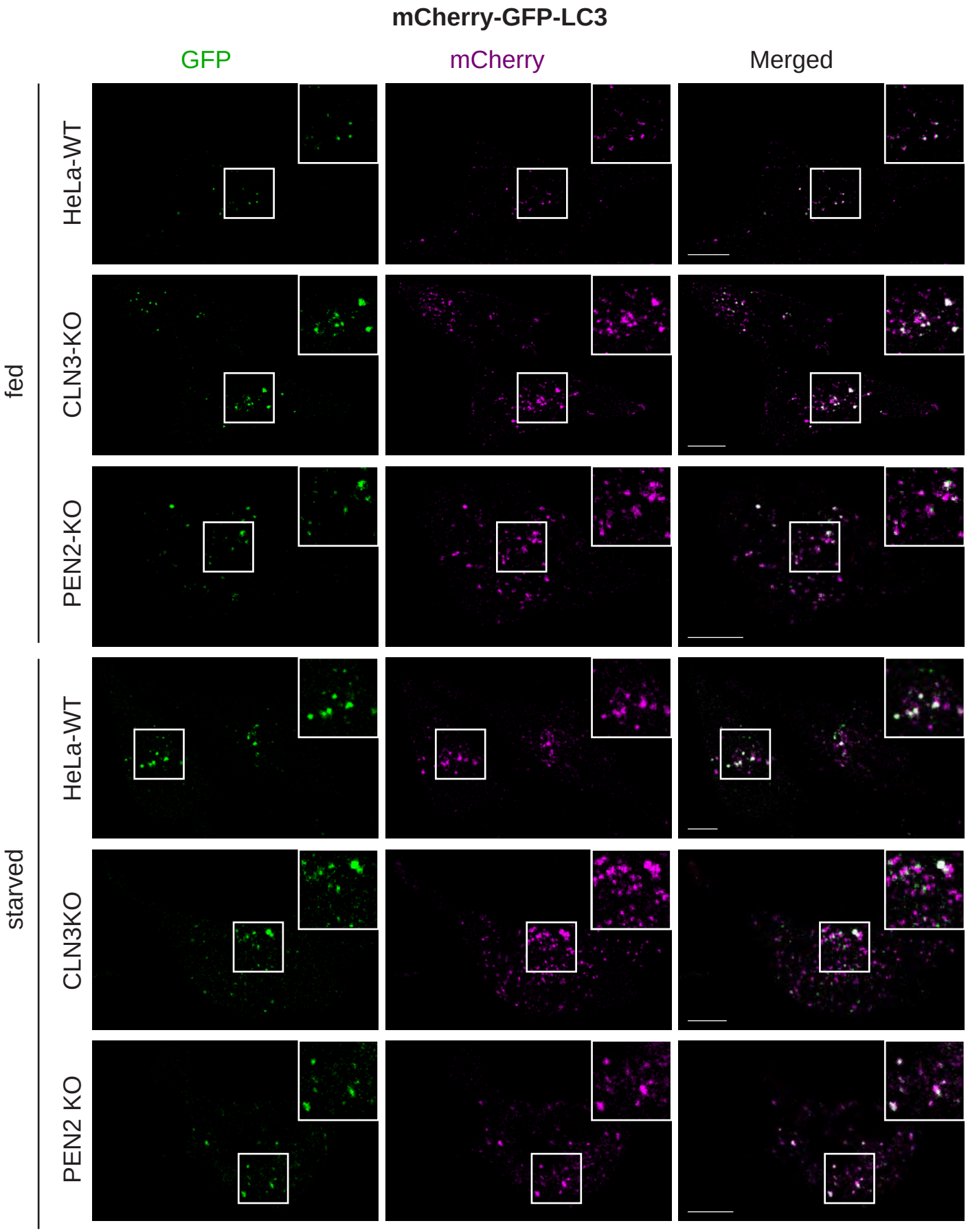

Figure S7. Representative images of cells expressing mCherry-GFP-LC3.
HeLa-WT, CLN3-KO or PEN2–KO cells were transfected with a mCherry-GFP-LC3 construct, cultured under control conditions (fed) or starved for 6 h in EBSS and analyzed by live confocal microscopy. The GFP signal is depicted in green (left panel), the mCherry signal is depicted in magenta (middle panel), colocalization occurs in white in the merged picture (right panel). Scale bars: 10 µm.

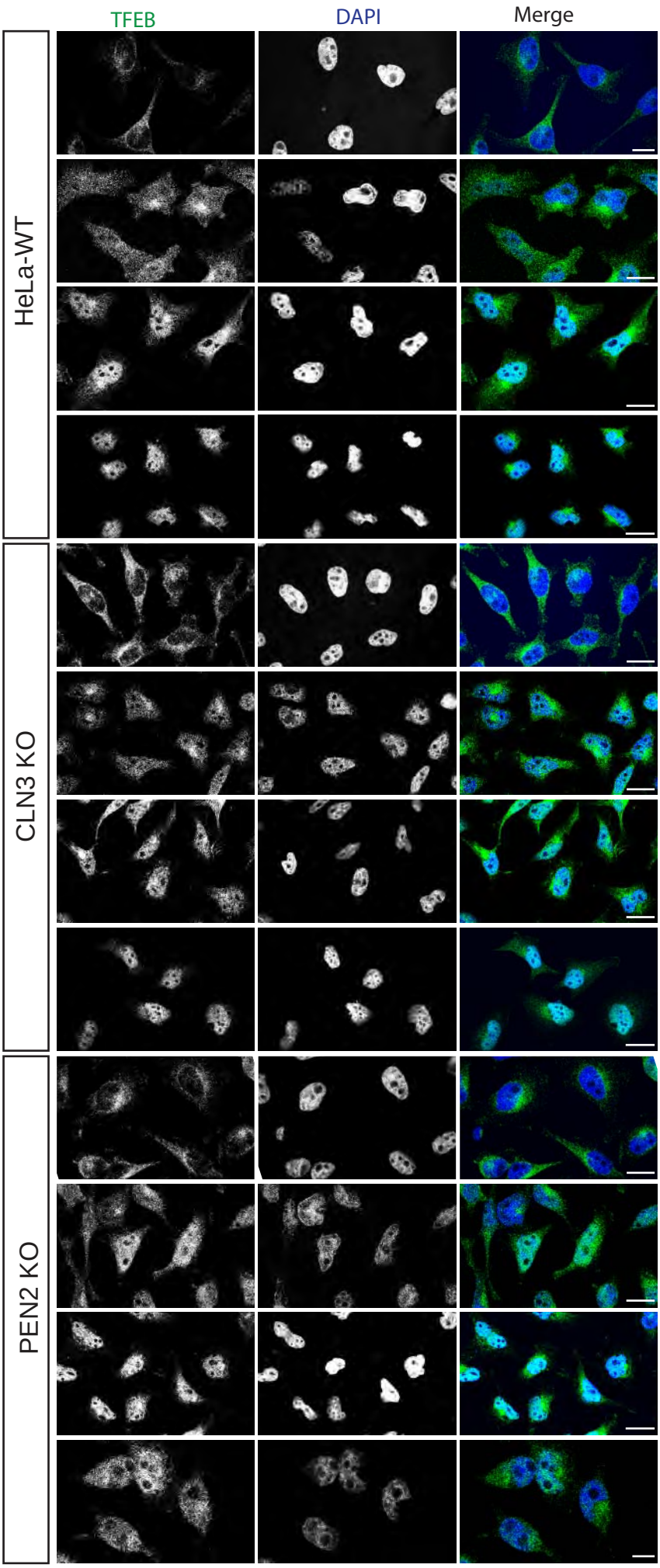

Figure S8. Representative images of TFEB nuclear translocation in WT, PEN2-KO and CLN3-KO cells

Images of TFEB immunolocalization in HeLa-WT, CLN3-KO and PEN2-KO cells under control conditions and 2 h, 4 h and 6 h after starvation. Scale bars: 10 µm.

3.

Converging links between adult-onset neurodegenerative Alzheimer's disease and early life neurodegenerative neuronal ceroid lipofuscinosis?

Marcel Klein and Guido Hermey

Review-Article

Neural Regen Res. 2023 Jul; 18(7), 1463-1471.
Epub ahead of print Dec. 2022.
DOI: 10.4103/1673-5374.361544

Personal contribution

Marcel Klein created the figure. Outline, literature search, writing and editorial work during the review process of the manuscript was performed by Marcel Klein and PD Dr. Guido Hermey.

21.12.2022 Hamburg

Date and City

Signature supervisor

PD Dr. Guido Hermey

Converging links between adult-onset neurodegenerative Alzheimer's disease and early life neurodegenerative neuronal ceroid lipofuscinosis?

Marcel Klein, Guido Hermey*

https://doi.org/10.4103/1673-5374.361544

Date of submission: September 19, 2022

Date of decision: October 10, 2022

Date of acceptance: October 26, 2022

Date of web publication: November 25, 2022

From the Contents

Abstract

Evidence from genetics and from analyzing cellular and animal models have converged to suggest links between neurodegenerative disorders of early and late life. Here, we summarize emerging links between the most common late life neurodegenerative disease, Alzheimer's disease, and the most common early life neurodegenerative diseases, neuronal ceroid lipofuscinoses. Genetic studies reported an overlap of clinically diagnosed Alzheimer's disease and mutations in genes known to cause neuronal ceroid lipofuscinoses. Accumulating data strongly suggest dysfunction of intracellular trafficking mechanisms and the autophagy-endolysosome system in both types of neurodegenerative disorders. This suggests shared cytopathological processes underlying these different types of neurodegenerative diseases. A better understanding of the common mechanisms underlying the different diseases is important as this might lead to the identification of novel targets for therapeutic concepts, the transfer of therapeutic strategies from one disease to the other and therapeutic approaches tailored to patients with specific mutations. Here, we review dysfunctions of the endolysosomal autophagy pathway in Alzheimer's disease and neuronal ceroid lipofuscinoses and summarize emerging etiologic and genetic overlaps.

Key Words: Alzheimer's disease; autophagy; Batten disease; CLN3 disease; dementia; endosome; lysosome; neurodegeneration; neuronal ceroid lipofuscinosis; presenilin

Introduction

Neurodegenerative diseases of early and late life demonstrate distinct clinical signatures and have traditionally been viewed independently. Early life neurodegenerative disorders are usually monogenetic and rare diseases. Whereas adult-onset neurodegenerative disorders are frequently genetically complex, with a high incidence rate among older adults, in several cases sporadic, and additionally driven by live style, environmental factors and therefore epigenetic modifications. In addition to the differential time of diagnosis and varying pathological hallmarks, neurodegenerative diseases can be categorized as disorders of specifically affected cellular pathways or organelles. Several monogenetic disorders have been classified by striking pathological abnormalities observed by biochemistry, cell biology or microscopy and include disorders of carbohydrate or amino acid metabolism, peroxisomal, mitochondrial or lysosomal disorders and the recently grouped autophagy disorders (Ballabio and Gieselmann, 2009; Ebrahimi-Fakhari et al., 2016; Sheng, 2017; Darios and Stevanin, 2020; Deb et al., 2021; Myerowitz et al., 2021). Several adult-onset neurodegenerative disorders show specific progressive abnormalities in varying organelles and can therefore also be classified accordingly.

Links between Parkinson's disease and Gaucher disease

Evidence from genetics and cellular and animal model investigations converged to suggest links between specific monogenetic early life and late life neurodegenerative diseases. An example of a rare disease linked to a common neurodegenerative disease is Gaucher disease (GD), a lysosomal storage disease that manifests early in life, which has been linked to Parkinson's disease (PD), one of the most common adult-onset neurodegenerative disorders. Epidemiological investigations disclosed hereditable forms causing familial autosomal dominant PD by mutations in the α-synuclein gene *SNCA* or *LRRK2* (de Lau and Breteler, 2006; Minakaki et al., 2020) and early onset autosomal recessive PD by mutations in *PARKIN*, *PINK1* or *DJ-1* (de Lau and Breteler, 2006; Minakaki et al., 2020). However, the majority of PD cases are regarded as sporadic and arise from an interplay of genetic and environmental factors. Today, known as the most common genetic risk factor for PD are heterozygous mutations in the glucocerebrosidase (GCase) gene *GBA1* (Sidransky et al., 2009). GCase is a lysosomal hydrolase that catalyzes the breakdown of glucosylceramide to glucose and ceramide. Heterozygous *GBA1* variants are thought to influence PD pathogenesis through multiple mechanisms. These include accumulation of misfolded GCase in the endoplasmic reticulum (ER), impairing ER-quality control, and its accumulation on the surface of lysosomes, inhibiting chaperone-mediated autophagy (CMA), resulting in impaired protein degradation and accumulation of GCase substrates (Ron and Horowitz, 2005; Mazzulli et al., 2011; Kuo et al., 2022a, b). Prior to its discovery as a PD risk locus, homozygous (or bi-allelic) missense mutations of *GBA1* were known to cause the autosomal recessive disorder GD (Roh et al., 2022). It results from GCase deficiency and the accumulation of its substrates within lysosomes leading to lysosomal dysfunction and impairments in the autophagy pathway (Roh et al., 2022). Due to the defective activity of a lysosomal protein and the accumulation of lysosomal storage material, GD is classified as a lysosomal storage disease and regarded as the most common form (Roh et al., 2022). Interestingly, there is also recent evidence for the involvement of additional lysosomal storage disease genes in PD risk (Robak et al., 2017; Huebecker et al., 2019). Moreover, patients affected by GD have a higher risk of PD (Goker-Alpan et al., 2004). Collectively, these findings classify PD on the cellular level also as a lysosomal disease. Different therapeutic strategies have been developed to treat GD employing enzyme replacement therapy and substrate reduction therapy involving small molecules (Do et al., 2019; Ivanova et al., 2021). Some of these strategies might actually as well be beneficial for PD patients. Congruously, a number of strategies targeting the GCase ceramide metabolism to improve autophagy-lysosome dynamics have been suggested to be therapeutic for both GD and PD (Bonam et al., 2019; Ysselstein et al., 2019). Together, findings from the last decades demonstrate how insights from a rare monogenic early life neurodegenerative disorder, such as GD, can direct research into the pathogenesis and therapy of a seemingly unrelated common and complex neurodegenerative disorder of late life such as PD. This raises the intriguing question whether there are also links between other late life and specific monogenetic early life neurodegenerative diseases.

Links between Alzheimer's disease and neuronal ceroid lipofuscinosis?

We recently reported biochemical and cellular evidence for converging roles of presenilin enhancer (PSENEN or PEN2) and ceroid-lipofuscinosis neuronal 3 (CLN3) in the autophagy-lysosome system (Klein et al., 2022). PEN2 is a subunit of the γ-secretase complex whose dysfunction relates to the adult-onset neurodegenerative disorder Alzheimer's disease (AD). Mutations in CLN3 are causative for CLN3 disease which belongs to the

Institute for Molecular and Cellular Cognition, Center for Molecular Neurobiology Hamburg, University Medical Center Hamburg-Eppendorf, Hamburg, Germany
***Correspondence to:** Guido Hermey, PhD, guido.hermey@zmnh.uni-hamburg.de.
https://orcid.org/0000-0003-4762-5262 (Guido Hermey); https://orcid.org/0000-0002-2365-9911 (Marcel Klein)

Funding: *The work was supported by the Deutsche Forschungsgemeinschaft (DFG; 425373668, HE 3220/4-1) (to GH).*
How to cite this article: *Klein M, Hermey G (2023) Converging links between adult-onset neurodegenerative Alzheimer's disease and early life neurodegenerative neuronal ceroid lipofuscinosis? Neural Regen Res 18(7):1463-1471.*

neuronal ceroid lipofuscinoses (NCLs), also named Batten disease, a group of neurodegenerative disorders of early life. On the cellular and molecular level, a growing number of independent studies strongly suggest dysfunction of intracellular trafficking and sorting mechanisms as well as of the autophagy-lysosome system in both types of neurodegenerative disorders (Festa et al., 2021; Kim et al., 2022). A better understanding of the shared mechanisms underlying the different diseases is important as this might lead to the identification of novel targets for therapeutic development, the transfer of therapeutic strategies from one disease to the other and therapeutic strategies tailored to patients with specific mutations.

In this review, we will highlight emerging links between the adult-onset neurodegenerative disorder AD and the early-onset neurodegenerative disorders NCL suggesting shared cytopathological processes underlying these different neurodegenerative diseases. We will first briefly introduce intracellular endosomal sorting and trafficking and the lysosome-autophagy system. We will then review dysfunction of these pathways in AD and NCL, and summarize etiologic and genetic overlaps.

Retrieval Strategy

To examine the published links between NCL and AD, we conducted a search of PubMed and Google Scholar between May and August 2022 without the restriction of publication dates for neurodegeneration, Alzheimer's disease, neuronal ceroid lipofuscinosis, Batten disease, CLN, intracellular sorting and trafficking, lysosome and autophagy.

Autophagy-Endolysosome System

Proteins are delivered post-translationally to specific subcellular compartments to exert their proper function. Protein sorting in the exo- and endocytic pathway occurs at three major sites, the Golgi complex, endosomes and the plasma membrane (**Figure 1**). Active transport of proteins is mediated by tubular or vesicular intermediates that bud from one compartment and fuse with the next. Adaptor proteins recognize sorting signals, short amino acid sequences in the cytosolic domains of transmembrane proteins, and convey selective transport (Bonifacino, 2014). Specific transmembrane proteins bind ligands through their luminal/extracellular domain and bind through their cytoplasmic domain adaptor proteins, which recruit additional components such as clathrin scaffolds and accessory proteins and direct receptor-ligand complexes to specific vesicle carriers (Braulke and Bonifacino, 2009). Secretory proteins synthesized in the ER are transported to the Golgi complex, sorted to secretory vesicles at the *trans*-Golgi network and targeted to the plasma membrane through regulated or constitutive pathways. At the plasma membrane transmembrane proteins can be internalized, enter early endosomes and segregate into separate trafficking itineraries. Transmembrane proteins can be recycled back to the plasma membrane through fast or slow recycling compartments. An alternative route directs internalized cargo from early endosomes to late endosomes, so-called multivesicular bodies, and retrogradely to the *trans*-Golgi network or further to lysosomes for degradation (Meraş et al., 2022; **Figure 1**). The majority of soluble lysosomal enzymes are modified with mannose 6-phosphate, allowing their recognition by mannose 6-phosphate receptors in the Golgi apparatus and their targeting to lysosomes. Other soluble lysosomal proteins are transported in a mannose 6-phosphate independent manner by alternative receptors, such as the lysosomal integral membrane protein 2 (LIMP2) or Sortilin (Braulke and Bonifacino, 2009). Lysosomes are degradative compartments that break down intracellular and exogenous substrates into their constituent building blocks. Pathogens, defective organelles or proteins and protein aggregates can be degraded by autophagy. Different types of autophagy are known, including macroautophagy, CMA and microautophagy. All route material to lysosomes for degradation (Fleming et al., 2022). Microautophagy mediates lysosomal degradation of cellular components through membrane invaginations in compartments of the endolysosomal system. In CMA, substrate proteins are targeted by the recognition of a KFERQ-like amino acid motif and translocated across the lysosomal membrane through a multimeric complex including the lysosome-associated membrane protein type 2A (LIMP-2A). Macroautophagy is an inducible catabolic process in which double membrane-bounded autophagosomes are formed around substrates and eventually fuse with lysosomes to autolysosomes for substrate degradation. The microtubule-associated protein 1 light chain 3 (LC3) plays key roles in macroautophagy and is frequently used as a marker protein for autophagosomes (Ballabio and Bonifacino, 2020). Lysosomes function also as metabolic signaling hubs. A key regulator of lysosomal function, nutrient sensing and regulation of gene expression is mammalian target of rapamycin complex 1 (mTORC1) that integrates nutrient availability and growth factor signaling. Downstream signaling of the multiprotein complex mTORC1 includes induction of autophagy and regulation of translation and transcription factors. Activation and inhibition of these different pathways are tightly regulated by phosphorylation of the different signal transducers. The transcription factor EB coordinates the expression of lysosomal and autophagy proteins in response to pathways sensing lysosomal stress and nutritional conditions (Ballabio and Bonifacino, 2020). Transcription factor EB localizes to the cytosol. Upon activation, it translocates to the nucleus and initiates gene expression.

Alzheimer's Disease

AD is the most prevalent progressive adult-onset neurodegenerative disorder characterized by cognitive and memory dysfunction. Hallmark

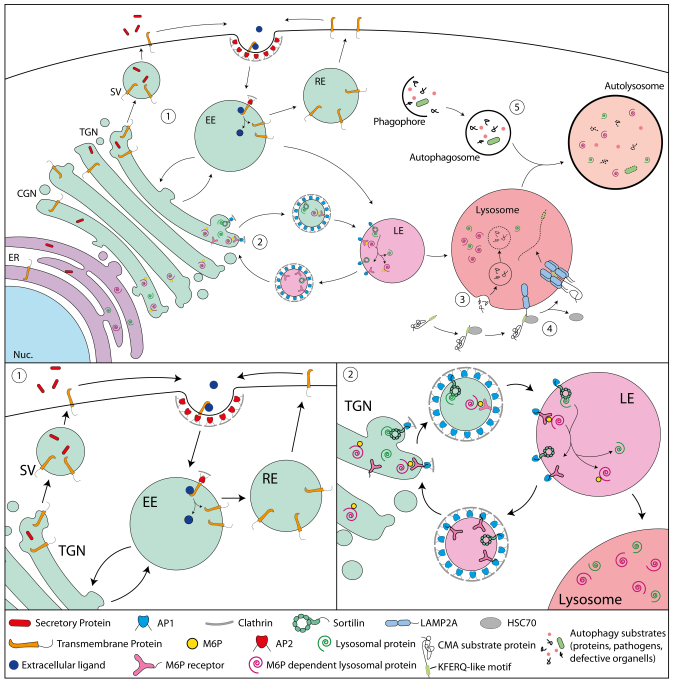

Figure 1 | Endosomal sorting and the lysosome-autophagosome system.
(1) After protein translation and folding, secretory and transmembrane proteins are transported from the endoplasmic reticulum (ER) to the Golgi apparatus and sorted towards the plasma membrane. Secretory proteins are released into the extracellular space. Transmembrane proteins presented at the cellular surface can interact with extracellular ligands. The cytosolic adapter protein 2 (AP2) mediates their internalization and targeting to early endosomes (EE). Transmembrane proteins are either recycled to the plasma membrane through recycling endosomes (RE) or transported retrograde to late endosomes (LE) or the *trans*-Golgi network (TGN). (2) Several lysosomal proteins are post-translationally modified with a mannose-6-phosphate (M6P) at the *cis*-Golgi network (CGN) and are then recognized by M6P receptors in the TGN. Other M6P independent lysosomal proteins interact with sorting receptors like Sortilin. Receptors interact with the cytosolic adapter protein 1 (AP1) and transport lysosomal proteins from the TGN to LE through clathrin coated vesicles. Lysosomal proteins then dissociate from their receptors due to low pH in LE and are targeted to lysosomes. (3) Microautophagy. Bulk of proteins can be taken up by invaginations and are then degraded in endolysosomal compartments. (4) Chaperone-mediated autophagy. Substrate proteins with a KFERQ-like amino acid motif bind to the chaperone heat-shock cognate protein of 70 kDa (HSC70), which guides them to the lysosomal protein lysosome-associated membrane protein type 2A (LAMP2A). The substrate protein unfolds its structure and is translocated by LAMP2 tetramers to the lysosomal lumen for degradation. (5) Macroautophagy. Proteins, protein aggregates, pathogens and defective organelles are enclosed by phagophores and form autophagosomes. Autophagosomes then fuse with lysosomes to form autolysosomes for degradation of the autophagy substrates.

histopathologies are intraneuronal neurofibrillary tangles, comprising the microtubule binding protein Tau, and extracellular amyloid plaques, composed of proteolytically cleaved amyloid β peptides (Aβ), which are fragments of the amyloid precursor protein (APP) (DeTure and Dickson, 2019). Genetic evidence strongly suggests that alterations in proteolytic APP processing have a significant impact on AD pathology. Dominantly inherited familial AD that manifests in the early twenties, with an average age of disease onset in the mid-forties, accounts for ~1% of AD cases (DeTure and Dickson, 2019). There are also other early onset forms of AD characterized by developing symptoms after 50 years and dementia in the mid-60s. Late onset AD is the most common form, accounting for ~95% of AD cases, regarded as sporadic and multifactorial with a high level of heritability.

The autophagy-endolysosome system in AD

Genomic studies identified genes linked to the development of the early onset familial forms and a larger number of genetic factors associated with increased risk for developing late onset AD. The encoded proteins have been functionally assigned to different biological pathways. Among the identified genetic variations, those found in genes coding for proteins related to the autophagy-endolysosome network attracted much attention, because of known prominent neuropathological features of the autophagy-endolysosome system in AD (Cataldo et al., 2000; Whyte et al., 2017). In addition, several studies strongly suggest that the genes in which mutations are causal for rare autosomal forms of AD encode proteins playing a role in the endosomal-lysosomal system (Wolfe et al., 2013; Nixon, 2017; Fleming et al., 2022; Szabo et al., 2022).

The prominent neuropathological features of the autophagy-endolysosome system in AD comprise an increase in size and volume of early endosomes, lysosomes and autophagic vacuoles, and an accumulation of lysosomal hydrolases, such as cathepsin D (CTSD) (Cataldo et al., 1991; Nixon, 2017; Whyte et al., 2017; Lee et al., 2022b). These findings suggest the deregulation

of the autophagy-endolysosome network in AD. Conversely, a gradual loss of CMA with age may be a risk factor for AD. CMA is inhibited in experimental models of tauopathies, in AD patient brains at an early disease stage and loss of CMA in a mouse model of AD accelerated disease progression (Bourdenx et al., 2021). Moreover, CMA deficiency increases the similarity between the proteomes of brains from an AD mouse model and AD patients, thus mimicking part of the disease. Furthermore, upregulation of CMA in two different mouse models of AD ameliorates the disease phenotype (Bourdenx et al., 2021).

Genes associated with familial AD

Mutations in *APP*, *PSEN1*, and *PSEN2* are causal for rare autosomal familial forms of AD and mutations in *SorL1* underlie additional rare early onset variants. APP, a type-I transmembrane protein, is sequentially processed by different enzymes in alternative pathways (Eggert et al., 2018; Checler et al., 2021). In one pathway, cleavage by β-secretase in the luminal/extracellular part produces the membrane embedded β-C-terminal fragment, also named C99. γ-Secretase cleaves this fragment and releases Aβ and the intracellular domain of APP. The proteolytic processing by β-secretase and subsequently by γ-secretase, regarded as the amyloidogenic pathway, occurs during APP's itinerary through the endolysosomal system. It has gained the most attention because it results in the plaque forming Aβ and mutations in APP and components of the γ-secretase have been genetically linked to familial forms of AD. γ-Secretase is composed of four transmembrane proteins PEN2, NCSTN, APH1 and presenilin 1 (PSEN1) or 2 (PSEN2), which harbor the catalytic site. Several mutations in *PSEN1* and *PSEN2* increase the production of Aβ. Cells co-express differing γ-secretase complexes including PSEN1 or PSEN2. PSEN1-containing complexes are broadly distributed in the cell whereas PSEN2 is mainly targeted to late endosomes and lysosomes (Meckler and Checler, 2016; Sannerud et al., 2016). In agreement, neuronal acidic compartments present γ-secretase activity (Maesako et al., 2022). Introduction of disease-causing mutations in or genetic ablation of *PSEN1* or *PSEN2* or depleting formation of γ-secretase by *PEN2* ablation results in altered lysosomal activity and accumulation of autophagosomes (Lee et al., 2010; Neely et al., 2011; Whyte et al., 2017; Fedeli et al., 2019; Klein et al., 2022). Initial studies proposed γ-secretase independent functions of PSENs in the autophagy-lysosome system because pharmacological inhibition of γ-secretase activity did not induce similar phenotypes as the genetic ablation, such as enlarged lysosomes and accumulation of the autophagosome marker LC3-II (Wilson et al., 2004; Neely et al., 2011). In contrast, other studies demonstrated the increased size of early endosomes, disrupted lysosomal proteolysis and autophagic impairment after pharmacological inhibition of γ-secretase (Jiang et al., 2010; Lauritzen et al., 2016; Hung and Livesey, 2018; Kwart et al., 2019). The congruent phenotype observed by genetic ablation, and pharmacological inhibition of PSENs suggests that the loss of γ-secretase activity is actually causing at least some of the observed alterations in the autophagy-endolysosome system. Notably, the introduction of mutations in *APP* and *PSEN1* causal for autosomal dominant early-onset monogenic AD led to converging defects in the autophagy-endolysosome system in human induced pluripotent stem cell (iPSC)-derived neurons (Hung and Livesey, 2018; Kwart et al., 2019). Checler and colleagues hypothesized that the PSEN1 phenotype relates to the accumulation of the C99 APP fragment, as β-secretase, but not γ-secretase, inhibition rescues the phenotype (Checler et al., 2021). Interestingly, C99 induces autophagy-lysosome impairments independently of Aβ (Lauritzen et al., 2016) and contains a KFERQ motif that could be utilized for its degradation through CMA (Fleming et al., 2022).

The sortilin-related receptor 1 (*Sorl1*) gene encodes SorLA, an established sorting receptor for APP, promotes retrograde sorting of APP from early endosomes to the *trans*-Golgi network and directs APP to a non-amyloidogenic pathway (Andersen et al., 2006). *SorL1* haploinsufficiency causes enlarged endosomes (Andersen et al., 2022) and *SorL1* ablation results in endosomal trafficking impairments and defects in the autophagy-endolysosome network (Knupp et al., 2020; Hung et al., 2021; Mishra et al., 2022). In conclusion, the genes linked to rare early onset forms of AD, *APP*, *PSEN1*, *PSEN2* and *SorL1*, encode proteins with proposed roles in the autophagy-endolysosome system.

Genes associated with sporadic AD

A large number of additional genes have been associated with AD risk and several of these relate to the autophagy-endolysosome system, too (Szabo et al., 2022). Among the encoded proteins are the SorLA related sorting receptors Sortilin and the sortilin related VPS10 domain containing receptor 1 (SorCS1) that also interact with APP, and the cytosolic regulators of endocytosis and trafficking, Bin1 and CALM (Reitz et al., 2011; Gustafsen et al., 2013; Hermey et al., 2015; Bellenguez et al., 2022).

Differentiated neurons with their long axons and complex dendritic trees are highly vulnerable to changes in the endolysosomal system, because they depend on functional long-range intracellular endosomal transport for proper function. In addition, neuronal cells are post mitotic and cannot dilute accumulated proteins by cell division. Thus, the defects in the autophagy-endolysosome system underlying AD may have a modest impact on autophagy-endolysosome function, but result in a long-term effect over lifetime probably in incorrect protein targeting, reduced degradation and accumulation of protein aggregates and finally cellular degeneration.

Together, AD occurs as sporadic forms with complex genetics or as monogenetic forms which have varying time points of manifestation. Different cellular mechanisms causing AD may exist in parallel, but accumulating evidence suggest that the autophagy-endolysosome pathway is critical to the pathology of AD.

Neuronal Ceroid Lipofuscinosis

NCLs, commonly named Batten disease, are a group of rare lysosomal storage disorders mainly affecting children and are considered the most common neurodegenerative disease in early life (Kohlschütter et al., 2019; Butz et al., 2020). NCLs are characterized by gradual neurodegeneration, including seizures and progressive loss of vision, motor function and cognition, and eventually premature death. The pathological hallmark is intracellular accumulation of autofluorescent lysosomal storage material, so-called lipofuscin (Mole et al., 2005; Radke et al., 2015). These deposits are found in neurons, but are also abundant in non-neuronal cells outside the nervous system. Depending on the subtype, the storage material is either predominantly composed of subunit C of the mitochondrial ATP synthase (SCMAS) or the sphingolipid activator proteins A and D (Mole et al., 2005; Radke et al., 2015; Butz et al., 2020). The storage material can comprise to a different degree additional components such as lysosomal proteins like palmitoyl protein thioesterase 1 (PPT1), tripeptidyl peptidase 1 (TPP1) and CTSD (Anderson et al., 2013), and strikingly, accumulation of Aβ has been reported in some cases (Wisniewski et al., 1990a; Wisniewski et al., 1990b; Herva et al., 2000). The age of disease manifestation differs between defined subtypes caused by mutations in different genes (Camp and Hofmann, 1993; Vesa et al., 1995; Wang et al., 1998; Lin et al., 2001; Steinfeld et al., 2006; Kohlschütter et al., 2019; Butz et al., 2020; Lee et al., 2022a; **Table 1**). The NCLs comprise 13 monogenetic diseases, which are all autosomal recessive and caused by homozygous or compound heterozygous mutations with the exception of the autosomal dominant CLN4 that is caused by heterozygous mutation in the *DNAJC5* gene (Kohlschütter et al., 2019). NCLs are thought to have partially shared, but also unique pathomechanisms involving alterations in the autophagy-endolysosome system (Huber, 2020; Nelvagal et al., 2020). In agreement, the majority of the disease-causing genes encode proteins with a predominant lysosomal localization, but some are located in other cellular compartments (**Table 1**).

Soluble CLN proteins

The CLN proteins can be classified into soluble and transmembrane proteins. The group of soluble proteins comprises lysosomal and cytosolic proteins. The lysosomal enzymes PPT1 (CLN1), TPP1 (CLN2), CTSD (CLN10) and cathepsin F (CTSF) (CLN13) are targeted directly from the Golgi to lysosomes where these hydrolases are activated (Butz et al., 2020). Whereas progranulin (granulin precursor, PGRN, encoded by the gene *GRN*) (CLN11) is either directly targeted from the Golgi to lysosomes or alternatively secreted to the extracellular space. Here, PGRN may be proteolytically processed to smaller peptides, so-called granulins, that possess function independent and sometimes in contrast to the granulin precursor, e.g. as a growth factor (Paushter et al., 2018). PGRN is translocated to lysosomes through direct interaction with the endocytic sorting receptor Sortilin (Hu et al., 2010) or through interaction with prosaposin and its receptors, mannose 6-phosphate receptor or low-density lipoprotein receptor-related protein 1 (LRP1), that mediate reuptake and intracellular targeting of the interactors to lysosomes (Zhou et al., 2015). Accumulating evidence suggests that lysosomal PGRN directly or indirectly regulates the activity of lysosomal enzymes such as CTSD or GCase (Paushter et al., 2018). Several soluble lysosomal CLN proteins, such as PPT1, TPP1, CTSD and CTSF, have been also detected extracellularly where these may serve additional functions (Huber, 2021).

Two soluble CLN proteins are cytosolic, DNAJC5 (CLN4) and KCTD7 (CLN14). DNAJC5 associates with endosomal and lysosomal membranes or perinuclear compartments (Benitez et al., 2011; Nosková et al., 2011; Lee et al., 2022a). Endolysosomal-associated DNAJC5 promotes ESCRT-dependent microautophagy and non-lysosomal DNAJC5 conveys misfolding-associated protein secretion (Lee et al., 2022a). KCTD7 ablation reduces lysosomal enzyme trafficking and causes lysosomal and autophagic defects (Wang et al., 2022). KCTD7 belongs to the BTB domain-containing adaptor subfamily (KCTD for potassium channel tetramerization domain). Several BTB domain-containing adaptors of the KCTD family act as substrate binding receptors for Cullin-3, a scaffolding protein component of E3 ubiquitin-ligase complexes that selectively tag proteins for degradation by the proteasome. Similarly, KCTD7 interacts with Cullin-3 and CLN14 patient-derived missense mutations in the BTB domain of KCTD7 disrupt the interaction with Cullin-3 (Staropoli et al., 2012). Moreover, KCTD7 serves as a Cullin-3 adaptor to recruit CLN5 to the ubiquitin-proteasome pathway (Wang et al., 2022).

Transmembrane CLN proteins

The remaining six CLN proteins are transmembrane proteins. CLN5 is a type-II transmembrane protein with a cytoplasmic N-terminus, one transmembrane domain and a large luminal C-terminal moiety. CLN5 is proteolytically processed (De Silva et al., 2015) and converted to a soluble form by signal peptidase and homologous signal peptidase-like proteases (Jules et al., 2017). One report suggested that CLN5 functions as a glycoside hydrolase, but endogenous substrates have not been identified (Huber and Mathavarajah, 2018). However, a more recent study identified CLN5 as a lysosomal cysteine-based S-depalmitoylase with the catalytic activity in the processed luminal moiety (Luebben et al., 2022). The other CLN transmembrane proteins are multi-spanning membrane proteins. These include the ER localized CLN6 and CLN8 that facilitate anterograde transport of lysosomal cargo from the ER to the Golgi (di Ronza et al., 2018; Bajaj et al., 2020). Moreover, CLN3 and

Table 1 | **Neuronal ceroid lipofuscinoses**

Disease	Typical age of manifestation*	Protein (gene)	Protein localization	Protein function
CLN1	Infantile (6–24 mon)	Palmitoyl protein thioesterase 1 (*PPT1*)	Lysosomal lumen, synaptic vesicles	S-depalmitoylase (long-chain fatty acyl hydrolase) (Camp and Hofmann, 1993; Vesa et al., 1995)
CLN2	Late infantile (2–4 yr)	Tripeptidyl peptidase 1 (*TPP1*)	Lysosomal lumen	Serine protease (Lin et al., 2001)
CLN3	Junvenile (4–10 yr)	CLN3 (*CLN3*)	Endolysosomal membrane	Unknown
CLN4	Adult (adult Kufs disease, Parry type)	Cysteine-string protein alpha, CSPα, DNAJC5 (*DNAJC5*)	Cytosol, association with endolysosomal membranes	Co-chaperone, conveys microautophagy and misfolding-associated protein secretion (Lee et al., 2022a)
CLN5	Late infantile (3–7 yr)	CLN5 (*CLN5*)	Endolysosomal	Cysteine based S-depalmitoylase (Luebben et al., 2022)
CLN6	Late infantile (1.5–8 yr)	CLN6 (*CLN6*)	Endoplasmic reticulum membrane	Involved in anterograde transport of lysosomal cargo (Bajaj et al., 2020)
CLN7	Late infantile (1.5–8 yr)	MFSD8 (*MFSD8*)	Endolysosomal membrane	Endolysosomal chloride channel (Wang et al., 2021)
CLN8	Late infantile (1.5–7 yr)	CLN8 (*CLN8*)	Endoplasmic reticulum/ endoplasmic reticulum Golgi intermediate compartment (ERGIC) membrane	Involved in anterograde transport of lysosomal cargo (di Ronza et al., 2018; Bajaj et al., 2020)
CLN10	Congenital (neonatal)	Cathepsin D (*CTSD*)	Lysosomal lumen	Aspartyl endoprotease (Steinfeld et al., 2006)
CLN11	Adult (early 20s)	Progranulin (*GRN*)	Lysosomal lumen, secretory pathway, secreted	Unknown (regulation of lysosomal enzyme activity?)
CLN12	Juvenile (8–12 yr)	ATP13A2, Park9 (*ATP13A2*)	Endolysosomal membrane	Polyamine transporter (van Veen et al., 2020)
CLN13	Adult (Kufs disease type B; 20+ yr)	Cathepsin F (*CTSF*)	Lysosomal lumen	Cysteine protease (Wang et al., 1998)
CLN14	Infantile/late infantile (8–9 mon)	Potassium channel tetramerization domain-containing protein 7 (*KCTD7*)	Cytosol	Cytosolic adaptor involved in transport and ubiquitin-proteasome degradation (Staropoli et al., 2012; Wang et al., 2022)

*The age of onset can deviate from the typical age of manifestation, as specific mutations can lead to a protracted course of the disease.

MFSD8 (CLN7) are mainly localized to lysosomes (Kyttälä et al., 2004; Storch et al., 2004; Steenhuis et al., 2010; Brandenstein et al., 2016; Oetjen et al., 2016). The function of CLN3 is still elusive. CLN3 has been constantly linked to the regulation of endosomal transport (Uusi-Rauva et al., 2012; Lojewski et al., 2014; Schmidtke et al., 2019; Yasa et al., 2020, 2021). Moreover, CLN3 loss of function studies demonstrate a role in lysosomal function, autophagy and phagocytosis (Cao et al., 2006; Chandrachud et al., 2015; Palmieri et al., 2017; Schmidtke et al., 2019; Zhong et al., 2020; Tang et al., 2021; Klein et al., 2022; Scotto Rosato et al., 2022). MFSD8 ablation causes alterations in lysosomal size, motility and exocytosis and impairs autophagy (Brandenstein et al., 2016; Danyukova et al., 2018; von Kleist et al., 2019; Lopez-Fabuel et al., 2022) and a function as an endolysosomal chloride channel has been recently reported (Wang et al., 2021). The transmembrane protein ATP13A2 (CLN12) is a member of the P5 subfamily of ATPases with a late endolysosomal localization (Ramirez et al., 2006). It functions as a polycation transporter that exports polyamines, specifically spermine, from lysosomes into the cytosol (van Veen et al., 2020).

Disease phenotypes and age of manifestation

Together, the CLN genes encode proteins that function in subcellular endosomal trafficking of lysosomal components or act in the lysosomal degradative pathway. Several NCL disease causing mutations in these proteins likely result in loss of function or dominant negative variants, in reduced lysosomal function and are associated with a characteristic disease phenotype with a typical age of manifestation (**Table 1**). With extending the use of exome sequencing in genetic disease diagnosis, it is more and more recognized that some mutations result in variable disease onset, severity, and progression and even in a clinically distinct phenotype (Kousi et al., 2012a; Butz et al., 2020). Several mutations underlie specific subphenotypes within the NCLs and can lead to a protracted course of the disease. For example, mutations in *CLN1* usually underlie classical infantile NCL with disease onset in the second half of the first year of life, but rare mutations in *CLN1* can cause also late infantile NCL with first symptoms occurring between 2 and 4 years of age, juvenile NCL with disease manifestation between 5 and 16 years and particularly rare adult forms (Kohlschütter et al., 2019).

Links to other neuronal diseases

Notably, several NCL genes have been linked to other neuronal diseases with an alternative clinical diagnosis (**Table 2**). Compound heterozygous mutations in the *TPP1* gene (CLN2) underlie a rare recessive type of spinocerebellar ataxia (Sun et al., 2013; Dy et al., 2015). Non-syndromic retinal degeneration and autophagic vacuolar myopathy have been also linked to mutations in *CLN3*. Specific homozygous or compound heterozygous mutations in *CLN6* lead to the development of the adult-onset Kufs type-A disease, a form of NCL without vision loss. These mutations appear to be mutually exclusive with those that underlie CLN6 disease (Arsov et al., 2011; Berkovic et al., 2019). Non-syndromic macular dystrophy can be caused by compound heterozygous mutations in *MFSD8* (CLN7) (Roosing et al., 2015). The gene has been also identified as a candidate risk factor for frontotemporal dementia (Geier et al., 2019) and amyotrophic lateral sclerosis (Huang et al., 2021). A form of progressive epilepsy with mental retardation, is caused by a mutation in the CLN8 gene (Ranta et al., 1999). *CTSD* (CLN10) has been genetically linked to PD (Robak et al., 2017). Homozygous or compound heterozygous mutations in *ATP13A2* (CLN12) cause the Kufor-Rakeb syndrome, a rare autosomal recessive form of juvenile-onset atypical PD (PARK9) (Ramirez et al., 2006) and biallelic mutations in ATP13A2 underlie autosomal recessive spastic paraplegia 78 (Estrada-Cuzcano et al., 2017). Homozygous or compound heterozygous mutations in *KCTD7* (CLN14) cause progressive myoclonic epilepsy-3, without NCL-type lysosomal storage (Van Bogaert et al., 2007; Kousi et al., 2012b; Krabichler et al., 2012).

GRN (CLN11) reveals an obvious link to late life neurodegeneration. Heterozygous mutations in *GRN*, resulting in haploinsufficiency, are the cause of frontotemporal lobar degeneration (FTLD) with TAR DNA-binding protein 43 (TDP-43) inclusions (Baker et al., 2006; Cruts et al., 2006; Gass et al., 2006). FTLD is a clinically heterogenous neurodegenerative disease characterized by progressive atrophy of the frontal and temporal lobes of the brain. Most often, it presents drastic alterations in behavior and personality, including social disinhibition as well as gradual decline in language capabilities. FTLD can be classified by clinical presentation, but also by common histopathological features which comprise inclusion bodies positive for tau protein (FTLD-Tau), ubiquitinated TDP-43 (FTLD-TDP) or fused-in sarcoma protein (FTLD-FUS). *GRN* mutations are primarily associated with the FTLD-TDP subtype. *GRN* mutations account for ~10% of all FTLD cases and ~20–25% of familial FTLD cases. NCL-related phenotypes, specifically elevated levels and accumulation of the NCL-like storage material, were observed in FTLD patients with *GRN* mutations (Götzl et al., 2014; Valdez et al., 2017; Ward et al., 2017) and some NCL-like features occurred already before dementia onset (Ward et al., 2017). These observations in autosomal dominant and recessive mutations point at converging pathological mechanisms underlying CLN11 disease and FTLD and dosage effects of PGRN are highly likely to playing a role in disease manifestation. Interestingly, a novel homozygous pathogenic variant in the *CTSF* gene was identified in a patient diagnosed with FTLD accompanied by parkinsonism (Gultekin et al., 2022) and, independently, heterozygous mutations in the *CTSF* gene were identified in FTLD patients (van der Zee et al., 2016), suggesting overlapping clinical features of CLN13 disease with FTLD.

Together, the autophagy-endolysosome pathway is critical to the pathology of NCLs. Some of the monogenetic NCLs present varying time points of manifestation. Independent mutations in several NCL genes can cause additional, clinically differentially diagnosed neuronal diseases.

Converging Links between Alzheimer's Disease and Neuronal Ceroid Lipofuscinosis

There is independent supporting evidence for an etiologic overlap between NCLs and AD. One arises from a study by Dolzhanskaya et al. (2014). A family with progressive dementia, motor deficits in their early 30s and lipofuscin containing phagocytic cells with distinct curvilinear lysosomal inclusion bodies was suspected to have CLN4 disease, but was negative for mutations in *DNAJC5*. Whole exome sequencing revealed a previously unknown mutation in *PSEN1*. Thus, the reported *PSEN1* mutation is associated with an unusually early onset dementia with a severe fast progressing disease course and lysosomal inclusions, previously believed to be specific for NCL (Dolzhanskaya et al., 2014).

Links from unexplained early onset AD cases

Examinations of unexplained early onset AD cases without clear inheritance patterns or mutations in *APP*, *PSEN1* or *PSEN2* and with two or more individuals with early onset AD identified a genomic region directly upstream of the *CLN3* gene using genetic linkage analysis (Cheng et al., 2018) and a missense variant in *CLN5* by whole-exome sequencing (Qureshi et al., 2018).

Table 2 | **Other diseases linked to *CLN* genes and their association with Alzheimer's disease**

Gene (neuronal ceroid lipofuscinose form)	Linkage to other neuronal diseases	Association with Alzheimer's disease
CLN1		CLN1 ablation results in altered targeting of the v-ATPase subunit V0a1 analogous to *PSEN1* knockout (Bagh et al., 2017)
TPP1 (CLN2)	Spinocerebellar ataxia, recessive type 7, caused by compound heterozygous mutation in the *TPP1* gene (Sun et al., 2013; Dy et al., 2015)	TPP1 promotes the degradation of amyloid β by cleavage of amyloid β fibrils *in vitro*, but elevated TPP1 levels do not ameliorate amyloid β accumulation *in vivo* (Solé-Domènech et al., 2018; Sleat et al., 2022)
CLN3	Non-syndromic retinal degeneration (retinitis pigmentosa, adult cone-rod dystrophy)	Examination of unexplained clinically diagnosed early onset Alzheimer's disease cases identified a genomic region directly upstream of the *CLN3* gene (Cheng et al., 2018)
		Pen2 and CLN3 ablation results in converging phenotypes in the autophagy-endolysosome system (Klein et al., 2022)
CLN5		Examination of unexplained clinically diagnosed early onset Alzheimer's disease cases identified rare missense variant in *CLN5* (Qureshi et al., 2018).
CLN6	Adult-onset Kufs disease, without vision loss, caused by homozygous or compound heterozygous mutations (Arsov et al., 2011; Berkovic et al., 2019)	
MFSD8 (CLN7)	Non-syndromic macular dystrophy caused by compound heterozygous mutation (Roosing et al., 2015)	
	Candidate risk factor for frontotemporal dementia (Geier et al., 2019)	
	Candidate risk factor for amyotrophic lateral sclerosis (Huang et al., 2021)	
CLN8	Northern epilepsy variant, without vision loss, also known as progressive epilepsy with mental retardation, caused by a homozygous mutation (Ranta et al., 1999)	
CTSD (CLN10)	Genetic linkage to Parkinson's disease (Robak et al., 2017).	Increased levels associate with Alzheimer's disease (Cataldo et al., 1991).
		Point mutations linked to Alzheimer's disease (Riemenschneider et al., 2006; Ehling et al., 2013).
GRN (CLN11)	Frontotemporal lobar degeneration with TAR DNA-binding protein 43 (TDP-43) inclusions, caused by heterozygous GRN mutations (Baker et al., 2006; Cruts et al., 2006; Gass et al., 2006)	Single-nucleotide polymorphism in the 3′-untranslated region is associated with Alzheimer's disease risk (Fenoglio et al., 2009; Viswanathan et al., 2009; Sheng et al., 2014; Xu et al., 2017)
ATP13A2 (CLN12)	Kufor-Rakeb syndrome (with Parkinsonism) caused by homozygous or compound heterozygous mutation (Ramirez et al., 2006)	
	Spastic paraplegia 78, autosomal recessive, caused by biallelic mutations (Estrada-Cuzcano et al., 2017)	
CTSF (CLN13)	Variant mutations in the gene suggest overlapping clinical features of CLN13 with frontotemporal lobar degeneration (van der Zee et al., 2016; Gultekin et al., 2022).	Examination of unexplained clinically diagnosed early onset Alzheimer's disease cases identified autosomal recessive gene variation (Bras et al., 2016).
KCTD7 (CLN14)	Progressive myoclonic epilepsy-3, without neuronal ceroid lipofuscinoses-type lysosomal storage, caused by homozygous or compound heterozygous mutation (Van Bogaert et al., 2007; Kousi et al., 2012b; Krabichler et al., 2012)	

In addition, *GRN* (CLN11) has been linked to AD pathophysiology. A single-nucleotide polymorphism in the 3′-untranslated region of *GRN* has been associated with AD risk (Fenoglio et al., 2009; Viswanathan et al., 2009; Sheng et al., 2014; Xu et al., 2017) and single nucleotide polymorphisms in intronic regions of *GRN* have been shown to increase the susceptibility for AD (Viswanathan et al., 2009). Moreover, an autosomal recessive *CTSF* (CLN13) gene variation in a clinically diagnosed early-onset AD family has been reported (Bras et al., 2016) and point mutations within the *CTSD* (CLN10) gene were linked to AD (Riemenschneider et al., 2006; Ehling et al., 2013). The latter findings are consistent with abnormal immunoreactivity of CTSD in senile plaques of AD patients, which already suggested a molecular link between CTSD and AD (Cataldo et al., 1991). However, the exact role of CTSD dysfunction in disease progression is not well understood, but investigations suggest that AD-associated variants of CTSD are enzymatically active, whereas CLN10-associated variants exhibited impairments of either CTSD maturation and/or enzymatic function (Bunk et al., 2021).

Links from cellular studies

In addition, cellular studies also suggest links between AD and NCL. Bagh and colleagues observed in *CLN1* ablated cells an altered targeting of the v-ATPase subunit V0a1 resulting in an endolysosomal phenotype analogous to that found in *PSEN1* knockouts (Lee et al., 2010; Bagh et al., 2017). TPP1 promotes the degradation of Aβ by cleavage of Aβ fibrils *in vitro* and this has been proposed as a therapeutic strategy to treat AD (Solé-Domènech et al., 2018). However, a subsequent study by the same research group demonstrated that elevated levels of TPP1 do not ameliorate pathogenesis in a mouse model of AD (Sleat et al., 2022). Early cellular studies suggested that overexpression of CLN3 modulates APP processing (Golabek et al., 2000). Our recent analysis demonstrates that *CLN3* ablation does not alter Aβ production or γ-secretase activity (Klein et al., 2022). However, we observed an interaction of the γ-secretase subunit Pen2 and CLN3, their co-expression, subcellular co-localization and endosomal co-transport. Using isogenic knockout cells for *Pen2* and *CLN3* respectively, we observed corresponding cellular alterations in the autophagy-endolysosome system (Klein et al., 2022). These include the reduced activity of lysosomal enzymes, an increased number of autophagosomes, increased lysosome-autophagosome fusion, and elevated levels of transcription factor EB. Our study strongly suggests converging roles of Pen2 and CLN3 in the autophagy-lysosome system supporting the idea of common cytopathological processes underlying an early and a late life neurodegenerative disease.

Taken together genetic studies suggest an overlap of clinically diagnosed AD and mutations in CLN genes and *vice versa* in one case clinically diagnosed NCL and a mutation in an AD gene. Moreover, cellular studies propose that NCL and AD risk genes functionally converge on the autophagy-endolysosome pathway. This convergence could allow for the buildup of shared therapeutic concepts and tools or the transfer of therapeutic strategies from one disease to the other. Such strategies may comprise pharmacological targeting of lysosome and autophagosome function, e.g lysosomal biogenesis or exocytosis. Accordingly, recent studies focused on the beneficial use of compounds modulating these pathways in NCL disease models (Soldati et al., 2021; Scotto Rosato et al., 2022).

Conclusion

Convergence between a rare neurodegenerative disease of early life and a "common" neurodegenerative disease of late life has been observed before, e.g. for GD and PD. Here, we summarized links between AD and NCLs and we found accumulating overlap.

Several overlapping data are based on clinical observations. These are complex considering that other dementia syndromes can mimic AD at the time of the initial evaluation, there is yet no single behavioral marker that can reliably discriminate AD from other dementias and AD often co-occurs with other pathologies at autopsy (Karantzoulis and Galvin, 2011). Apart from such diagnostic complexity, AD and NCLs present distinct clinical signatures. These may be explained in large parts by the different ages of onset. In NCLs, neurodegeneration occurs mostly in a still developing brain and not in a mature brain as in AD. The early neurodegeneration of neurons may cause several symptoms, such as frequently observed progressive epilepsies that are also found in other lysosomal childhood neurodegenerative diseases (Minassian, 2014). Notably, patients with common AD will in the most advanced stages develop also myoclonus, and patients with the aggressive AD of Down syndrome develop a typical and severe progressive myoclonus epilepsy. However, the time point of manifestation clearly results in modified clinical signatures and different severity as observed in classical *versus* protracted forms of NCLs or early onset *versus* late onset AD.

As summarized above, several studies demonstrate an etiologic and genetic overlap between NCLs and AD. Notably, the number of studies is still restricted and limits this review and our view on converging links between AD and NCLs. Extending the use of genetic disease diagnosis and genetic linkage analysis will be important to provide additional corroboration.

There is abundant evidence for dysfunction of the autophagy-endolysosome system contributing to the pathogenesis of both, AD and NCLs, and that this dysfunction is a major driver of neurodegeneration in both diseases. Different mutations and gene dosage effects are likely dictating the severity of dysfunction and the time point of manifestation in different subtypes. Loss of function or gradual residual functions may result in a phenotypic continuum ranging from severe and early onset to less severe, protracted, or late onset and even to asymptomatic cases. The severity of the diseases is likely also modulated by additional comorbidities and genetic risk factors.

The convergence of lysosomal and autophagy dysfunction could provide a foundation for the development of common therapeutic designs or the transfer of therapeutic strategies from one disease to the other. However, dysfunction of the autophagy-endolysosome system is not limited to NCLs and AD. Such dysfunction and progressive loss of nerve cells are commonly observed also in other neurodegenerative diseases, such as FTLD or PD. Strikingly, a distinct pattern of regional atrophy, neuronal degeneration and accumulation of specific material are characteristic pathological hallmarks of the individual disorders. Thus, lysosome and autophagosome dysfunction alone cannot explain the disease specific occurrence of neuronal vulnerability in each disease and understanding the specific underlying mechanisms is still a challenging task. However, the development of targeted therapies that enhance or repair lysosome and autophagosome function in the developing and aged brain may have broad therapeutic utility and are a particularly promising area for future research.

Acknowledgments: *The authors apologize to all colleagues whose important contributions to this field could not be cited due to space constrains.*
Author contributions: *MK and GH performed literature searches, outlined and wrote the manuscript. MK created the figure. Both authors approved the final manuscript.*
Conflicts of interest: *No potential conflict of interest by the authors.*

References

Andersen OM, Schmidt V, Spoelgen R, Gliemann J, Behlke J, Galatis D, McKinstry WJ, Parker MW, Masters CL, Hyman BT, Cappai R, Willnow TE (2006) Molecular dissection of the interaction between amyloid precursor protein and its neuronal trafficking receptor SorLA/LR11. Biochemistry 45:2618-2628.

Andersen OM, Bøgh N, Landau AM, Pløen GG, Jensen AMG, Monti G, Ulhøi BP, Nyengaard JR, Jacobsen KR, Jørgensen MM, Holm IE, Kristensen ML, Alstrup AKO, Hansen ESS, Teunissen CE, Breidenbach L, Droescher M, Liu Y, Pedersen HS, Callesen H, et al. (2022) A genetically modified minipig model for Alzheimer's disease with SORL1 haploinsufficiency. Cell Rep Med 3:100740.

Anderson GW, Goebel HH, Simonati A (2013) Human pathology in NCL. Biochim Biophys Acta 1832:1807-1826.

Arsov T, Smith KR, Damiano J, Franceschetti S, Canafoglia L, Bromhead CJ, Andermann E, Vears DF, Cossette P, Rajagopalan S, McDougall A, Sofia V, Farrell M, Aguglia U, Zini A, Meletti S, Morbin M, Mullen S, Andermann F, Mole SE, et al. (2011) Kufs disease, the major adult form of neuronal ceroid lipofuscinosis, caused by mutations in CLN6. Am J Hum Genet 88:566-573.

Bagh MB, Peng S, Chandra G, Zhang Z, Singh SP, Pattabiraman N, Liu A, Mukherjee AB (2017) Misrouting of v-ATPase subunit V0a1 dysregulates lysosomal acidification in a neurodegenerative lysosomal storage disease model. Nat Commun 8:14612.

Bajaj L, Sharma J, di Ronza A, Zhang P, Eblimit A, Pal R, Roman D, Collette JR, Booth C, Chang KT, Sifers RN, Jung SY, Weimer JM, Chen R, Schekman RW, Sardiello M (2020) A CLN6-CLN8 complex recruits lysosomal enzymes at the ER for Golgi transfer. J Clin Invest 130:4118-4132.

Baker M, Mackenzie IR, Pickering-Brown SM, Gass J, Rademakers R, Lindholm C, Snowden J, Adamson J, Sadovnick AD, Rollinson S, Cannon A, Dwosh E, Neary D, Melquist S, Richardson A, Dickson D, Berger Z, Eriksen J, Robinson T, Zehr C, et al. (2006) Mutations in progranulin cause tau-negative frontotemporal dementia linked to chromosome 17. Nature 442:916-919.

Ballabio A, Gieselmann V (2009) Lysosomal disorders: from storage to cellular damage. Biochim Biophys Acta 1793:684-696.

Ballabio A, Bonifacino JS (2020) Lysosomes as dynamic regulators of cell and organismal homeostasis. Nat Rev Mol Cell Biol 21:101-118.

Bellenguez C, Küçükali F, Jansen IE, Kleineidam L, Moreno-Grau S, Amin N, Naj AC, Campos-Martin R, Grenier-Boley B, Andrade V, Holmans PA, Boland A, Damotte V, van der Lee SJ, Costa MR, Kuulasmaa T, Yang Q, de Rojas I, Bis JC, Yaqub A, et al. (2022) New insights into the genetic etiology of Alzheimer's disease and related dementias. Nat Genet 54:412-436.

Benitez BA, Alvarado D, Cai Y, Mayo K, Chakraverty S, Norton J, Morris JC, Sands MS, Goate A, Cruchaga C (2011) Exome-sequencing confirms DNAJC5 mutations as cause of adult neuronal ceroid-lipofuscinosis. PLoS One 6:e26741.

Berkovic SF, Oliver KL, Canafoglia L, Krieger P, Damiano JA, Hildebrand MS, Morbin M, Vears DF, Sofia V, Giuliano L, Garavaglia B, Simonati A, Santorelli FM, Gambardella A, Labate A, Belcastro V, Castellotti B, Ozkara C, Zeman A, Rankin J, et al. (2019) Kufs disease due to mutation of CLN6: clinical, pathological and molecular genetic features. Brain 142:59-69.

Bonam SR, Wang F, Muller S (2019) Lysosomes as a therapeutic target. Nat Rev Drug Discov 18:923-948.

Bonifacino JS (2014) Adaptor proteins involved in polarized sorting. J Cell Biol 204:7-17.

Bourdenx M, Martín-Segura A, Scrivo A, Rodriguez-Navarro JA, Kaushik S, Tasset I, Diaz A, Storm NJ, Xin Q, Juste YR, Stevenson E, Luengo E, Clement CC, Choi SJ, Krogan NJ, Mosharov EV, Santambrogio L, Grueninger F, Collin L, Swaney DL, et al. (2021) Chaperone-mediated autophagy prevents collapse of the neuronal metastable proteome. Cell 184:2696-2714.e25.

Brandenstein L, Schweizer M, Sedlacik J, Fiehler J, Storch S (2016) Lysosomal dysfunction and impaired autophagy in a novel mouse model deficient for the lysosomal membrane protein Cln7. Hum Mol Genet 25:777-791.

Bras J, Djaldetti R, Alves AM, Mead S, Darwent L, Lleo A, Molinuevo JL, Blesa R, Singleton A, Hardy J, Clarimon J, Guerreiro R (2016) Exome sequencing in a consanguineous family clinically diagnosed with early-onset Alzheimer's disease identifies a homozygous CTSF mutation. Neurobiol Aging 46:236.e1-6.

Braulke T, Bonifacino JS (2009) Sorting of lysosomal proteins. Biochim Biophys Acta 1793:605-614.

Bunk J, Prieto Huarcaya S, Drobny A, Dobert JP, Walther L, Rose-John S, Arnold P, Zunke F (2021) Cathepsin D variants associated with neurodegenerative diseases show dysregulated functionality and modified α-synuclein degradation properties. Front Cell Dev Biol 9:581805.

Butz ES, Chandrachud U, Mole SE, Cotman SL (2020) Moving towards a new era of genomics in the neuronal ceroid lipofuscinoses. Biochim Biophys Acta Mol Basis Dis 1866:165571.

Camp LA, Hofmann SL (1993) Purification and properties of a palmitoyl-protein thioesterase that cleaves palmitate from H-Ras. J Biol Chem 268:22566-22574.

Cao Y, Espinola JA, Fossale E, Massey AC, Cuervo AM, MacDonald ME, Cotman SL (2006) Autophagy is disrupted in a knock-in mouse model of juvenile neuronal ceroid lipofuscinosis. J Biol Chem 281:20483-20493.

Cataldo AM, Paskevich PA, Kominami E, Nixon RA (1991) Lysosomal hydrolases of different classes are abnormally distributed in brains of patients with Alzheimer disease. Proc Natl Acad Sci U S A 88:10998-11002.

Cataldo AM, Peterhoff CM, Troncoso JC, Gomez-Isla T, Hyman BT, Nixon RA (2000) Endocytic pathway abnormalities precede amyloid beta deposition in sporadic Alzheimer's disease and Down syndrome: differential effects of APOE genotype and presenilin mutations. Am J Pathol 157:277-286.

Chandrachud U, Walker MW, Simas AM, Heetveld S, Petcherski A, Klein M, Oh H, Wolf P, Zhao WN, Norton S, Haggarty SJ, Lloyd-Evans E, Cotman SL (2015) Unbiased cell-based screening in a neuronal cell model of batten disease highlights an interaction between Ca2+ homeostasis, autophagy, and CLN3 protein function. J Biol Chem 290:14361-14380.

Checler F, Afram E, Pardossi-Piquard R, Lauritzen I (2021) Is γ-secretase a beneficial inactivating enzyme of the toxic APP C-terminal fragment C99? J Biol Chem 296:100489.

Cheng R, Tang M, Martinez I, Ayodele T, Baez P, Reyes-Dumeyer D, Lantigua R, Medrano M, Jimenez-Velazquez I, Lee JH, Beecham GW, Reitz C (2018) Linkage analysis of multiplex Caribbean Hispanic families loaded for unexplained early-onset cases identifies novel Alzheimer's disease loci. Alzheimers Dement (Amst) 10:554-562.

Cruts M, Gijselinck I, van der Zee J, Engelborghs S, Wils H, Pirici D, Rademakers R, Vandenberghe R, Dermaut B, Martin JJ, van Duijn C, Peeters K, Sciot R, Santens P, De Pooter T, Mattheijssens M, Van den Broeck M, Cuijt I, Vennekens K, De Deyn PP, et al. (2006) Null mutations in progranulin cause ubiquitin-positive frontotemporal dementia linked to chromosome 17q21. Nature 442:920-924.

Danyukova T, Ariunbat K, Thelen M, Brocke-Ahmadinejad N, Mole SE, Storch S (2018) Loss of CLN7 results in depletion of soluble lysosomal proteins and impaired mTOR reactivation. Hum Mol Genet 27:1711-1722.

Darios F, Stevanin G (2020) Impairment of lysosome function and autophagy in rare neurodegenerative diseases. J Mol Biol 432:2714-2734.

de Lau LM, Breteler MM (2006) Epidemiology of Parkinson's disease. Lancet Neurol 5:525-535.

De Silva B, Adams J, Lee SY (2015) Proteolytic processing of the neuronal ceroid lipofuscinosis related lysosomal protein CLN5. Exp Cell Res 338:45-53.

Deb R, Joshi N, Nagotu S (2021) Peroxisomes of the brain: distribution, functions, and associated diseases. Neurotox Res 39:986-1006.

DeTure MA, Dickson DW (2019) The neuropathological diagnosis of Alzheimer's disease. Mol Neurodegener 14:32.

di Ronza A, Bajaj L, Sharma J, Sanagasetti D, Lotfi P, Adamski CJ, Collette J, Palmieri M, Amawi A, Popp L, Chang KT, Meschini MC, Leung HE, Segatori L, Simonati A, Sifers RN, Santorelli FM, Sardiello M (2018) CLN8 is an endoplasmic reticulum cargo receptor that regulates lysosome biogenesis. Nat Cell Biol 20:1370-1377.

Do J, McKinney C, Sharma P, Sidransky E (2019) Glucocerebrosidase and its relevance to Parkinson disease. Mol Neurodegener 14:36.

Dolzhanskaya N, Gonzalez MA, Sperziani F, Stefl S, Messing J, Wen GY, Alexov E, Zuchner S, Velinov M (2014) A novel p.Leu(381)Phe mutation in presenilin 1 is associated with very early onset and unusually fast progressing dementia as well as lysosomal inclusions typically seen in Kufs disease. J Alzheimers Dis 39:23-27.

Dy ME, Sims KB, Friedman J (2015) TPP1 deficiency: rare cause of isolated childhood-onset progressive ataxia. Neurology 85:1259-1261.

Ebrahimi-Fakhari D, Saffari A, Wahlster L, Lu J, Byrne S, Hoffmann GF, Jungbluth H, Sahin M (2016) Congenital disorders of autophagy: an emerging novel class of inborn errors of neuro-metabolism. Brain 139:317-337.

Eggert S, Thomas C, Kins S, Hermey G (2018) Trafficking in Alzheimer's disease: modulation of APP transport and processing by the transmembrane proteins LRP1, SorLA, SorCS1c, Sortilin, and Calsyntenin. Mol Neurobiol 55:5809-5829.

Ehling R, Nosková L, Stránecký V, Hartmannová H, Přistoupilová A, Hodaňová K, Benke T, Kovacs GG, Ströbel T, Niedermüller U, Wagner M, Nachbauer W, Janecke A, Budka H, Boesch S, Kmoch S (2013) Cerebellar dysfunction in a family harboring the PSEN1 mutation co-segregating with a cathepsin D variant p.A58V. J Neurol Sci 326:75-82.

Estrada-Cuzcano A, Martin S, Chamova T, Synofzik M, Timmann D, Holemans T, Andreeva A, Reichbauer J, De Rycke R, Chang DI, van Veen S, Samuel J, Schöls L, Pöppel T, Mollerup Sørensen D, Asselbergh B, Klein C, Zuchner S, Jordanova A, Vangheluwe P, et al. (2017) Loss-of-function mutations in the ATP13A2/PARK9 gene cause complicated hereditary spastic paraplegia (SPG78). Brain 140:287-305.

Fedeli C, Filadi R, Rossi A, Mammucari C, Pizzo P (2019) PSEN2 (presenilin 2) mutants linked to familial Alzheimer disease impair autophagy by altering Ca(2+) homeostasis. Autophagy 15:2044-2062.

Fenoglio C, Galimberti D, Cortini F, Kauwe JS, Cruchaga C, Venturelli E, Villa C, Serpente M, Scalabrini D, Mayo K, Piccio LM, Clerici F, Albani D, Mariani C, Forloni G, Bresolin N, Goate AM, Scarpini E (2009) Rs5848 variant influences GRN mRNA levels in brain and peripheral mononuclear cells in patients with Alzheimer's disease. J Alzheimers Dis 18:603-612.

Festa BP, Barbosa AD, Rob M, Rubinsztein DC (2021) The pleiotropic roles of autophagy in Alzheimer's disease: From pathophysiology to therapy. Curr Opin Pharmacol 60:149-157.

Fleming A, Bourdenx M, Fujimaki M, Karabiyik C, Krause GJ, Lopez A, Martín-Segura A, Puri C, Scrivo A, Skidmore J, Son SM, Stamatakou E, Wrobel L, Zhu Y, Cuervo AM, Rubinsztein DC (2022) The different autophagy degradation pathways and neurodegeneration. Neuron 110:935-966.

Gass J, Cannon A, Mackenzie IR, Boeve B, Baker M, Adamson J, Crook R, Melquist S, Kuntz K, Petersen R, Josephs K, Pickering-Brown SM, Graff-Radford N, Uitti R, Dickson D, Wszolek Z, Gonzalez J, Beach TG, Bigio E, Johnson N, et al. (2006) Mutations in progranulin are a major cause of ubiquitin-positive frontotemporal lobar degeneration. Hum Mol Genet 15:2988-3001.

Geier EG, Bourdenx M, Storm NJ, Cochran JN, Sirkis DW, Hwang JH, Bonham LW, Ramos EM, Diaz A, Van Berlo V, Dokuru D, Nana AL, Karydas A, Balestra ME, Huang Y, Russo SP, Spina S, Grinberg LT, Seeley WW, Myers RM, et al. (2019) Rare variants in the neuronal ceroid lipofuscinosis gene MFSD8 are candidate risk factors for frontotemporal dementia. Acta Neuropathol 137:71-88.

Goker-Alpan O, Schiffmann R, LaMarca ME, Nussbaum RL, McInerney-Leo A, Sidransky E (2004) Parkinsonism among Gaucher disease carriers. J Med Genet 41:937-940.

Golabek AA, Kida E, Walus M, Kaczmarski W, Michalewski M, Wisniewski KE (2000) CLN3 protein regulates lysosomal pH and alters intracellular processing of Alzheimer's amyloid-beta protein precursor and cathepsin D in human cells. Mol Genet Metab 70:203-213.

Götzl JK, Mori K, Damme M, Fellerer K, Tahirovic S, Kleinberger G, Janssens J, van der Zee J, Lang CM, Kremmer E, Martin JJ, Engelborghs S, Kretzschmar HA, Arzberger T, Van Broeckhoven C, Haass C, Capell A (2014) Common pathobiochemical hallmarks of progranulin-associated frontotemporal lobar degeneration and neuronal ceroid lipofuscinosis. Acta Neuropathol 127:845-860.

Gultekin M, Tufekcioglu Z, Baydemir R (2022) Novel frameshift CTSF mutation causing kufs disease type B mimicking frontotemporal dementia-parkinsonism. Neurocase 28:107-109.

Gustafsen C, Glerup S, Pallesen LT, Olsen D, Andersen OM, Nykjær A, Madsen P, Petersen CM (2013) Sortilin and SorLA display distinct roles in processing and trafficking of amyloid precursor protein. J Neurosci 33:64-71.

Hermey G, Schmidt N, Bluhm B, Mensching D, Ostermann K, Rupp C, Kuhl D, Kins S (2015) SorCS1 variants and amyloid precursor protein (APP) are co-transported in neurons but only SorCS1c modulates anterograde APP transport. J Neurochem 135:60-75.

Herva R, Tyynelä J, Hirvasniemi A, Syrjäkallio-Ylitalo M, Haltia M (2000) Northern epilepsy: a novel form of neuronal ceroid-lipofuscinosis. Brain Pathol 10:215-222.

Hu F, Padukkavidana T, Vægter CB, Brady OA, Zheng Y, Mackenzie IR, Feldman HH, Nykjaer A, Strittmatter SM (2010) Sortilin-mediated endocytosis determines levels of the frontotemporal dementia protein, progranulin. Neuron 68:654-667.

Huang L, Liu Z, Yuan Y, Shen L, Jiang H, Tang B, Wang J, Lei L (2021) Mutation analysis of MFSD8 in an amyotrophic lateral sclerosis cohort from mainland China. Eur J Neurosci 53:1197-1206.

Huber RJ, Mathavarajah S (2018) Cln5 is secreted and functions as a glycoside hydrolase in Dictyostelium. Cell Signal 42:236-248.

Huber RJ (2020) Molecular networking in the neuronal ceroid lipofuscinoses: insights from mammalian models and the social amoeba Dictyostelium discoideum. J Biomed Sci 27:64.

Huber RJ (2021) Altered protein secretion in Batten disease. Dis Model Mech 14:dmm049152.

Huebecker M, Moloney EB, van der Spoel AC, Priestman DA, Isacson O, Hallett PJ, Platt FM (2019) Reduced sphingolipid hydrolase activities, substrate accumulation and ganglioside decline in Parkinson's disease. Mol Neurodegener 14:40.

Hung C, Tuck E, Stubbs V, van der Lee SJ, Aalfs C, van Spaendonk R, Scheltens P, Hardy J, Holstege H, Livesey FJ (2021) SORL1 deficiency in human excitatory neurons causes APP-dependent defects in the endolysosome-autophagy network. Cell Rep 35:109259.

Hung COY, Livesey FJ (2018) Altered γ-secretase processing of APP disrupts lysosome and autophagosome function in monogenic Alzheimer's disease. Cell Rep 25:3647-3660. e2.

Ivanova MM, Dao J, Kasaci N, Adewale B, Nazari S, Noll L, Fikry J, Sanati AH, Goker-Alpan O (2021) Cellular and biochemical response to chaperone versus substrate reduction therapies in neuropathic Gaucher disease. PLoS One 16:e0247211.

Jiang Y, Mullaney KA, Peterhoff CM, Che S, Schmidt SD, Boyer-Boiteau A, Ginsberg SD, Cataldo AM, Mathews PM, Nixon RA (2010) Alzheimer's-related endosome dysfunction in Down syndrome is Abeta-independent but requires APP and is reversed by BACE-1 inhibition. Proc Natl Acad Sci U S A 107:1630-1635.

Jules F, Sauvageau E, Dumaresq-Doiron K, Mazzaferri J, Haug-Kröper M, Fluhrer R, Costantino S, Lefrancois S (2017) CLN5 is cleaved by members of the SPP/SPPL family to produce a mature soluble protein. Exp Cell Res 357:40-50.

Karantzoulis S, Galvin JE (2011) Distinguishing Alzheimer's disease from other major forms of dementia. Expert Rev Neurother 11:1579-1591.

Kim WD, Wilson-Smillie M, Thanabalasingam A, Lefrancois S, Cotman SL, Huber RJ (2022) Autophagy in the neuronal ceroid lipofuscinoses (Batten disease). Front Cell Dev Biol 10:812728.

Klein M, Kaleem A, Oetjen S, Wünkhaus D, Binkle L, Schilling S, Gjorgjieva M, Scholz R, Gruber-Schoffnegger D, Storch S, Kins S, Drewes G, Hoffmeister-Ullerich S, Kuhl D, Hermey G (2022) Converging roles of PSENEN/PEN2 and CLN3 in the autophagy-lysosome system. Autophagy 18:2068-2085.

Knupp A, Mishra S, Martinez R, Braggin JE, Szabo M, Kinoshita C, Hailey DW, Small SA, Jayadev S, Young JE (2020) Depletion of the AD risk gene SORL1 selectively impairs neuronal endosomal traffic independent of amyloidogenic APP processing. Cell Rep 31:107719.

Kohlschütter A, Schulz A, Bartsch U, Storch S (2019) Current and emerging treatment strategies for neuronal ceroid lipofuscinoses. CNS Drugs 33:315-325.

Kousi M, Lehesjoki AE, Mole SE (2012a) Update of the mutation spectrum and clinical correlations of over 360 mutations in eight genes that underlie the neuronal ceroid lipofuscinoses. Hum Mutat 33:42-63.

Kousi M, Anttila V, Schulz A, Calafato S, Jakkula E, Riesch E, Myllykangas L, Kalimo H, Topçu M, Gökben S, Alehan F, Lemke JR, Alber M, Palotie A, Kopra O, Lehesjoki AE (2012b) Novel mutations consolidate KCTD7 as a progressive myoclonus epilepsy gene. J Med Genet 49:391-399.

Krabichler B, Rostasy K, Baumann M, Karall D, Scholl-Bürgi S, Schwarzer C, Gautsch K, Spreiz A, Kotzot D, Zschocke J, Fauth C, Haberlandt E (2012) Novel mutation in potassium channel related gene KCTD7 and progressive myoclonic epilepsy. Ann Hum Genet 76:326-331.

Kuo SH, Tasset I, Cuervo AM, Sulzer D (2022a) Misfolded GBA/β-glucocerebrosidase impairs ER-quality control by chaperone-mediated autophagy in Parkinson disease. Autophagy doi: 10.1080/15548627.2022.2071383.

Kuo SH, Tasset I, Cheng MM, Diaz A, Pan MK, Lieberman OJ, Hutten SJ, Alcalay RN, Kim S, Ximénez-Embún P, Fan L, Kim D, Ko HS, Yacoubian T, Kanter E, Liu L, Tang G, Muñoz J, Sardi SP, Li A, et al. (2022b) Mutant glucocerebrosidase impairs α-synuclein degradation by blockade of chaperone-mediated autophagy. Sci Adv 8:eabm6393.

Kwart D, Gregg A, Scheckel C, Murphy EA, Paquet D, Duffield M, Fak J, Olsen O, Darnell RB, Tessier-Lavigne M (2019) A large panel of isogenic APP and PSEN1 mutant human iPSC neurons reveals shared endosomal abnormalities mediated by APP β-CTFs, Not Aβ. Neuron 104:1022.

Kyttälä A, Ihrke G, Vesa J, Schell MJ, Luzio JP (2004) Two motifs target Batten disease protein CLN3 to lysosomes in transfected nonneuronal and neuronal cells. Mol Biol Cell 15:1313-1323.

Lauritzen I, Pardossi-Piquard R, Bourgeois A, Pagnotta S, Biferi MG, Barkats M, Lacor P, Klein W, Bauer C, Checler F (2016) Intraneuronal aggregation of the β-CTF fragment of APP (C99) induces Aβ-independent lysosomal-autophagic pathology. Acta Neuropathol 132:257-276.

Lee J, Xu Y, Saidi L, Xu M, Zinsmaier K, Ye Y (2022a) Abnormal triaging of misfolded proteins by adult neuronal ceroid lipofuscinosis-associated DNAJC5/CSPα mutants causes lipofuscin accumulation. Autophagy doi: 10.1080/15548627.2022.2065618.

Lee JH, Yu WH, Kumar A, Lee S, Mohan PS, Peterhoff CM, Wolfe DM, Martinez-Vicente M, Massey AC, Sovak G, Uchiyama Y, Westaway D, Cuervo AM, Nixon RA (2010) Lysosomal proteolysis and autophagy require presenilin 1 and are disrupted by Alzheimer-related PS1 mutations. Cell 141:1146-1158.

Lee JH, Yang DS, Goulbourne CN, Im E, Stavrides P, Pensalfini A, Chan H, Bouchet-Marquis C, Bleiwas C, Berg MJ, Huo C, Peddy J, Pawlik M, Levy E, Rao M, Staufenbiel M, Nixon RA (2022b) Faulty autolysosome acidification in Alzheimer's disease mouse models induces autophagic build-up of Aβ in neurons, yielding senile plaques. Nat Neurosci 25:688-701.

Lin L, Sohar I, Lackland H, Lobel P (2001) The human CLN2 protein/tripeptidyl-peptidase I is a serine protease that autoactivates at acidic pH. J Biol Chem 276:2249-2255.

Lojewski X, Staropoli JF, Biswas-Legrand S, Simas AM, Haliw L, Selig MK, Coppel SH, Goss KA, Petcherski A, Chandrachud U, Sheridan SD, Lucente D, Sims KB, Gusella JF, Sondhi D, Crystal RG, Reinhardt P, Sterneckert J, Schöler H, Haggarty SJ, et al. (2014) Human iPSC models of neuronal ceroid lipofuscinosis capture distinct effects of TPP1 and CLN3 mutations on the endocytic pathway. Hum Mol Genet 23:2005-2022.

Lopez-Fabuel I, Garcia-Macia M, Buondelmonte C, Burmistrova O, Bonora N, Alonso-Batan P, Morant-Ferrando B, Vicente-Gutierrez C, Jimenez-Blasco D, Quintana-Cabrera R, Fernandez E, Llop J, Ramos-Cabrer P, Sharaireh A, Guevara-Ferrer M, Fitzpatrick L, Thompton CD, McKay TR, Storch S, Medina DL, et al. (2022) Aberrant upregulation of the glycolytic enzyme PFKFB3 in CLN7 neuronal ceroid lipofuscinosis. Nat Commun 13:536.

Luebben AV, Bender D, Becker S, Crowther LM, Erven I, Hofmann K, Söding J, Klemp H, Bellotti C, Stäuble A, Qiu T, Kathayat RS, Dickinson BC, Gärtner J, Sheldrick GM, Krätzner R, Steinfeld R (2022) Cln5 represents a new type of cysteine-based S-depalmitoylase linked to neurodegeneration. Sci Adv 8:eabj8633.

Maesako M, Houser MCQ, Turchyna Y, Wolfe MS, Berezovska O (2022) Presenilin/γ-secretase activity is located in acidic compartments of live neurons. J Neurosci 42:145-154.

Mazzulli JR, Xu YH, Sun Y, Knight AL, McLean PJ, Caldwell GA, Sidransky E, Grabowski GA, Krainc D (2011) Gaucher disease glucocerebrosidase and α-synuclein form a bidirectional pathogenic loop in synucleinopathies. Cell 146:37-52.

Meckler X, Checler F (2016) Presenilin 1 and presenilin 2 target γ-secretase complexes to distinct cellular compartments. J Biol Chem 291:12821-12837.

Meraş İ, Maes J, Lefrancois S (2022) Mechanisms regulating the sorting of soluble lysosomal proteins. Biosci Rep 42:BSR20211856.

Minakaki G, Krainc D, Burbulla LF (2020) The convergence of alpha-synuclein, mitochondrial, and lysosomal pathways in vulnerability of midbrain dopaminergic neurons in Parkinson's disease. Front Cell Dev Biol 8:580634.

Minassian BA (2014) The progressive myoclonus epilepsies. Prog Brain Res 213:113-122.

Mishra S, Knupp A, Szabo MP, Williams CA, Kinoshita C, Hailey DW, Wang Y, Andersen OM, Young JE (2022) The Alzheimer's gene SORL1 is a regulator of endosomal traffic and recycling in human neurons. Cell Mol Life Sci 79:162.

Mole SE, Williams RE, Goebel HH (2005) Correlations between genotype, ultrastructural morphology and clinical phenotype in the neuronal ceroid lipofuscinoses. Neurogenetics 6:107-126.

Myerowitz R, Puertollano R, Raben N (2021) Impaired autophagy: the collateral damage of lysosomal storage disorders. EBioMedicine 63:103166.

Neely KM, Green KN, LaFerla FM (2011) Presenilin is necessary for efficient proteolysis through the autophagy-lysosome system in a γ-secretase-independent manner. J Neurosci 31:2781-2791.

Nelvagal HR, Lange J, Takahashi K, Tarczyluk-Wells MA, Cooper JD (2020) Pathomechanisms in the neuronal ceroid lipofuscinoses. Biochim Biophys Acta Mol Basis Dis 1866:165570.

Nixon RA (2017) Amyloid precursor protein and endosomal-lysosomal dysfunction in Alzheimer's disease: inseparable partners in a multifactorial disease. FASEB J 31:2729-2743.

Nosková L, Stránecký V, Hartmannová H, Přistoupilová A, Barešová V, Ivánek R, Hůlková H, Jahnová H, van der Zee J, Staropoli JF, Sims KB, Tyynelä J, Van Broeckhoven C, Nijssen PC, Mole SE, Elleder M, Kmoch S (2011) Mutations in DNAJC5, encoding cysteine-string protein alpha, cause autosomal-dominant adult-onset neuronal ceroid lipofuscinosis. Am J Hum Genet 89:241-252.

Oetjen S, Kuhl D, Hermey G (2016) Revisiting the neuronal localization and trafficking of CLN3 in juvenile neuronal ceroid lipofuscinosis. J Neurochem 139:456-470.

Palmieri M, Pal R, Nelvagal HR, Lotfi P, Stinnett GR, Seymour ML, Chaudhury A, Bajaj L, Bondar VV, Bremner L, Saleem U, Tse DY, Sanagasetti D, Wu SM, Neilson JR, Pereira FA, Pautler RG, Rodney GG, Cooper JD, Sardiello M (2017) mTORC1-independent TFEB activation via Akt inhibition promotes cellular clearance in neurodegenerative storage diseases. Nat Commun 8:14338.

Paushter DH, Du H, Feng T, Hu F (2018) The lysosomal function of progranulin, a guardian against neurodegeneration. Acta Neuropathol 136:1-17.

Qureshi YH, Patel VM, Berman DE, Kothiya MJ, Neufeld JL, Vardarajan B, Tang M, Reyes-Dumeyer D, Lantigua R, Medrano M, Jiménez-Velázquez IJ, Small SA, Reitz C (2018) An Alzheimer's disease-linked loss-of-function CLN5 variant impairs cathepsin d maturation, consistent with a retromer trafficking defect. Mol Cell Biol 38:e00011-18.

Radke J, Stenzel W, Goebel HH (2015) Human NCL Neuropathology. Biochim Biophys Acta 1852:2262-2266.

Ramirez A, Heimbach A, Gründemann J, Stiller B, Hampshire D, Cid LP, Goebel I, Mubaidin AF, Wriekat AL, Roeper J, Al-Din A, Hillmer AM, Karsak M, Liss B, Woods CG, Behrens MI, Kubisch C (2006) Hereditary parkinsonism with dementia is caused by mutations in ATP13A2, encoding a lysosomal type 5 P-type ATPase. Nat Genet 38:1184-1191.

Ranta S, Zhang Y, Ross B, Lonka L, Takkunen E, Messer A, Sharp J, Wheeler R, Kusumi K, Mole S, Liu W, Soares MB, Bonaldo MF, Hirvasniemi A, de la Chapelle A, Gilliam TC, Lehesjoki AE (1999) The neuronal ceroid lipofuscinoses in human EPMR and mnd mutant mice are associated with mutations in CLN8. Nat Genet 23:233-236.

Reitz C, Tokuhiro S, Clark LN, Conrad C, Vonsattel JP, Hazrati LN, Palotás A, Lantigua R, Medrano M, I ZJ-V, Vardarajan B, Simkin I, Haines JL, Pericak-Vance MA, Farrer LA, Lee JH, Rogaeva E, George-Hyslop PS, Mayeux R (2011) SORCS1 alters amyloid precursor protein processing and variants may increase Alzheimer's disease risk. Ann Neurol 69:47-64.

Riemenschneider M, Blennow K, Wagenpfeil S, Andreasen N, Prince JA, Laws SM, Förstl H, Kurz A (2006) The cathepsin D rs17571 polymorphism: effects on CSF tau concentrations in Alzheimer disease. Hum Mutat 27:532-537.

Robak LA, Jansen IE, van Rooij J, Uitterlinden AG, Kraaij R, Jankovic J, International Parkinson's Disease Genomics Consortium (IPDGC), Heutink P, Shulman JM (2017) Excessive burden of lysosomal storage disorder gene variants in Parkinson's disease. Brain 140:3191-3203.

Roh J, Subramanian S, Weinreb NJ, Kartha RV (2022) Gaucher disease- more than just a rare lipid storage disease. J Mol Med (Berl) 100:499-518.

Ron I, Horowitz M (2005) ER retention and degradation as the molecular basis underlying Gaucher disease heterogeneity. Hum Mol Genet 14:2387-2398.

Roosing S, van den Born LI, Sangermano R, Banfi S, Koenekoop RK, Zonneveld-Vrieling MN, Klaver CC, van Lith-Verhoeven JJ, Cremers FP, den Hollander AI, Hoyng CB (2015) Mutations in MFSD8, encoding a lysosomal membrane protein, are associated with nonsyndromic autosomal recessive macular dystrophy. Ophthalmology 122:170-179.

Sannerud R, Esselens C, Ejsmont P, Mattera R, Rochin L, Tharkeshwar AK, De Baets G, De Wever V, Habets R, Baert V, Vermeire W, Michiels C, Groot AJ, Wouters R, Dillen K, Vints K, Baatsen P, Munck S, Derua R, Waelkens E, et al. (2016) Restricted location of PSEN2/γ-secretase determines substrate specificity and generates an intracellular Aβ pool. Cell 166:193-208.

Schmidtke C, Tiede S, Thelen M, Käkelä R, Jabs S, Makrypidi G, Sylvester M, Schweizer M, Braren I, Brocke-Ahmadinejad N, Cotman SL, Schulz A, Gieselmann V, Braulke T (2019) Lysosomal proteome analysis reveals that CLN3-defective cells have multiple enzyme deficiencies associated with changes in intracellular trafficking. J Biol Chem 294:9592-9604.

Scotto Rosato A, Krogsaeter EK, Jaślan D, Abrahamian C, Montefusco S, Soldati C, Spix B, Pizzo MT, Grieco G, Böck J, Wyatt A, Wünkhaus D, Passon M, Stieglitz M, Keller M, Hermey G, Markmann S, Gruber-Schoffnegger D, Cotman S, Johannes L, et al. (2022) TPC2 rescues lysosomal storage in mucolipidosis type IV, Niemann-Pick type C1, and Batten disease. EMBO Mol Med 14:e15377.

Sheng J, Su L, Xu Z, Chen G (2014) Progranulin polymorphism rs5848 is associated with increased risk of Alzheimer's disease. Gene 542:141-145.

Sheng ZH (2017) The interplay of axonal energy homeostasis and mitochondrial trafficking and anchoring. Trends Cell Biol 27:403-416.

Sidransky E, Nalls MA, Aasly JO, Aharon-Peretz J, Annesi G, Barbosa ER, Bar-Shira A, Berg D, Bras J, Brice A, Chen CM, Clark LN, Condroyer C, De Marco EV, Dürr A, Eblan MJ, Fahn S, Farrer MJ, Fung HC, Gan-Or Z, et al. (2009) Multicenter analysis of glucocerebrosidase mutations in Parkinson's disease. N Engl J Med 361:1651-1661.

Sleat DE, Maita I, Banach-Petrosky W, Larrimore KE, Liu T, Cruz D, Baker L, Maxfield FR, Samuels B, Lobel P (2022) Elevated levels of tripeptidyl peptidase 1 do not ameliorate pathogenesis in a mouse model of Alzheimer disease. Neurobiol Aging 118:106-107.

Soldati C, Lopez-Fabuel I, Wanderlingh LG, Garcia-Macia M, Monfregola J, Esposito A, Napolitano G, Guevara-Ferrer M, Scotto Rosato A, Krogsaeter EK, Paquet D, Grimm CM, Montefusco S, Braulke T, Storch S, Mole SE, De Matteis MA, Ballabio A, Sampaio JL, McKay T, et al. (2021) Repurposing of tamoxifen ameliorates CLN3 and CLN7 disease phenotype. EMBO Mol Med 13:e13742.

Solé-Domènech S, Rojas AV, Maisuradze GG, Scheraga HA, Lobel P, Maxfield FR (2018) Lysosomal enzyme tripeptidyl peptidase 1 destabilizes fibrillar Aβ by multiple endoproteolytic cleavages within the β-sheet domain. Proc Natl Acad Sci U S A 115:1493-1498.

Staropoli JF, Karaa A, Lim ET, Kirby A, Elbalalesy N, Romansky SG, Leydiker KB, Coppel SH, Barone R, Xin W, MacDonald ME, Abdenur JE, Daly MJ, Sims KB, Cotman SL (2012) A homozygous mutation in KCTD7 links neuronal ceroid lipofuscinosis to the ubiquitin-proteasome system. Am J Hum Genet 91:202-208.

Steenhuis P, Herder S, Gelis S, Braulke T, Storch S (2010) Lysosomal targeting of the CLN7 membrane glycoprotein and transport via the plasma membrane require a dileucine motif. Traffic 11:987-1000.

Steinfeld R, Reinhardt K, Schreiber K, Hillebrand M, Kraetzner R, Bruck W, Saftig P, Gartner J (2006) Cathepsin D deficiency is associated with a human neurodegenerative disorder. Am J Hum Genet 78:988-998.

Storch S, Pohl S, Braulke T (2004) A dileucine motif and a cluster of acidic amino acids in the second cytoplasmic domain of the batten disease-related CLN3 protein are required for efficient lysosomal targeting. J Biol Chem 279:53625-53634.

Sun Y, Almomani R, Breedveld GJ, Santen GW, Aten E, Lefeber DJ, Hoff JI, Brusse E, Verheijen FW, Verdijk RM, Kriek M, Oostra B, Breuning MH, Losekoot M, den Dunnen JT, van de Warrenburg BP, Maat-Kievit AJ (2013) Autosomal recessive spinocerebellar ataxia 7 (SCAR7) is caused by variants in TPP1, the gene involved in classic late-infantile neuronal ceroid lipofuscinosis 2 disease (CLN2 disease). Hum Mutat 34:706-713.

Szabo MP, Mishra S, Knupp A, Young JE (2022) The role of Alzheimer's disease risk genes in endolysosomal pathways. Neurobiol Dis 162:105576.

Tang C, Han J, Dalvi S, Manian K, Winschel L, Volland S, Soto CA, Galloway CA, Spencer W, Roll M, Milliner C, Bonilha VL, Johnson TB, Latchney L, Weimer JM, Augustine EF, Mink JW, Gullapalli VK, Chung M, Williams DS, et al. (2021) A human model of Batten disease shows role of CLN3 in phagocytosis at the photoreceptor-RPE interface. Commun Biol 4:161.

Uusi-Rauva K, Kyttälä A, van der Kant R, Vesa J, Tanhuanpää K, Neefjes J, Olkkonen VM, Jalanko A (2012) Neuronal ceroid lipofuscinosis protein CLN3 interacts with motor proteins and modifies location of late endosomal compartments. Cell Mol Life Sci 69:2075-2089.

Valdez C, Wong YC, Schwake M, Bu G, Wszolek ZK, Krainc D (2017) Progranulin-mediated deficiency of cathepsin D results in FTD and NCL-like phenotypes in neurons derived from FTD patients. Hum Mol Genet 26:4861-4872.

Van Bogaert P, Azizieh R, Désir J, Aeby A, De Meirleir L, Laes JF, Christiaens F, Abramowicz MJ (2007) Mutation of a potassium channel-related gene in progressive myoclonic epilepsy. Ann Neurol 61:579-586.

van der Zee J, Mariën P, Crols R, Van Mossevelde S, Dillen L, Perrone F, Engelborghs S, Verhoeven J, D'Aes T, Ceuterick-De Groote C, Sieben A, Versijpt J, Cras P, Martin JJ, Van Broeckhoven C (2016) Mutated CTSF in adult-onset neuronal ceroid lipofuscinosis and FTD. Neurol Genet 2:e102.

van Veen S, Martin S, Van den Haute C, Benoy V, Lyons J, Vanhoutte R, Kahler JP, Decuypere JP, Gelders G, Lambie E, Zielich J, Swinnen JV, Annaert W, Agostinis P, Ghesquière B, Verhelst S, Baekelandt V, Eggermont J, Vangheluwe P (2020) ATP13A2 deficiency disrupts lysosomal polyamine export. Nature 578:419-424.

Vesa J, Hellsten E, Verkruyse LA, Camp LA, Rapola J, Santavuori P, Hofmann SL, Peltonen L (1995) Mutations in the palmitoyl protein thioesterase gene causing infantile neuronal ceroid lipofuscinosis. Nature 376:584-587.

Viswanathan J, Mäkinen P, Helisalmi S, Haapasalo A, Soininen H, Hiltunen M (2009) An association study between granulin gene polymorphisms and Alzheimer's disease in Finnish population. Am J Med Genet B Neuropsychiatr Genet 150B:747-750.

von Kleist L, Ariunbat K, Braren I, Stauber T, Storch S, Danyukova T (2019) A newly generated neuronal cell model of CLN7 disease reveals aberrant lysosome motility and impaired cell survival. Mol Genet Metab 126:196-205.

Wang B, Shi GP, Yao PM, Li Z, Chapman HA, Brömme D (1998) Human cathepsin F. Molecular cloning, functional expression, tissue localization, and enzymatic characterization. J Biol Chem 273:32000-32008.

Wang Y, Zeng W, Lin B, Yao Y, Li C, Hu W, Wu H, Huang J, Zhang M, Xue T, Ren D, Qu L, Cang C (2021) CLN7 is an organellar chloride channel regulating lysosomal function. Sci Adv 7:eabj9608.

Wang Y, Cao X, Liu P, Zeng W, Peng R, Shi Q, Feng K, Zhang P, Sun H, Wang C, Wang H (2022) KCTD7 mutations impair the trafficking of lysosomal enzymes through CLN5 accumulation to cause neuronal ceroid lipofuscinoses. Sci Adv 8:eabm5578.

Ward ME, Chen R, Huang HY, Ludwig C, Telpoukhovskaia M, Taubes A, Boudin H, Minami SS, Reichert M, Albrecht P, Gelfand JM, Cruz-Herranz A, Cordano C, Alavi MV, Leslie S, Seeley WW, Miller BL, Bigio E, Mesulam MM, Bogyo MS, et al. (2017) Individuals with progranulin haploinsufficiency exhibit features of neuronal ceroid lipofuscinosis. Sci Transl Med 9:eaah5642.

Whyte LS, Lau AA, Hemsley KM, Hopwood JJ, Sargeant TJ (2017) Endo-lysosomal and autophagic dysfunction: a driving factor in Alzheimer's disease? J Neurochem 140:703-717.

Wilson CA, Murphy DD, Giasson BI, Zhang B, Trojanowski JQ, Lee VM (2004) Degradative organelles containing mislocalized alpha-and beta-synuclein proliferate in presenilin-1 null neurons. J Cell Biol 165:335-346.

Wisniewski KE, Kida E, Gordon-Majszak W, Saitoh T (1990a) Altered amyloid beta-protein precursor processing in brains of patients with neuronal ceroid lipofuscinosis. Neurosci Lett 120:94-96.

Wisniewski KE, Maslinska D, Kitaguchi T, Kim KS, Goebel HH, Haltia M (1990b) Topographic heterogeneity of amyloid B-protein epitopes in brains with various forms of neuronal ceroid lipofuscinoses suggesting defective processing of amyloid precursor protein. Acta Neuropathol 80:26-34.

Wolfe DM, Lee JH, Kumar A, Lee S, Orenstein SJ, Nixon RA (2013) Autophagy failure in Alzheimer's disease and the role of defective lysosomal acidification. Eur J Neurosci 37:1949-1961.

Xu HM, Tan L, Wan Y, Tan MS, Zhang W, Zheng ZJ, Kong LL, Wang ZX, Jiang T, Tan L, Yu JT (2017) PGRN is associated with late-onset Alzheimer's disease: a case-control replication study and meta-analysis. Mol Neurobiol 54:1187-1195.

Yasa S, Modica G, Sauvageau E, Kaleem A, Hermey G, Lefrancois S (2020) CLN3 regulates endosomal function by modulating Rab7A-effector interactions. J Cell Sci 133:jcs234047.

Yasa S, Sauvageau E, Modica G, Lefrancois S (2021) CLN5 and CLN3 function as a complex to regulate endolysosome function. Biochem J 478:2339-2357.

Ysselstein D, Shulman JM, Krainc D (2019) Emerging links between pediatric lysosomal storage diseases and adult parkinsonism. Mov Disord 34:614-624.

Zhong Y, Mohan K, Liu J, Al-Attar A, Lin P, Flight RM, Sun Q, Warmoes MO, Deshpande RR, Liu H, Jung KS, Mitov MI, Lin N, Butterfield DA, Lu S, Liu J, Moseley HNB, Fan TWM, Kleinman ME, Wang QJ (2020) Loss of CLN3, the gene mutated in juvenile neuronal ceroid lipofuscinosis, leads to metabolic impairment and autophagy induction in retinal pigment epithelium. Biochim Biophys Acta Mol Basis Dis 1866:165883.

Zhou X, Sun L, Bastos de Oliveira F, Qi X, Brown WJ, Smolka MB, Sun Y, Hu F (2015) Prosaposin facilitates sortilin-independent lysosomal trafficking of progranulin. J Cell Biol 210:991-1002.

C-Editors: Zhao M, Liu WJ, Yu J; T-Editor: Jia Y

4.

The adaptor protein PICK1 targets the sorting receptor SorLA

Lars Binkle, Marcel Klein, Uwe Borgmeyer, Dietmar Kuhl and Guido Hermey

Research-Article

Mol Brain. 2022 Feb; 15(1), 18.
DOI: 10.1186/s13041-022-00903-0

Personal contribution

Experiments in Fig. 3 were performed by Marcel Klein and analyzed together by Marcel Klein and Dr. Lars Binkle. Experiments in Fig. 4 were performed by Marcel Klein and Dr. Lars Binkle and analyzed by Marcel Klein. Additional experiments during the review process were performed by Marcel Klein, Dr. Lars Binkle, and PD Dr. Guido Hermey.

21.12.2022 Hamburg

Date and City

Signature supervisor

PD Dr. Guido Hermey

Binkle *et al. Molecular Brain* (2022) 15:18
https://doi.org/10.1186/s13041-022-00903-0

Molecular Brain

SHORT REPORT Open Access

The adaptor protein PICK1 targets the sorting receptor SorLA

Lars Binkle, Marcel Klein, Uwe Borgmeyer, Dietmar Kuhl and Guido Hermey*

Abstract

SorLA is a member of the Vps10p-domain (Vps10p-D) receptor family of type-I transmembrane proteins conveying neuronal endosomal sorting. The extracellular/luminal moiety of SorLA has a unique mosaic domain composition and interacts with a large number of different and partially unrelated ligands, including the amyloid precursor protein as well as amyloid-β. Several studies support a strong association of SorLA with sporadic and familial forms of Alzheimer's disease (AD). Although SorLA seems to be an important factor in AD, the large number of different ligands suggests a role as a neuronal multifunctional receptor with additional intracellular sorting capacities. Therefore, understanding the determinants of SorLA's subcellular targeting might be pertinent for understanding neuronal endosomal sorting mechanisms in general. A number of cytosolic adaptor proteins have already been demonstrated to determine intracellular trafficking of SorLA. Most of these adaptors and several ligands of the extracellular/luminal moiety are shared with the Vps10p-D receptor Sortilin. Although SorLA and Sortilin show both a predominant intracellular and endosomal localization, they are targeted to different endosomal compartments. Thus, independent adaptor proteins may convey their differential endosomal targeting. Here, we hypothesized that Sortilin and SorLA interact with the cytosolic adaptors PSD95 and PICK1 which have been shown to bind the Vps10p-D receptor SorCS3. We observed only an interaction for SorLA and PICK1 in mammalian-two-hybrid, pull-down and cellular recruitment experiments. We demonstrate by mutational analysis that the C-terminal minimal PDZ domain binding motif VIA of SorLA mediates the interaction. Moreover, we show co-localization of SorLA and PICK1 at vesicular structures in primary neurons. Although the physiological role of the interaction between PICK1 and SorLA remains unsolved, our study suggests that PICK1 partakes in regulating SorLA's intracellular itinerary.

Keywords: SorLA, Sorting receptor, Vps10p-domain, PICK1, PDZ-domain, Protein interaction, Neuronal endosomal sorting and trafficking

Introduction

SorLA (also known as LR11 or SORL1) a transmembrane protein with a short cytosolic and a large extracellular/luminal part is prominently, but not exclusively, expressed in the brain [1–3]. It constitutes together with Sortilin, SorCS1, SorCS2 and SorCS3 the vacuolar protein sorting 10 domain (Vps10p-D) receptor family [4, 5]. SorLA's extracellular/luminal moiety has a unique domain composition. It consists of an N-terminal Vps10p-D, followed by EGF- and complement-type repeats, which are also characteristics of the low-density-lipoprotein receptor (LDLR) family, and fibronectin type-III domains. A large number of different ligands have been described to interact with SorLA. Some neuropeptides and growth factors, such as neurotensin, amyloid-β (Aβ), and ciliary and glial cell line-derived neurotrophic factor bind to the Vps10p-D [6–10]. Other ligands are shared with LDLRs and probably all interact with the cluster of complement-type repeats, including apolipoproteins, lipoprotein lipase, plasminogen activators and

*Correspondence: guido.hermey@zmnh.uni-hamburg.de
Institute for Molecular and Cellular Cognition, Center for Molecular Neurobiology Hamburg, University Medical Center Hamburg-Eppendorf, Falkenried 94, 20251 Hamburg, Germany

the amyloid precursor protein (APP) [1, 8, 11–14]. In addition, SorLA binds and regulates endosomal trafficking of ERBB2 (also termed HER2) [15].

Genetic analysis revealed an association of *SORL1* with both sporadic and familial forms of Alzheimer's disease (AD) [16]. AD brains show lower expression of SorLA [17], which was also observed in mouse models following amyloidosis [18, 19]. In mice, deletion of SorLA leads to elevated Aβ-levels in the brain and increased SorLA levels go along with a reduced Aβ load [20]. In neurons, SorLA alters the intracellular trafficking of APP and this reduces amyloidogenic processing [14, 20, 21]. Depending on pH, SorLA also binds Aβ in its monomeric form, which probably regulates lysosomal targeting of Aβ [6, 22]. These data substantiate SorLA's sorting function for APP and Aβ. Although SorLA seems an important factor in AD, the large number of different ligands suggests a role as a multifunctional receptor with additional, APP-independent, cellular functions.

SorLA locates to the TGN and endosomes and only a minority is found on the cell surface [8, 23, 24]. In polarized MDCK cells, SorLA is targeted to the basolateral membrane and to sorting endosomes, in cultured neurons, to the somato-dendritic area [25]. In SorLA deficient hiPSC-derived neurons, altered endosomal trafficking of APP was confirmed, but an overall endosome enlargement was also observed [26, 27]. SorLA ablation seemed to disrupt endosomal cargo processing and cause intracellular traffic jams, supporting a broader role in regulating endosomal transport and sorting [26, 27]. Therefore, understanding the determinants of SorLA's subcellular itinerary might be pertinent for understanding neuronal endosomal sorting in general.

Cellular uptake of ligands conveyed by SorLA is rather slow when compared to LDLRs such as LRP1 [11]. The cytoplasmic domain contains canonical binding motifs, and the interaction of several cytosolic adaptors has been reported. SorLA interacts with adaptor protein-2 (AP-2), AP-1, GGAs, and retromer [28–31]. It is of note, that these adaptors and many ligands of the extracellular/luminal moiety are shared with the Vps10p-D receptor Sortilin. Although SorLA and Sortilin show both a predominant intracellular and endosomal localization, they are targeted to different endosomal compartments [24, 28]. This indicates differential subcellular sorting of both receptors by exclusive adaptor proteins interacting only with one of the two receptors. So far, the cytosolic adaptor HSPA12A has been shown to target specifically the cytoplasmic domain of SorLA but not of Sortilin [32].

To date, only a few adaptor proteins have been described to bind the cytosolic domains of the SorCS subset of Vps10p-D receptors. SorCS1 interacts with AP-2 that likely mediates the internalization of all Vps10p-D receptors [33]. The SorCS3 cytosolic domain binds the PDZ (postsynaptic density-95/disc-large/zona-occludens-1) domain proteins PSD95 and PICK1 [34]. Here, we hypothesized that Sortilin and SorLA share these interactions. We assessed the binding of PSD95 and PICK1 to Sortilin and SorLA and observed an interaction only for SorLA and PICK1.

PICK1 has a unique domain composition with a single N-terminal PDZ domain followed by a BAR (Bin-Amphiphysin-Rvs) domain [35, 36]. PICK1 has been first described as an interactor and substrate of protein kinase C [37]. In addition, the PDZ domain mediates binding to the C-termini of many transmembrane proteins, ion channels and kinases, including the AMPA receptor subunit GluA2, mGluR7, monoamine transporters, ADP ribosylation factors, and ERBB2 [36, 38–44]. The BAR domain is a protein module thought to induce and stabilize lipid membrane curvature [45]. In agreement, an amphipathic helix N-terminal to the PICK1 BAR domain conveys membrane curvature sensing [46]. Initial studies demonstrated a prominent perinuclear localization of PICK1 [37]. Subsequent studies demonstrated localization of PICK1 to Golgi compartments and secretory vesicles [47, 48]. It plays a critical role in the budding of immature secretory vesicles from the TGN [48], and in secretory vesicle biogenesis [47, 49]. In neurons, PICK1 localizes to pre- and postsynaptic membranes [38, 50, 51]. It controls activity-regulated synaptic endosomal cargo retrieval at presynaptic nerve terminals [50]. At postsynaptic membranes, PICK1 binds GluA2 and is participating in NMDA receptor-induced calcium-dependent internalization of AMPA receptors, a critical process for multiple forms of synaptic plasticity [35, 52–57].

The PICK1 PDZ domain tethers transmembrane proteins as cargo and the BAR domain binds curved-membranes which can bud and form transport vesicles. It becomes fully functional through homo- or hetero-dimerization with another BAR domain protein. PICK1 constitutes a heteromeric BAR-domain complex with ICA69 [47, 48]. These complexes are mainly localized to the TGN, on budding immature dense core vesicles containing either proinsulin (in pancreactic beta cells) or growth hormone (in pituitary cells). In contrast, PICK1-positive but ICA69-negative complexes that are likely PICK1 homomeric complexes are found at mature secretory granules [47, 48]. Moreover, a change from PICK1-ICA69 heterodimers to PICK1 homodimers has been suggested to control the neuronal trafficking of AMPA receptors to synapses [58].

Although the physiological significance of the interaction of PICK1 and several of its ligands remains poorly understood, PICK1 regulates the trafficking of

transmembrane proteins through binding their C-termini with its PDZ domain.

Results

We investigated the potential interaction of the cytoplasmic domains of SorLA and Sortilin with PICK1 by mammalian-2-hybrid analysis (Fig. 1A, B). The mammalian 2-hybrid system is based on the yeast DNA-binding domain (DBD) of GAL4 and the transcription activation domain (TAD) VP16 of the herpes simplex virus. Both domains are separated and reconstitution occurs only by interaction of fused proteins (Fig. 1A). When reconstituted, DBD binds to an upstream activating sequence (UAS) and TAD drives firefly luciferase (Luc) expression from a reporter plasmid. To analyze the interaction of SorLA and Sortilin with PICK1, we fused the cytoplasmic domain of SorLA as well as of Sortilin with the DBD and fused PICK1 with the TAD (Fig. 1A). The luciferase activity of transfected N2a cells showed binding of PICK1 to the cytoplasmic domain of SorLA (SorLA-CD), but not to the cytoplasmic domain of Sortilin (Sortilin-CD) (Fig. 1B, C). To demonstrate the specificity of the interaction, we generated SorLA-CD mutants and analyzed their binding capabilities to PICK1 (Fig. 1C). PICK1 binding was abolished by mutating I^{53} or V^{52} and I^{53} to alanine (Fig. 1C). Mutation of only V^{52} showed an attenuated interaction. There was no detectable PICK1 binding when the C-terminal amino acids were removed. Mutations of M^{51} or P^{50} to alanine or to a basic or acidic amino acid did not affect the binding. Moreover, mutations of

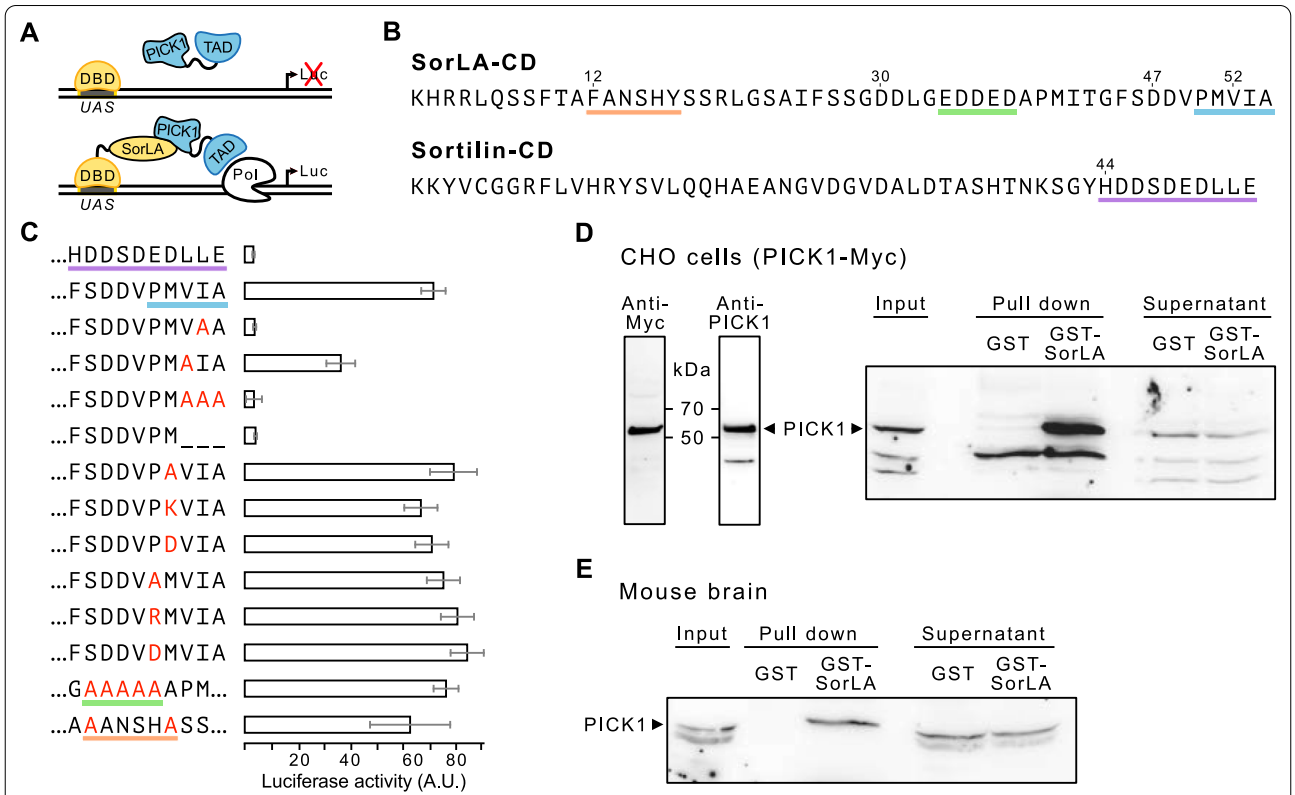

Fig. 1 SorLA interacts with PICK1. **A** Principle of the mammalian-2-hybrid system. DBD, DNA-binding domain; Luc, firefly luciferase; Pol, polymerase; TAD, transcription activation domain; UAS, upstream activating sequence. **B** Primary sequence of the SorLA cytoplasmic domain (CD) (top) and of the Sortilin cytoplasmic domain. Protein interaction motifs mutated in (**C**) are underlined. **C** Mammalian-2-Hybrid analysis of PICK1 with the cytoplasmic domain of Sortilin or SorLA. Co-transfections of N2a cells with fusion constructs of the GAL4 DNA binding domain with wild-type Sortilin or SorLA or the mutant cytoplasmic domain of SorLA and a fusion construct of the VP16 transcriptional activation domain with full length PICK1 were analyzed. Terminal or mutated amino acid sequences of the cytoplasmic domains are indicated on the left. Motifs marked in (**B**) are indicated with the same color code. Luciferase activity was normalized to the fluorescence generated by a co-transfected eGFP vector. Relative luciferase activity (mean ± SD) based on a typical experiment performed in septuplicate. **D** Detection of PICK1-Myc in stably transfected CHO-cells by immunoblotting using an anti-Myc or anti-PICK1 antibody (left). Pull-down of PICK1-Myc from stably transfected CHO-cells (right). Precipitation was performed with GST or GST fused to the cytoplasmic domain of SorLA and analyzed by immunoblotting using an anti-Pick1 antibody. **E** Pull down of PICK1 from murine brain lysates. GST or GST fused to the cytoplasmic domain of SorLA was used to pull down from brain lysates and analyzed by immunoblotting using an anti-PICK1 antibody

the pentameric acidic cluster E^{34}-D^{38} to AAAAA (Fig. 1B, C indicated in green), which is essential for interaction with AP-1 and AP-2 [28] as well as alanine mutations of the retromer interaction motif FANSHY to AANSHA [29] (Fig. 1B, C indicated in orange) did not alter the binding. These analyses demonstrate an interaction of PICK1 with the C-terminus of SorLA-CD of which the three C-terminal amino acids appear critical for binding. To corroborate the observed interaction, we performed GST pull-down experiments. We stably transfected CHO cells with Myc-tagged PICK1 and confirmed the expression through immunoblot analysis using anti-Myc and anti-PICK1 antibodies demonstrating the specificity of the applied anti-PICK1 antibody (Fig. 1D). A fusion protein of GST and SorLA-CD but not GST alone pulled down PICK1-myc from lysates of the stable transfectants (Fig. 1D). Subsequently, we used GST and GST-SorLA to pull-down proteins from mouse brain extracts and PICK1 was detected only in the GST-SorLA fraction (Fig. 1E).

To study the interaction in a physiological cellular environment, we ectopically expressed the SorLA-CD or Sortilin-CD in COS7 cells and analyzed subsequent recruitment of PICK1, GGA2 or PSD95 to the ectopic site. GGA2 has been shown before to interact with Sortilin and SorLA [30, 59]. Ectopic expression of the SorLA and Sortilin cytoplasmic domains on mitochondria was achieved by their fusion to the first 88 amino acids of the yeast mitochondrial protein Tom70 (T70). The fluorophore mVenus (mV) was inserted between T70 and the cytoplasmic domains (CD) for visualization and these constructs were named T70mV-SorLA-CD and T70mV-Sortilin-CD respectively. We used the fusion of nanoLuc luciferase (nanoLuc) to T70mV as a negative control. Co-expression of T70mV-SorLA-CD and tdTomato-PICK1 or tdTomato-GGA2, but not of PSD95-tdTomato, resulted in the recruitment of tdTomato tagged proteins to mitochondria (Fig. 2A). T70mV-Sortilin-CD recruited tdTomato-GGA2, but not tdTomato-PICK1 or PSD95-tdTomato. Co-expression of T70mV-nanoLuc with tdTomato-PICK1, tdTomato-GGA2 or PSD95-tdTomato led to no recruitment and a diffuse tdTomato staining was observed (Fig. 2A). However, the ectopic expression of T70mV-nanoLuc on mitochondria was confirmed by immunostaining for the mitochondrial marker protein Tom20 (Fig. 2C). These results confirm the interaction of SorLA-CD with GGA2 and PICK1 whereas Sortilin-CD interacts with GGA2 but not with PICK1. Mutating the last three C-terminal amino acids of SorLA from VIA to AAA in T70mV-SorLA-CD abolished the recruitment of tdTomato-PICK1 (Fig. 2B). Mutating the second last amino acid of the SorLA-CD (I^{53}) to alanine (T70mV-SorLA-CD-VAA) strongly reduced, but did not impede completely the recruitment of tdTomato-PICK1 (Fig. 2B). None of these mutations affected the recruitment of tdTomato-GGA2 to mitochondria (Fig. 2B). Figure 2D summarizes the results of these analyses. Next, we asked if the SorLA-CD fused to a transmembrane domain of a type-I transmembrane receptor recruits PICK1 in COS7 cells which do not express PICK1. To this end, we expressed a chimeric receptor composed of the extracellular and transmembrane moiety of the interleukin 2 receptor alpha (IL2R) fused to the SorLA-CD (IL2R-SorLA-CD). This construct was expressed together with tdTomato-PICK1 in COS7 cells and we observed co-localization of both proteins to perinuclear and vesicular structures (Fig. 3A). Expression of constructs with a deletion of the three terminal amino acids of SorLA (IL2R-SorLA-CD-Del3) or mutation of the second last amino acid of SorLA (I^{53}) to alanine (IL2R-SorLA-CD-VAA) resulted in a similar subcellular localization as compared to IL2R-SorLA-CD (Fig. 3A). However, both did not co-localize with tdTomato-PICK1, which shows a diffuse distribution (Fig. 3A). These results suggest that expression of IL2R-SorLA-CD leads to perinuclear and vesicular localization of the interacting tdTomato-PICK1 in cells with no endogenous PICK1 expression. In contrast, the subcellular localization of GGA2 and of the trans-Golgi marker protein Arfip1 expressed as tdTomato fusion proteins appeared not altered in cells co-expressing IL2R-SorLA-CD mutants as compared to the wild type construct (Fig. 3A). These experiments demonstrate the interaction of SorLA-CD and PICK1 under physiological conditions in cells. They also corroborate the results obtained by mammalian-2-hybrid analysis, showing that the interaction of PICK1 with SorLA-CD depends on the three C-terminal amino acids.

A previous study showed that the truncation of the terminal four amino acids of SorLA (M^{51}-A^{54}) does not change its internalization rate in CHO cells [28]. We used SY5Y cells that express PICK1 endogenously to determine its role in SorLA internalization. PICK1 interacts with the three C-terminal amino acids of SorLA-CD. If PICK1 plays a prominent role in SorLA internalization, deletion of the three terminal amino acids of SorLA should impede its endocytosis. We expressed IL2R-SorLA-CD and the mutant IL2R-SorLA-CD-Del3 in SY5Y cells, incubated cells at 4 °C with an anti-IL2R antibody, washed the cells and incubated the cells for 0 or 30 min at 37 °C (Fig. 3B). Without incubation at 37 °C, IL2R-SorLA-CD and IL2R-SorLA-CD-Del3 showed a prominent surface localization. After incubation at 37 °C for 30 min, both constructs were detected to a similar degree in intracellular vesicular structures. As we did not detect any differences between the uptake of the two constructs, the results strongly suggest that the interaction of

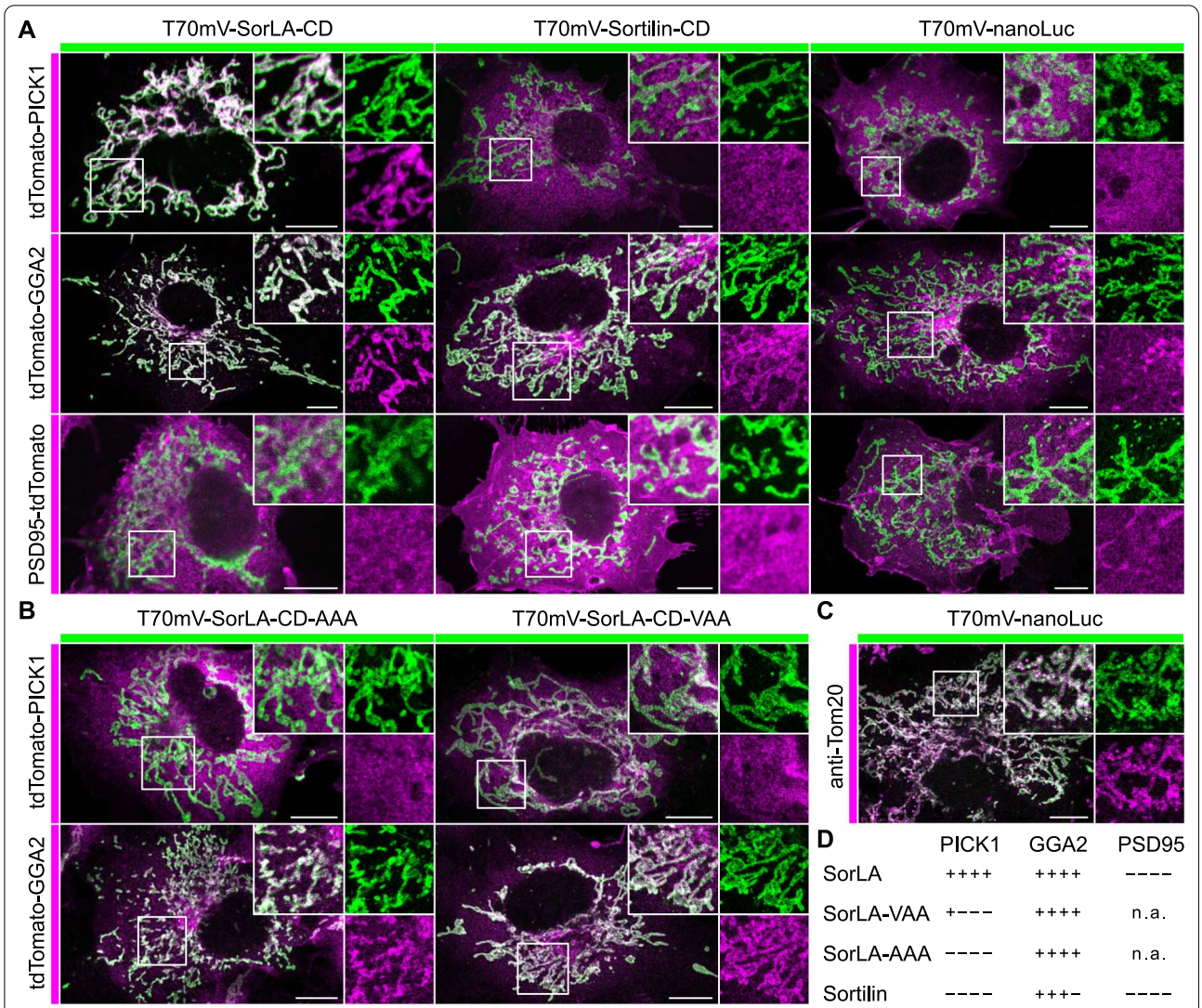

Fig. 2 Ectopically localized SorLA cytoplasmic domain recruits PICK1. **A** COS7 cells were transfected with T70mV-SorLA-CD, T70mV-Sortilin-CD or T70mV-nanoLuc (green) and co-transfected with tdTomato-PICK1, tdTomato-GGA2 or PSD95-tdTomato (magenta) as indicated. Magnifications of selected areas (boxes) are shown as insets. mVenus and tdTomato signals were enhanced by immunostainings with respective antibodies. **B** COS7 cells were transfected with the mutated SorLA constructs T70mV-SorLA-CD-AAA or T70mV-SorLA-CD-VAA (green) and co-transfected with tdTomato-PICK1 or tdTomato-GGA2 (magenta) as indicated. **C** Ectopic localization of T70mV-nanoLuc at mitochondria. COS7 cells were transfected with T70mV-nanoLuc (green) and stained with an antibody against the mitochondrial protein Tom20 (magenta). **D** Summary of the recruitment of the tdTomato fusion constructs of PICK1, GGA2 and PSD95 by the analyzed cytoplasmic domains to mitochondria. Scale bars: 10 µm

PICK1 with SorLA-CD does not mediate internalization of SorLA.

In order to assess localization of endogenous SorLA and PICK1, we immunostained SY5Y cells using antibodies against PICK1 and SorLA and observed co-localization at larger vesicular structures (Fig. 4A, D). We expressed IL2R-SorLA-CD together with tdTomato-PICK1 in dissociated primary cultured hippocampal neurons, which have no endogenous expression of IL2R. Immunocytochemical analysis demonstrated for both proteins a predominant somatic distribution that extended into neurites. We observed co-localization to a large number of vesicular structures in the soma and in proximal neurites (Fig. 4B, D). Finally, we immunostained dissociated primary cultured hippocampal neurons for endogenous SorLA and PICK1 and observed colocalization at endosomal structures in the soma and proximal parts of neurites (Fig. 4C, D).

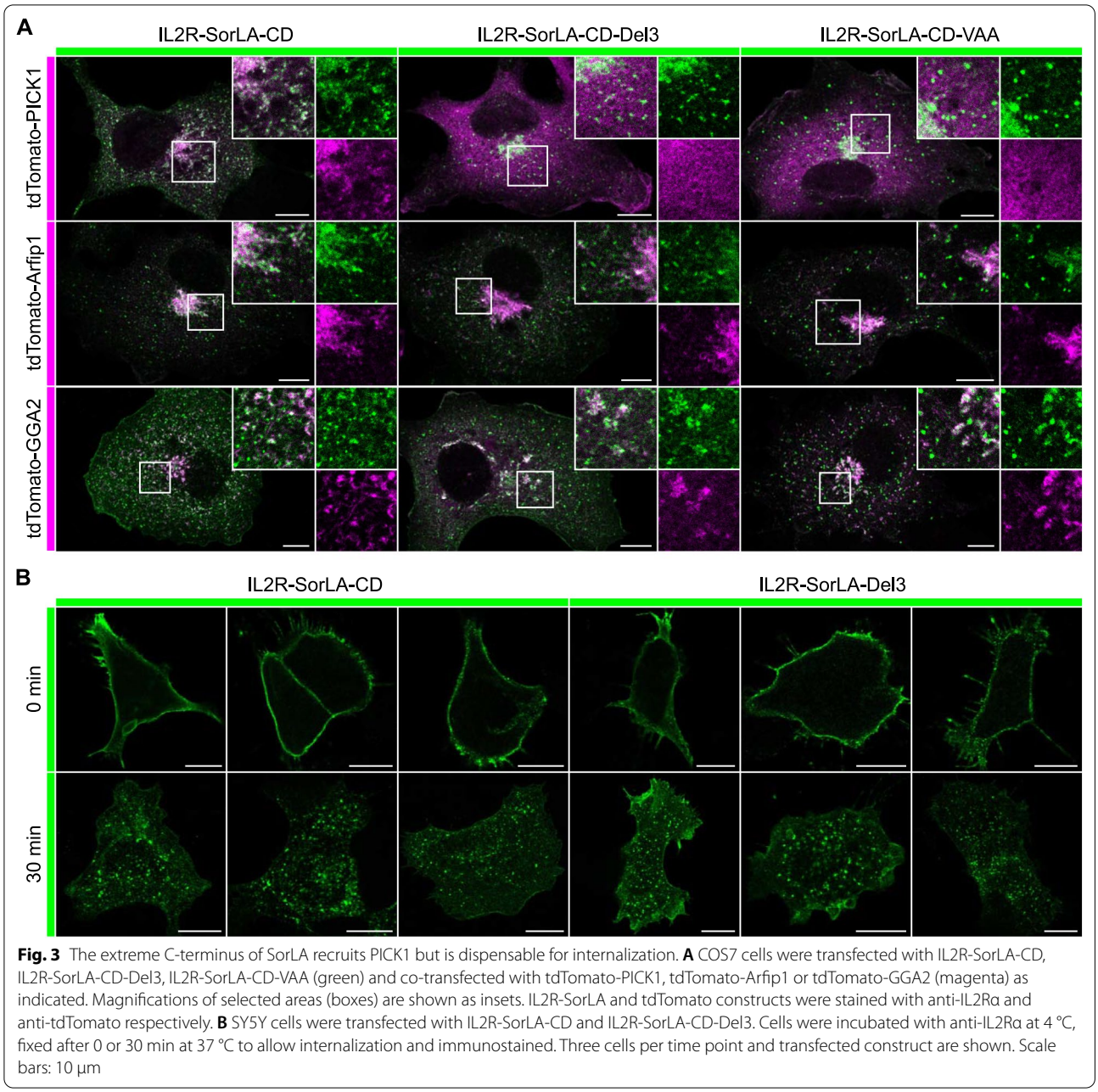

Fig. 3 The extreme C-terminus of SorLA recruits PICK1 but is dispensable for internalization. **A** COS7 cells were transfected with IL2R-SorLA-CD, IL2R-SorLA-CD-Del3, IL2R-SorLA-CD-VAA (green) and co-transfected with tdTomato-PICK1, tdTomato-Arfip1 or tdTomato-GGA2 (magenta) as indicated. Magnifications of selected areas (boxes) are shown as insets. IL2R-SorLA and tdTomato constructs were stained with anti-IL2Rα and anti-tdTomato respectively. **B** SY5Y cells were transfected with IL2R-SorLA-CD and IL2R-SorLA-CD-Del3. Cells were incubated with anti-IL2Rα at 4 °C, fixed after 0 or 30 min at 37 °C to allow internalization and immunostained. Three cells per time point and transfected construct are shown. Scale bars: 10 µm

Discussion

Here, we show an interaction of PICK1 with SorLA mediated by the last three C-terminal amino acids, VIA, of SorLA. This corresponds to a type II PDZ domain interaction motif. The canonical classification of PDZ domain interactions with C-termini assorts four major classes; I interacts with (S/T)-X-Φ, II interacts with Φ-X-Φ, III interacts with Ψ-X-Φ, and IV which interacts with (D/E)-X-Φ as preferred C-terminal motif, where X is any residue, Φ is a hydrophobic residue and Ψ is a basic hydrophilic residue [60]. Most PDZ domains interact with only one classified sequence type. In contrast, the PICK1 PDZ domain belongs to a small group of promiscuous PDZ domains with a mixed specificity. PICK1 binds sequences of class I and II interaction motifs and also some atypical motifs [61, 62]. Thus, it is highly likely that the PICK1 PDZ domain mediates the interaction with SorLA-CD. Another PICK1 interactor is ERBB2, which is also forming a complex with SorLA [39]. It is tempting to speculate that a SorLA ERBB2/HER2 complex recruits PICK1,

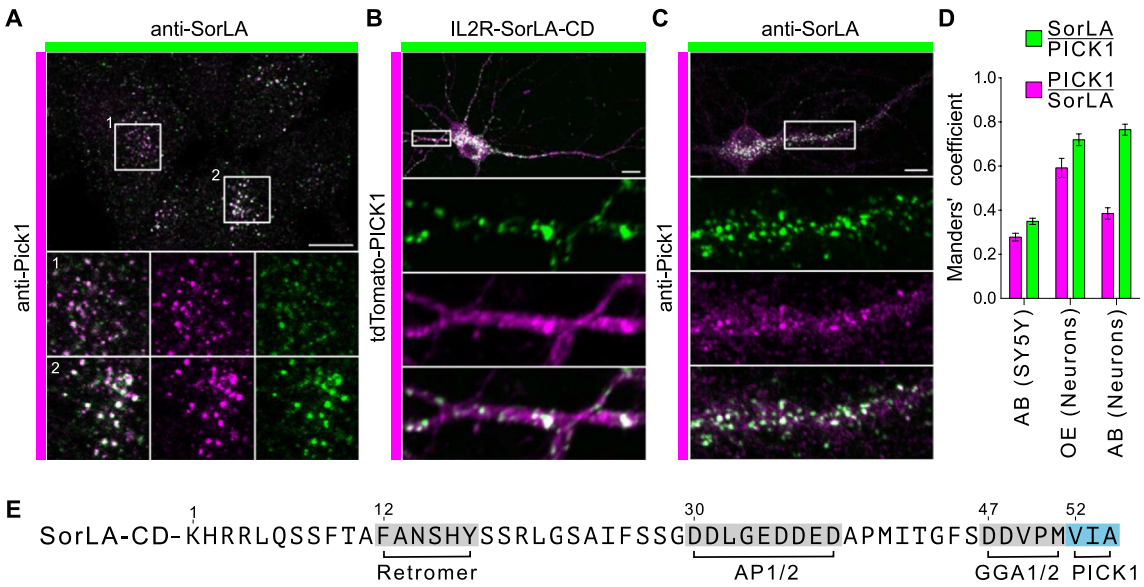

Fig. 4 SorLA and PICK1 co-localize. **A** SY5Y cells were stained with anti-PICK1 (green) and anti-SorLA (magenta) antibodies. Magnifications of two selected areas (boxes) are shown. **B** Immunocytochemical localization of IL2R-SorLA and tdTomato-PICK1 in transfected dissociated primary cultured hippocampal neurons using anti-IL2R (green) and anti-tdTomato (magenta) antibodies. Magnification of a selected area (boxes) are shown. **C** Immunolocalization of endogenous SorLA and PICK1 in dissociated primary cultured hippocampal neurons using anti-SorLA (green) and anti-PICK1 (magenta) antibodies. Magnification of a selected area (boxes) are shown. **D** Respective Manders' coefficient of SorLA and PICK1 using antibodies (AB) against the endogenous proteins or of overexpressed (OE) IL2R-SorLA and tdTomato-PICK1. **E** Primary sequence of the SorLA cytoplasmic domain. Amino acid motifs mediating interaction with retromer, AP-1 and AP-2 and GGA1 and GGA2 are indicated in grey. The here described PICK1 interaction motif is indicated in blue. Scale bars: 10 µm

which homodimerizes through its BAR domain and facilitates endosomal transport of the complex.

Our study adds PICK1 to the portfolio of cytosolic SorLA interacting proteins. In general, short linear amino acid motifs mediate the binding of cytosolic domains of transmembrane proteins to adaptor proteins. A number of previous studies addressed the interaction of SorLA-CD with adaptor proteins, identified specific amino acid motifs that mediate the interaction and analyzed the consequences of their mutation or deletion for the subcellular localization of SorLA. The cytoplasmic domain of SorLA interacts through the F^{12}ANSHY^{17} motif with retromer [29], the acidic cluster D^{30}–D^{38} facilitates binding of AP-1, AP-2 and PACS1, the heat shock protein HSPA12A binds the SorLA-CD via the acidic residues E^{34}-D^{38} and $D^{47}D^{48}$ in an ADP/ATP-dependent manner and D^{47}DXXM is regarded as the minimal GGA interaction motif (Fig. 4E) [28, 30–32]. Accordingly, the here identified PICK1 binding site is located adjacent to the minimal GGA binding motif (Fig. 4E).

Partial ablation or mutation of the retromer interaction motif in SorLA-CD caused endosomal accumulation of SorLA, altered APP sorting and increased APP processing [29, 63]. Additional mutational analysis revealed that the pentameric acidic cluster (E^{34}-D^{38}) is crucial for SorLA's internalization, TGN to endosome transport and polarized neuronal targeting [25, 28]. SorLA's anterograde TGN to endosome transport relies on the acidic cluster in combination with the minimal GGA-binding motif D^{48}XXM^{51} [28]. Here, we observed unaltered uptake of a chimeric construct in SY5Y cells after deletion of the terminal three amino acids (V^{52}-A^{54}). Truncation of the terminal four amino acids (M^{51}-A^{54}) does also not change the internalization rate in CHO cells [28] nor the polarized sorting of SorLA in neurons [25]. However, the subcellular distribution of such a mutant is changed towards a reduced TGN and increased endosomal localization as compared to the wild-type receptor [28, 31]. Taken together, we demonstrate that SorLA-CD interacts with PICK1 via its three C-terminal residues (VIA). In addition, a function of the last four amino acids in the transport of SorLA between Golgi and endosomes has already be shown. Considering the role of PICK1 in endosomal transport, it is likely that PICK1 is capable of regulating SorLA's intracellular itinerary.

Methods

Antibodies and DNA constructs

The following primary antibodies were used: rabbit anti-dsRed (tdTomato) (632496, Clontech Takara); chicken

anti-GFP (mVenus) (ab139701, Abcam); mouse monoclonal anti-interleukin receptor 2 alpha (IL2R-alpha, Tac/CD25) (ab8235, Abcam); mouse monoclonal anti-Myc – 9E10 (MMS-150P, Covance); rabbit polyclonal anti-PICK1 (ab3420, Abcam); mouse monoclonal anti-PICK1 (MABN75, Millipore); rabbit anti-SorLA (SorLA-Vps10p domain) (a gift from C.M. Petersen, Aarhus University, Denmark) [8]; rabbit anti-Tom20 (sc-11415, Santa Cruz Biotechnology Inc.). As secondary antibodies, fluorescent Alexa Fluor-conjugated (Invitrogen) or horseradish peroxidase (HRP)-conjugated (Dianova) antibodies were used.

The construct of the SorLA-cd inserted in pGEX4T-1 (Amersham Pharmacia) has been described before [28]. To generate expression constructs encoding PICK1-Myc, the PICK1 cDNA was cloned into pcDNA4/Myc-His (Invitrogen). To generate VP16 fusion proteins, PICK1 or PSD95 cDNA was cloned in frame via BamHI and NotI into pAct (Promega). To express GAL4 fusion proteins cDNA encoding wild-type or mutant cytoplasmic domains of SorLA or Sortilin were cloned in frame via BamHI and NotI into pBind3-D [64]. Mutations in the amino acid sequence of the SorLA cytoplasmic domain were introduced by PCR using appropriate primers. To recruit the SorLA or the Sortilin cytoplasmic domain to mitochondria, a modified pFUGW vector was used harboring a CMV promoter and a multiple cloning site (Binkle, unpublished). T70mV-SorLA-cd or T70mV-Sortilin-cd were generated by inserting the coding sequence of the first 88 amino acids of yeast Tom70 (T70) followed by the fluorophore mVenus (mV) and the cytoplasmic domains of SorLA, its mutant sequence, or Sortilin respectively. NanoLuc luciferase (nanoLuc) was cloned via PCR using pNL1.1 (Promega) as template and together with T70mV into the modified expression vector. To tag PICK1, PSD95, GGA2 and Arfip1 with the fluorophore tdTomato respective coding sequence was cloned into the expression vector L21C-Nt-tdTomato (Binkle, unpublished). GGA2 was cloned from pcDNA3-Flag-HA-GGA2 (obtained from W. Sellers through Addgene). The chimeric receptor construct (IL2R-SorLA-CD) corresponds to the extracellular and transmembrane domains of the interleukin-2 receptor alpha and SorLA's cytoplasmic domain or mutated versions of the SorLA cytoplasmic domain. Fragments were PCR amplified and cloned into pcDNA3.1/Zeo (Invitrogen).

Cell culture

CHO and COS7 cells were cultured in DMEM (Invitrogen) supplemented with 10% (v/v) fetal calf serum (FCS). SH-SY5Y cells were cultured in DMEM (Invitrogen) supplemented with 20% (v/v) fetal calf serum (FCS). Murine neuroblastoma N2a (Neuro-2a) cells were grown in Opti-MEM™ without Phenol Red (Invitrogen) supplemented with 5% (v/v) FCS. All cells were cultured at 37 °C and 5% CO_2. Lipofectamine™ 2000 (Invitrogen) was used for transfection of cells. Generation of stable transfected cells was described before [65]. Dissociated hippocampal neurons were prepared and cultured as described before [66]. Animal husbandry was authorized under German regulations on animal welfare in accordance with the European Communities Council Directive (2010/63/EU). After 3 days in vitro, neurons were transfected with Lipofectamine® LTX (Invitrogen) and immunostained at 14 days in vitro.

Mammalian two-hybrid analysis

Interaction of proteins was determined using a modification of the Checkmate mammalian two-hybrid system (Promega). Two vectors were used, pAct and pBind3-D. pAct (Promega) contains the herpes simplex virus VP16 activation domain followed by a multiple cloning site. pBind3-D [64] is a modification of pBind (Promega) in which the DNA-binding domain of the yeast GAL4 gene followed by an altered multiple cloning site and the vector lacks the *Renilla* luciferase module.

N2a cells were seeded on 96-well plates and transfected in parallel with pAct, pBind3-D, peGFP (Clontech), and a pG5luc (Promega) expressing firefly luciferase under control of GAL4 [64]. The next day fluorescence generated by eGFP was determined for normalization and light emission generated by luciferase activity was detected after adding Bright-Glo (Luciferase Assay System, Promega) with a Multilabel Counter (PerkinElmer). Luciferase activity was normalized to eGFP-fluorescence. All transfections and analysis were performed in septuplicate and experiments repeated three times. Average relative luciferase light units and S.D. were determined using the Prism software.

Pull down analysis

GST or GST-fusion proteins were expressed in BL21(DE3) cells, and purified by using glutathione-sepharose beads according to the manufacturer's recommendations (Amersham Pharmacia). Stable transfected CHO cells expressing PICK1-Myc were lysed in 150 mM NaCl, 1% Triton X-100, 20 mM Tris–HCl, 10 mM EDTA, pH 8.0 supplemented with protease inhibitors (Complete Mini, Roche), cell debris sedimented for 20 min at 16.000 g and 10% of each supernatant was used as an expression control (input). Supernatants were incubated with 30 µl Pierce™ glutathione magnetic agarose beads (ThermoFisher Scientific) prebound with GST or GST-SorLA-cd for 2 h at 4 °C. Subsequently, protein complexes were subjected to immunoblotting.

For pull down of endogenous proteins, brain homogenates were prepared from 2 mouse forebrains in 320 mM Sucrose, 4 mM Hepes, 2 mM MgCl, 2 mM CaCl, pH 7.5 supplemented with protease inhibitors (Complete Mini, Roche) using a glass homogenizer (12 passes) (modified from [38]). Homogenates were centrifuged at 1000 g for 10 min, and the supernatant (S1) was centrifuged at 48,000 g for 30 min to obtain the pellet (p2) fraction. This fraction was resuspended in 0.1 mM EDTA, 1% Triton, pH 7.4 plus protease inhibitor, sonicated and solubilized for 1 h at 4 °C. After centrifugation at 100,000 g for 1 h the supernatant (S3) was used for GST pull-down assays. GST fusion proteins coupled to Pierce™ glutathione magnetic agarose beads were incubated overnight, washed with PBS, 0.1 mM EDTA, 0.1% Triton, pH 7.4 plus protease inhibitor and analyzed by immunoblotting as described before [65].

Immunocytochemistry and internalization assay

Cells were cultured on coverslips, fixed, permeabilized and stained as described before [65]. To visualize internalization, cells were surface labeled with primary antibody (anti-IL2Rα) at 4 °C for 1 h followed by fixation or incubation at 37 °C for 30 min, fixation and staining with secondary fluorescent antibody. All immunocytochemical stainings were performed in triplicates. Cells were analyzed by confocal microscopy using a Leica TCS SP8 microscope and a 63x (NA = 1.4) oil immersion objective.

Abbreviations

Aβ: Amyloid-β; AD: Alzheimer's disease; APP: Amyloid precursor protein; ERBB2: Epidermal growth factor receptor 2; DBD: DNA-binding domain; hiPSC: Human induced pluripotent stem cell; IL2R: Interleukin 2 receptor alpha; LDLR: Low-density-lipoprotein receptor; Luc: Firefly luciferase; SorLA-CD: Cytoplasmic domain of SorLA; Sortilin-CD: Cytoplasmic domain of Sortilin; TAD: Transcription activation domain; TGN: Trans-Golgi-network; Vps10p-D: Vacuolar protein sorting 10 domain; UAS: Upstream activating sequence.

Acknowledgements

We thank Barbara Merz and Andrea Zaisser for skilled technical assistance and the UKE microscopy imaging facility (umif) for providing confocal microscopes and support.

Authors' contributions

Experimental execution and data analysis: LB, MK, UB, GH; data interpretation: LB, UB, DK, GH; design of the study and drafting the manuscript: GH; all authors read and approved the final manuscript.

Funding

Open Access funding enabled and organized by Projekt DEAL.

Availability of data and materials

All data generated or analyzed during this study are included in this article. Materials are available from the corresponding author on reasonable request.

Declarations

Ethics approval and consent to participate

Not applicable.

Consent for publication

Not applicable.

Competing interests

The authors declare that they have no competing interests.

Received: 6 October 2021 Accepted: 7 February 2022
Published online: 19 February 2022

References

1. Jacobsen L, Madsen P, Moestrup SK, Lund AH, Tommerup N, Nykjaer A, Sottrup-Jensen L, Gliemann J, Petersen CM. Molecular characterization of a novel human hybrid-type receptor that binds the alpha2-macroglobulin receptor-associated protein. J Biol Chem. 1996;271(49):31379–83.
2. Yamazaki H, Bujo H, Kusunoki J, Seimiya K, Kanaki T, Morisaki N, Schneider WJ, Saito Y. Elements of neural adhesion molecules and a yeast vacuolar protein sorting receptor are present in a novel mammalian low density lipoprotein receptor family member. J Biol Chem. 1996;271(40):24761–8.
3. Hermans-Borgmeyer I, Hampe W, Schinke B, Methner A, Nykjaer A, Susens U, Fenger U, Herbarth B, Schaller HC. Unique expression pattern of a novel mosaic receptor in the developing cerebral cortex. Mech Dev. 1998;70(1–2):65–76.
4. Hermey G. The Vps10p-domain receptor family. Cell Mol Life Sci. 2009;66(16):2677–89.
5. Malik AR, Willnow TE. VPS10P domain receptors: sorting out brain health and disease. Trends Neurosci. 2020;43(11):870–85.
6. Caglayan S, Takagi-Niidome S, Liao F, Carlo AS, Schmidt V, Burgert T, Kitago Y, Fuchtbauer EM, Fuchtbauer A, Holtzman DM, et al. Lysosomal sorting of amyloid-beta by the SORLA receptor is impaired by a familial Alzheimer's disease mutation. Sci Transl Med. 2014. https://doi.org/10.1126/scitranslmed.3007747.
7. Glerup S, Lume M, Olsen D, Nyengaard JR, Vaegter CB, Gustafsen C, Christensen EI, Kjolby M, Hay-Schmidt A, Bender D, et al. SorLA controls neurotrophic activity by sorting of GDNF and its receptors GFRalpha1 and RET. Cell Rep. 2013;3(1):186–99.
8. Jacobsen L, Madsen P, Jacobsen C, Nielsen MS, Gliemann J, Petersen CM. Activation and functional characterization of the mosaic receptor SorLA/LR11. J Biol Chem. 2001;276(25):22788–96.
9. Larsen JV, Kristensen AM, Pallesen LT, Bauer J, Vaegter CB, Nielsen MS, Madsen P, Petersen CM. Cytokine-like factor 1, an essential facilitator of cardiotrophin-like cytokine: ciliary neurotrophic factor receptor alpha signaling and sorLA-mediated turnover. Mol Cell Biol. 2016;36(8):1272–86.
10. Westergaard UB, Sorensen ES, Hermey G, Nielsen MS, Nykjaer A, Kirkegaard K, Jacobsen C, Gliemann J, Madsen P, Petersen CM. Functional organization of the sortilin Vps10p domain. J Biol Chem. 2004;279(48):50221–9.
11. Gliemann J, Hermey G, Nykjaer A, Petersen CM, Jacobsen C, Andreasen PA. The mosaic receptor sorLA/LR11 binds components of the plasminogen-activating system and platelet-derived growth factor-BB similarly to LRP1 (low-density lipoprotein receptor-related protein), but mediates slow internalization of bound ligand. Biochem J. 2004;381(Pt 1):203–12.
12. Klinger SC, Glerup S, Raarup MK, Mari MC, Nyegaard M, Koster G, Prabakaran T, Nilsson SK, Kjaergaard MM, Bakke O, et al. SorLA regulates the activity of lipoprotein lipase by intracellular trafficking. J Cell Sci. 2011;124(Pt 7):1095–105.
13. Taira K, Bujo H, Hirayama S, Yamazaki H, Kanaki T, Takahashi K, Ishii I, Miida T, Schneider WJ, Saito Y. LR11, a mosaic LDL receptor family member, mediates the uptake of ApoE-rich lipoproteins in vitro. Arterioscler Thromb Vasc Biol. 2001;21(9):1501–6.
14. Andersen OM, Schmidt V, Spoelgen R, Gliemann J, Behlke J, Galatis D, McKinstry WJ, Parker MW, Masters CL, Hyman BT, et al. Molecular dissection of the interaction between amyloid precursor protein and its neuronal trafficking receptor SorLA/LR11. Biochemistry. 2006;45(8):2618–28.
15. Pietila M, Sahgal P, Peuhu E, Jantti NZ, Paatero I, Narva E, Al-Akhrass H, Lilja J, Georgiadou M, Andersen OM, et al. SORLA regulates endosomal trafficking and oncogenic fitness of HER2. Nat Commun. 2019;10(1):2340.
16. Andersen OM, Rudolph IM, Willnow TE. Risk factor SORL1: from genetic association to functional validation in Alzheimer's disease. Acta Neuropathol. 2016. https://doi.org/10.1007/s00401-016-1615-4.

17. Scherzer CR, Offe K, Gearing M, Rees HD, Fang G, Heilman CJ, Schaller C, Bujo H, Levey AI, Lah JJ. Loss of apolipoprotein E receptor LR11 in Alzheimer disease. Arch Neurol. 2004;61(8):1200–5.
18. Nunes AF, Amaral JD, Lo AC, Fonseca MB, Viana RJ, Callaerts-Vegh Z, D'Hooge R, Rodrigues CM. TUDCA, a bile acid, attenuates amyloid precursor protein processing and amyloid-β deposition in APP/PS1 mice. Mol Neurobiol. 2012;45(3):440–54.
19. Hermey G, Hoffmeister-Ullerich SA, Merz B, Gross D, Kuhl D, Kins S. Amyloidosis causes downregulation of SorLA, SorCS1 and SorCS3 expression in mice. Biol Chem. 2019;400(9):1181–9.
20. Andersen OM, Reiche J, Schmidt V, Gotthardt M, Spoelgen R, Behlke J, von Arnim CA, Breiderhoff T, Jansen P, Wu X, et al. Neuronal sorting protein-related receptor sorLA/LR11 regulates processing of the amyloid precursor protein. Proc Natl Acad Sci USA. 2005;102(38):13461–6.
21. Eggert S, Gonzalez AC, Thomas C, Schilling S, Schwarz SM, Tischer C, Adam V, Strecker P, Schmidt V, Willnow TE, et al. Dimerization leads to changes in APP (amyloid precursor protein) trafficking mediated by LRP1 and SorLA. Cell Mol Life Sci. 2018;75(2):301–22.
22. Kitago Y, Nagae M, Nakata Z, Yagi-Utsumi M, Takagi-Niidome S, Mihara E, Nogi T, Kato K, Takagi J. Structural basis for amyloidogenic peptide recognition by sorLA. Nat Struct Mol Biol. 2015;22(3):199–206.
23. Burgert T, Schmidt V, Caglayan S, Lin F, Fuchtbauer A, Fuchtbauer EM, Nykjaer A, Carlo AS, Willnow TE. SORLA-dependent and -independent functions for PACS1 in control of amyloidogenic processes. Mol Cell Biol. 2013;33(21):4308–20.
24. Gustafsen C, Glerup S, Pallesen LT, Olsen D, Andersen OM, Nykjaer A, Madsen P, Petersen CM. Sortilin and SorLA display distinct roles in processing and trafficking of amyloid precursor protein. J Neurosci. 2013;33(1):64–71.
25. Klinger SC, Hojland A, Jain S, Kjolby M, Madsen P, Svendsen AD, Olivecrona G, Bonifacino JS, Nielsen MS. Polarized trafficking of the sorting receptor SorLA in neurons and MDCK cells. FEBS J. 2016;283(13):2476–93.
26. Knupp A, Mishra S, Martinez R, Braggin JE, Szabo M, Kinoshita C, Hailey DW, Small SA, Jayadev S, Young JE. Depletion of the AD risk gene SORL1 selectively impairs neuronal endosomal traffic independent of amyloidogenic APP processing. Cell Rep. 2020;31(9): 107719.
27. Hung C, Tuck E, Stubbs V, van der Lee SJ, Aalfs C, van Spaendonk R, Scheltens P, Hardy J, Holstege H, Livesey FJ. SORL1 deficiency in human excitatory neurons causes APP-dependent defects in the endolysosome-autophagy network. Cell Rep. 2021;35(11): 109259.
28. Nielsen MS, Gustafsen C, Madsen P, Nyengaard JR, Hermey G, Bakke O, Mari M, Schu P, Pohlmann R, Dennes A, et al. Sorting by the cytoplasmic domain of the amyloid precursor protein binding receptor SorLA. Mol Cell Biol. 2007;27(19):6842–51.
29. Fjorback AW, Seaman M, Gustafsen C, Mehmedbasic A, Gokool S, Wu C, Militz D, Schmidt V, Madsen P, Nyengaard JR, et al. Retromer binds the FANSHY sorting motif in SorLA to regulate amyloid precursor protein sorting and processing. J Neurosci. 2012;32(4):1467–80.
30. Jacobsen L, Madsen P, Nielsen MS, Geraerts WP, Gliemann J, Smit AB, Petersen CM. The sorLA cytoplasmic domain interacts with GGA1 and -2 and defines minimum requirements for GGA binding. FEBS Lett. 2002;511(1–3):155–8.
31. Schmidt V, Sporbert A, Rohe M, Reimer T, Rehm A, Andersen OM, Willnow TE. SorLA/LR11 regulates processing of amyloid precursor protein via interaction with adaptors GGA and PACS-1. J Biol Chem. 2007;282(45):32956–64.
32. Madsen P, Isaksen TJ, Siupka P, Toth AE, Nyegaard M, Gustafsen C, Nielsen MS. HSPA12A targets the cytoplasmic domain and affects the trafficking of the Amyloid Precursor Protein receptor SorLA. Sci Rep. 2019;9(1):611.
33. Nielsen MS, Keat SJ, Hamati JW, Madsen P, Gutzmann JJ, Engelsberg A, Pedersen KM, Gustafsen C, Nykjaer A, Gliemann J, et al. Different motifs regulate trafficking of SorCS1 isoforms. Traffic. 2008;9(6):980–94.
34. Breiderhoff T, Christiansen GB, Pallesen LT, Vaegter C, Nykjaer A, Holm MM, Glerup S, Willnow TE. Sortilin-related receptor SORCS3 is a postsynaptic modulator of synaptic depression and fear extinction. PLoS ONE. 2013;8(9): e75006.
35. Hanley JG, Henley JM. PICK1 is a calcium-sensor for NMDA-induced AMPA receptor trafficking. EMBO J. 2005;24(18):3266–78.
36. Xia J, Zhang X, Staudinger J, Huganir RL. Clustering of AMPA receptors by the synaptic PDZ domain-containing protein PICK1. Neuron. 1999;22(1):179–87.
37. Staudinger J, Zhou J, Burgess R, Elledge SJ, Olson EN. PICK1: a perinuclear binding protein and substrate for protein kinase C isolated by the yeast two-hybrid system. J Cell Biol. 1995;128(3):263–71.
38. Dev KK, Nakajima Y, Kitano J, Braithwaite SP, Henley JM, Nakanishi S. PICK1 interacts with and regulates PKC phosphorylation of mGLUR7. J Neurosci. 2000;20(19):7252–7.
39. Jaulin-Bastard F, Saito H, Le Bivic A, Ollendorff V, Marchetto S, Birnbaum D, Borg JP. The ERBB2/HER2 receptor differentially interacts with ERBIN and PICK1 PSD-95/DLG/ZO-1 domain proteins. J Biol Chem. 2001;276(18):15256–63.
40. Dev KK, Nishimune A, Henley JM, Nakanishi S. The protein kinase C alpha binding protein PICK1 interacts with short but not long form alternative splice variants of AMPA receptor subunits. Neuropharmacology. 1999;38(5):635–44.
41. Boudin H, Doan A, Xia J, Shigemoto R, Huganir RL, Worley P, Craig AM. Presynaptic clustering of mGluR7a requires the PICK1 PDZ domain binding site. Neuron. 2000;28(2):485–97.
42. El Far O, Airas J, Wischmeyer E, Nehring RB, Karschin A, Betz H. Interaction of the C-terminal tail region of the metabotropic glutamate receptor 7 with the protein kinase C substrate PICK1. Eur J Neurosci. 2000;12(12):4215–21.
43. Takeya R, Takeshige K, Sumimoto H. Interaction of the PDZ domain of human PICK1 with class I ADP-ribosylation factors. Biochem Biophys Res Commun. 2000;267(1):149–55.
44. Torres GE, Yao WD, Mohn AR, Quan H, Kim KM, Levey AI, Staudinger J, Caron MG. Functional interaction between monoamine plasma membrane transporters and the synaptic PDZ domain-containing protein PICK1. Neuron. 2001;30(1):121–34.
45. Rao Y, Haucke V. Membrane shaping by the Bin/amphiphysin/Rvs (BAR) domain protein superfamily. Cell Mol Life Sci. 2011;68(24):3983–93.
46. Herlo R, Lund VK, Lycas MD, Jansen AM, Khelashvili G, Andersen RC, Bhatia V, Pedersen TS, Albornoz PBC, Johner N, et al. An amphipathic helix directs cellular membrane curvature sensing and function of the BAR domain protein PICK1. Cell Rep. 2018;23(7):2056–69.
47. Cao M, Mao Z, Kam C, Xiao N, Cao X, Shen C, Cheng KK, Xu A, Lee KM, Jiang L, et al. PICK1 and ICA69 control insulin granule trafficking and their deficiencies lead to impaired glucose tolerance. PLoS Biol. 2013;11(4): e1001541.
48. Holst B, Madsen KL, Jansen AM, Jin C, Rickhag M, Lund VK, Jensen M, Bhatia V, Sorensen G, Madsen AN, et al. PICK1 deficiency impairs secretory vesicle biogenesis and leads to growth retardation and decreased glucose tolerance. PLoS Biol. 2013;11(4): e1001542.
49. Li J, Mao Z, Huang J, Xia J. PICK1 is essential for insulin production and the maintenance of glucose homeostasis. Mol Biol Cell. 2018;29(5):587–96.
50. Yong XLH, Cousin MA, Anggono V. PICK1 controls activity-dependent synaptic vesicle cargo retrieval. Cell Rep. 2020;33(4): 108312.
51. Perez JL, Khatri L, Chang C, Srivastava S, Osten P, Ziff EB. PICK1 targets activated protein kinase Calpha to AMPA receptor clusters in spines of hippocampal neurons and reduces surface levels of the AMPA-type glutamate receptor subunit 2. J Neurosci. 2001;21(15):5417–28.
52. Xia J, Chung HJ, Wihler C, Huganir RL, Linden DJ. Cerebellar long-term depression requires PKC-regulated interactions between GluR2/3 and PDZ domain-containing proteins. Neuron. 2000;28(2):499–510.
53. Kim CH, Chung HJ, Lee HK, Huganir RL. Interaction of the AMPA receptor subunit GluR2/3 with PDZ domains regulates hippocampal long-term depression. Proc Natl Acad Sci U S A. 2001;98(20):11725–30.
54. Seidenman KJ, Steinberg JP, Huganir R, Malinow R. Glutamate receptor subunit 2 Serine 880 phosphorylation modulates synaptic transmission and mediates plasticity in CA1 pyramidal cells. J Neurosci. 2003;23(27):9220–8.
55. Iwakura Y, Nagano T, Kawamura M, Horikawa H, Ibaraki K, Takei N, Nawa H. N-methyl-D-aspartate-induced alpha-amino-3-hydroxy-5-methyl-4-isoxazolepropionic acid (AMPA) receptor down-regulation involves interaction of the carboxyl terminus of GluR2/3 with Pick1. Ligand-binding studies using Sindbis vectors carrying AMPA receptor decoys. J Biol Chem. 2001;276(43):40025–32.
56. Terashima A, Cotton L, Dev KK, Meyer G, Zaman S, Duprat F, Henley JM, Collingridge GL, Isaac JT. Regulation of synaptic strength and AMPA receptor subunit composition by PICK1. J Neurosci. 2004;24(23):5381–90.
57. Terashima A, Pelkey KA, Rah JC, Suh YH, Roche KW, Collingridge GL, McBain CJ, Isaac JT. An essential role for PICK1 in NMDA

receptor-dependent bidirectional synaptic plasticity. Neuron. 2008;57(6):872–82.
58. Cao M, Xu J, Shen C, Kam C, Huganir RL, Xia J. PICK1-ICA69 heteromeric BAR domain complex regulates synaptic targeting and surface expression of AMPA receptors. J Neurosci. 2007;27(47):12945–56.
59. Nielsen MS, Madsen P, Christensen EI, Nykjaer A, Gliemann J, Kasper D, Pohlmann R, Petersen CM. The sortilin cytoplasmic tail conveys Golgi-endosome transport and binds the VHS domain of the GGA2 sorting protein. EMBO J. 2001;20(9):2180–90.
60. Dev KK. Making protein interactions druggable: targeting PDZ domains. Nat Rev Drug Discov. 2004;3(12):1047–56.
61. Madsen KL, Beuming T, Niv MY, Chang CW, Dev KK, Weinstein H, Gether U. Molecular determinants for the complex binding specificity of the PDZ domain in PICK1. J Biol Chem. 2005;280(21):20539–48.
62. Erlendsson S, Rathje M, Heidarsson PO, Poulsen FM, Madsen KL, Teilum K, Gether U. Protein interacting with C-kinase 1 (PICK1) binding promiscuity relies on unconventional PSD-95/discs-large/ZO-1 homology (PDZ) binding modes for nonclass II PDZ ligands. J Biol Chem. 2014;289(36):25327–40.
63. Dumanis SB, Burgert T, Caglayan S, Fuchtbauer A, Fuchtbauer EM, Schmidt V, Willnow TE. Distinct functions for anterograde and retrograde sorting of SORLA in amyloidogenic processes in the brain. J Neurosci. 2015;35(37):12703–13.
64. Hentschke M, Susens U, Borgmeyer U. Transcriptional ERRgamma2-mediated activation is regulated by sentrin-specific proteases. Biochem J. 2009;419(1):167–76.
65. Hermey G, Keat SJ, Madsen P, Jacobsen C, Petersen CM, Gliemann J. Characterization of sorCS1, an alternatively spliced receptor with completely different cytoplasmic domains that mediate different trafficking in cells. J Biol Chem. 2003;278(9):7390–6.
66. Oetjen S, Mahlke C, Hermans-Borgmeyer I, Hermey G. Spatiotemporal expression analysis of the growth factor receptor SorCS3. J Comp Neurol. 2014;522(15):3386–402.

Publisher's Note

5.

Internally tagged Vps10p-Domain receptors reveal BDNF uptake

Marcel Klein, Antonio Virgilio Failla, and Guido Hermey

Research-Article

Under review in *J Biol Chem.*

Personal contribution

All experiments were performed and analyzed by Marcel Klein. The FRET experiments in Fig. 6 B-C were performed and analyzed by Marcel Klein and Dr. Antonio Virgilio Failla. The first version of the manuscript was written by Marcel Klein.

21.12.2022 Hamburg

Date and City

Signature supervisor

PD Dr. Guido Hermey

Internally tagged Vps10p-Domain receptors reveal BDNF uptake

Marcel Klein[1*], Antonio Virgilio Failla[2], Guido Hermey[1*]

[1]Institute for Molecular and Cellular Cognition, Center for Molecular Neurobiology Hamburg, University Medical Center Hamburg-Eppendorf, Hamburg, Germany

[2]Microscopy Imaging Facility, University Medical Center Hamburg-Eppendorf, Hamburg, Germany

[*]Authors for correspondence: marcel.klein@zmnh.uni-hamburg.de and guido.hermey@zmnh.uni-hamburg.de

Running title: Fluorophore tagged Vps10p-D receptors

Keywords*:* Sortilin; SORLA; SorCS; neurotrophin; BDNF; protein sorting; receptor internalization; live-cell imaging

Abstract

The Vps10p-Domain (Vps10p-D) receptor family consists of Sortilin, SorLA, SorCS1, SorCS2 and SorCS3. They convey internalization, secretion and intracellular sorting of specific cargo in different cell types, including neurons, but the underlying molecular determinants are incompletely understood. Their malfunctioning is associated with several neurodegenerative, neuropsychiatric, and metabolic diseases including Alzheimer's disease and diabetes. Decoding the dynamic intracellular itineraries of Vps10p-D receptors is crucial to understand their role in physiological and cytopathological processes. The direct observation of their interactions at spatial and temporal levels to examine local dynamics by live imaging has been challenging as terminal fluorophore tagging presumably impedes a large number of their protein interactions and functions. For such imaging studies, we designed functional internally fluorophore tagged versions of all family members. We used bioinformatics and predict protein folding and structures of the tagged Vps10p-D receptors. In accordance, we demonstrate exit of the newly designed receptor constructs from the endoplasmic reticulum. We examined their subcellular localization by immunocytochemistry and live imaging, which was identical to that of the wild type counterparts as far as known. The ligand induced internalization of the fluorophore tagged Vps10p-D receptors strongly suggests functionality of the Vps10p-D domains and homodimerization of fluorophore tagged SorCS2 demonstrates intact leucine rich domains. We show for the first time BDNF uptake mediated by all Vps10p-D receptors and interaction of SorLA and SorCS1 with a neurotrophin. Together, the here designed fluorophore tagged receptors are novel powerful tools for accurate live surveys of the individual cellular functions of Vps10p-D receptors.

Introduction

The Vps10p-Domain (Vps10p-D) receptor family consists in mammals of the five type-I transmembrane proteins Sortilin, SorLA, SorCS1, SorCS2 and SorCS3 (1). All family members are predominantly expressed in the developing and adult nervous system with specific spatiotemporal expression patterns (2-6). All, with exception of SorCS3, are also expressed in varying peripheral tissues (7-11). A large number of genetic linkage analysis and functional studies demonstrated an association of the receptors with several neurodegenerative and psychiatric disorders, including Alzheimer's disease and autism spectrum disorders (12-19), and metabolic diseases, including diabetes, atherosclerosis and hypercholesterolemia (20-24).

The shared hallmark of the family is the N-terminal Vps10p-D, which was first described in the yeast sorting receptor Vps10p (25). Due to the intracellular sorting function of yeast Vps10p, sorting properties were also proposed for the mammalian Vps10p-D receptors. In agreement, these bind different ligands and mediate their secretion, internalization and sorting through the endosomal system (1,26,27). All family members present a large luminal/extracellular moiety followed by a transmembrane domain and a short cytoplasmic tail (Fig. 1*A*). The Vps10p-D forms at its N-terminus a β-propeller resembling a conical funnel with binding sites for different ligands followed by two small cysteine-rich domains, named 10CC module (28-30). In Sortilin, the luminal/extracellular moiety comprises only the Vps10p-D (8,31). In the SorCS subgroup, a leucine rich domain is located between the Vps10p-D and the transmembrane domain. It contains imperfect leucine-rich repeats, but also regions with homology to polycystic kidney disease (PKD) domains and is thought to allow receptor dimerization (10,30,32). In SorLA, the Vps10p-D is followed by structural motifs shared with the low-density lipoprotein (LDL) receptor family, a YWTD β-propeller domain, an EGF precursor type repeat, LDLR class A repeats and fibronectin type III repeats (7).

An N-terminal propeptide precedes all Vps10p-Ds (Fig. 1*A*), which in Sortilin and SorLA, but not in the SorCS subgroup, is binding to their own Vps10p-Ds, causing an inability of additional binding of most ligands to this domain (33-37). The proprotein convertase furin cleaves the propeptides of all family members within the trans-Golgi network (TGN). This proteolytic step activates the Vps10p-D of Sortilin and SorLA for ligand binding. At least in SorCS1 alternative functional furin cleavage sites for the propetide exist, indicating possible differential proprotein convertase processing (38).

The receptors interact with a broad range of transmembrane and secreted proteins, including trophic factors. In particular, the role of Sortilin and SorCS2 in neuronal plasticity and apopototic signaling by interacting through their Vps10p-Ds with neurotrophins are well studied. The four members of the neurotrophin family, nerve growth factor (NGF), brain derived neurotrophic factor (BDNF), neurotrophin-3 (NT-3), and neurotrophin-4/5 (NT-4/5), are synthesized as precursors, so called pro-neurotrophins (39). Proteolytic cleavage of the pro-domain releases the mature neurotrophin. Both

the pro and mature forms can be secreted and display distinct and often opposing biological activities. Mature neurotrophins bind their cognate tropomyosin receptor kinase (Trk) family receptors promoting growth and survival of neurons, whereas pro-neurotrophins form a ternary complex with p75 neurotrophin receptor (p75NTR) and Sortilin or SorCS2 and induce apoptotic signaling. Both, pro- and mature neurotrophins bind to TrKs, p75NTR and Vps10p-D receptors. In general, mature neurotrophins bind p75NTR and Trks with higher affinity whereas the affinity of proneurotrophins seems to be higher for Vps10p-D receptors (30,34,40-42). The latter assumption is mainly based on binding studies of pro-BDNF, pro-NGF and NGF to Sortilin and SorCS2. However, there are exceptions as SorCS3 binds mature NGF with higher affinity than pro-NGF (43). Due to the homologous structure of the Vps10p-Ds within the receptor family, it is expected that all family members bind neurotrophins, but so far, this concept awaits experimental corroboration.

On the receptor level, there is accumulating evidence for a complex orchestration of interactions. Trks and p75NTR can form a complex to enhance trophic signaling (44). Moreover, Sortilin and SorCS2 interact directly with p75NTR (34,45). Vps10p-D receptors interact also with the BDNF receptor TrkB (46-48). SorLA promotes, whereas SorCS1 and SorCS3 inhibit TrkB surface activity and Sortilin promotes cell and synaptic surface expression of all Trks (47,49,50).

The cytoplasmic domains of all Vps10p-D receptors contain internalization motifs and varying adaptor protein binding sites. SorCS1 is expressed as different splice variants with alternative cytoplasmic domains (33). Notably, the variant SorCS1b is the only Vps10p-D receptor lacking a functional internalization motif in its cytoplasmic domain and is localized predominantly to the cell surface (33). In contrast, all other SorCS1 splice variants, such as the here studied SorCS1c-α, and all other Vps10p-D receptors are endocytic receptors targeted mainly to Golgi and endosomal compartments (1,26,27). The assumption that Vps10p-D receptors convey intracellular sorting is based on the interaction of their cytoplasmic domains with various adaptor proteins involved in endosomal targeting (51-58). Moreover, studies employing knockout models revealed altered localization or miss-targeting of interacting proteins (24,48,49,56,59-62) and the expression of chimeric receptor constructs demonstrated internalization and intracellular targeting of ligands or rescued specific phenotypes in knockout models (6,33,43,53-55). In previous studies, the subcellular localization of endogenous Vps10p-D receptors was determined by subcellular fractionation or by immunocytochemistry of fixed cells. There have been also attempts to perform direct and live imaging of Vps10p-D receptor localization and trafficking. These include the fusion of a fluorophore N-terminal to the transmembrane and cytoplasmic domain of Sortilin or SorLA (63,64). These constructs lack the receptor specific luminal/extracellular moieties, but revealed important information on the subcellular targeting and transport dynamics mediated by the respective cytoplasmic domains. In a number of other studies full length Sortilin, SorLA or SorCS2 were tagged at the C-terminus with a fluorophore

(52,56,61,65-67). These constructs retained full functionality of the respective luminal/extracellular domains, but the C-terminal tag likely interferes with different interactions of the cytosolic tails. Binding of several cytosolic adaptor proteins, such as GGAs and PDZ-domain proteins, to their specific amino acid motifs depends on a free C-terminus (68,69). Notably, already small C-terminal peptide tags, such as a myc-tag, impede GGA interaction (68). GGAs are known functional Sortilin and SorLA interactors (55,56,68,70,71), the PDZ-domain protein PICK1 targets SorLA and SorCS3 (51,57) and additional yet unidentified C-terminal interactors are most likely. Therefore, C-terminal tagging probably leads to aberrant subcellular localization of Vps10p-D receptors. Hence, other tagging strategies are needed to study Vps10p-D receptors by live and in vivo imaging.

Here, we designed functional genetically encoded constructs of each member of the Vps10p-D receptor family tagged with fluorophores. We excluded an N-terminal tag, because it would be cleaved off by furin in the secretory pathway, furin cleavage is critical for some receptor function and a fluorophore tag following the furin cleavage site probably interferes with the ligand binding capacity of the Vps10p-D. We also excluded a C-terminal tag because it impedes specific interactions with adaptor proteins binding to C-terminal sites and also an insertion of a fluorophore tag between the transmembrane and the cytoplasmic domain, because several sorting motifs depend on the correct spacing relative to the plasma membrane (72). Therefore, we designed versions of the receptors harboring an internal tag in the luminal/extracellular moiety between functional modules and the transmembrane domain.

Previously, we presented versions of different SorCS1 splice variants with an internal mVenus tag between their transmembrane and extracellular domains to analyze their intracellular transport and differences in amyloid precursor protein (APP) sorting (73). Here, we applied this tagging strategy to all members of the Vps10p-D receptor family. We examine the subcellular localization of the constructs which is identical to their wild type counterparts as far as known, show internalization after ligand binding to the extracellular/luminal domain and functional dimerization of constructs of the SorCS subgroup. Finally, we demonstrate for the first time that all Vps10p-D receptors facilitate internalization of BDNF independent of TrkB.

Results

Design and structure prediction of fluorophore tagged Vps10p-D receptors

We aimed at generating tools to investigate dynamic localizations of each member of the Vps10p-D receptor family by live imaging. To this end, we tagged the receptors with fluorophores. The position of the tag insertion is critical to preserve receptor functions. To retain the functionality of the Vps10p-D receptors, we excluded N- or C-terminal positioning of fluorophore tags. Instead, we designed expression constructs encoding receptors tagged internally in the luminal/extracellular moieties. The

luminal/extracellular segments of Sortilin, SorCS1, SorCS2 and SorCS3 and the Vps10p-D of SorLA have been previously expressed in eukaryotic cells, purified from cell culture media and successfully used in functional ligand binding experiments (33-35,37,43). This demonstrated that these segments are functional units. In addition, extracellular moieties of Sortilin, SorLA and SorCS2 have been also expressed to resolve their structures (28-30). Considering these results, we predicted functional segments after which fluorophore tags could be inserted without altering receptor functionality. We designed respective full-length receptors with mVenus or tdTomato tag insertions between the luminal/extracellular moieties and the transmembrane domains of Sortilin, SorCS1b, SorCS1c-α, SorCS2 and SorCS3 (Fig. 1*A*). For SorLA a tag between the transmembrane domain and the fibronectin type III repeats revealed constantly errors in protein folding predictions (data not shown) and thus, tag insertions were positioned directly after the SorLA Vps10p-D (Fig. 1*A*).

We predicted correct folding of the designed proteins computationally using AlphaFold 2.0 (74). Figure 1B shows that transmembrane domains (indicated in orange) of Sortilin, SorCS1, SorCS2 and SorCS3 fold as full α-helices in wild type (wt) proteins and after insertion of either mVenus or tdTomato. The TopPred tool also recognized these transmembrane domains respectively (75,76). The leucine rich domains (indicated in green) of the SorCS subgroup preceding the respective tag show the same folding sequence of α-helices and β-sheets as in the wt proteins (Fig. 1*B*). Each fluorophore is followed in tagged SorLA by an YWTD β-propeller domain that folds identical to the domain in wt SorLA (indicated in dark blue). These predictions indicate that the structures of the domains next to the fluorophores in the internally tagged Vps10p-D receptors are unaltered by mVenus or tdTomato insertions at the selected positions as compared to the wt receptors. Together, the structure predictions suggest preserved receptor structures and functionality after tag insertion.

Expression of internally tagged Vps10p-D receptors

Correctly folded proteins are exported from the endoplasmic reticulum (ER), whereas misfolded proteins are retained and eventually degraded. We cloned and expressed the designed Vps10p-D receptors tagged with mVenus or tdTomato in COS7 cells. Co-transfection of the mVenus constructs with an ER marker construct (KDEL-tdTomato) demonstrates low localization of the mVenus tagged Vps10p-D receptors at the ER (Fig. 2*A*). SorCS3 constructs were expressed in HEK293 cells, because in COS7 cells varying amounts of the construct were constantly trapped in the ER (data not shown). For mVenus tagged Sortilin, SorCS1c-α, SorCS2 and SorCS3 vesicular and surface expression was observed. SorLA-mVenus predominated in vesicular structures and SorCS1b-mVenus mainly localized at the cell surface. Together, these findings indicate the successful exit of the tagged Vps10p-D receptors from the ER and therefore suggest correct protein folding.

Subsequent immunoblotting of cell lysates with tag specific antibodies revealed full-length expression of the mVenus or the tdTomato tagged receptors, because observed estimated molecular weights resemble the expected calculated molecular weights of the respective proteins (Fig. 2, *B* and *C*).

Subcellular localization of internally tagged Vps10p-D receptors

Next, we asked to which specific subcellular compartments the tagged receptors localize and if these localizations are in accordance with the previously reported localization of the Vps10p-D receptors. Therefore, the subcellular localizations of the mVenus or tdTomato tagged Vps10p-D receptors were specified by their expression and co-staining of transfected cells with antibodies against subcellular marker proteins for the cis-Golgi network (CGN), early endosomes or lysosomes (Fig. 3). In addition, we co-expressed fluorophore tagged marker proteins for the TGN, the TGN – endosome transition or endosome – lysosome transition (Fig. 4). Subsequently, Mander`s co-localization coefficients were calculated from confocal images of single cells and compared between the sorting receptors. mVenus tagged Sortilin, SorCS1c-α, SorCS2, SorCS3 and SorCS1b showed co-localization with the CGN marker protein GM130 (Fig. 3, *A* and *B*). For SorLA-mVenus, however, we observed significantly lower co-localization with GM130. Antibody staining against the early endosomal protein Rab5 showed significantly higher co-localization with mVenus tagged Sortilin, SorLA, SorCS1c-α, SorCS2 and SorCS3 than with SorCS1b-mVenus (Fig. 3, *C* and *D*). The mVenus tagged Vps10p-D receptors showed relatively low co-localization with the lysosomal protein LAMP1 without significant differences between the receptors (Fig. 3, *E* and *F*). Co-expression of the GFP tagged C-terminal fragment of the TGN localized β-1,4-galactosyltransferase (β-1,4-GT) with tdTomato tagged Vps10p-D receptors demonstrates high co-localization with Sortilin-tdTomato and with SorLA-tdTomato (Fig. 4, *A* and *B*). Whereas SorCS1c-α-, SorCS2- and SorCS3-tdTomato showed significantly lower co-localization with the TGN marker and almost no co-localization was observed with SorCS1b-tdTomato. VPS35, is part of the retromer complex which conveys endosome-to-TGN retrieval of different cargo proteins (77) and, hence, localizes to endosomes and the TGN. GFP-VPS35 co-localized to a minor degree with SorCS1b-tdTomato (Fig. 4, *C* and *D*), but revealed significant co-localization with tdTomato tagged SorCS1c-α, SorCS2 and SorCS3, and even higher co-localization with Sortilin- and SorLA-tdTomato (Fig. 4, *C* and *D*). Rab9 mediates transport from late endosomes to the TGN and towards endolysosomal compartments (78). mCherry-Rab9 co-localized with mVenus tagged Sortilin, SorLA, SorCS1c-α, SorCS2 and only to a limited degree with SorCS3- and SorCS1b-mVenus (Fig. 4, *E* and *F*).

In addition, COS7 or HEK293 cells and primary hippocampal neurons were transfected with GFP-Rab5 and the tdTomato tagged Vps10p-D receptors. Expression in COS7 and HEK293 cells was monitored *in vivo* by confocal live-cell imaging. Time-lapse recordings demonstrate frequent endosomal co-transport of tdTomato tagged Sortilin, SorLA, SorCS1c-α, SorCS2 and SorCS3 with GFP-Rab5 (Movies 1-

5 and Fig. 5). SorCS1b-tdTomato positive vesicular structures were only rarely positive for GFP-Rab5 (Movies 6 and Fig. 5). Transfected primary hippocampal neurons were stained for GFP and tdTomato. A large number of vesicles positive for tdTomato tagged Sortilin, SorLA, SorCS1c-α, SorCS2 and SorCS3 were also positive for GFP-Rab5 (Fig. 6*A*). In accordance with the previous experiments, we observed almost no colocalization of the surface localized SorCS1b-tdTomato with GFP-Rab5. Co-staining of primary cultured neurons expressing td-Tomato tagged Sortilin, SorLA, SorCS1b, SorCS1c-α, SorCS2 or SorCS3 with the somatodendritic marker microtubule-associated protein 2 (MAP2) and the axonal initial segment marker ankyrin G (AnkG) demonstrated a predominant somatodendritic localization of all tagged Vps10p-D receptors (Fig. 6*B*). However, tagged SorCS3 and SorCS1b also showed some expression in the axonal initial segment.

Taken together, we observed somatodendritic and endosomal expression of all receptors except for SorCS1b, which presented a predominant cell surface localization, in neurons. All tagged Vps10p-D receptors, but not SorCS1b, showed an endosomal localization also in non-polarized cells. Tagged Sortilin, SorLA, SorCS1c-α, SorCS2 and SorCS3 were all expressed in early to late endosomes including Rab5, VPS35 and Rab9 positive endosomes. SorCS3, however, was found only to a minor extend in Rab9 positive endosomes. The subcellular localization has not been completely described for all Vps10p-D receptors, but our findings are to a large extend in accordance with so far reported localizations. Therefore, our results indicate functional C-terminal interaction of the tagged Vps10p-D receptors with adaptor proteins, which are crucial regulators for the subcellular targeting of Vps10p-D receptors.

Dimerization of SorCS2

The correct subcellular localization of the fluorophore tagged Vps10p-D receptors and therefore assumed functionality of their cytoplasmic tails interacting with different cytosolic adaptor proteins opened the intriguing question if their extracellular domains are also functional. The leucine rich domain of the SorCS subgroup interacts with other leucine rich domains of the SorCS subgroup which consequently form homo- and heterodimers. As this domain is adjacent to the tag insert area in the SorCS subgroup, we regarded dimerization, which likely underlies functionality, as crucial. As a proof, we investigated the ability of tagged SorCS2 to form homodimers. To this end, we expressed mVenus and tdTomato tagged SorCS2 and performed co-immunoprecipitation experiments. As a control, these experiments were also performed with cells transfected with SorCS2-mVenus and Sortilin-tdTomato. Sortilin, which lacks a leucine rich domain, has not been shown to dimerize with any member of the SorCS subgroup. We observed co-immunoprecipitation of SorCS2-tdTomato with SorCS2-mVenus, but not of Sortilin-tdTomato with SorCS2-mVenus from the respective cell lysates (Fig. 7*A*).

Next, we assessed homodimerization of fluorophore tagged SorCS2 by employing fluorescence lifetime imaging (FLIM). Again, we co-expressed SorCS2-mVenus with either SorCS2-tdTomato or Sortilin-tdTomato. Cells were fixed and the fluorescence lifetime of the mVenus fluorophores was measured using STED microscopy. Here, mVenus emission acts as a donor for the excitation of tdTomato. If both fluorophores are in close proximity, the fluorescence lifetime of mVenus decreases due to photon energy transfer to tdTomato. When co-expressing SorCS2-mVenus with SorCS2-tdTomato the fluorescence lifetime of the mVenus fluorophore was significantly lower as compared to SorCS2-mVenus co-expressed with Sortilin-tdTomato (Fig. 7, *B* and *C*). This proves close proximity between the tagged SorCS2 proteins and strongly suggests their direct interaction and homodimerization.

Vps10p-D receptors mediate BDNF uptake

To assess functional ligand binding of the fluorophore tagged Vps10p-D receptors, we assessed BDNF binding abilities of the Vps10p domains. Cells were transfected with the tdTomato tagged Vps10p-D receptors, incubated at 4°C with mature BDNF-Biotin, washed, incubated for 10 min at 37°C to allow receptor internalization and after fixation BDNF-Biotin was visualized by a fluorescent streptavidin conjugate (Fig. 8*A*). Cells transfected with tdTomato tagged Sortilin, SorLA, SorCS1c-α, SorCS2 and SorCS3 internalized BDNF-Biotin (Fig. 8*B*). The BDNF signal was restricted to vesicular structures which were also positive for the respective tagged Vps10p-D receptors. Cells transfected with tdTomato tagged SorCS1b yielded BDNF staining only at the cellular surface and no internalization of BDNF was observed (Fig. 8*B*). We performed immunoblotting for the BDNF receptor TrkB. We compared lysates of HEK293 cells transfected with TrkB-GFP and non-transfected HeLa and HEK293 cells (Fig. 8*C*). Using an antibody against TrkB, we detected in transfected cells TrkB-GFP, with the expected molecular weight of approximately 167 kDa, and its dominant-negative truncated version TrkB.t1-GFP, which originates from post-translational cleavage of TrkB-GFP within its cytoplasmic domain by calpain (79) with an expected molecular weight of approximately 117 kDa. As we could not detect TrkB in the employed HeLa and HEK293 cells by immunoblotting, we conclude that internalization of BDNF through the tagged Vps10p-D receptors in HeLa or HEK293 cells was TrkB independent.

We assessed BDNF internalization also by live cell imaging by co-culturing cells expressing BDNF-GFP with cells expressing tdTomato tagged Sortilin, SorLA, SorCS1b, SorCS1c-α or SorCS2. In these experiments, one set of HeLa cells was transfected with BDNF-GFP (Fig. 8*D*). These cells secrete BDNF-GFP into the cell culture medium. Another set of HeLa cells was transfected with the tdTomato tagged Vps10p-D receptors. 24 h after transfection, the differently treated cells were co-cultured and analyzed by confocal live microscopy. Time-lapse images of cells expressing either of the tdTomato tagged Vps10p-D receptors also show vesicular co-localization and co-transport of BDNF-GFP with tdTomato tagged Sortilin, SorLA, SorCS1c-α or SorCS2 (Movies 7-10, Fig. 8*E*). As BDNF-GFP is expressed in

independently transfected cells, tdTomato tagged Vps10p-D receptor expressing cells took up BDNF-GFP from the cell culture medium. In accordance with the previous experiments, BDNF-GFP was observed predominantly at the cellular surface in cells expressing SorCS1b-tdTomato (Movie 11, Fig. 8*E*).

In conclusion, we demonstrate for the first time that all Vps10p-D receptors interact with BDNF, that tagged Sortilin, SorLA, SorCS1c-α, SorCS2 and SorCS3 mediate internalization of BDNF independent of TrkB and that tagged SorCS1b overexpressing cells exposed to BDNF accumulate BDNF at their cellular surface. The functional interaction of the receptors with BDNF strongly suggests ligand binding ability of the fluorophore tagged Vps10p-D receptors through their Vps10p-Ds.

Discussion

Proteins are delivered post-translationally to specific subcellular compartments to exert their proper function. Accurate sorting of proteins is one factor that underlies the compartmentalization of cells into distinct membrane-bound organelles and the asymmetric arrangement of polarized cells such as neurons. Alterations of these processes can underlie tremendous cytopathological defects. Sorting receptors of the Vps10p-D family play a role in endosomal targeting, secretion and internalization of soluble ligands. In addition, they govern also the subcellular localization of other transmembrane proteins, but the underlying molecular determinants are incompletely understood (1,26,27).

Deciphering the localization and mobility of Vps10p-D receptors inside a cell and directly observing their interactions at spatial and temporal levels to examine local dynamics by live imaging has been challenging. The most widely applied strategy for live imaging of proteins is the use of fluorescent protein tags. Such fusion proteins enable the non-invasive analysis of protein localization and dynamics in living cells owing to the unique ability of GFP-like fluorescent proteins to form chromophores autocatalytically without the involvement of external enzymes and cofactors (80). When genetically fused to a protein of interest, fluorophores offer an exquisite labeling specificity. Adding a fluorophore to the N- or C-terminus of a protein is the simplest strategy to tag a protein. However, terminal tagging of Vps10p-D receptors presumably impedes a large number of specific protein interactions and functions. Therefore, we excluded terminal tagging and designed internally tagged receptors. The positioning of the internal tag is critical to retain receptor structure and function. For the selection of the tag position, we benefitted from previous studies expressing the extracellular/luminal parts of the receptors as functional segments and from structural analyses (28-30,33-35,37,43).

To maintain function and ligand binding properties of tagged receptors, the correct folding of their individual domains is essential. Protein folding, along with different protein modifications, occurs co- and post-translationally in the ER by several chaperoning proteins and the functional protein is then sorted from the ER to the Golgi apparatus (81). Misfolding of proteins generally prevents their exit

from the ER, leads to accumulation in the ER and eventually to a stress response and degradation. We predicted the structures of mVenus and tdTomato tagged Vps10p-D receptors computationally, observed their exit from the ER and concluded correct domain folding of the tagged Vps10p-D receptors. Only the SorCS3 construct was partially trapped in the ER when expressed in COS7 or HeLa cells, but not in HEK293 cells and in primary cultured neurons. SorCS3 is the only Vps10p-D family member with an exclusive expression in the brain (6) and it is tempting to speculate that in some non-neuronal cells, such as COS7 cells, specific factors for successful folding of the receptor are lacking.

We specified the intracellular localizations of the tagged receptors and our observations are largely in agreement with previous studies assessing subcellular localization of wt or chimeric Vps10p-D receptors by immunocytochemistry. Notably, a detailed subcellular localization has not been performed for all Vps10p-D receptors so far. This turned out difficult for SorCS1 and SorCS3, because both proteins are highly homologous and specific antibodies for each receptor are not available. Thus, we present additional tools to detect the receptors independently. We show significant co-localization of all fluorophore tagged Vps10p-D receptors, but not of SorLA, with the CGN marker protein GM130. Still, the absence of SorLA co-localization with GM130 corroborates previous investigations (82). We observed that the receptors are targeted from the Golgi apparatus to the plasma membrane and to various endosomes of which several were Rab5 and VPS35 positive (6,34,48,52,54,58,73,82-85). Only SorCS1b, which is lacking internalization motifs in its cytoplasmic tail, is predominantly localized to the plasma membrane (33). Specific post-Golgi and post-endocytic pathways are so far not completely characterized for all Vps10p-D receptors. The itineraries of Sortilin and SorLA are best characterized. Both interact directly with the retromer complex (52,58). This is likely reflected in the high co-localization of fluorophore tagged Sortilin and SorLA with the retromer subunit VPS35. Fluorophore tagged SorCS1c-α, SorCS2 and SorCS3 demonstrated a significantly lower co-localization, presumably due to an indirect interaction with the retromer complex, indicated by the lack of canonical retromer interaction motifs in their cytoplasmic domains. However, co-immunoprecipitation of VPS35 with SorCS1 has been observed (86), supporting SorCS1 transport in VPS35 positive endosomes.

In accordance with a number of other studies, we found predominant somatodendritic expression of all fluorophore tagged Vps10p-D receptors in primary cultured neurons (6,46,82,87,88). However, we also observed some additional expression of SorCS1b and SorCS3 in the axonal initial segment.

The receptors of the SorCS subgroup homo- and heterodimerize through their leucine rich domains (32). The demonstration of the homodimerization of fluorophore tagged SorCS2 suggests functional leucine rich domains and hints at an equally functional dimerization of fluorophore tagged SorCS1 or SorCS3. Our successful FLIM application points at the use of fluorophore tagged Vps10p-D receptors in additional interaction studies based on FRET-FLIM experiments in fixed and living cells. The here established internal insertion site may be also applied to other tags including application-tailored

fluorophores with specialized photophysical properties. Thus, live cell analysis can be expanded by the introduction of alternative fluorophore tags, such as pH sensitive fluorophores. The tag position is also useable for insertion in other experiments, e.g. to identify additional protein interaction partners. Moreover, the genetically encoded tags can be introduced by gene editing methods to overcome overexpression effects.

The here conducted live imaging experiments proved the applicability of the designed fluorophore tagged Vps10p-D receptors in live assays. For all tagged receptors except for SorCS1b our data shows *in vivo* cotransport with GFP-Rab5 as well as TrkB independent internalization of biotin labeled or GFP tagged BDNF. These observations corroborate the endocytic function of all Vps10p-D receptors, but not SorCS1b, and their transport through Rab5 positive early endosomes. Previous studies highlighted the high affinity interaction of pro-NGF and pro-BDNF with Sortilin and SorCS2 (30,40). However, a lower affinity binding of mNGF has been observed for Sortilin and SorCS2 (30,40) and SorCS3 also binds proNGF but, in contrast, an even higher affinity to mNGF (43). We observed an endocytic uptake of biotin labeled mBDNF by all fluorophore tagged Vps10p-D receptors, but not SorCS1b which promotes accumulation of mBDNF on the cell surface. In the executed experiments, we focused on the functionality of the Vps10p-Ds in the tagged receptors. Accordingly, saturating concentrations of mBDNF-Biotin were used in the internalization experiments and binding of lower affinity ligands might already result in receptor internalization. In addition, cells expressing either fluorophore tagged Vps10p-D receptor, but not SorCS1b, internalized BDNF-GFP secreted by co-cultured cells. The BDNF-GFP construct encoded full length BDNF and internalized BDNF-GFP might correspond to both pro- or mature-BDNF-GFP. Together, our experiments demonstrate for the first time BDNF uptake by all Vps10p-D receptors. Notably, an interaction of SorLA and SorCS1 with a neurotrophin has not been demonstrated before. Future experiments are needed to determine specific affinities of the receptors for the specific forms of BDNF.

In summary, we designed functional fluorophore tagged Vps10p-D receptors. Using immortalized cells as well as primary cultured neurons, we observed functional subcellular targeting, ligand binding, cargo transport and dimerization of the tagged receptors. Overall, the here designed fluorophore tagged Vps10p-D receptors are novel powerful tools for future accurate surveys of the individual roles of the receptors in intracellular sorting which might be key to understand cytopathological mechanisms underlying neuronal and metabolic diseases.

Experimental procedures

Constructs for protein expression and structure prediction

To generate expression constructs, tdTomato or mVenus, as well as one N-terminal and one C-terminal fragment of (human) hSortilin, hSorLA, hSorCS1b, hSorCS1c-α, (murine) mSorCS2 and hSorCS3

respective cDNAs were amplified by PCR using Q5® High-Fidelity DNA Polymerase (New England Biolabs). Using appropriate primers generating an ApaI site at the 3'-ends of cDNA encoding the N-terminal fragments of the Vps10p-D receptors and at the 5'-ends of tdTomato or mVenus cDNA. To the 5'-ends of cDNA encoding the C-terminal fragments and to the 3'-ends of tdTomato or mVenus cDNA an XbaI site was added. For hSortilin, hSorCS1b, hSorCS1c-α, mSorCS2 and hSorCS3 the N-terminal fragment contained their extracellular domains, and the C-terminal fragment comprised their transmembrane and cytosolic domain respectively. The transition point to the respective transmembrane domain was predicted using the TMHMM 2.0 (89,90) and the TopPred tool (75,76). Accordingly, the transition from the extracellular domain to the transmembrane domain of hSortilin is at V^{757} (UniProtKB ID: Q99523-1), for the hSorCS1 splice variants at G^{1100} (UniprotKB ID: Q8WY21-1), for mSorCS2 at Y^{1080} (UniprotKB ID: Q9EPR5-1) and for hSorCS3 at S^{1124} (UniprotKB ID: Q9UPU3-1). However, to enhance correct protein folding, C-terminal fragments of hSorCS1 and hSorCS3 were extended until the next proline which often functions as a structure breaker between domains (91). Hence, the C-terminal fragments of the hSorCS1 variants start from P^{1096} and of hSorCS3 from P^{1114}. For hSorLA (UniprotKB ID: Q92673-1) the N-terminal fragment contains the propeptide and the Vps10p-D (M^1 – E^{759}), and the C-terminal fragment contains all domains starting with the YWTD repeat to the C-terminus (F^{760} – A^{2214}). cDNA encoding the respective N-terminal and C-terminal fragments were first cloned into the pcDNA3.1/Zeo(-) vector (Invitrogen). Between these two fragments the amplified cDNA of tdTomato or mVenus were inserted respectively. For lentiviral expression these constructs were then also cloned into the L21 vector (57). The subcellular markers were all tagged at their termini. Accordingly, cDNA encoding GFP was cloned to the 3'-ends of the respective cDNAs encoding BDNF, TrkB, Vps35 or β-1.4-GT and cloned into an L21C-M2 destination vector. GFP-Rab5 has been described before (92). mCherry-Rab9a was purchased from Addgene (Plasmid #78592) (93). The ER marker, tdTomato tagged Calreticulin signal peptide carrying a KDEL sequence, was a generous gift from Jakob Gutzmann.

The structures of the wildtype sorting receptors were predicted using the AlphaFold Structure Database. To confirm correct protein folding of the tagged proteins their structures were predicted employing the Robetta server and AlphaFold 2.0 (74,94,95). Due to computational limitations, however, the tagged protein predictions contain only the critical neighboring domains of the inserted fluorophores, respectively.

Cell culture and transfection

COS7 (DSMZ, ACC60), HeLa (DSMZ, ACC57) and HEK293 (DSMZ, ACC305) cells were cultured at 37°C and 5% CO_2 in Gibco Dulbecco's MEM (DMEM, Thermo Fisher Scientific) supplemented with 10% fetal calf serum (FCS, Capricorn Scientific GmbH) and 100 U ml^{-1} Penicilin-Streptomycin (Thermo Fisher

Scientific). Transfection was performed using Lipofectamine 2000 (Invitrogen) according to manufacturer's protocol.

For primary hippocampal cell culture hippocampi were dissected from E16 embryos of pregnant C57BL/6J mice collected in 10 mM glucose, rinsed with Hanks' Balanced Salt Solution (HBSS, Thermo Fisher Scientific) and treated with 0.05% Trypsin-EDTA (Thermo Fisher Scientific) for 5 min at 37°C. Trypsin reaction was stopped using 10% FCS in HBSS and neurons were dissociated in HBSS by triturating with fire polished Pasteur pipettes. HBSS was removed and approximately 60,000 cells/cm² were seeded in PNGM™ (Lonza) supplemented with 100 U/ml Penicilin-Streptomycin on poly-L-lysine coated 12 mm glass coverslips. After 3 days *in vitro* (DIV), neurons were incubated with PNGM™ (Lonza) supplemented with NSF-1 (Lonza) for 30 min and transfected with 3 µg plasmid DNA using 125 mM $CaCl_2$ in HeBS (137 mM NaCl, 5 mM KCl, 0.7 mM Na_2HPO_4, 7.5 mM glucose, 21 mM HEPES pH 7.12) for 40 min per coverslip. Transfected neurons were then fixed and immunostained 7–14 days *in vitro* (DIV).

Immunocytochemistry, antibodies and conjugates

Cells were fixed using ice cold 4% paraformaldehyde (PFA) and 4% sucrose in PBS or with ice cold methanol for 20 min and permeabilized with 0.05 % Triton X-100 in PBS for 30 min. For immunostaining the following antibodies were used: rabbit α-dsRed (to stain tdTomato) (632496, Clontech; 1:500); chicken α-GFP (to stain mVenus) (ab139701, Abcam; 1:5000); mouse α-GM130 (ab169276, Abcam; 1:100); rabbit α-Rab5 (ab18211, Abcam; 1:200); rabbit mouse α-Lamp1 (555798, BD Biosciences; 1:2000); chicken α-Map2 (ab5392, Abcam; 1:10,000); mouse α-Ankyrin G (sc-12719, Santa Cruz; 1:100); goat α-chicken Alexa Fluor 488 (A11039, Invitrogen; 1:400); goat α-rabbit Alexa Fluor 555 (A21428, Invitrogen; 1:400); goat α-mouse Alexa Fluor 555 (A21422, Invitrogen; 1:400); goat α-mouse Alexa Fluor 633 (35513, Thermo Scientific; 1:400).

Immunoblotting

To verify qualitative expression of indicated proteins transfected or non-transfected cells were harvested and lysed in lysis buffer (150 mM NaCl, PBS pH 7.4, 2% NP-40, 0.1% SDS, 0.5% sodium deoxycholate, 1 mM PMSF and Complete proteinase inhibitor cocktail (Roche)) for 1 h at 4°C. Protein concentrations of lysates were determined using the bicinchoninic acid method (BCA Protein Assay; Pierce). Equal amounts of protein were mixed with SDS sample buffer, boiled at 95°C for 5 min, separated in 8% acrylamide gels and transferred on polyvinylidene fluoride (PVDF) membranes. Specific proteins were then detected with respective primary antibodies and HRP-conjugated secondary antibodies and visualized by ECL with SuperSignal™ West Pico PLUS Chemiluminescent Substrate (Thermo Scientific) using a Fujifilm LAS 4000 mini. For detection the following antibodies

were used: α-dsRed (to detect tdTomato) (632496, Clontech; 1:1000); chicken α-GFP (to detect mVenus) (ab139701, Abcam; 1:10,000); mouse α-TrkB (610101, BD Biosciences; 1:1000); mouse α-β-actin (A5441, Sigma; 1:1000); goat α-rabbit HRP (65-6120, Invitrogen; 1:5000); rabbit α-chicken HRP (W4011, Promega; 1:5000); goat α-mouse HRP (W4021, Promega; 1:5000).

Co-immunoprecipitation (co-IP)

Transfected cells were harvested and lysed with co-IP lysis buffer (150 mM NaCl, PBS pH 7.4, 0.5% Triton X-100, 1 mM PMSF and Complete proteinase inhibitor cocktail (Roche)). A fraction of the lysates was saved and supplemented with SDS sample buffer as the input fraction and the remaining lysates were coupled to GFP-Trap® Nanobodies/VHH coupled to magnetic agarose beads (ChromoTek) by inverting them for 30 min at 4°C. A part of the supernatant was saved and supplemented with SDS sample buffer. The beads were washed five times with dilution buffer (150 mM NaCl, PBS pH 7.4, 1 mM PMSF and Complete proteinase inhibitor cocktail (Roche)) and finally supplemented with SDS sample buffer as the precipitate fraction. For visualization, input and supernatant fractions as well as the precipitates were immunoblotted.

Fluorescence lifetime imaging microscopy (FLIM)

Hela cells were transfected with mVenus tagged SorCS2 and either tdTomato tagged SorCS2 or Sortilin. Two days post transfection cells were fixed with 4% PFA in PBS for 20 min. Confocal images were taken and fluorescence lifetimes of the mVenus fluorophores were measured using an Abberior STED-confocal expert line system (Abberior Instruments). The images were acquired in confocal mode. Pixel by pixel the fluorescence lifetime intensity curve was acquired. An image of the sample was obtained by summing up the fluorescence lifetime intensity curves associated to each pixel.

During the pixel by pixel analysis an equal intensity threshold was set, to exclude from the analysis lifetime profiles which signal to noise ratio was too poor to provide reliable estimates. In the end, only the pixels above the threshold were analyzed. Statistical differences between lifetimes were validated through Kruskal-Wallis analysis with a post-hoc Mann-Whitney-U test using IBM SPSS Statistics 25. For lifetime images, pixels above the threshold were color-coded based on their fluorescence lifetimes. Normalized frequencies were calculated as the relative number of pixels at a lifetime in a range of 0.01 ns in relation to the amount of pixels at the respective lifetime with the maximum amount of pixels.

BDNF uptake assay

HeLa or HEK293 cells were transfected with tdTomato tagged Vps10p-D receptors respectively. Two days post transfection cells were starved for 2 h in Opti-MEM™ without FCS (OptiMEM, Thermo Fisher Scientific). Subsequently, the cells were cooled down to 4°C and incubated for 1 h with 0.1 µg/ml ice-

cold hBDNF-Biotin (B-250-B, Alomone Labs Ltd) in OptiMEM for receptor binding at the plasma membrane. Non-binding hBDNF-Biotin was removed by washing twice with ice cold OptiMEM. For internalization of the receptors, the cells were incubated 10 min at 37°C, followed by immediate fixation with 4% paraformaldehyde and 4% sucrose in PBS at 4°C. hBDNF-Biotin was visualized by using Streptavidin, DyLight™ 488 conjugated (21832, Thermo Scientific; 1:500).

For live-cell analysis of BDNF uptake one set of HeLa cells was transfected with BDNF-GFP and another set in parallel with the tdTomato tagged Vps10p-D receptors respectively. 24 h post transfection the two differently treated sets of cells were co-cultured with a ratio of 40% BDNF-GFP expressing cells and 60% tdTomato tagged Vps10p-D receptors expressing cells. After another 24 h live time-lapse images were taken from HeLa cells expressing the tdTomato tagged Vps10p-D receptors.

Confocal imaging and co-localization

Immunofluorescent images were taken by confocal microscopy using a TCS SP8 microscope (Leica) with a 60x magnification objective. For time-lapse microscopy, cells were seeded in glass bottom dishes and transfected with indicated fluorophore tagged fusion proteins. During live-cell imaging temperature was kept at 37°C and CO_2 levels at 5%. Time-lapse movies were taken with the TCS SP8 microscope (Leica) and formatted using Fiji ImageJ.

For colocalization analysis, Laser Power and Gain was kept identical between images. Using the Fiji ImageJ plugin JaCoP the Mander's coefficients for colocalization were calculated. These represent the amount of immunoreactivity of one channel colocalizing with the immunoreactivity of the other channel. Bar graphs were produced using Graph Pad Prism 5. Statistical differences were validated through one-way-Anova with post hoc Tukey tests for parametric data sets or Kruskal-Wallis and post hoc Mann-Whittney-U tests for non-parametric data sets in IBM SPSS Statistics 25.

Data availability

All data are contained within the manuscript and are available upon reasonable request.

The plasmids generated here will be deposited on Addgene.

Supporting information

This article contains supporting information.

Acknowledgements

We are grateful to Lars Binkle for discussions and indebted to Dietmar Kuhl for continuous support.

Conflict of interest

The authors declare that they have no conflicts of interest with the contents of this article.

References

1. Hermey, G. (2009) The Vps10p-domain receptor family. *Cell Mol Life Sci* **66**, 2677-2689
2. Sarret, P., Krzywkowski, P., Segal, L., Nielsen, M. S., Petersen, C. M., Mazella, J., Stroh, T., and Beaudet, A. (2003) Distribution of NTS3 receptor/sortilin mRNA and protein in the rat central nervous system. *J Comp Neurol* **461**, 483-505
3. Hermans-Borgmeyer, I., Hermey, G., Nykjaer, A., and Schaller, C. (1999) Expression of the 100-kDa neurotensin receptor sortilin during mouse embryonal development. *Brain Res Mol Brain Res* **65**, 216-219
4. Rezgaoui, M., Hermey, G., Riedel, I. B., Hampe, W., Schaller, H. C., and Hermans-Borgmeyer, I. (2001) Identification of SorCS2, a novel member of the VPS10 domain containing receptor family, prominently expressed in the developing mouse brain. *Mech Dev* **100**, 335-338
5. Hermey, G., Schaller, H. C., and Hermans-Borgmeyer, I. (2001) Transient expression of SorCS in developing telencephalic and mesencephalic structures of the mouse. *Neuroreport* **12**, 29-32
6. Oetjen, S., Mahlke, C., Hermans-Borgmeyer, I., and Hermey, G. (2014) Spatiotemporal expression analysis of the growth factor receptor SorCS3. *J Comp Neurol* **522**, 3386-3402
7. Jacobsen, L., Madsen, P., Moestrup, S. K., Lund, A. H., Tommerup, N., Nykjaer, A., Sottrup-Jensen, L., Gliemann, J., and Petersen, C. M. (1996) Molecular characterization of a novel human hybrid-type receptor that binds the alpha2-macroglobulin receptor-associated protein. *J Biol Chem* **271**, 31379-31383
8. Petersen, C. M., Nielsen, M. S., Nykjaer, A., Jacobsen, L., Tommerup, N., Rasmussen, H. H., Roigaard, H., Gliemann, J., Madsen, P., and Moestrup, S. K. (1997) Molecular identification of a novel candidate sorting receptor purified from human brain by receptor-associated protein affinity chromatography. *J Biol Chem* **272**, 3599-3605
9. Boggild, S., Molgaard, S., Glerup, S., and Nyengaard, J. R. (2016) Spatiotemporal patterns of sortilin and SorCS2 localization during organ development. *BMC Cell Biol* **17**, 8
10. Hermey, G., Riedel, I. B., Hampe, W., Schaller, H. C., and Hermans-Borgmeyer, I. (1999) Identification and characterization of SorCS, a third member of a novel receptor family. *Biochem Biophys Res Commun* **266**, 347-351
11. Hermans-Borgmeyer, I., Hampe, W., Schinke, B., Methner, A., Nykjaer, A., Susens, U., Fenger, U., Herbarth, B., and Schaller, H. C. (1998) Unique expression pattern of a novel mosaic receptor in the developing cerebral cortex. *Mech Dev* **70**, 65-76
12. Andersen, O. M., Reiche, J., Schmidt, V., Gotthardt, M., Spoelgen, R., Behlke, J., von Arnim, C. A. F., Breiderhoff, T., Jansen, P., Wu, X., Bales, K. R., Cappai, R., Masters, C. L., Gliemann, J., Mufson, E. J., Hyman, B. T., Paul, S. M., Nykjaer, A., and Willnow, T. E. (2005) Neuronal sorting protein-related receptor sorLA/LR11 regulates processing of the amyloid precursor protein. *P Natl Acad Sci USA* **102**, 13461-13466
13. Rogaeva, E., Meng, Y., Lee, J. H., Gu, Y., Kawarai, T., Zou, F., Katayama, T., Baldwin, C. T., Cheng, R., Hasegawa, H., Chen, F., Shibata, N., Lunetta, K. L., Pardossi-Piquard, R., Bohm, C., Wakutani, Y., Cupples, L. A., Cuenco, K. T., Green, R. C., Pinessi, L., Rainero, I., Sorbi, S., Bruni, A., Duara, R., Friedland, R. P., Inzelberg, R., Hampe, W., Bujo, H., Song, Y. Q., Andersen, O. M., Willnow, T. E., Graff-Radford, N., Petersen, R. C., Dickson, D., Der, S. D., Fraser, P. E., Schmitt-Ulms, G., Younkin, S., Mayeux, R., Farrer, L. A., and St George-Hyslop, P. (2007) The neuronal sortilin-related receptor SORL1 is genetically associated with Alzheimer disease. *Nat Genet* **39**, 168-177
14. Reitz, C., Tokuhiro, S., Clark, L. N., Conrad, C., Vonsattel, J. P., Hazrati, L. N., Palotas, A., Lantigua, R., Medrano, M., I, Z. J.-V., Vardarajan, B., Simkin, I., Haines, J. L., Pericak-Vance, M. A., Farrer, L. A., Lee, J. H., Rogaeva, E., George-Hyslop, P. S., and Mayeux, R. (2011) SORCS1

alters amyloid precursor protein processing and variants may increase Alzheimer's disease risk. *Ann Neurol* **69**, 47-64

15. Reitz, C., Tosto, G., Vardarajan, B., Rogaeva, E., Ghani, M., Rogers, R. S., Conrad, C., Haines, J. L., Pericak-Vance, M. A., Fallin, M. D., Foroud, T., Farrer, L. A., Schellenberg, G. D., George-Hyslop, P. S., Mayeux, R., and Alzheimer's Disease Genetics, C. (2013) Independent and epistatic effects of variants in VPS10-d receptors on Alzheimer disease risk and processing of the amyloid precursor protein (APP). *Transl Psychiatry* **3**, e256
16. Bellenguez, C., Kucukali, F., Jansen, I. E., Kleineidam, L., Moreno-Grau, S., Amin, N., Naj, A. C., Campos-Martin, R., Grenier-Boley, B., Andrade, V., Holmans, P. A., Boland, A., Damotte, V., van der Lee, S. J., Costa, M. R., Kuulasmaa, T., Yang, Q., de Rojas, I., Bis, J. C., Yaqub, A., Prokic, I., Chapuis, J., Ahmad, S., Giedraitis, V., Aarsland, D., Garcia-Gonzalez, P., Abdelnour, C., Alarcon-Martin, E., Alcolea, D., Alegret, M., Alvarez, I., Alvarez, V., Armstrong, N. J., Tsolaki, A., Antunez, C., Appollonio, I., Arcaro, M., Archetti, S., Pastor, A. A., Arosio, B., Athanasiu, L., Bailly, H., Banaj, N., Baquero, M., Barral, S., Beiser, A., Pastor, A. B., Below, J. E., Benchek, P., Benussi, L., Berr, C., Besse, C., Bessi, V., Binetti, G., Bizarro, A., Blesa, R., Boada, M., Boerwinkle, E., Borroni, B., Boschi, S., Bossu, P., Brathen, G., Bressler, J., Bresner, C., Brodaty, H., Brookes, K. J., Brusco, L. I., Buiza-Rueda, D., Burger, K., Burholt, V., Bush, W. S., Calero, M., Cantwell, L. B., Chene, G., Chung, J., Cuccaro, M. L., Carracedo, A., Cecchetti, R., Cervera-Carles, L., Charbonnier, C., Chen, H. H., Chillotti, C., Ciccone, S., Claassen, J., Clark, C., Conti, E., Corma-Gomez, A., Costantini, E., Custodero, C., Daian, D., Dalmasso, M. C., Daniele, A., Dardiotis, E., Dartigues, J. F., de Deyn, P. P., de Paiva Lopes, K., de Witte, L. D., Debette, S., Deckert, J., Del Ser, T., Denning, N., DeStefano, A., Dichgans, M., Diehl-Schmid, J., Diez-Fairen, M., Rossi, P. D., Djurovic, S., Duron, E., Duzel, E., Dufouil, C., Eiriksdottir, G., Engelborghs, S., Escott-Price, V., Espinosa, A., Ewers, M., Faber, K. M., Fabrizio, T., Nielsen, S. F., Fardo, D. W., Farotti, L., Fenoglio, C., Fernandez-Fuertes, M., Ferrari, R., Ferreira, C. B., Ferri, E., Fin, B., Fischer, P., Fladby, T., Fliessbach, K., Fongang, B., Fornage, M., Fortea, J., Foroud, T. M., Fostinelli, S., Fox, N. C., Franco-Macias, E., Bullido, M. J., Frank-Garcia, A., Froelich, L., Fulton-Howard, B., Galimberti, D., Garcia-Alberca, J. M., Garcia-Gonzalez, P., Garcia-Madrona, S., Garcia-Ribas, G., Ghidoni, R., Giegling, I., Giorgio, G., Goate, A. M., Goldhardt, O., Gomez-Fonseca, D., Gonzalez-Perez, A., Graff, C., Grande, G., Green, E., Grimmer, T., Grunblatt, E., Grunin, M., Gudnason, V., Guetta-Baranes, T., Haapasalo, A., Hadjigeorgiou, G., Haines, J. L., Hamilton-Nelson, K. L., Hampel, H., Hanon, O., Hardy, J., Hartmann, A. M., Hausner, L., Harwood, J., Heilmann-Heimbach, S., Helisalmi, S., Heneka, M. T., Hernandez, I., Herrmann, M. J., Hoffmann, P., Holmes, C., Holstege, H., Vilas, R. H., Hulsman, M., Humphrey, J., Biessels, G. J., Jian, X., Johansson, C., Jun, G. R., Kastumata, Y., Kauwe, J., Kehoe, P. G., Kilander, L., Stahlbom, A. K., Kivipelto, M., Koivisto, A., Kornhuber, J., Kosmidis, M. H., Kukull, W. A., Kuksa, P. P., Kunkle, B. W., Kuzma, A. B., Lage, C., Laukka, E. J., Launer, L., Lauria, A., Lee, C. Y., Lehtisalo, J., Lerch, O., Lleo, A., Longstreth, W., Jr., Lopez, O., de Munain, A. L., Love, S., Lowemark, M., Luckcuck, L., Lunetta, K. L., Ma, Y., Macias, J., MacLeod, C. A., Maier, W., Mangialasche, F., Spallazzi, M., Marquie, M., Marshall, R., Martin, E. R., Montes, A. M., Rodriguez, C. M., Masullo, C., Mayeux, R., Mead, S., Mecocci, P., Medina, M., Meggy, A., Mehrabian, S., Mendoza, S., Menendez-Gonzalez, M., Mir, P., Moebus, S., Mol, M., Molina-Porcel, L., Montrreal, L., Morelli, L., Moreno, F., Morgan, K., Mosley, T., Nothen, M. M., Muchnik, C., Mukherjee, S., Nacmias, B., Ngandu, T., Nicolas, G., Nordestgaard, B. G., Olaso, R., Orellana, A., Orsini, M., Ortega, G., Padovani, A., Paolo, C., Papenberg, G., Parnetti, L., Pasquier, F., Pastor, P., Peloso, G., Perez-Cordon, A., Perez-Tur, J., Pericard, P., Peters, O., Pijnenburg, Y. A. L., Pineda, J. A., Pinol-Ripoll, G., Pisanu, C., Polak, T., Popp, J., Posthuma, D., Priller, J., Puerta, R., Quenez, O., Quintela, I., Thomassen, J. Q., Rabano, A., Rainero, I., Rajabli, F., Ramakers, I., Real, L. M., Reinders, M. J. T., Reitz, C., Reyes-Dumeyer, D., Ridge, P., Riedel-Heller, S., Riederer, P., Roberto, N., Rodriguez-Rodriguez, E., Rongve, A., Allende, I. R., Rosende-Roca, M., Royo, J. L., Rubino, E., Rujescu, D., Saez, M. E., Sakka, P., Saltvedt, I., Sanabria, A., Sanchez-Arjona, M. B., Sanchez-Garcia, F., Juan, P. S., Sanchez-Valle, R., Sando, S. B., Sarnowski, C., Satizabal, C. L., Scamosci, M., Scarmeas, N., Scarpini, E., Scheltens, P.,

Scherbaum, N., Scherer, M., Schmid, M., Schneider, A., Schott, J. M., Selbaek, G., Seripa, D., Serrano, M., Sha, J., Shadrin, A. A., Skrobot, O., Slifer, S., Snijders, G. J. L., Soininen, H., Solfrizzi, V., Solomon, A., Song, Y., Sorbi, S., Sotolongo-Grau, O., Spalletta, G., Spottke, A., Squassina, A., Stordal, E., Tartan, J. P., Tarraga, L., Tesi, N., Thalamuthu, A., Thomas, T., Tosto, G., Traykov, L., Tremolizzo, L., Tybjaerg-Hansen, A., Uitterlinden, A., Ullgren, A., Ulstein, I., Valero, S., Valladares, O., Broeckhoven, C. V., Vance, J., Vardarajan, B. N., van der Lugt, A., Dongen, J. V., van Rooij, J., van Swieten, J., Vandenberghe, R., Verhey, F., Vidal, J. S., Vogelgsang, J., Vyhnalek, M., Wagner, M., Wallon, D., Wang, L. S., Wang, R., Weinhold, L., Wiltfang, J., Windle, G., Woods, B., Yannakoulia, M., Zare, H., Zhao, Y., Zhang, X., Zhu, C., Zulaica, M., Eadb, Gr@Ace, Degesco, Eadi, Gerad, Demgene, FinnGen, Adgc, Charge, Farrer, L. A., Psaty, B. M., Ghanbari, M., Raj, T., Sachdev, P., Mather, K., Jessen, F., Ikram, M. A., de Mendonca, A., Hort, J., Tsolaki, M., Pericak-Vance, M. A., Amouyel, P., Williams, J., Frikke-Schmidt, R., Clarimon, J., Deleuze, J. F., Rossi, G., Seshadri, S., Andreassen, O. A., Ingelsson, M., Hiltunen, M., Sleegers, K., Schellenberg, G. D., van Duijn, C. M., Sims, R., van der Flier, W. M., Ruiz, A., Ramirez, A., and Lambert, J. C. (2022) New insights into the genetic etiology of Alzheimer's disease and related dementias. *Nat Genet* **54**, 412-436

17. Mattheisen, M., Grove, J., Als, T. D., Martin, J., Voloudakis, G., Meier, S., Demontis, D., Bendl, J., Walters, R., Carey, C. E., Rosengren, A., Strom, N. I., Hauberg, M. E., Zeng, B., Hoffman, G., Zhang, W., Bybjerg-Grauholm, J., Baekvad-Hansen, M., Agerbo, E., Cormand, B., Nordentoft, M., Werge, T., Mors, O., Hougaard, D. M., Buxbaum, J. D., Faraone, S. V., Franke, B., Dalsgaard, S., Mortensen, P. B., Robinson, E. B., Roussos, P., Neale, B. M., Daly, M. J., and Borglum, A. D. (2022) Identification of shared and differentiating genetic architecture for autism spectrum disorder, attention-deficit hyperactivity disorder and case subgroups. *Nat Genet* **54**, 1470-1478
18. Singh, T., Poterba, T., Curtis, D., Akil, H., Al Eissa, M., Barchas, J. D., Bass, N., Bigdeli, T. B., Breen, G., Bromet, E. J., Buckley, P. F., Bunney, W. E., Bybjerg-Grauholm, J., Byerley, W. F., Chapman, S. B., Chen, W. J., Churchhouse, C., Craddock, N., Cusick, C. M., DeLisi, L., Dodge, S., Escamilla, M. A., Eskelinen, S., Fanous, A. H., Faraone, S. V., Fiorentino, A., Francioli, L., Gabriel, S. B., Gage, D., Gagliano Taliun, S. A., Ganna, A., Genovese, G., Glahn, D. C., Grove, J., Hall, M. H., Hamalainen, E., Heyne, H. O., Holi, M., Hougaard, D. M., Howrigan, D. P., Huang, H., Hwu, H. G., Kahn, R. S., Kang, H. M., Karczewski, K. J., Kirov, G., Knowles, J. A., Lee, F. S., Lehrer, D. S., Lescai, F., Malaspina, D., Marder, S. R., McCarroll, S. A., McIntosh, A. M., Medeiros, H., Milani, L., Morley, C. P., Morris, D. W., Mortensen, P. B., Myers, R. M., Nordentoft, M., O'Brien, N. L., Olivares, A. M., Ongur, D., Ouwehand, W. H., Palmer, D. S., Paunio, T., Quested, D., Rapaport, M. H., Rees, E., Rollins, B., Satterstrom, F. K., Schatzberg, A., Scolnick, E., Scott, L. J., Sharp, S. I., Sklar, P., Smoller, J. W., Sobell, J. L., Solomonson, M., Stahl, E. A., Stevens, C. R., Suvisaari, J., Tiao, G., Watson, S. J., Watts, N. A., Blackwood, D. H., Borglum, A. D., Cohen, B. M., Corvin, A. P., Esko, T., Freimer, N. B., Glatt, S. J., Hultman, C. M., McQuillin, A., Palotie, A., Pato, C. N., Pato, M. T., Pulver, A. E., St Clair, D., Tsuang, M. T., Vawter, M. P., Walters, J. T., Werge, T. M., Ophoff, R. A., Sullivan, P. F., Owen, M. J., Boehnke, M., O'Donovan, M. C., Neale, B. M., and Daly, M. J. (2022) Rare coding variants in ten genes confer substantial risk for schizophrenia. *Nature* **604**, 509-516
19. Wu, Y., Cao, H., Baranova, A., Huang, H., Li, S., Cai, L., Rao, S., Dai, M., Xie, M., Dou, Y., Hao, Q., Zhu, L., Zhang, X., Yao, Y., Zhang, F., Xu, M., and Wang, Q. (2020) Multi-trait analysis for genome-wide association study of five psychiatric disorders. *Transl Psychiatry* **10**, 209
20. Clee, S. M., Yandell, B. S., Schueler, K. M., Rabaglia, M. E., Richards, O. C., Raines, S. M., Kabara, E. A., Klass, D. M., Mui, E. T., Stapleton, D. S., Gray-Keller, M. P., Young, M. B., Stoehr, J. P., Lan, H., Boronenkov, I., Raess, P. W., Flowers, M. T., and Attie, A. D. (2006) Positional cloning of Sorcs1, a type 2 diabetes quantitative trait locus. *Nat Genet* **38**, 688-693
21. Mitok, K. A., Keller, M. P., and Attie, A. D. (2022) Sorting through the extensive and confusing roles of sortilin in metabolic disease. *J Lipid Res* **63**, 100243

22. Vongpromek, R., Bujo, H., Hoekstra, M., Schneider, W. J., van der Zee, L., Schinkel, A. F., Korporaal, S. J., Dik, W. A., Ebinuma, H., Jiang, M., Verhoeven, A. J., Sijbrands, E. J., and Mulder, M. T. (2015) LR11/SorLA links triglyceride-rich lipoproteins to risk of developing cardiovascular disease in FH patients. *Atherosclerosis* **243**, 429-437
23. Whittle, A. J., Jiang, M., Peirce, V., Relat, J., Virtue, S., Ebinuma, H., Fukamachi, I., Yamaguchi, T., Takahashi, M., Murano, T., Tatsuno, I., Takeuchi, M., Nakaseko, C., Jin, W., Jin, Z., Campbell, M., Schneider, W. J., Vidal-Puig, A., and Bujo, H. (2015) Soluble LR11/SorLA represses thermogenesis in adipose tissue and correlates with BMI in humans. *Nat Commun* **6**, 8951
24. Kjolby, M., Andersen, O. M., Breiderhoff, T., Fjorback, A. W., Pedersen, K. M., Madsen, P., Jansen, P., Heeren, J., Willnow, T. E., and Nykjaer, A. (2010) Sort1, encoded by the cardiovascular risk locus 1p13.3, is a regulator of hepatic lipoprotein export. *Cell Metab* **12**, 213-223
25. Marcusson, E. G., Horazdovsky, B. F., Cereghino, J. L., Gharakhanian, E., and Emr, S. D. (1994) The sorting receptor for yeast vacuolar carboxypeptidase Y is encoded by the VPS10 gene. *Cell* **77**, 579-586
26. Malik, A. R., and Willnow, T. E. (2020) VPS10P Domain Receptors: Sorting Out Brain Health and Disease. *Trends Neurosci* **43**, 870-885
27. Salasova, A., Monti, G., Andersen, O. M., and Nykjaer, A. (2022) Finding memo: versatile interactions of the VPS10p-Domain receptors in Alzheimer's disease. *Mol Neurodegener* **17**, 74
28. Kitago, Y., Nagae, M., Nakata, Z., Yagi-Utsumi, M., Takagi-Niidome, S., Mihara, E., Nogi, T., Kato, K., and Takagi, J. (2015) Structural basis for amyloidogenic peptide recognition by sorLA. *Nature Structural & Molecular Biology* **22**, 199-206
29. Quistgaard, E. M., Madsen, P., Groftehauge, M. K., Nissen, P., Petersen, C. M., and Thirup, S. S. (2009) Ligands bind to Sortilin in the tunnel of a ten-bladed beta-propeller domain. *Nat Struct Mol Biol* **16**, 96-98
30. Leloup, N., Chataigner, L. M. P., and Janssen, B. J. C. (2018) Structural insights into SorCS2-Nerve Growth Factor complex formation. *Nat Commun* **9**, 2979
31. Mazella, J., Zsurger, N., Navarro, V., Chabry, J., Kaghad, M., Caput, D., Ferrara, P., Vita, N., Gully, D., Maffrand, J. P., and Vincent, J. P. (1998) The 100-kDa neurotensin receptor is gp95/sortilin, a non-G-protein-coupled receptor. *J Biol Chem* **273**, 26273-26276
32. Januliene, D., Manavalan, A., Ovesen, P. L., Pedersen, K. M., Thirup, S., Nykjaer, A., and Moeller, A. (2017) Hidden Twins: SorCS Neuroreceptors Form Stable Dimers. *J Mol Biol* **429**, 2907-2917
33. Hermey, G., Keat, S. J., Madsen, P., Jacobsen, C., Petersen, C. M., and Gliemann, J. (2003) Characterization of sorCS1, an alternatively spliced receptor with completely different cytoplasmic domains that mediate different trafficking in cells. *J Biol Chem* **278**, 7390-7396
34. Glerup, S., Olsen, D., Vaegter, C. B., Gustafsen, C., Sjoegaard, S. S., Hermey, G., Kjolby, M., Molgaard, S., Ulrichsen, M., Boggild, S., Skeldal, S., Fjorback, A. N., Nyengaard, J. R., Jacobsen, J., Bender, D., Bjarkam, C. R., Sorensen, E. S., Fuchtbauer, E. M., Eichele, G., Madsen, P., Willnow, T. E., Petersen, C. M., and Nykjaer, A. (2014) SorCS2 regulates dopaminergic wiring and is processed into an apoptotic two-chain receptor in peripheral glia. *Neuron* **82**, 1074-1087
35. Jacobsen, L., Madsen, P., Jacobsen, C., Nielsen, M. S., Gliemann, J., and Petersen, C. M. (2001) Activation and functional characterization of the mosaic receptor SorLA/LR11. *J Biol Chem* **276**, 22788-22796
36. Westergaard, U. B., Sorensen, E. S., Hermey, G., Nielsen, M. S., Nykjaer, A., Kirkegaard, K., Jacobsen, C., Gliemann, J., Madsen, P., and Petersen, C. M. (2004) Functional organization of the sortilin Vps10p domain. *J Biol Chem* **279**, 50221-50229
37. Munck Petersen, C., Nielsen, M. S., Jacobsen, C., Tauris, J., Jacobsen, L., Gliemann, J., Moestrup, S. K., and Madsen, P. (1999) Propeptide cleavage conditions sortilin/neurotensin receptor-3 for ligand binding. *EMBO J* **18**, 595-604

38. Larsen, J. V., Hermey, G., Sorensen, E. S., Prabakaran, T., Christensen, E. I., Gliemann, J., Madsen, P., and Petersen, C. M. (2014) Human sorCS1 binds sortilin and hampers its cellular functions. *Biochem J* **457**, 277-288
39. Chao, M. V. (2003) Neurotrophins and their receptors: a convergence point for many signalling pathways. *Nat Rev Neurosci* **4**, 299-309
40. Nykjaer, A., Lee, R., Teng, K. K., Jansen, P., Madsen, P., Nielsen, M. S., Jacobsen, C., Kliemannel, M., Schwarz, E., Willnow, T. E., Hempstead, B. L., and Petersen, C. M. (2004) Sortilin is essential for proNGF-induced neuronal cell death. *Nature* **427**, 843-848
41. Teng, H. K., Teng, K. K., Lee, R., Wright, S., Tevar, S., Almeida, R. D., Kermani, P., Torkin, R., Chen, Z. Y., Lee, F. S., Kraemer, R. T., Nykjaer, A., and Hempstead, B. L. (2005) ProBDNF induces neuronal apoptosis via activation of a receptor complex of p75NTR and sortilin. *J Neurosci* **25**, 5455-5463
42. Deinhardt, K., Kim, T., Spellman, D. S., Mains, R. E., Eipper, B. A., Neubert, T. A., Chao, M. V., and Hempstead, B. L. (2011) Neuronal growth cone retraction relies on proneurotrophin receptor signaling through Rac. *Sci Signal* **4**, ra82
43. Westergaard, U. B., Kirkegaard, K., Sorensen, E. S., Jacobsen, C., Nielsen, M. S., Petersen, C. M., and Madsen, P. (2005) SorCS3 does not require propeptide cleavage to bind nerve growth factor. *FEBS Lett* **579**, 1172-1176
44. Conroy, J. N., and Coulson, E. J. (2022) High-affinity TrkA and p75 neurotrophin receptor complexes: A twisted affair. *J Biol Chem* **298**, 101568
45. Skeldal, S., Sykes, A. M., Glerup, S., Matusica, D., Palstra, N., Autio, H., Boskovic, Z., Madsen, P., Castren, E., Nykjaer, A., and Coulson, E. J. (2012) Mapping of the interaction site between sortilin and the p75 neurotrophin receptor reveals a regulatory role for the sortilin intracellular domain in p75 neurotrophin receptor shedding and apoptosis. *J Biol Chem* **287**, 43798-43809
46. Glerup, S., Bolcho, U., Molgaard, S., Boggild, S., Vaegter, C. B., Smith, A. H., Nieto-Gonzalez, J. L., Ovesen, P. L., Pedersen, L. F., Fjorback, A. N., Kjolby, M., Login, H., Holm, M. M., Andersen, O. M., Nyengaard, J. R., Willnow, T. E., Jensen, K., and Nykjaer, A. (2016) SorCS2 is required for BDNF-dependent plasticity in the hippocampus. *Mol Psychiatry* **21**, 1740-1751
47. Rohe, M., Hartl, D., Fjorback, A. N., Klose, J., and Willnow, T. E. (2013) SORLA-mediated trafficking of TrkB enhances the response of neurons to BDNF. *PLoS One* **8**, e72164
48. Savas, J. N., Ribeiro, L. F., Wierda, K. D., Wright, R., DeNardo-Wilke, L. A., Rice, H. C., Chamma, I., Wang, Y. Z., Zemla, R., Lavallee-Adam, M., Vennekens, K. M., O'Sullivan, M. L., Antonios, J. K., Hall, E. A., Thoumine, O., Attie, A. D., Yates, J. R., 3rd, Ghosh, A., and de Wit, J. (2015) The Sorting Receptor SorCS1 Regulates Trafficking of Neurexin and AMPA Receptors. *Neuron* **87**, 764-780
49. Vaegter, C. B., Jansen, P., Fjorback, A. W., Glerup, S., Skeldal, S., Kjolby, M., Richner, M., Erdmann, B., Nyengaard, J. R., Tessarollo, L., Lewin, G. R., Willnow, T. E., Chao, M. V., and Nykjaer, A. (2011) Sortilin associates with Trk receptors to enhance anterograde transport and neurotrophin signaling. *Nat Neurosci* **14**, 54-61
50. Subkhangulova, A., Malik, A. R., Hermey, G., Popp, O., Dittmar, G., Rathjen, T., Poy, M. N., Stumpf, A., Beed, P. S., Schmitz, D., Breiderhoff, T., and Willnow, T. E. (2018) SORCS1 and SORCS3 control energy balance and orexigenic peptide production. *EMBO Rep* **19**
51. Breiderhoff, T., Christiansen, G. B., Pallesen, L. T., Vaegter, C., Nykjaer, A., Holm, M. M., Glerup, S., and Willnow, T. E. (2013) Sortilin-related receptor SORCS3 is a postsynaptic modulator of synaptic depression and fear extinction. *PLoS One* **8**, e75006
52. Fjorback, A. W., Seaman, M., Gustafsen, C., Mehmedbasic, A., Gokool, S., Wu, C., Militz, D., Schmidt, V., Madsen, P., Nyengaard, J. R., Willnow, T. E., Christensen, E. I., Mobley, W. B., Nykjaer, A., and Andersen, O. M. (2012) Retromer binds the FANSHY sorting motif in SorLA to regulate amyloid precursor protein sorting and processing. *J Neurosci* **32**, 1467-1480
53. Nielsen, M. S., Gustafsen, C., Madsen, P., Nyengaard, J. R., Hermey, G., Bakke, O., Mari, M., Schu, P., Pohlmann, R., Dennes, A., and Petersen, C. M. (2007) Sorting by the cytoplasmic domain of the amyloid precursor protein binding receptor SorLA. *Mol Cell Biol* **27**, 6842-6851

54. Nielsen, M. S., Keat, S. J., Hamati, J. W., Madsen, P., Gutzmann, J. J., Engelsberg, A., Pedersen, K. M., Gustafsen, C., Nykjaer, A., Gliemann, J., Hermans-Borgmeyer, I., Kuhl, D., Petersen, C. M., and Hermey, G. (2008) Different motifs regulate trafficking of SorCS1 isoforms. *Traffic* **9**, 980-994
55. Nielsen, M. S., Madsen, P., Christensen, E. I., Nykjaer, A., Gliemann, J., Kasper, D., Pohlmann, R., and Petersen, C. M. (2001) The sortilin cytoplasmic tail conveys Golgi-endosome transport and binds the VHS domain of the GGA2 sorting protein. *EMBO J* **20**, 2180-2190
56. Schmidt, V., Sporbert, A., Rohe, M., Reimer, T., Rehm, A., Andersen, O. M., and Willnow, T. E. (2007) SorLA/LR11 regulates processing of amyloid precursor protein via interaction with adaptors GGA and PACS-1. *J Biol Chem* **282**, 32956-32964
57. Binkle, L., Klein, M., Borgmeyer, U., Kuhl, D., and Hermey, G. (2022) The adaptor protein PICK1 targets the sorting receptor SorLA. *Mol Brain* **15**, 18
58. Canuel, M., Lefrancois, S., Zeng, J., and Morales, C. R. (2008) AP-1 and retromer play opposite roles in the trafficking of sortilin between the Golgi apparatus and the lysosomes. *Biochem Biophys Res Commun* **366**, 724-730
59. Hung, C., Tuck, E., Stubbs, V., van der Lee, S. J., Aalfs, C., van Spaendonk, R., Scheltens, P., Hardy, J., Holstege, H., and Livesey, F. J. (2021) SORL1 deficiency in human excitatory neurons causes APP-dependent defects in the endolysosome-autophagy network. *Cell Rep* **35**, 109259
60. Mishra, S., Knupp, A., Szabo, M. P., Williams, C. A., Kinoshita, C., Hailey, D. W., Wang, Y., Andersen, O. M., and Young, J. E. (2022) The Alzheimer's gene SORL1 is a regulator of endosomal traffic and recycling in human neurons. *Cell Mol Life Sci* **79**, 162
61. Malik, A. R., Szydlowska, K., Nizinska, K., Asaro, A., van Vliet, E. A., Popp, O., Dittmar, G., Fritsche-Guenther, R., Kirwan, J. A., Nykjaer, A., Lukasiuk, K., Aronica, E., and Willnow, T. E. (2019) SorCS2 Controls Functional Expression of Amino Acid Transporter EAAT3 and Protects Neurons from Oxidative Stress and Epilepsy-Induced Pathology. *Cell Rep* **26**, 2792-2804 e2796
62. Glerup, S., Lume, M., Olsen, D., Nyengaard, J. R., Vaegter, C. B., Gustafsen, C., Christensen, E. I., Kjolby, M., Hay-Schmidt, A., Bender, D., Madsen, P., Saarma, M., Nykjaer, A., and Petersen, C. M. (2013) SorLA controls neurotrophic activity by sorting of GDNF and its receptors GFRalpha1 and RET. *Cell Rep* **3**, 186-199
63. Progida, C., Nielsen, M. S., Koster, G., Bucci, C., and Bakke, O. (2012) Dynamics of Rab7b-dependent transport of sorting receptors. *Traffic* **13**, 1273-1285
64. Klinger, S. C., Hojland, A., Jain, S., Kjolby, M., Madsen, P., Svendsen, A. D., Olivecrona, G., Bonifacino, J. S., and Nielsen, M. S. (2016) Polarized trafficking of the sorting receptor SorLA in neurons and MDCK cells. *FEBS J* **283**, 2476-2493
65. Eggert, S., Gonzalez, A. C., Thomas, C., Schilling, S., Schwarz, S. M., Tischer, C., Adam, V., Strecker, P., Schmidt, V., Willnow, T. E., Hermey, G., Pietrzik, C. U., Koo, E. H., and Kins, S. (2018) Dimerization leads to changes in APP (amyloid precursor protein) trafficking mediated by LRP1 and SorLA. *Cell Mol Life Sci* **75**, 301-322
66. Huang, T. Y., Zhao, Y., Li, X., Wang, X., Tseng, I. C., Thompson, R., Tu, S., Willnow, T. E., Zhang, Y. W., and Xu, H. (2016) SNX27 and SORLA Interact to Reduce Amyloidogenic Subcellular Distribution and Processing of Amyloid Precursor Protein. *J Neurosci* **36**, 7996-8011
67. Pietila, M., Sahgal, P., Peuhu, E., Jantti, N. Z., Paatero, I., Narva, E., Al-Akhrass, H., Lilja, J., Georgiadou, M., Andersen, O. M., Padzik, A., Sihto, H., Joensuu, H., Blomqvist, M., Saarinen, I., Bostrom, P. J., Taimen, P., and Ivaska, J. (2019) SORLA regulates endosomal trafficking and oncogenic fitness of HER2. *Nat Commun* **10**, 2340
68. Cramer, J. F., Gustafsen, C., Behrens, M. A., Oliveira, C. L., Pedersen, J. S., Madsen, P., Petersen, C. M., and Thirup, S. S. (2010) GGA autoinhibition revisited. *Traffic* **11**, 259-273
69. Hung, A. Y., and Sheng, M. (2002) PDZ domains: structural modules for protein complex assembly. *J Biol Chem* **277**, 5699-5702
70. Herskowitz, J. H., Offe, K., Deshpande, A., Kahn, R. A., Levey, A. I., and Lah, J. J. (2012) GGA1-mediated endocytic traffic of LR11/SorLA alters APP intracellular distribution and amyloid-beta production. *Mol Biol Cell* **23**, 2645-2657

71. Jacobsen, L., Madsen, P., Nielsen, M. S., Geraerts, W. P., Gliemann, J., Smit, A. B., and Petersen, C. M. (2002) The sorLA cytoplasmic domain interacts with GGA1 and -2 and defines minimum requirements for GGA binding. *FEBS Lett* **511**, 155-158
72. Geisler, C., Dietrich, J., Nielsen, B. L., Kastrup, J., Lauritsen, J. P., Odum, N., and Christensen, M. D. (1998) Leucine-based receptor sorting motifs are dependent on the spacing relative to the plasma membrane. *J Biol Chem* **273**, 21316-21323
73. Hermey, G., Schmidt, N., Bluhm, B., Mensching, D., Ostermann, K., Rupp, C., Kuhl, D., and Kins, S. (2015) SorCS1 variants and amyloid precursor protein (APP) are co-transported in neurons but only SorCS1c modulates anterograde APP transport. *J Neurochem* **135**, 60-75
74. Jumper, J., Evans, R., Pritzel, A., Green, T., Figurnov, M., Ronneberger, O., Tunyasuvunakool, K., Bates, R., Zidek, A., Potapenko, A., Bridgland, A., Meyer, C., Kohl, S. A. A., Ballard, A. J., Cowie, A., Romera-Paredes, B., Nikolov, S., Jain, R., Adler, J., Back, T., Petersen, S., Reiman, D., Clancy, E., Zielinski, M., Steinegger, M., Pacholska, M., Berghammer, T., Bodenstein, S., Silver, D., Vinyals, O., Senior, A. W., Kavukcuoglu, K., Kohli, P., and Hassabis, D. (2021) Highly accurate protein structure prediction with AlphaFold. *Nature* **596**, 583-589
75. Claros, M. G., and von Heijne, G. (1994) TopPred II: an improved software for membrane protein structure predictions. *Comput Appl Biosci* **10**, 685-686
76. von Heijne, G. (1992) Membrane protein structure prediction. Hydrophobicity analysis and the positive-inside rule. *J Mol Biol* **225**, 487-494
77. Seaman, M. N. (2012) The retromer complex - endosomal protein recycling and beyond. *J Cell Sci* **125**, 4693-4702
78. Kucera, A., Bakke, O., and Progida, C. (2016) The multiple roles of Rab9 in the endolysosomal system. *Commun Integr Biol* **9**, e1204498
79. Fenner, B. M. (2012) Truncated TrkB: beyond a dominant negative receptor. *Cytokine Growth Factor Rev* **23**, 15-24
80. Dean, K. M., and Palmer, A. E. (2014) Advances in fluorescence labeling strategies for dynamic cellular imaging. *Nat Chem Biol* **10**, 512-523
81. Braakman, I., and Hebert, D. N. (2013) Protein folding in the endoplasmic reticulum. *Cold Spring Harb Perspect Biol* **5**, a013201
82. Offe, K., Dodson, S. E., Shoemaker, J. T., Fritz, J. J., Gearing, M., Levey, A. I., and Lah, J. J. (2006) The lipoprotein receptor LR11 regulates amyloid beta production and amyloid precursor protein traffic in endosomal compartments. *J Neurosci* **26**, 1596-1603
83. Ribeiro, L. F., Verpoort, B., Nys, J., Vennekens, K. M., Wierda, K. D., and de Wit, J. (2019) SorCS1-mediated sorting in dendrites maintains neurexin axonal surface polarization required for synaptic function. *PLoS Biol* **17**, e3000466
84. Bhalla, A., Vetanovetz, C. P., Morel, E., Chamoun, Z., Di Paolo, G., and Small, S. A. (2012) The location and trafficking routes of the neuronal retromer and its role in amyloid precursor protein transport. *Neurobiol Dis* **47**, 126-134
85. Kebede, M. A., Oler, A. T., Gregg, T., Balloon, A. J., Johnson, A., Mitok, K., Rabaglia, M., Schueler, K., Stapleton, D., Thorstenson, C., Wrighton, L., Floyd, B. J., Richards, O., Raines, S., Eliceiri, K., Seidah, N. G., Rhodes, C., Keller, M. P., Coon, J. L., Audhya, A., and Attie, A. D. (2014) SORCS1 is necessary for normal insulin secretory granule biogenesis in metabolically stressed beta cells. *J Clin Invest* **124**, 4240-4256
86. Lane, R. F., Raines, S. M., Steele, J. W., Ehrlich, M. E., Lah, J. A., Small, S. A., Tanzi, R. E., Attie, A. D., and Gandy, S. (2010) Diabetes-associated SorCS1 regulates Alzheimer's amyloid-beta metabolism: evidence for involvement of SorL1 and the retromer complex. *J Neurosci* **30**, 13110-13115
87. Hermey, G., Riedel, I. B., Rezgaoui, M., Westergaard, U. B., Schaller, C., and Hermans-Borgmeyer, I. (2001) SorCS1, a member of the novel sorting receptor family, is localized in somata and dendrites of neurons throughout the murine brain. *Neurosci Lett* **313**, 83-87
88. Sarret, P., Perron, A., Stroh, T., and Beaudet, A. (2003) Immunohistochemical distribution of NTS2 neurotensin receptors in the rat central nervous system. *J Comp Neurol* **461**, 520-538

89. Krogh, A., Larsson, B., von Heijne, G., and Sonnhammer, E. L. (2001) Predicting transmembrane protein topology with a hidden Markov model: application to complete genomes. *J Mol Biol* **305**, 567-580
90. Sonnhammer, E. L., von Heijne, G., and Krogh, A. (1998) A hidden Markov model for predicting transmembrane helices in protein sequences. *Proc Int Conf Intell Syst Mol Biol* **6**, 175-182
91. Chou, P. Y., and Fasman, G. D. (1978) Empirical predictions of protein conformation. *Annu Rev Biochem* **47**, 251-276
92. Klein, M., Kaleem, A., Oetjen, S., Wunkhaus, D., Binkle, L., Schilling, S., Gjorgjieva, M., Scholz, R., Gruber-Schoffnegger, D., Storch, S., Kins, S., Drewes, G., Hoffmeister-Ullerich, S., Kuhl, D., and Hermey, G. (2022) Converging roles of PSENEN/PEN2 and CLN3 in the autophagy-lysosome system. *Autophagy* **18**, 2068-2085
93. Lee, J. G., Takahama, S., Zhang, G., Tomarev, S. I., and Ye, Y. (2016) Unconventional secretion of misfolded proteins promotes adaptation to proteasome dysfunction in mammalian cells. *Nat Cell Biol* **18**, 765-776
94. Kim, D. E., Chivian, D., and Baker, D. (2004) Protein structure prediction and analysis using the Robetta server. *Nucleic Acids Res* **32**, W526-531
95. Varadi, M., Anyango, S., Deshpande, M., Nair, S., Natassia, C., Yordanova, G., Yuan, D., Stroe, O., Wood, G., Laydon, A., Zidek, A., Green, T., Tunyasuvunakool, K., Petersen, S., Jumper, J., Clancy, E., Green, R., Vora, A., Lutfi, M., Figurnov, M., Cowie, A., Hobbs, N., Kohli, P., Kleywegt, G., Birney, E., Hassabis, D., and Velankar, S. (2022) AlphaFold Protein Structure Database: massively expanding the structural coverage of protein-sequence space with high-accuracy models. *Nucleic Acids Res* **50**, D439-D444

Figure legends

Figure 1. Domain organization and structural analysis of the Vps10p-D receptors with and without fluorophore insertion. *A*, domain organization of the Vps10p-D receptors (top) and design of fluorophore tagged versions of the Vps10p-D receptors, tagged with mVenus (bottom left) and tagged with tdTomato (bottom right). *B*, structural predictions of the wildtype Vps10p-D receptors and their domains surrounding the insert area before and after mVenus or tdTomato insertion using AlphaFold 2.0. Purple represents the propeptide, light blue the Vps10p domain, dark blue the YWTD repeat, grey the EGF precursor type repeat, magenta the LDLR class A repeat, green the fibronectine type III repeat in SorLA and the leucine rich domain in the SorCS subgroup, orange the transmembrane domain and red the cytoplasmic domain.

Figure 2. Expression and ER exit of the tagged Vps10p-D receptors. *A*, confocal images of cells transfected with the ER marker KDEL-tdTomato (magenta) and mVenus tagged Vps10p-D receptors (green). mVenus tagged Sortilin, SorLA, SorCS1b, SorCS1c-α and SorCS2 were expressed in COS7 cells and mVenus tagged SorCS3 was expressed in HEK293 cells. mVenus and tdTomato signals were enhanced by immunostainings with respective antibodies. *B*, *C*, full-length expression of fluorophore tagged Vps10p-D receptors. Lysates of indicated non-transfected cells and COS7 cells transfected with fluorophore tagged Sortilin, SorLA, SorCS1b, SorCS1c-α and SorCS2 and HEK293 cells transfected with

fluorophore tagged SorCS3 were analyzed by immunoblotting with respective antibodies for (*B*) mVenus or (*C*) tdTomato. Data are representative of three independent experiments.

Figure 3. Colocalization analysis of mVenus tagged Vps10p-D receptors with endogenous GM130, Rab5 or Lamp1. *A*, *C*, *E*, mVenus tagged Sortilin, SorLA, SorCS1b, SorCS1c-α and SorCS2 were expressed in COS7 cells and mVenus tagged SorCS3 was expressed in HEK293 cells, immunostained for endogenous (*A*) GM130, (*C*) Rab5 or (*E*) Lamp1 (magenta), mVenus signals (green) were enhanced by immunostaining and cells analyzed by confocal microscopy. Magnifications of selected areas (boxes) are shown as insets. *B*, *D*, *F*, Manders' colocalization coefficients of the Vps10p-D receptors tagged with mVenus and (*B*) GM130, (*D*) Rab5 or (*F*) Lamp1. Values represent mean ± s.e.m. Statistical differences were validated through Kruskal-Wallis and post hoc Mann-Whittney-U tests. *B*, Manders' coefficient of GM130/SorLA-mVenus (n=9) is significantly lower than GM130/Sortilin-mVenus (n=14, p=0.003), GM130/SorC1c-α-mVenus (n=10, p=0.008), GM130/SorCS2-mVenus (n=10, p=0.001), GM130/SorCS3-mVenus (n=16, p≤0.001) and GM130/SorC1b-mVenus (n=11, p=0.001). *D*, Manders' coefficient of SorCS1b-mVenus/Rab5 (n=19) is significantly lower than Sortilin-mVenus/Rab5 (n=13, p≤0.001), SorLA-mVenus/Rab5 (n=10, p≤0.001), SorCS1c-α-mVenus/Rab5 (n=14, p≤0.001), SorCS2-mVenus/Rab5 (n=7, p≤0.001) and SorCS3-mVenus/Rab5 (n=24, p≤0.001). Manders' coefficient of Rab5/SorCS1b-mVenus (p≤0.001) is significantly lower than Rab5/Sortilin-mVenus (p≤0.001), Rab5/SorLA-mVenus (p≤0.001), Rab5/SorCS1b-mVenus (p≤0.001), Rab5/SorCS1c-α-mVenus (p≤0.001), Rab5/SorCS2-mVenus (p≤0.001) and Rab5/SorCS3-mVenus (p≤0.001). *F*, Manders' coefficients form co-localization between Lamp1 and Sortilin-mVenus (n=13), SorLA-mVenus (n=12), SorCS1b-mVenus (n=9), SorCS1c-α-mVenus (n=12), SorCS2-mVenus (n=12) or SorCS3-mVenus (n=14) were all similarly low. **, p≤0,01. ***, p≤0,001.

Figure 4. Colocalization analysis of fluorophore tagged Vps10p-D receptors with β-1,4-GT-GFP, VPS35-GFP and mCherry-Rab9. *A*, *C*, *E*, confocal images of cells transfected with Vps10p-D receptors tagged with (*A*, *C*) tdTomato (magenta) or (*E*) mVenus (green) and (*A*) β-1,4-GT-GFP, (*C*) VPS35-GFP or (*E*) mCherry-Rab9. Tagged Sortilin, SorLA, SorCS1b, SorCS1c-α and SorCS2 were expressed in COS7 cells and tagged SorCS3 was expressed in HEK293 cells. Fluorophore signals were enhanced by immunostainings with respective antibodies. Magnifications of selected areas (boxes) are shown as insets. *B*, *D*, *F*, Manders' colocalization coefficients for the fluorophore tagged Vps10p-D receptors with (*B*) β-1,4-GT-GFP, (*D*) VPS35-GFP or (*F*) Rab9-mCherry. Values represent mean ± s.e.m. Statistical differences were validated through Kruskal-Wallis and post hoc Mann-Whittney-U tests. *B*, Manders' coefficient of β-1,4-GT-GFP/Sortilin-tdTomato (n=11) is significantly higher than β-1,4-GT-GFP/SorLA-tdTomato (n=11, p=0.028), β-1,4-GT-GFP/SorCS1c-α-tdTomato (n=10, p≤0.001), β-1,4-GT-GFP/SorCS2-

tdTomato (n=9, p≤0.001), β-1,4-GT-GFP/SorCS3-tdTomato (n=11, p≤0.001) and β-1,4-GT-GFP/SorCS1b-tdTomato (n=22, p≤0.001). Manders' coefficient of β-1,4-GT-GFP/SorLA-tdTomato is significantly higher than β-1,4-GT-GFP/SorCS1c-α-tdTomato (p=0.013), β-1,4-GT-GFP/SorCS2-tdTomato (p=0.001), β-1,4-GT-GFP/SorCS3-tdTomato (p≤0.001) and β-1,4-GT-GFP/SorCS1b-tdTomato (p≤0.001). Manders' coefficient of β-1,4-GT-GFP/ SorCS1c-α-tdTomato is significantly higher than β-1,4-GT-GFP/SorCS3-tdTomato (p=0.002) and β-1,4-GT-GFP/SorCS1b-tdTomato (p≤0.001). Manders' coefficient of β-1,4-GT-GFP/SorCS2-tdTomato is significantly higher than β-1,4-GT-GFP/SorCS1b-tdTomato (p≤0.001). *D*, Manders' coefficient of VPS35-GFP/SorCS1b-tdTomato (n=10) is significantly lower than VPS35-GFP/Sortilin-tdTomato (n=14, p≤0,001), VPS35-GFP/SorLA-tdTomato (n=10, p≤0,001), VPS35-GFP/SorCS1c-α-tdTomato (n=15, p≤0,001), VPS35-GFP/SorCS2-tdTomato (n=12, p≤0,001) and VPS35-GFP/SorCS3-tdTomato (n=13, p≤0,001). Manders' coefficients of VPS35-GFP/Sortilin-tdTomato (n=14) and VPS35-GFP/SorLA-tdTomato (n=10) significantly higher than VPS35-GFP/SorCS1c-α-tdTomato (n=15, $p_{Sortilin}$=0.029, p_{SorLA}=0.031), VPS35-GFP/SorCS2-tdTomato (n=12, $p_{Sortilin}$=0.041, p_{SorLA}=0.043) and VPS35-GFP/SorCS3-tdTomato (n=13, $p_{Sortilin}$=0.048, p_{SorLA}=0.042). *F*, Manders' coefficient of SorCS1b-mVenus/Rab9-mCherry (n=11) is significantly lower than Sortilin-mVenus/ mCherry-Rab9 (n=18, p≤0.001), SorLA-mVenus/mCherry-Rab9 (n=16, p≤0.001), SorCS1c-α-mVenus/mCherry-Rab9 (n=10, p≤0.001) and SorCS2-mVenus/mCherry-Rab9 (n=12, p≤0.001). Manders' coefficient of SorCS2-mVenus/mCherry-Rab9 is significantly lower than Sortilin-mVenus/mCherry-Rab9 (p≤0.001) and SorCS1c-α-mVenus/mCherry-Rab9 (p=0.004). Manders' coefficient of SorCS3-mVenus/mCherry-Rab9 (n=12) is significantly lower than Sortilin-mVenus/mCherry-Rab9 (p≤0.001), SorLA-mVenus/mCherry-Rab9 (p=0,006) and SorCS1c-α-mVenus/ mCherry-RAB9 (p≤0.001). *, p≤0,05. **, p≤0,01. ***, p≤0,001.

Figure 5. Cotransport of tdTomatot tagged Vps10p-D receptors with GFP-Rab5.

Confocal live image analysis of a COS7 cell transfected with SorCS1c-α-tdTomato, SorCS2-tdTomato, or SorCS1b-tdTomato (magenta) and GFP-Rab5 (green). Single images show initial position (0 s) and after indicated time points. The images correspond to movies 3, 4 and 6.

Figure 6. Endosomal and somatodendritic localization of fluorophore tagged Vps10p-D receptors in neurons. *A*, dissociated hippocampal neurons were transfected at 3 days *in vitro* (DIV 3) with the indicated tdTomato tagged Vps10p-D receptors and GFP-Rab5 and immunostained at 7–14 DIV and analyzed by confocal microscopy. GFP and tdTomato signals were enhanced by immunostainings with respective antibodies. *B*, dissociated hippocampal neurons were transfected at 3 DIV with the indicated tdTomato tagged Vps10p-D receptors and immunostained for MAP2, as a marker for

dendrites, and for Ankyrin G, as a marker for the axonal initial segment at DIV 7-14. Magnifications of selected areas (boxed areas) are shown on the right.

Figure 7. SorCS2-mVenus interacts with SorCS2-tdTomato but not with Sortilin-tdTomato. *A*, HeLa cells were transfected with SorCS2-mVenus and Sortilin-tdTomato or SorCS2-tdTomato as indicated. SorCS2-mVenus was precipitated from cell lysates with anti-mVenus beads and fractions analyzed by immunoblotting for the indicated fluorophore tags. I, Input; P, Precipitate; S, Supernatant. The depicted immunoblot is representative out of three independent experiments. *B*, *C*, FLIM analysis of HeLa cells transfected with SorCS2-mVenus and Sortilin-tdTomato or SorCS2-tdTomato. *B*, mean ± s.e.m. lifetimes of excited mVenus in pixels showing tdTomato (acceptor) excitation by mVenus (donor) emission. mVenus lifetime is significantly lower in cells co-expressing SorCS2-tdTomato (n_{cells}=25, n_{pixels}=79,984) than in cells co-expressing Sortilin-tdTomato (n_{cells}=25, n_{pixels}=82,816, $p \leq 0.001$). *C*, intensity images of SorCS2-mVenus in cells co-expressing Sortilin-tdTomato or SorCS2-tdTomato (left), FLIM representation of excited mVenus in pixels showing tdTomato (acceptor) excitation by mVenus (donor) emission (middle). Lifetime distribution of pixels with acceptor excitation (right). mVenus lifetime is represented as indicated in the color bar, black pixels represent pixels without acceptor excitation.

Figure 8. Fluorophore tagged Vps10p-D receptors mediate BDNF uptake. *A*, experimental design of BDNF-Biotin uptake. *B*, tdTomato tagged Sortilin, SorLA, SorCS1b, SorCS1c-α and SorCS2 were expressed in HeLa cells and tdTomato tagged SorCS3 was expressed in HEK293 cells. Cells were incubated with BDNF-Biotin for 1 h at 4°C, washed, incubated for 10 min at 37°C and fixed. BDNF-Biotin visualized by a fluorescent streptavidin conjugate (green) and the tdTomato signal (magenta) was enhanced by immunostaining. Magnifications of selected areas (boxes) of confocal images are shown as insets. *C*, lysates of non-transfected HEK293 and HeLa cells as well as HEK293 cells transfected with TrkB-GFP were analyzed by immunoblotting with antibodies against TrkB (upper panel) and β-actin (lower). The immunoblot shows a representative image out of three independent experiments. *D*, experimental design of BDNF-GFP uptake. HeLa cells were transfected with tdTomato tagged Vps10p-D receptors (magenta) and in parallel another set of HeLa cells transfected with BDNF-GFP (green). After 24 h cells were co-cultured and imaged after 24 h by live confocal microscopy. *E*, single images show selected areas of cells of initial recordings (0 s) and after indicated time points. The images correspond to movies 9, 10 and 11.

Supporting information

Movies:

Movie 1. Confocal live image analysis of a COS7 cell transfected with Sortilin-tdTomato (magenta) and GFP-Rab5 (green) representing co-transport of Sortilin and Rab5. Scale bar represents 10 µm. Images were recorded with a framerate of 2.2 fps and are represented with a framerate of 2 fps.

Movie 2. Confocal live image analysis of COS7 cells transfected with SorLA-tdTomato (magenta) and GFP-Rab5 (green) representing co-transport of SorLA and Rab5. Scale bar represents 10 µm. Images were recorded with a framerate of 2.16 fps and are represented with a framerate of 2 fps.

Movie 3. Confocal live image analysis of a COS7 cell transfected with SorCS1c-α-tdTomato (magenta) and GFP-Rab5 (green) representing co-transport of SorCS1c-α and Rab5. Scale bar represents 10 µm. Images were recorded with a framerate of 4.97 fps and are represented with a framerate of 2 fps.

Movie 4. Confocal live image analysis of COS7 cells transfected with SorCS2-tdTomato (magenta) and GFP-Rab5 (green) representing co-transport of SorCS2 and Rab5. Scale bar represents 10 µm. Images were recorded with a framerate of 4.48 fps and are represented with a framerate of 2 fps.

Movie 5. Confocal live image analysis of a HEK293 cell transfected with SorCS3-tdTomato (magenta) and GFP-Rab5 (green) representing co-transport of SorCS3 and Rab5. Scale bar represents 10 µm. Images were recorded with a framerate of 2.16 fps and are represented with a framerate of 2 fps.

Movie 6. Confocal live image analysis of a COS7 cell transfected with SorCS1b-tdTomato (magenta) and GFP-Rab5 (green) representing no co-transport of SorCS1b and Rab5. Scale bar represents 10 µm. Images were recorded with a framerate of 4.39 fps and are represented with a framerate of 2 fps.

Movie 7. Confocal live image analysis of a HeLa cell transfected with Sortilin-tdTomato (magenta) co-cultured with HeLa cells transfected with BDNF-GFP (green) representing vesicular co-transport of Sortilin and BDNF. Scale bar represents 10 µm. Images were recorded with a framerate of 1.71 fps and are represented with a framerate of 2 fps.

Movie 8. Confocal live image analysis of a HeLa cell transfected with SorLA-tdTomato (magenta) co-cultured with HeLa cells transfected with BDNF-GFP (green) representing vesicular co-transport of SorLA and BDNF. Scale bar represents 10 µm. Images were recorded with a framerate of 1.72 fps and are represented with a framerate of 2 fps.

Movie 9. Confocal live image analysis of a HeLa cell transfected with SorCS1c-α-tdTomato (magenta) co-cultured with HeLa cells transfected with BDNF-GFP (green) representing vesicular co-transport of SorCS1c-α and BDNF. Scale bar represents 10 µm. Images were recorded with a framerate of 1.73 fps and are represented with a framerate of 2 fps.

Movie 10. Confocal live image analysis of a HeLa cell transfected with SorCS2-tdTomato (magenta) co-cultured with HeLa cells transfected with BDNF-GFP (green) representing vesicular co-transport of SorCS2 and BDNF. Scale bar represents 10 µm. Images were recorded with a framerate of 1.71 fps and are represented with a framerate of 2 fps.

Movie 11. Confocal live image analysis of a HeLa cell transfected with SorCS1b-tdTomato (magenta) co-cultured with HeLa cells transfected with BDNF-GFP (green) representing co-localization of SorCS1b and BDNF on the cell surface. Scale bar represents 10 µm. Images were recorded with a framerate of 1.71 fps and are represented with a framerate of 2 fps.

Click to open movies:

Movie 1 

Movie 2 

Movie 3 

Movie 4 

Movie 5 

Movie 6 

Movie 7 

Movie 8 

Movie 9 

Movie 10 

Movie 11 

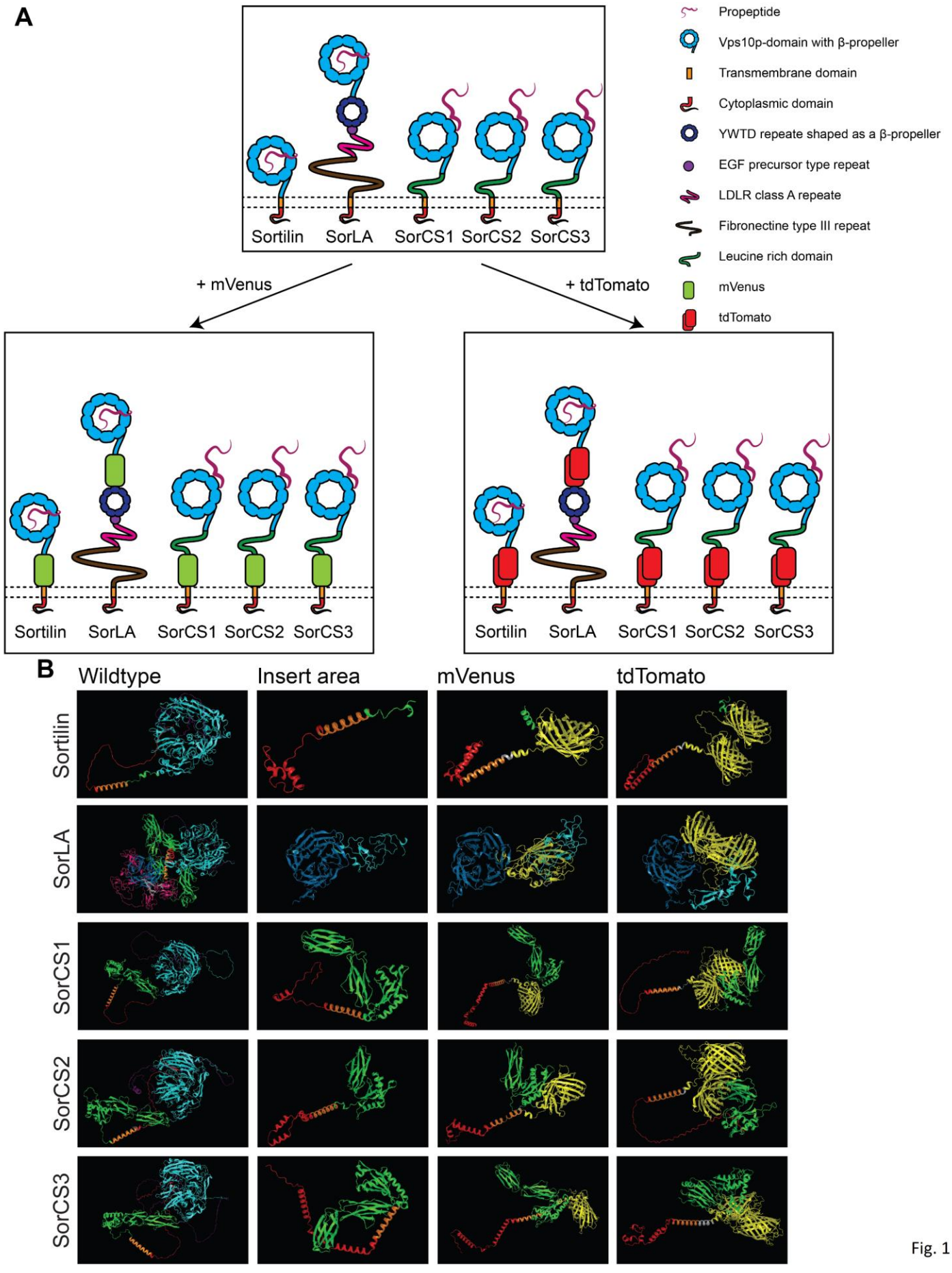
A
Propeptide
Vps10p-domain with β-propeller
Transmembrane domain
Cytoplasmic domain
YWTD repeate shaped as a β-propeller
EGF precursor type repeat
LDLR class A repeate
Fibronectine type III repeat
Leucine rich domain
mVenus
tdTomato
Sortilin
SorLA
SorCS1
SorCS2
SorCS3
+ mVenus
+ tdTomato
B
Wildtype
Insert area
mVenus
tdTomato

Fig. 1

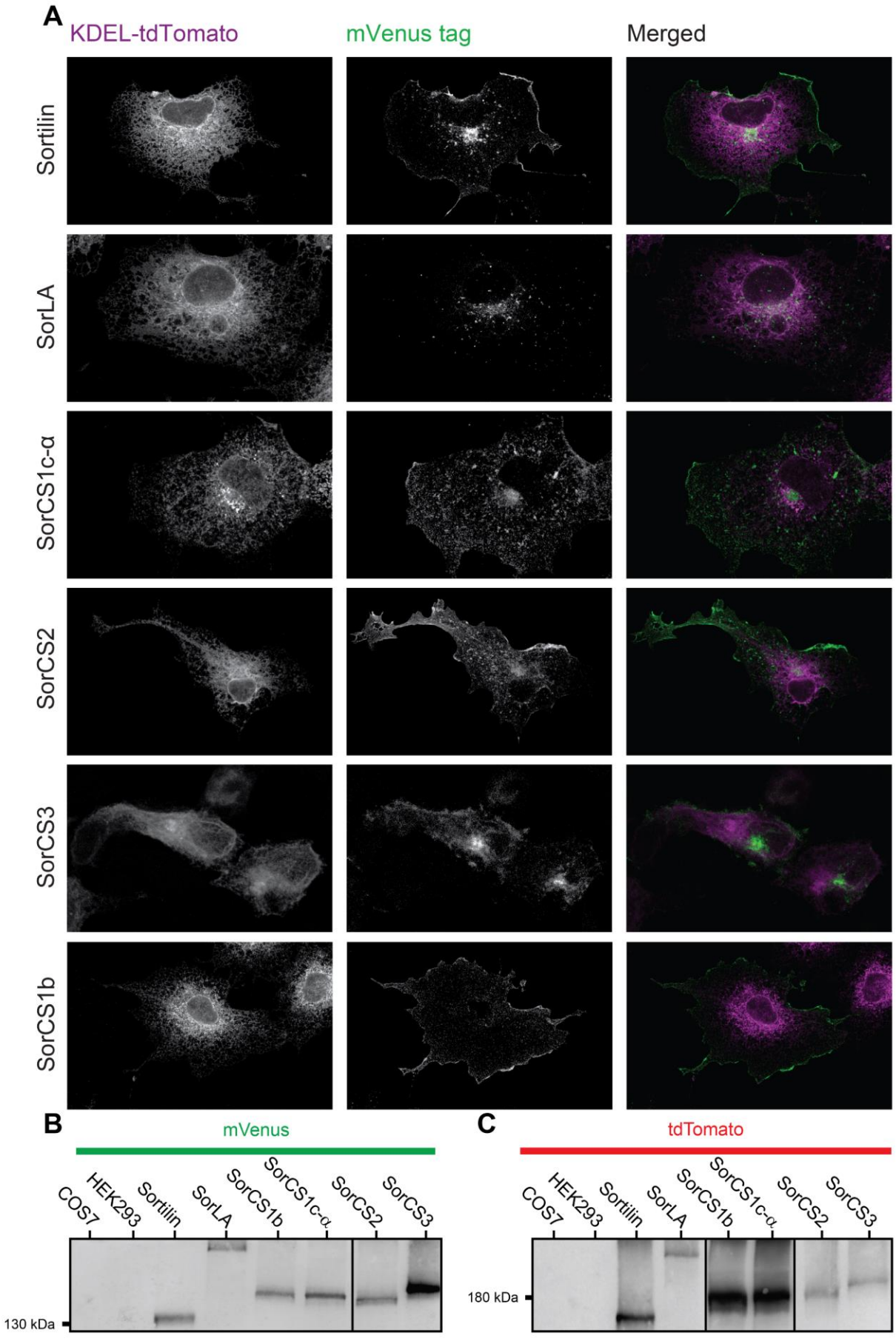
A
KDEL-tdTomato
mVenus tag
Merged
Sortilin
SorLA
SorCS1c-α
SorCS2
SorCS3
SorCS1b
B
mVenus
COS7
HEK293
Sortilin
SorLA
SorCS1b
SorCS1c-α
SorCS2
SorCS3
130 kDa
C
tdTomato
COS7
HEK293
Sortilin
SorLA
SorCS1b
SorCS1c-α
SorCS2
SorCS3
180 kDa

Fig. 2

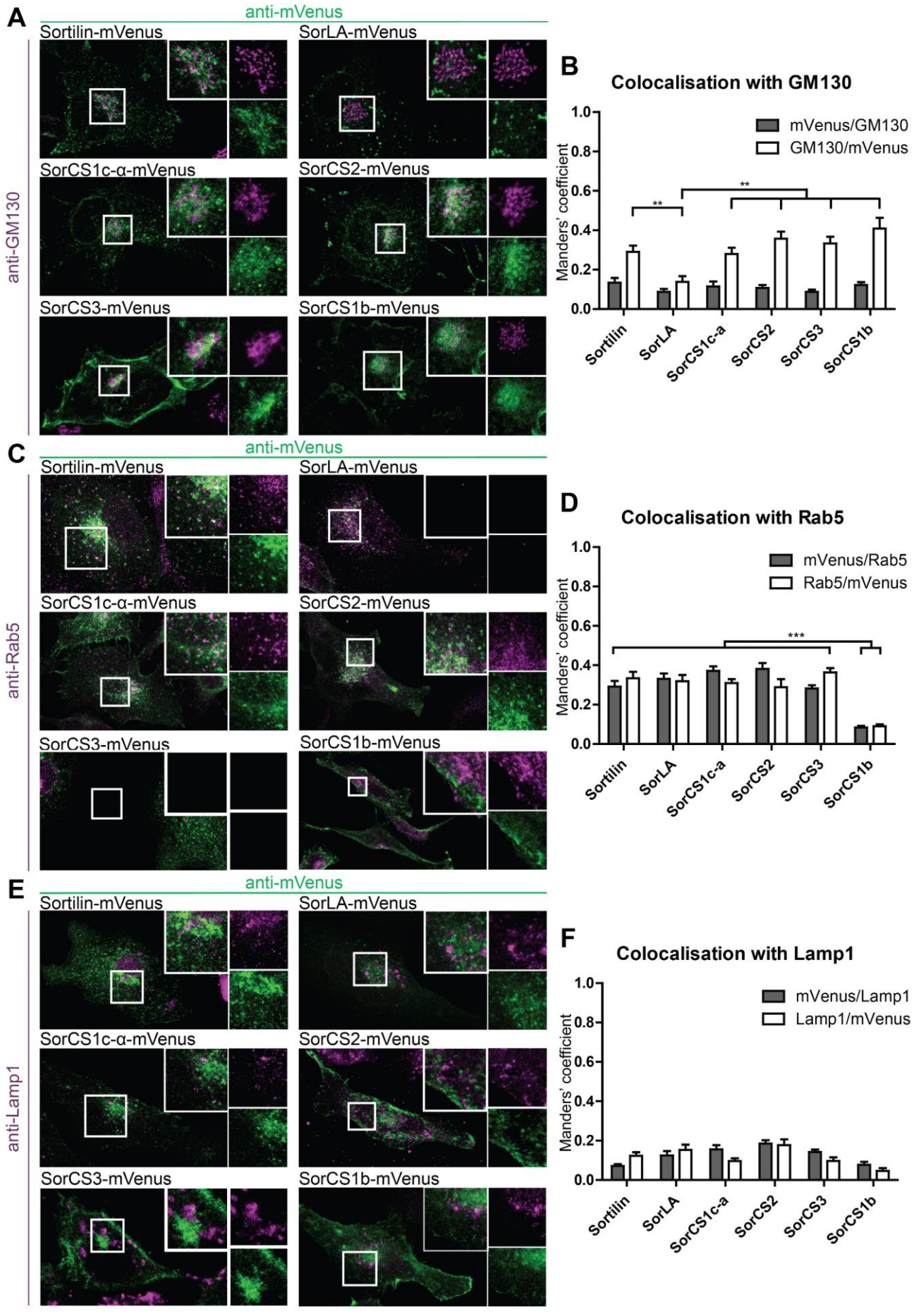
A
anti-mVenus
Sortilin-mVenus
SorLA-mVenus
anti-GM130
SorCS1c-α-mVenus
SorCS2-mVenus
SorCS3-mVenus
SorCS1b-mVenus
B
Colocalisation with GM130
mVenus/GM130
GM130/mVenus
Manders' coefficient
1.0
0.8
0.6
0.4
0.2
0.0
**
**
Sortilin
SorLA
SorCS1c-a
SorCS2
SorCS3
SorCS1b
C
anti-mVenus
Sortilin-mVenus
SorLA-mVenus
anti-Rab5
SorCS1c-α-mVenus
SorCS2-mVenus
SorCS3-mVenus
SorCS1b-mVenus
D
Colocalisation with Rab5
mVenus/Rab5
Rab5/mVenus
Manders' coefficient
1.0
0.8
0.6
0.4
0.2
0.0
***
Sortilin
SorLA
SorCS1c-a
SorCS2
SorCS3
SorCS1b
E
anti-mVenus
Sortilin-mVenus
SorLA-mVenus
anti-Lamp1
SorCS1c-α-mVenus
SorCS2-mVenus
SorCS3-mVenus
SorCS1b-mVenus
F
Colocalisation with Lamp1
mVenus/Lamp1
Lamp1/mVenus
Manders' coefficient
1.0
0.8
0.6
0.4
0.2
0.0
Sortilin
SorLA
SorCS1c-a
SorCS2
SorCS3
SorCS1b

Fig. 3

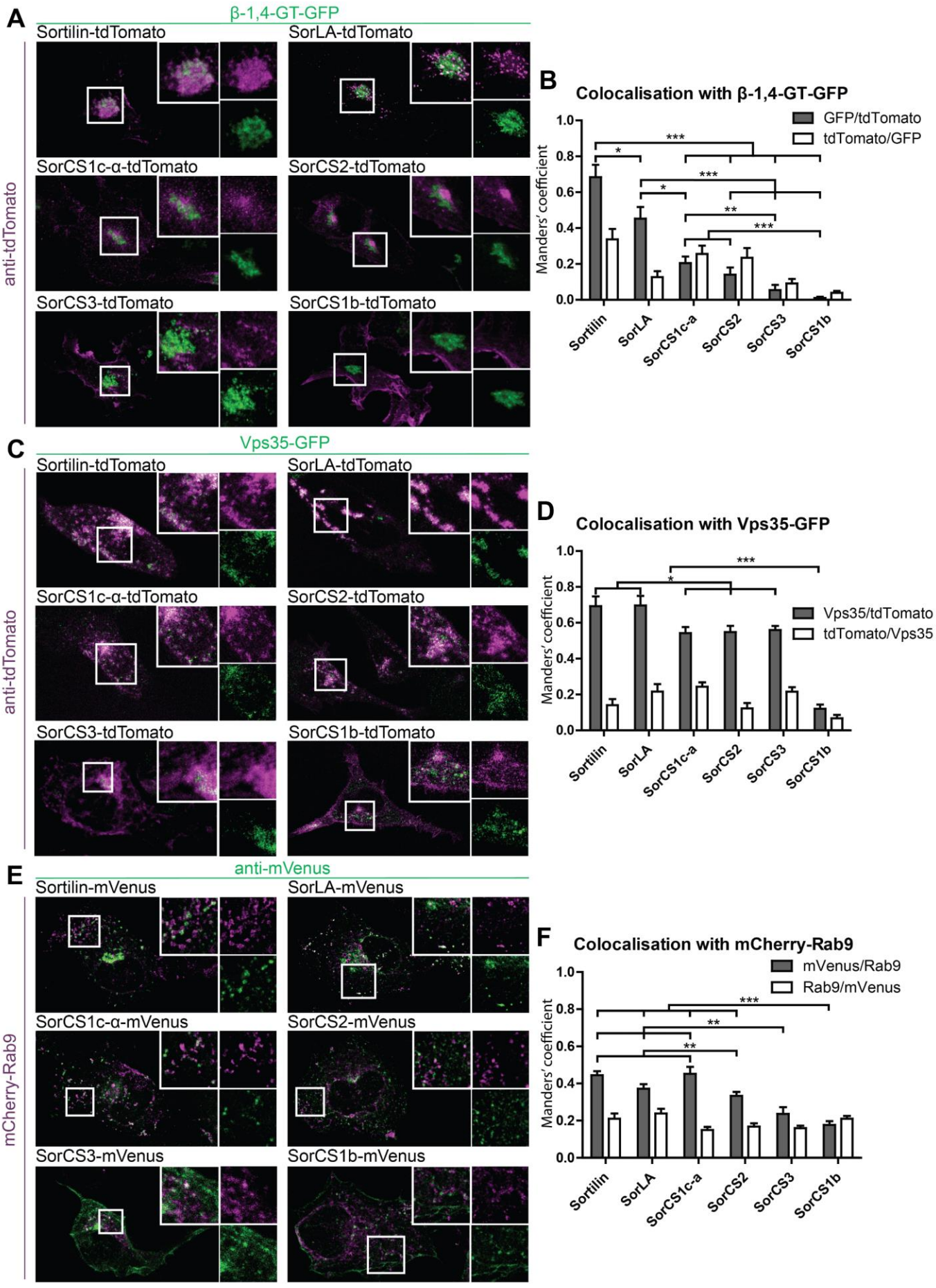
A
β-1,4-GT-GFP
Sortilin-tdTomato
SorLA-tdTomato
SorCS1c-α-tdTomato
SorCS2-tdTomato
SorCS3-tdTomato
SorCS1b-tdTomato
anti-tdTomato
B
Colocalisation with β-1,4-GT-GFP
GFP/tdTomato
tdTomato/GFP
Manders' coefficient
1.0
0.8
0.6
0.4
0.2
0.0
***
*
***
*
**
***
Sortilin
SorLA
SorCS1c-a
SorCS2
SorCS3
SorCS1b
C
Vps35-GFP
Sortilin-tdTomato
SorLA-tdTomato
SorCS1c-α-tdTomato
SorCS2-tdTomato
SorCS3-tdTomato
SorCS1b-tdTomato
anti-tdTomato
D
Colocalisation with Vps35-GFP
Vps35/tdTomato
tdTomato/Vps35
Manders' coefficient
1.0
0.8
0.6
0.4
0.2
0.0
***
*
Sortilin
SorLA
SorCS1c-a
SorCS2
SorCS3
SorCS1b
E
anti-mVenus
Sortilin-mVenus
SorLA-mVenus
SorCS1c-α-mVenus
SorCS2-mVenus
SorCS3-mVenus
SorCS1b-mVenus
mCherry-Rab9
F
Colocalisation with mCherry-Rab9
mVenus/Rab9
Rab9/mVenus
Manders' coefficient
1.0
0.8
0.6
0.4
0.2
0.0
***
**
**
Sortilin
SorLA
SorCS1c-a
SorCS2
SorCS3
SorCS1b

Fig. 4

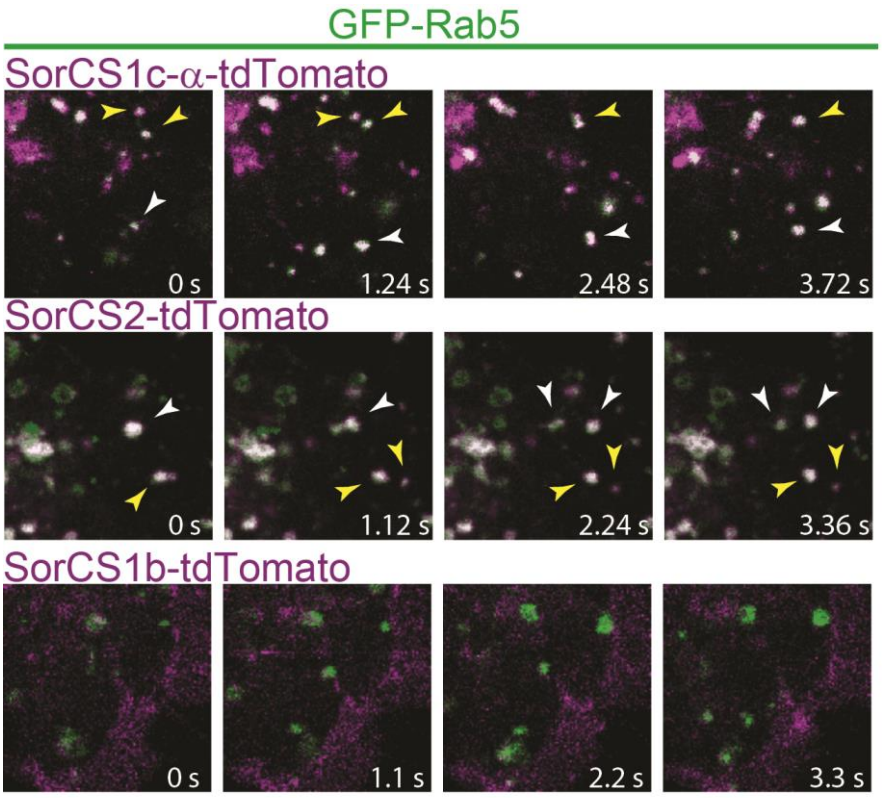
GFP-Rab5
SorCS1c-α-tdTomato
0 s
1.24 s
2.48 s
3.72 s
SorCS2-tdTomato
0 s
1.12 s
2.24 s
3.36 s
SorCS1b-tdTomato
0 s
1.1 s
2.2 s
3.3 s

Fig. 5

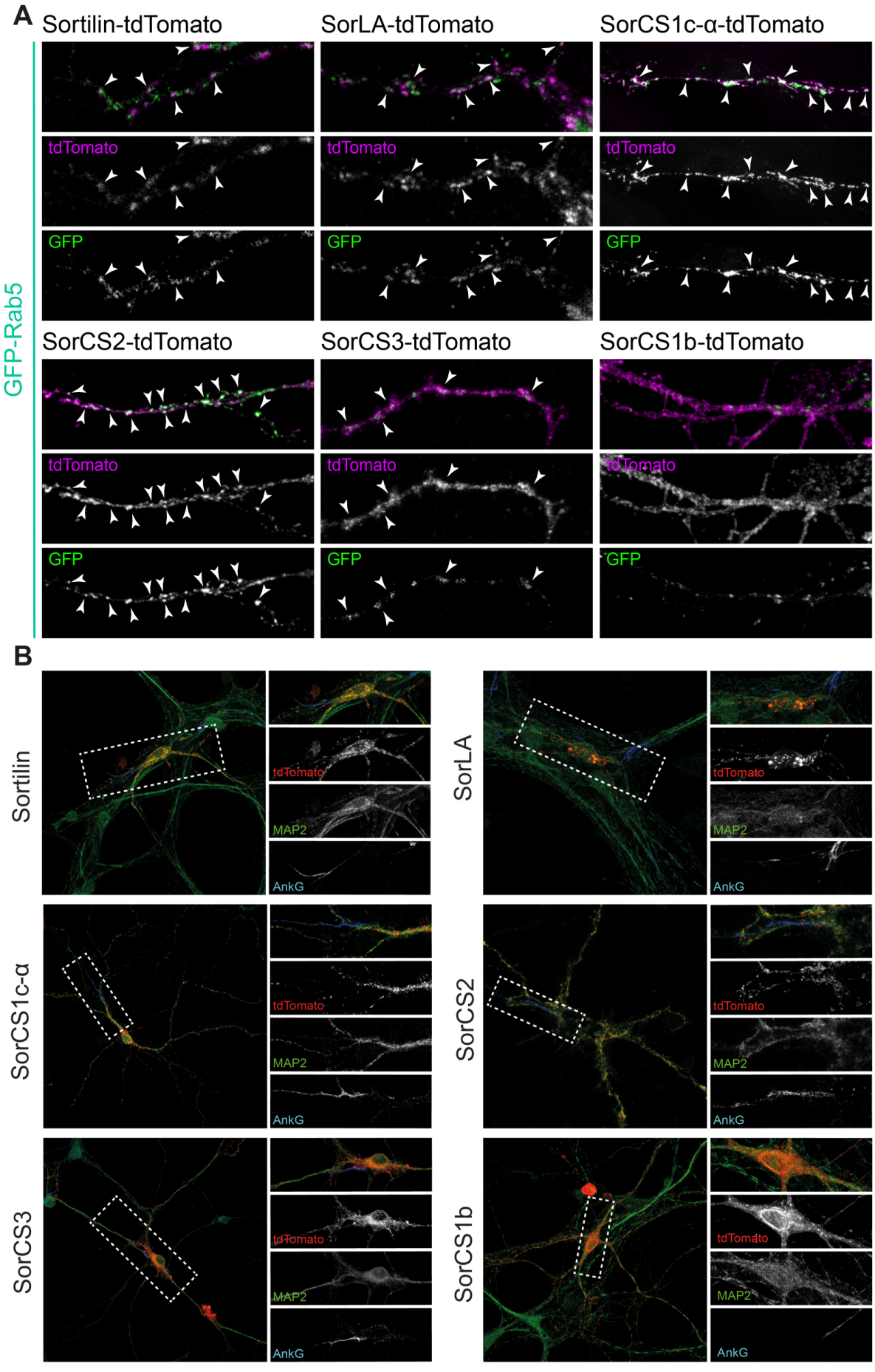
A
Sortilin-tdTomato
SorLA-tdTomato
SorCS1c-α-tdTomato
GFP-Rab5
tdTomato
GFP
SorCS2-tdTomato
SorCS3-tdTomato
SorCS1b-tdTomato
B
Sortilin
SorLA
SorCS1c-α
SorCS2
SorCS3
SorCS1b
tdTomato
MAP2
AnkG

Fig. 6

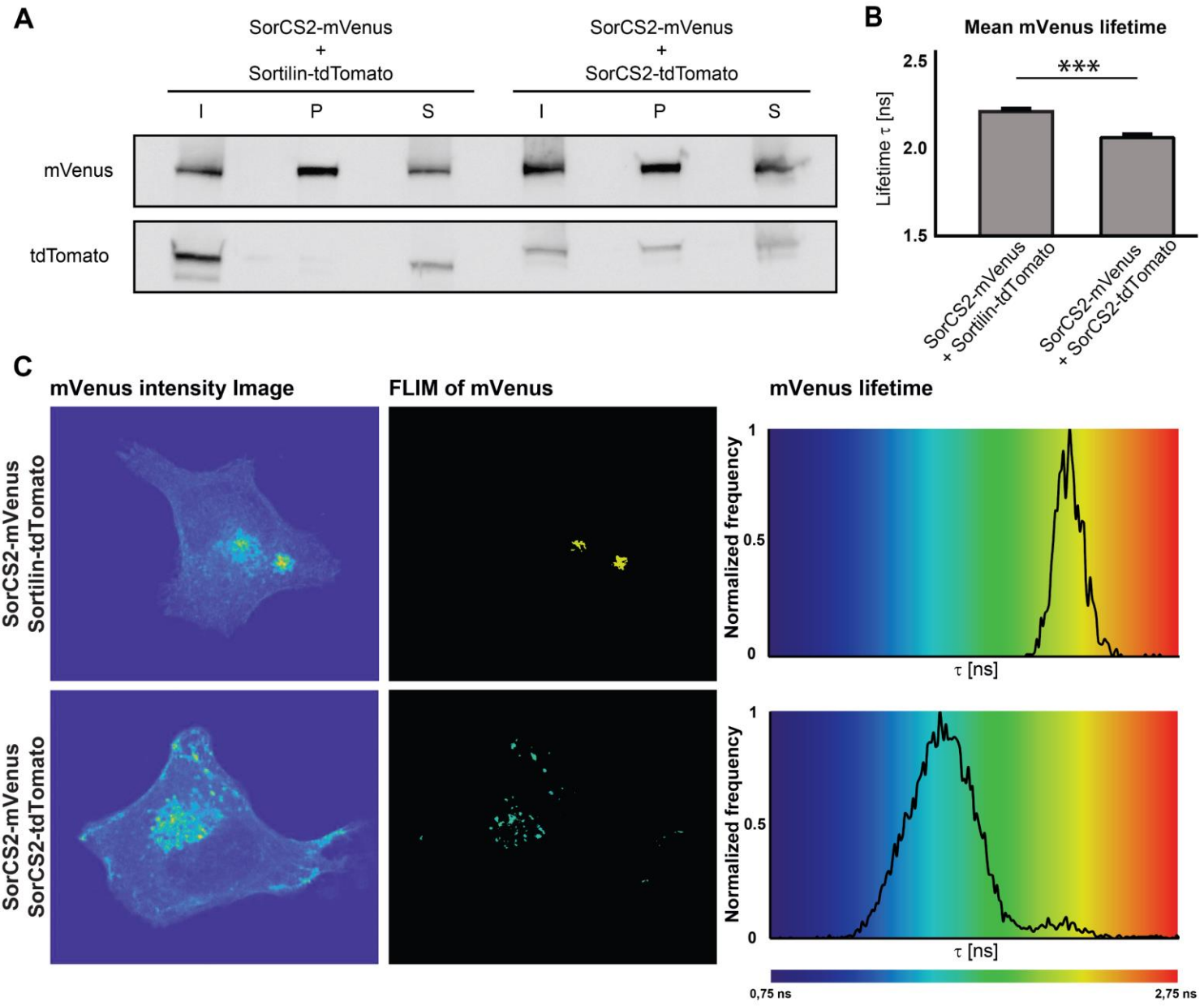
A
SorCS2-mVenus
+
Sortilin-tdTomato
SorCS2-mVenus
+
SorCS2-tdTomato
I
P
S
I
P
S
mVenus
tdTomato
B
Mean mVenus lifetime
***
Lifetime τ [ns]
2.5
2.0
1.5
SorCS2-mVenus
+ Sortilin-tdTomato
SorCS2-mVenus
+ SorCS2-tdTomato
C
mVenus intensity Image
FLIM of mVenus
mVenus lifetime
SorCS2-mVenus
Sortilin-tdTomato
SorCS2-mVenus
SorCS2-tdTomato
Normalized frequency
1
0.5
0
τ [ns]
Normalized frequency
1
0.5
0
τ [ns]
0,75 ns
2,75 ns

Fig. 7

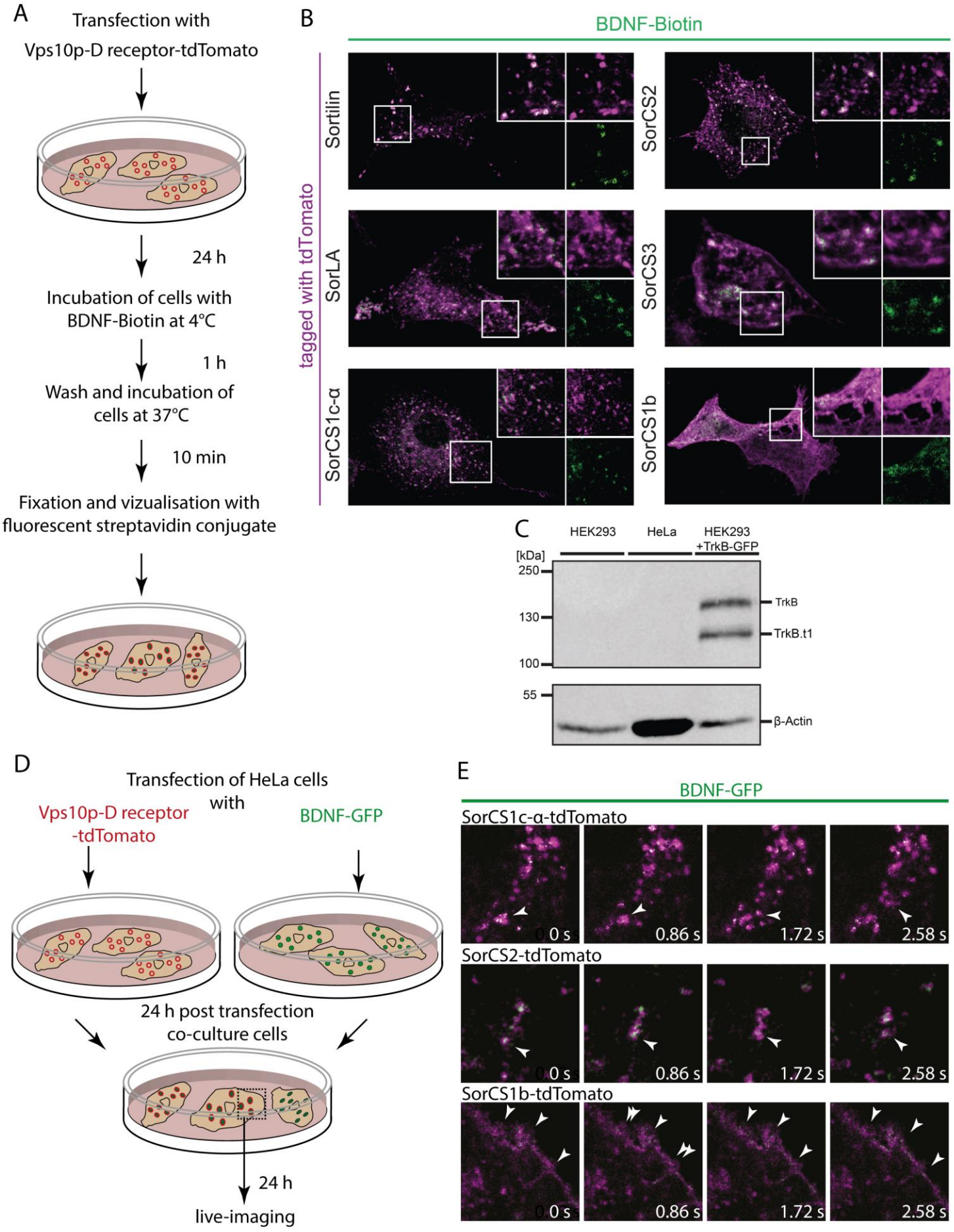
A
Transfection with
Vps10p-D receptor-tdTomato
24 h
Incubation of cells with
BDNF-Biotin at 4°C
1 h
Wash and incubation of
cells at 37°C
10 min
Fixation and vizualisation with
fluorescent streptavidin conjugate
B
BDNF-Biotin
tagged with tdTomato
Sortilin
SorCS2
SorLA
SorCS3
SorCS1c-α
SorCS1b
C
HEK293
HeLa
HEK293
+TrkB-GFP
[kDa]
250
130
100
55
TrkB
TrkB.t1
β-Actin
D
Transfection of HeLa cells
with
Vps10p-D receptor
-tdTomato
BDNF-GFP
24 h post transfection
co-culture cells
24 h
live-imaging
E
BDNF-GFP
SorCS1c-α-tdTomato
SorCS2-tdTomato
SorCS1b-tdTomato
0 s
0.86 s
1.72 s
2.58 s

Fig. 8

6. Discussion

Overall, in the presented publications I examine different functions and dysfunctions of endolysosomal protein sorting in the lysosome-autophagosome system and endosomal trafficking. I demonstrate congruent deficits in autophagic processes after ablation of the juvenile NCL protein CLN3 or the AD risk factor Pen2 in HeLa cells. Accordingly, I compare converging links of NCLs with AD in the literature. These suggest that protein aggregates that accumulate in NCL and AD are possibly caused by deficits in the lysosome-autophagosome system. I further investigate the novel interaction of the AD risk factor SorLA with the scaffold protein PICK1. PICK1 and SorLA might mediate the intracellular trafficking of other PICK1 or SorLA interactors in concert. SorLA is a member of the Vps10p-D receptor family that are involved in several endosomal sorting processes and their dysfunction has been involved to several neurological diseases. I established functional internal fluorophore tagged versions of all Vps10p-D receptors as powerful tools for live applications to investigate their role in protein sorting. With these fluorophore tagged Vps10p-D receptors I examine their detailed subcellular localizations and show for the first time that all Vps10p-D receptors interact with BDNF independent of TrkB.

6.1. Converging links between CLN3, other lysosomal storage disorders, and Alzheimer's disease

Impairments in trafficking and function of the autophagy-endolysosome system underlie different neurodegenerative diseases such as the NCLs. The function of *CLN3*, the most prevalent mutated gene of NCLs, is still elusive. Thus, in section 2, its implications in the autophagy-endolysosome system were investigated by employing a previously generated HeLa KO cell line of CLN3 (Kaleem, 2017; Klein et al., 2022). In these cells, a decreased activity of lysosomal enzymes including CTSB and a lower number of lysosomes when compared to wild type cells was observed (Klein et al., 2022). These observations were accompanied by minor alterations in endosome compartmentalization as shown in increased colocalization of Lamp1 or Lamp2 with Rab9. As Rab9 conveys transport between the TGN, late endosomes and lysosomes, and Lamp1 and Lamp2 are lysosome resident this either hints at a mislocalization of Rab9 or an increased protein transport towards lysosomes. Lysosomal

formation and degradation deficiencies are both common pathological initiators of NCLs as described for CLN6, CLN8, CLN12 and CLN14 (Bajaj et al., 2020; di Ronza et al., 2018; Nyuzuki et al., 2020; Wang et al., 2022). Autophagosome formation as well as autophagosome fusion with lysosomes to autolysosomes appear to be functional and even elevated upon CLN3 KO in HeLa cells. In contrast, in numerous other lysosomal storage disorders including CLN1, CLN5, CLN10 and CLN11 this autophagic flux has been demonstrated to show major deficits (Sarkar et al. 2020; Marques et al. 2020; Zhou et al. 2019; Kim et al. 2022). In CLN11, however, these deficits may origin from impairments in general autophagosome formation (Zhou et al., 2019). Our analysis demonstrated in the established CLN3 KO HeLa cells elevated levels of nuclear TFEB as demonstrated by immunocytochemistry and elevated levels of transcripts of autophagy related TFEB targets as shown by qPCR, with even stronger effects after nutrient deprivation. The levels of the CLN10 protein CTSD were elevated in the KO cells under normal conditions and even increased after nutrient deprivation. Expression of the CLN2 protein TPP1, however, was decreased in CLN3 KO cells under conditions with full nutrient supply but increased after nutrient deprivation. As in CLN10 disease the autophagic flux is inhibited (Marques et al., 2020), the increased expression of CTSD in the CLN3 KO HeLa cells possibly promotes further autolysosome formation. The altered expression levels of different TFEB targets, especially after nutrient deprivation, therefore, possibly regulates autophagosome formation. An increased fusion of autophagosomes with lysosomes in the CLN3 KO cells maybe explain the observed decreased number of lysosomes. Overall, the findings of significantly reduced lysosomal activity and compartmentalization, and increased formation of autophagosomes and autolysosomes in the CLN3 KO HeLa cells are concordant with previous findings of impaired lysosomal functions upon CLN3 deficiency in other cellular and biological models (Fossale et al., 2004; Lojewski et al., 2014; Ramirez-Montealegre and Pearce, 2005; Schmidtke et al., 2019) and the accumulation of autophagy related proteins in CLN3 disease (Cao et al., 2006) (See 1.3.2 Transmembrane CLN proteins).

Excitingly, an interaction of CLN3 with the γ-secretase subunit and AD disease risk factor Pen2 was identified (Klein et al., 2022; Oetjen, 2014). Moreover, their co-expression in tissue, co-localization in endo-lysosomal compartments, like late endosomes and lysosomes, and co-transport in HeLa cells and primary hippocampal neurons was exhibited (Klein et al., 2022; Oetjen, 2014). A KO of Pen2 in HeLa cells demonstrated expected deficits of γ-secretase activity, which, however, were not shared by the CLN3 KO cells (Kaleem, 2017; Klein et al.,

2022). Consequently, CLN3 seems not to regulate γ-secretase activity. Interestingly, an analysis of unexplained clinically diagnosed EOAD cases identified a genomic region directly upstream of the CLN3 gene suggesting other links between CLN3 and AD, independent of γ-secretase function (Cheng et al., 2018). In mice, Pen2 deficiency is lethal at an embryonic stage (Bammens et al., 2011) but in our established Pen2 KO HeLa cell we did not observe any changes in cell proliferation and survival (Klein et al., 2022). This suggests that γ-secretase inhibition itself and therefore the processing of its target proteins like APP is not a major cause for cellular death or that their processing or removal can also be achieved differently (Wolfe, 2020).

Pen2 is the last protein to be incorporated in the γ-secretase complex, regulates the exit of the γ-secretase from the ER, and plays a role in the proteolytic autoactivation of PSENs (Kaether et al., 2007; Prokop et al., 2005). Interestingly recent studies suggest its involvement in AMPK activation particularly when interacting with the diabetes type 2 drug metformin at the lysosome membrane (Liu et al., 2022; Ma et al., 2022; Sakamoto and Jessen, 2022). When investigating the autophagy-lysosome system in the employed Pen2 KO HeLa cells we observe striking overlaps with the phenotype of CLN3 KO cells (Klein et al., 2022). Precisely, the findings in the two congenic KO cell lines are almost identical which indicates a shared involvement of Pen2 and CLN3 in the autophagy-lysosome system. The performed qPCR experiments also demonstrated increased Pen2 transcript levels in CLN3 KO and increased CLN3 transcript levels in Pen2 KO. This suggests compensatory effects of the two proteins. Moreover, the KO cell lines partially mimic the phenotype of nutrient deprived 'starved' wild type cells. Thus, the consequent enhancement of the autophagy-lysosome system as demonstrated by increased nuclear TFEB, increased transcript levels of autophagy related TFEB targets, and increased autophagosome and autolysosome formation in starved Pen2 KO and CLN3 KO cells may be explained by a compensatory stress response to an impaired energy metabolism as already earlier suggested for CLN3 deficiency (Zhong et al., 2020). The observations in the autophagy-lysosome systems in the CLN3 KO and Pen2 KO HeLa cells are coherent with those in sub-confluent cerebellar neuronal precursor cells after *CLN3Δ$^{exon7/8}$* mutation (CbCLN3Δ$^{exon7/8}$) (Cao et al., 2011; Chandrachud et al., 2015; Fossale et al., 2004). The typical ATP5MC accumulation observed in neurons from CLN3 disease patients, however, only occurs in confluent CbCLN3Δ$^{exon7/8}$ cells, and not under sub-confluent conditions (Fossale et al., 2004). Such accumulation was also not observed in the CLN3 KO nor Pen2 KO HeLa cells. Hence, it is

plausible that CLN3 KO and Pen2 KO HeLa cells and the CbCLN3Δ$^{exon7/8}$ cells upon sub-confluency are still more adaptable to deficits in the autophagy-lysosome system than CbCLN3Δ$^{exon7/8}$ cells upon confluency or post-mitotic neurons. In the established KO cell lines said deficits are possibly rescued through TFEB activation which has been proposed to counteract disease progression in neurodegenerative diseases (Bajaj et al., 2019).

In the last years, in contrast to the conventional amyloid hypothesis, where Aβ occurrence and accumulation is regarded as the primary cause for AD, impairments of the autophagy-endolysosomal system that eventually lead to an imbalance of the energy metabolism have been suggested more frequently to be causative for AD (Funderburk et al., 2010; Liu and Li, 2019; Nixon and Yang, 2011; Uddin et al., 2018; Whyte et al., 2017; Zare-Shahabadi et al., 2015; Zhang et al., 2021). Accordingly, several overlaps between AD and NCLs in the autophagy-lysosome system have been reported. In NCL patients sometimes the accumulation of Aβ in lysosomes as part of the lysosomal storage material has been reported (Herva et al., 2000; Wisniewski et al., 1990a; Wisniewski et al., 1990b) and TPP1 (CLN2) is capable of Aβ degradation by cleaving Aβ fibrils *in vitro* (Solé-Domènech et al., 2018). A decrease of Aβ accumulation *in vivo* by elevating levels of TPP1, however, was so far unsuccessful (Sleat et al., 2022). Moreover, in a set of early onset dementia patients with mutations in the *PSEN1* gene, that are typical for familial AD, lysosomal inclusions were observed that were previously believed to be specific for NCLs (Dolzhanskaya et al., 2014). PSEN1 KO and depletion of the CLN1 gene *PPT1* both result in a defective vacuolar ATPase (v-ATPase) causing impairments of lysosome acidification (Lee et al. 2020; Bagh et al. 2017). Additionally, rare mutations of *CLN5*, *CTSD* (CLN10), *GRN* (CLN11) and *CTSF* (CLN13) have been linked to different forms of AD (Bras et al., 2016; Ehling et al., 2013; Fenoglio et al., 2009; Lee et al., 2011; Qureshi et al., 2018; Riemenschneider et al., 2006; Sheng et al., 2014; Viswanathan et al., 2009; Xu et al., 2017). In contrast to CLN10-associated mutations of *CTSD,* AD-associated mutants seem to be enzymatically active and not impaired in CTSD maturation or function (Bunk et al., 2021). Additional converging links between AD and other lysosomal storage disorders have also been identified. Accordingly, the typical NFTs in the brain of AD patients have been observed also in Nielmann Pick type C disease and mucopolysaccharidosis type IIB (Ohmi et al., 2009). Nielmann Pick type C disease pathology is further modified by increased BACE1 activity, mild Aβ deposition and APOE (Nixon, 2004).

6.2. The involvement of autophagy in Alzheimer's disease

Very early in AD pathology and prior to the formation of amyloid plaques dystopic neurons display an increased size and volume of EEs as well as an accumulation of autophagic vesicles, including autophagosomes and autolysosomes (Cataldo et al., 1997; Haung Yu et al., 2005). Aβ and Aβ aggregates have been shown to localize to these EEs and autophagic vesicles, making an involvement of endocytic and autophagic processes in AD pathogenesis very likely (Funderburk et al., 2010; Ginsberg et al., 2010; Haung Yu et al., 2005). To remain protein homeostasis neurons heavily depend on autophagy to degrade large and insoluble protein aggregates (Malampati et al., 2020). Such aggregates accumulate not only in lysosomal storage disorders and AD but also in other neurodegenerative diseases. Among others, α-synuclein accumulates in Parkinson's disease, TAR DNA-binding protein 43 (TDP43) and superoxide dismutase 1 (SOD1) in amyotrophic lateral sclerosis (ALS) and mutated huntingtin (HTT) in Huntington's disease (Peng et al., 2020). The polarized nature of neurons makes them especially vulnerable to dysfunctional autophagy as neuronal lysosomes localize primarily to their soma and axonal phagosomes must be transported into the soma to fuse with these lysosomes (Cheng et al., 2015; Maday et al., 2012). In the AD brain the cytoplasmic content of dystopic neurites gets almost completely filled by autophagic vesicles which is an extreme burden that is comparable to that in lysosomal storage disorders (Nixon and Yang, 2011; Nixon et al., 2008). Along with autophagosome formation, lysosomal number and mRNA and protein levels of lysosomal genes like hydrolases, as well as autophagy related proteins like ATGs are upregulated in AD (Bordi et al., 2016; Cataldo et al., 1995; Cataldo et al., 1996; Nixon and Cataldo, 2006).

Similar to our observations concerning Pen2, γ-secretase activity independent functions in the autophagy-lysosome system have been proposed for the exchangeable γ-secretase catalytic subunits PSEN1 and PSEN2 (Neely et al., 2011; Wolfe et al., 2013). Upon PSEN1 mutations, enlarged endosomes, deficits in lysosome acidification, and deficient lysosomal Ca^{2+} signaling and proteolysis have been demonstrated (Lee et al., 2010; Lee et al., 2015; Wilson et al., 2004). Depletion of PSEN1 further induces an increase in autophagic lysosomes that selectively accumulate autophagic maker proteins, α- and β-synuclein and, hence, possibly play a role in α-synuclein lesions typical for Parkinson's disease (PD) but also observed in AD (Fujiwara et al., 2002; Neely et al., 2011). PSEN2 containing γ-secretases are targeted to lysosomes as

PSEN2 harbors a lysosomal targeting signal (Meckler and Checler, 2016; Sannerud et al., 2016). Mutations in PSEN2 impair autophagy by blocking autolysosome fusion which is seemingly related to its regulation capacities for intracellular Ca^{2+} homeostasis (Fedeli et al., 2019). Cytosolic Ca^{2+} levels are known to mediate autophagic processes (Criollo et al., 2007; Wang et al., 2008). Initially, phenotypes from such γ-secretase ablations through *PSEN1/2* mutations were different from phenotypes from pharmacological γ-secretase inhibition. Therefore, the involvement of presenilins in the autophagy-lysosome system independent from γ-secretase activity in lysosomal storage disorders and other neurodegenerative diseases like AD was suggested. Other studies, however, demonstrated congruent effects upon pharmacological γ-secretase inhibition like an increased size of EEs, disrupted lysosomal proteolysis and autophagic impairments (Hung and Livesey, 2018; Jiang et al., 2010; Kwart et al., 2019; Lauritzen et al., 2016). Therefore, impairments of γ-secretase may be causative for at least some of the alterations in the autophagy-endolysosome system. Studies in human induced pluripotent stem cell-derived neurons further demonstrated remarkable converging effects in the autophagy-lysosome system of *PSEN1* and *APP* mutations (Hung and Livesey, 2018; Kwart et al., 2019).

It has further been demonstrated that the earlier described hallmarks of AD i.e., senile plaques and NFTs, can derive from deficits in the autophagy-lysosome system. APP is to a significant degree processed in the endosomal-lysosomal pathway (Grbovic et al., 2003; Koo et al., 1996; Pasternak et al., 2003) and γ-secretase is highly active in autophagic vesicles (Haung Yu et al., 2005; Yu et al., 2004). In the healthy brain, Aβ is rapidly degraded by the autophagy-lysosome system but it accumulates in autophagic vesicles in the aging and pathological brain (Haung Yu et al., 2005). Hyperphosphorylated tau also localizes first to autophagic vesicles (Nixon et al., 2005) where it aggregates after autophagic flux blockage (Hamano et al., 2008). Further, the activation of autophagy by inhibiting mTOR or the overexpression of cathepsins in AD models rescues intra- and extracellular deposition of Aβ and cognitive functions (Caccamo et al., 2010; Majumder et al., 2011; Mueller-Steiner et al., 2006). In accordance, the depletion of autophagy related proteins worsens the AD phenotype by inducing Aβ inclusions (Nilsson et al., 2015; Tian et al., 2011) and the inhibition of cathepsins causes rapid autophagic vesicle accumulation (Boland et al., 2008). Similarly, phosphorylation of tau or mutant tau aggregation gets upregulated by ATG7 depletion (Inoue et al., 2012) and autophagy inhibition (Caccamo et al., 2013; Wang et al., 2009) and downregulated by autophagy activation through

inhibition of mTOR (Berger et al., 2006; Silva et al., 2020) or TFEB upregulation (Polito et al., 2014; Wang et al., 2016). The APP fragment CTFβ as well as tau are substrates for chaperone mediated autophagy and can induce autophagy-lysosome impairments (Lauritzen et al., 2016). Mutant tau targets to LAMP2 oligomers but cannot enter the lysosome lumen completely and the remaining tau fragments on the lysosome membrane thereby block chaperone mediated autophagy (Caballero et al., 2021; Wang et al., 2009). Finally, it was suggested that autophagic vesicles are released into the extracellular space where they associate with deposits of Aβ after the degeneration of dystopic neurons (Cataldo et al., 1994).

The typical synaptic loss in AD patients has also been described to be partially autophagy dependent. The clearance of different neurotransmitter receptors like AMPARs and $GABA_A$ is dependent on autophagy (Lieberman and Sulzer, 2020) and autophagy suppression was demonstrated to increase dopamine release of dopaminergic neurons (Hernandez et al., 2012). Autophagy is further important for LTP. BDNF, which induces LTP, reduces neuronal autophagy and BDNF deficiency promotes autophagosome formation (Nikoletopoulou and Tavernarakis, 2018). In contrast, autophagy stimulation, however, also seems to be required for memory formation and LTP generation (Glatigny et al., 2019).

In the healthy brain autophagic vesicles are relatively uncommon in neurons (Mizushima et al., 2004; Nixon et al., 2005). Healthy neurons exhibit low basal autophagic activity and an extremely efficient clearance of autophagosomes through rapid autolysosome formation (Boland et al., 2008). Autophagic vesicle accumulation as observed in the AD brain can therefore be caused by increased autophagy initiation, impaired autophagic vesicle transport towards lysosomes, an impaired autophagic flux or decreased lysosomal degradation (Liu and Li, 2019). There is evidence that autophagy initiation is impaired in the AD brain as it displays downregulation of p62 (Du et al., 2009) and Beclin-1 (BECN-1), a major autophagy initiator (Pickford et al., 2008). Upon BECN-1 deficiency autophagy is disrupted and intracellular Aβ accumulation in autophagic vesicles is increased. Its overexpression causes an intra- and extracellular reduction of Aβ (Pickford et al., 2008). Aβ itself also directly induces autophagic vesicle production (Hung et al., 2009). Nerve ligations and toxic agents focally interrupt axonal transport of autophagic vesicles by cytoskeletal elements (Griffin and Watson, 1988; Wirtschafter et al., 1977). This interruption induces rapid autophagosome accumulation that is trapped in neurites (Boland et al., 2008). Accordingly, insoluble tau aggregates in dystopic

AD neurons are primarily localized to axons rather than to dendrites or the soma (Binder et al., 1985) and functional tau protein is essential for retrograde autophagosome trafficking and maturation by regulating the assembly and stabilization of microtubules (Dixit et al., 2008). A blockage of the autophagic flux in AD has also been suggested as the lysosomal and autolysosomal marker LAMP1 was abundant in accumulating autophagic vesicles around amyloid plaques (Gowrishankar et al., 2015). Finally, lysosomal degradation deficits are also plausible in dystopic AD neurons as their autophagic vesicles are filled with undigested and partially digested substrates (Nixon et al., 2005) and the blockage of cathepsin mediated proteolysis in the healthy brain leads to an AD like accumulation of autophagic vesicles (Boland et al., 2008). Further, Aβ disrupts the physical integrity of the autolysosomal membrane and thereby impairs substrate degradation (Ling et al., 2009). Chung et al. therefore suggested that initially autophagy increases as a protective response against stress but that autophagic flux is ultimately impaired with AD progression (Chung et al., 2019).

Our findings of the involvement of Pen2 in the autophagy-lysosome system supports the previously reported AD dependency on autophagy. Precisely, they suggest Pen2 and CLN3 involvement in autophagy induction, lysosomal protein degradation but not in autophagosome-autolysosome fusion. The observed efficient autophagic flux in Pen2 KO and CLN3 KO HeLa cells, however, might be due to the adaptiveness to stress of HeLa cells as they are, in contrast to neurons, unpolarized and highly mitotic cells. As in other studies and models for AD and CLN3 disease impairments of the autophagic flux were observed, the here employed cells possibly mimic early stages of these diseases that are still able to respond to the increased metabolic stress levels.

6.3. PICK1 and its interaction with SorLA

Recent studies demonstrate that deficiency of the Vps10p-D receptor SorLA causes APP-dependent defects in the endolysosome-autophagy system. They display endosome enlargements, lysosome dysfunction and defects in autophagic degradation (Hung et al., 2021) that are congruent to the observations after APP of PSEN1 ablation (Hung and Livesey, 2018; Kwart et al., 2019). As described earlier, some proteins like APP are retrogradely transported to the TGN through SorLA in a retromer-dependent way (see 1.5.2 SorLA). SorLA

expression is downregulated in the AD brain. It also promotes Aβ degradation through its transportation towards lysosomes (Caglayan et al., 2014; Dumanis et al., 2015).

With regard to the cytosolic adaptors of SorLA, the fact that SorLA promotes surface expression of some of its ligands, such as TrkB and APP, and lysosomal localization of other ligands like Aβ, the involvement of SorLA in intracellular trafficking processes has been suggested. It has been proposed that SorLA recruits in a complex with the retromer complex some ligands from endosomes to the TGN where they re-enter the secretory pathway and are transported to the plasma membrane. Moreover, it has been proposed that SorLA also transports specific ligands from the TGN to late endosomes and lysosomes via its interaction with AP-1, similar to Sortilin (Caglayan et al., 2014; Fjorback et al., 2012; Rohe et al., 2013).

In section 4 the novel interaction and co-localization of SorLA with the protein interacting with C kinase 1 (PICK1) in neurons was identified and characterized. PICK1 is a cytosolic scaffold protein comprised of one PDZ domain and one BAR domain (Xu and Xia, 2006). PDZ domains, named after PSD95, DLG1 and ZO1 as the first proteins found to harbour such a domain, are small highly reactive domains that interact with short protein cytoplasmic termini of transmembrane proteins. PDZ domain containing proteins (PDZ proteins) often promote the itinerary of these transmembrane proteins through their interaction with cytoskeletal compartments (Lee and Zheng, 2010). BAR domains, also named after three proteins they were first found in Bin, Amphiphysin and Rvs, on the other hand are composed out of only α-helices and induce membrane curvature upon homodimerization (Peter et al., 2004). We also demonstrate that Sortilin, another Vps10p-D receptor, is not interacting with PICK1 and that SorLA is not interacting with the cytosolic scaffold protein PSD95, which harbours three PDZ domains and like PICK1 has been identified to interact with the Vps10p-D receptor SorCS3 (Breiderhoff et al., 2013). Thus, SorLA interaction with PDZ proteins is not arbitrary, but seems to be rather specific to PICK1 and PICK1 is not interacting with all other Vps10p-D receptors, although PICK1 belongs to a small group of promiscuous PDZ domains with a mixed specificity. The last C-terminal amino acids of the SorLA cytoplasmic tail valine(V)-isoleucine(I)-alanine(A) are hydrophobic and therefore make up a typical type II PDZ domain interaction motif Φ-X-Φ, with Φ being a hydrophobic residue, and X being any residue (Kalyoncu et al., 2010). Ablation of the V-I-A motif in the SorLA cytoplasmic tail impaired its interaction with PICK1 as shown by mammalian-2-hybrid analysis and recruitment experiments of PICK1 with ectopically

localized cytoplasmic tails of SorLA to mitochondria. SorLA, hence, interacts most likely with the PDZ domain of PICK1. We further demonstrate that PICK1 interaction seems to have no impact on the internalization of SorLA, as ablation of the V-I-A motif did not alter internalization properties of the employed chimeric IL2-receptor with a SorLA cytoplasmic tail. Expression of both, SorLA and PICK1, are inducible by BDNF (Jourdi et al., 2003; Rohe et al., 2013). Thus, PICK1-dependent SorLA trafficking might be altered by induction of neuronal activity. PICK1 and SorLA possibly form a complex with the oncogene erb-b2 receptor tyrosine kinase 2 (ERBB2), a growth factor receptor that activates signal transduction and cell proliferation. ERBB2 is a known PICK1 interactor that also forms a complex with SorLA (Jaulin-Bastard et al., 2001; Pietilä et al., 2019).

PICK1 is localized to the pre- and post-synaptic density, interacts with numerous proteins and has been genetically linked to various neurodegenerative and neuropsychological diseases through its ability to modulate the trafficking of its interactors (Li et al., 2016). In the presynapse it interacts with the metabotropic glutamate receptor mGluR7 and the dopamine transporter (DAT) (Jin et al., 2006; Torres et al., 2001). Interference of the PICK1-mGluR7 interaction causes pre-synaptic mGluR7 clusters leading to prominent epileptic seizures (Arstikaitis and Gauthier-Campbell, 2006; Jin et al., 2006; Meldrum et al., 1999). In the schizophrenia brain PICK1-dependent surface expression of DAT is increased (Torres et al., 2001). PICK1 involvement in schizophrenia has also been shown by its interaction with the NMDA receptor activating serine racemase which synthesizes D-serine (Nomura et al., 2016). PICK1 further regulates local protein translation by interacting with argonaute protein and inhibiting its RNA silencing processes (Antoniou et al., 2014). Phosphorylation and palmitoylation of PICK1 are essential regulating factors during LTD (Thomas et al., 2013; Yagishita et al., 2015) and PICK1 ubiquitination through Parkin impairs its interaction with acid sensing ion-channel 2a (ASIC2a) which possibly leads to the loss of dopaminergic neurons in PD (Joch et al., 2007). PICK1 deficiency generally causes oxidative stress in aged neurons. Hence, its abnormal function has been suggested to facilitate neuronal loss in oxidative-stress related diseases like AD, PD and ALS (Wang et al., 2015).

The best investigated function of PICK1 is its role in regulating trafficking of AMPARs. PICK1 interacts with the AMPAR subunit GluA2 (Hanley and Henley, 2005; Yagishita et al., 2015). Like other transmembrane proteins, the intracellular trafficking of neurotransmitter receptors is

regulated by the cytosolic motifs of their respective subunits and their interaction with different adaptor and scaffolding proteins, including PDZ-proteins. These interactions can be regulated by the phosphorylations of specific amino acids in the cytoplasmic tails of the subunits or in the interacting intracellular proteins (Anggono and Huganir, 2012; Collingridge et al., 2004; Díaz-Alonso and Nicoll, 2021; Lau and Zukin, 2007; Lerma and Marques, 2013). AMPAR can additionally form complexes with transmembrane AMPAR regulatory proteins (TARPs) for directed trafficking (Chen et al., 2000; Fukata et al., 2005). All AMPAR subunits also interact directly with the TARP stargazin and, consequently, form a complex with the stargazin interacting PDZ protein PSD95. The stargazing-AMPAR interaction is induced by stargazing phosphorylation through CAMKII. The stargazin-PSD95 interaction then traps and transiently stabilizes diffusing AMPAR at the post-synapse and its disruption increases the surface diffusion of AMPAR (Bats et al., 2007; Chen et al., 2000; Opazo et al., 2010). The most common AMPA receptors are composed of GluA1/GluA2 heterotetramers. In its cytosolic tail the AMPAR subunit GluA1 contains a type I PDZ domain binding motif which directly interacts with the PDZ protein synapse-associated protein 97 (SAP97). This interaction can rescue AMPAR transmission when reduced by PSD95 loss and, thus, is critical for synaptic targeting of GluA1 containing AMPAR (Anggono and Huganir, 2012; Rumbaugh et al., 2003; Wu et al., 2002). It is believed, that SAP97 interacts with the motor protein myosin VI to transport AMPARs towards the dendritic plasma membrane and that AMPAR insertion, but not its diffusional trapping at the synapse, is promoted by SAP97 phosphorylation through CAMKII (Collingridge et al., 2004; Opazo et al., 2010). After AMPAR insertion in the plasma membrane they travel laterally into the postsynaptic membrane. The GluA2 subunit, like SorLA, contains a type II PDZ domain binding motif which directly interacts with GRIP1 and PICK1 (Anggono and Huganir, 2012; Dong et al., 1997; Won et al., 2017). GRIP1 phosphorylation increases AP-2 mediated clathrin-dependent internalization of AMPAR, which causes LTD and the knockout of GRIP1 causes LTD absence in the cerebellum (Anggono and Huganir, 2012; Collingridge et al., 2004; Yong et al., 2020). PICK1-GluA2 interaction underlies hippocampal and cerebral long-term depression and the internalization of AMPAR (Steinberg et al., 2006). This interaction especially drives the synaptic removal of GluA2-containing AMPA receptors (Hanley, 2008). Phosphorylation of a serine residue within the GluA2 PDZ binding motif by PKC greatly reduces the GRIP1 binding affinity for GluA2 without affecting PICK1 binding (Collingridge et al., 2004). This reduces synaptic GluA2 expression and is therefore thought to drive storage of AMPAR

at extrasynaptic sites and in intracellular vesicles (Sørensen et al., 2022). The N-terminal acid region of PICK1, however, regulates GluA2 interaction and internalization in a Ca^{2+}-dependent way. Increased NMDAR induced intracellular Ca^{2+} currents seem to increase PICK1-GluA2 interaction and promotes AMPAR internalization (Hanley and Henley, 2005). PICK1 regulates endocytosis of membrane AMPAR during LTD (Kim et al., 2001; Xia et al., 2000) or after stroke induced oxygen-glucose deprivation (Dixon et al., 2009) but, in contrast, its deficiency or PDZ domain blockage prevents LTP as its overexpression increases LTP essential synaptic expression of GluA2-deficient AMPAR (Terashima et al., 2008; Xu et al., 2014). Interestingly, PICK1 also recruits AMPAR to immature postsynaptic sites and promotes neurexin-induced synaptogenesis (Xu et al., 2014) and possibly effects spinogenesis by regulating actin polymerization (Rocca and Hanley, 2015).

The interaction of SorLA with the PDZ domain of PICK1 either competes with other PICK1 PDZ domain interactors or, more likely, forms a complex with them through PICK1 homodimerization facilitated by its BAR domain. This homodimerization is essential to mediate the endosomal transport of PICK1 and its bound partners. Given the retraction capabilities of PICK1 from the plasma membrane, the internalization and sorting capacity of SorLA to lysosomes and retrogradely to the TGN, it is possible that such hypothetic SorLA-PICK1 complexes internalize other PICK1 interactors upon PICK1 homodimerization and either sort them back to the TGN for subsequential secretion or direct them towards lysosomes for subsequential degradation. As LTD induced AMPAR removal is autophagy dependent the latter itinerary could be a possible pathway for GluA2 containing AMPAR degradation. As SorCS3 interacts with PSD95, PICK1 (Breiderhoff et al., 2013) and SAP97 (Klein, 2019), SorCS1c-δ interacts with PICK1 and GRIP1 (Klein and Hermey, unpublished) and a KO of SorCS1 leads to decreased AMPAR surface expression in primary neurons (Savas et al., 2015), Vps10p-D receptor involvement in the regulation of AMPAR trafficking is highly likely. The C-termini of the Vps10p-D receptors can further be phosphorylated which can alter their interactions with PDZ proteins. The phosphorylation of the SorCS1c-δ C-terminus inhibits its interaction with GRIP1 but not with PICK1, which suggests a kinase dependent interaction and trafficking of Vps10p-D receptors (Klein and Hermey, unpublished). Interestingly, recent studies also demonstrate impaired GluA1 trafficking upon SorLA deficiency (Mishra et al., 2022).

6.4. Investigating the role of Vps10p-D receptors in intracellular sorting

The intracellular protein sorting in neurons underlies their polarization and compartmentalization, which directly regulates their physiological functions. Misregulation in neuronal intracellular protein trafficking processes likely causes disease and, therefore, their examination is a crucial matter to understand the healthy and the diseased brain. Protein trafficking pathways that are affected in neurodegenerative diseases include general protein folding, endocytosis, EE formation, EE to LE transition, and retrograde TGN transmission (Schreij et al., 2016). Mutant forms of proteins can cause misfolding of their structure in the ER or the cytosol that leads to their intracellular accumulation like in mutant tau protein. The uncoating of AP-2 mediated clathrin-coated endosomes, like synaptic vesicles, is regulated by synaptojanin and auxilin (Cremona et al., 1999; Xing et al., 2010), which can both underlie mutations causative for early-onset PD (Edvardson et al., 2012; Krebs et al., 2013; Quadri et al., 2013). EE enlargement in AD and down syndrome, which has a shared pathogenesis with AD through their shared elevated expression of APP, can be induced by increased CTFβ and Rab5 levels (Cataldo et al., 2008; Jiang et al., 2010). Mutations in the genetic ALS risk factor *ALS2* further cause decreased levels of active Rab5 and dysregulate EE association to the actin cytoskeleton (Topp et al., 2004). Active Rab5 levels are also decreased in the most common mutation of familial PD in the leucine rich repeat kinase 2 (LRRK2). This LRRK2 mutation causes impairments in the transition of proteins from Rab5 positive EEs to Rab7 positive LEs (Henry et al., 2015). Retrograde transport from the endosomes to the TGN is facilitated through the retromer complex and mutations in the retromer subunit VPS35 are causative for some forms of late-onset PD (Vilariño-Güell et al., 2011; Zimprich et al., 2011).

One of the most straight-forward ways to investigate intracellular protein trafficking is live imaging. This approach enables the dynamic observation of proteins rather than gathering stationary information like in fixed cells. Live imaging, however, requires special tools, such as fluorescent protein tags, for respective protein visualization. The members of the Vps10p-D receptor sorting family Sortilin, SorLA, SorCS1, SorCS2 and SorCS3 (See 1.5 The Vps10p-D receptor family) have been proposed to convey several intracellular sorting processes and have been linked to different neurodegenerative and psychiatric diseases. Particularly, they interact with transmembrane, extracellular, and lysosomal proteins and are involved in their anterograde transport and secretion, internalization processes, retrograde transport to the

TGN for their reintegration in the secretory pathway and transportation towards lysosomes. Apart from the earlier described involvement of SorLA, Sortilin and SorCS1 in AD, previous investigations have linked Sortilin and SorCS2 to Huntington's disease, as SorCS2 promotes recycling of the NMDAR subunit NR2A and Sortilin and SorCS2 associate with HAP1 which mediates BDNF secretion and stabilization of TrkB complexes (Ma et al., 2017; Nykjaer and Willnow, 2012). Sortilin further facilitates endocytosis of the CLN11 disease and frontotemporal dementia risk factor PGRN and delivers it to lysosomes (Hu et al., 2010). Therefore, these sorting receptors are valuable substrates for live cell imaging investigations. The specific sorting mechanisms of each of these receptors may be distinct due to their partially complementary expression patterns and different cytoplasmic motifs for interactions with auxiliary proteins (Hermey, 2009; Hermey et al., 2004; Malik and Willnow, 2020). Hence, fluorophore tagged Vps10p-D receptors can be used to decipher various protein itineraries in the healthy and diseased brain using live assays and other methods as discussed below.

Earlier studies used subcellular fractionation or immunocytochemistry of fixed cells to examine the subcellular localizations of endogenous Vps10p-D receptors. This, however, gives only stationary information at specific time points and the partial lack of specific antibodies due to the high homology between some of the Vps10p-D receptors limits such investigations. To overcome these issues, cellular investigations of Vps10p-D receptors therefore highly relied on the generation of chimeric receptors and their tagging with fluorophores. Some of such fluorophore-tagged Vps10p-D receptors have also been employed for live assays. Fusion of the Sortilin transmembrane and cytoplasmic domains with an N-terminal extracellular green fluorescent protein (GFP) tag have been used to investigate the association of Sortilin with Rab7b (Progida et al., 2012). A similar approach was used by fusing the SorLA transmembrane and cytoplasmic domain with an N-terminal extracellular mCherry tag to investigate the somatodendritic localization of SorLA (Klinger et al., 2016) or with the extracellular moiety of IL2-R to investigate its cytoplasmic interaction with PICK1 (Binkle et al., 2022; see section 4. The adaptor protein PICK1 targets the sorting receptor SorLA). SorLA has been tagged C-terminally with red fluorescent protein (RFP) or mCherry for live imaging experiments to track APP trafficking, to investigate the SorLA-APP interaction (Eggert et al., 2018; Schmidt et al., 2007) and its subcellular colocalization with SNX27, an endosomal trafficking factor and negative regulator of the γ-secretase complex (Huang et al., 2016). C-terminal tagging of SorLA with GFP was used to investigate its interaction with ERBB2 (Pietilä et al., 2019). C-terminal

tagged SorCS2 with GFP was further used for co-immunoprecipitation studies with the excitatory amino acid transporter 3 (EAAT3) (Malik et al., 2019). N- and C-terminal tagging of proteins is a fairly easy tagging strategy, but, although these studies give us valuable information about the interactors and itineraries of Vps10p-D receptors, such tags likely interfere with some interactions and functionalities of the receptors. Complex proteins like the multidomain transmembrane Vps10p-D receptors have a variety of interaction sites and motifs that can easily be impaired by protein tags. Thus, a number of known and likely of so far unknown interacting cytosolic adaptor proteins require freely accessible C-termini. Even small C-terminal tags interfere with their interaction with GGAs, PDZ proteins and possibly other adaptor proteins and consequently dysregulate their subcellular localization (Cramer et al., 2010; Lee and Zheng, 2010). Precisely, C-terminal tagging would maybe interfere with the earlier described phosphorylation-dependent PDZ protein interactions, which would result in altered trafficking of the Vps10p-D receptors and their interactors. A tag at the N-terminus of a Vps10p-D receptor would be cleaved off together with its N-terminal propeptide in the Golgi complex. Accordingly, I aimed for internal tags of the Vps10p-D receptors. Internal tagging strategies, however, are challenging as a misplaced internal tag easily interferes with specific functions or interaction sites of the protein or even impairs its structural folding. Misfolding of proteins generally prevents their exit from the ER, leads to accumulation in the ER and eventually to a stress response and degradation (Rao and Bredesen, 2004). To reduce the chance of such interferences, internal protein tags have to be placed between structural protein domains. A tag between the cytosolic tail and the transmembrane domain of Vps10p-D receptors was excluded because several sorting motifs like the AP-2 internalization motifs rely on the correct spacing between the motif and the plasma membrane (Geisler et al., 1998). A tag between the Vps10p-D and the cleavage site of the propeptide, on the other hand, might interfere with ligand binding of the Vps10p-D.

Therefore, in section 5, I established Vps10p-D receptors with an internal mVenus or tdTomato tag between their transmembrane domain and their extracellular moiety or between the Vps10p-D and the YWTD repeat for SorLA that can be used for their examination in live assays. Structural analyses of the tagged receptors were performed computationally using the novel AlphaFold 2.0 tool and compared with the predicted structures of the wild type proteins (Jumper et al., 2021; Varadi et al., 2022). Only after the computational analyses demonstrated a structural overlap between the domains surrounding the inserted tag and the

domains in the wild type proteins, the respective plasmid DNAs were generated for functional experiments. AlphaFold 2.0 predicts protein structures with nearly experimental accuracy (Jumper et al., 2021) but the functionality of the tagged receptors had still to be validated. Indeed, AlphaFold 2.0 gave very good approximations of the individual domain borders within the Vps10p-D receptors according to the literature (Glerup et al., 2014; Hermey et al., 2003; Jacobsen et al., 2001; Kitago et al., 2015; Leloup et al., 2017; Leloup et al., 2018; Petersen et al., 1999; Quistgaard et al., 2009; Westergaard et al., 2005) and therefore helped to set the exact sites for tag insertion. Some computationally correct folded proteins, however, still accumulated in the ER after construct expression in cell culture by transfection and consequently were adjusted again. Interestingly, fluorophore tagged SorCS3, which is the only Vps10p-D receptor that is exclusively expressed in the brain (Oetjen et al., 2014), failed to exit the ER in COS7 cells but was distributed in vesicular structures and at the surface in HEK293 cells and primary hippocampal neurons. This highly suggest, that SorCS3 needs specific factors for successful folding that are present in neurons and HEK293 but not in COS7 cells. Human embryonic kidney or HEK293 cells express a variety of neuron-specific genes as they most probably originate from an adrenal precursor structure that is adjacent to the kidney during development (Lin et al., 2014; Shaw et al., 2002). Accordingly, neuron-specific factors are very likely to be involved in SorCS3 folding.

Only after I observed successful exit of the fluorophore tagged receptors from the ER by immunocytochemistry further functional tests were executed. Western blot analysis of cells transfected with the plasmids coding for the tagged receptors revealed full length expression of the fluorophore tagged Vps10p-D receptors without further degradation. Then, the subcellular localizations of the fluorophore tagged Vps10p-D receptors were determined by colocalization experiments with different subcellular marker proteins. Previous studies report Sortilin localization to EEs, the TGN and to a low level to lysosomes (Al-Akhrass et al., 2017). SorLA was identified to localize to the ER, EEs, LEs, REs and the Golgi complex with a more prominent localization to the TGN than to the CGN (Andersen et al., 2005; Offe et al., 2006; Shih et al., 2022). SorCS1 has differing subcellular localizations depending on the specific splice variant. Generally, SorCS1 splice variants localize to the plasma membrane, vesicular and perinuclear structures. SorCS1b, however, is thought to localize to secretory vesicles and the plasma membrane and not to a significant degree to endosomes due to its lack of internalization motifs (Hermey et al., 2003). SorCS1c-β on the other hand localizes to EEs and

REs (Savas et al., 2015). SorCS3 was demonstrated to localize to the TGN and EEs (Oetjen et al., 2014). In neurons all Vps10p-D receptors are found primarily at somatodendritic compartments and for SorCS3 minor axonal localizations have been reported (Glerup et al., 2016; Hermey et al., 2001b; Oetjen et al., 2014; Sarret et al., 2003; Savas et al., 2015). The performed co-localization experiments in section 5 are in accordance with the yet known subcellular localizations of the receptors and add new insights to the yet only partially deciphered subcellular localizations of Vps10p-D receptors. They demonstrate localization of all Vps10p-D receptors in the CGN and TGN. As all Vps10p-D receptors are sorted to the plasma membrane through the secretory pathway they necessarily traverse the CGN and the TGN. Yet, the localization of SorLA in the CGN was relatively low in comparison to other Vps10p-D receptors. The mentioned earlier studies found similarly low levels or missing localization of SorLA in the CGN (Andersen et al., 2005; Offe et al., 2006). Thus, SorLA possibly traverses the CGN in a rapid fashion making its detection in this compartment difficult. My data also presents localization of all Vps10p-D receptors but SorCS1b to different endosomes like EEs in fixed immortalised cell lines and primary hippocampal neurons and under live imaging conditions. As SorCS1b is the only Vps10p-D receptor lacking internalization motifs like an AP-2 binding site, all other Vps10p-D receptors are internalized and subsequently present in EEs. Sortilin and SorLA directly interact with retromer subunits and, accordingly, show a relatively high co-localization with the retromer subunit VPS35. As the retromer complex confers the retrograde transport from endosomes to the TGN and is therefore localized to those compartments colocalization with VPS35 was also found for SorCS1c-α, SorCS2 and SorCS3. As Rab9 plays a role in the LE to endolysosome and LE to TGN transition it is expressed mainly in LEs. We demonstrate especially high co-localization with Rab9 for Sortilin, SorLA and SorCS1c-α and lower co-localization for SorCS2 and SorCS3. As described earlier, Sortilin and SorLA have AP-1 and GGA interaction motifs and play important roles in targeting proteins towards lysosomes, whereas proteins of the SorCS subfamily do not interact with GGAs and are so far believed to rather facilitate endocytosis of proteins at the plasma membrane. Lower co-localization with Rab9 could be due to targeting of the receptors for lysosomal degradation or the low Rab9 presence in EEs. The similarly high co-localization of Rab9 with SorCS1c-α as with Sortilin and SorLA might also be a hint to its involvement in trafficking processes of proteins in LEs. Lysosomal localization of the tagged Vps10p-D receptors, however, is relatively

low. These localization results demonstrated the functional sorting of the fluorophore tagged Vps10p-D receptors, which is dependent on their sorting motifs in their cytoplasmic domains.

Further functional dimerization of the fluorophore tagged SorCS subfamily, which is facilitated by their leucine rich domain (Januliene et al., 2017b; Leloup et al., 2018) was tested with tagged SorCS2 as an example. Thus, SorCS2-tdTomato was successfully co-immunoprecipitated using SorCS2-mVenus. To confirm that these effects were dimerization-dependent and not due to indirect interactions fluorescence lifetime microscopy (FLIM) experiments were performed. During FLIM a lifetime reduction of the acceptor protein can only be observed by very close proximity of the acceptor to the donor fluorophore as found in direct protein interactions. This lifetime reduction of mVenus in cells expressing SorCS2-mVenus and SorCS2-tdTomato was observed when comparing it to cells expressing SorCS2-mVenus and Sortilin-tdTomato. Sortilin lacks a leucine rich domain and, therefore, is not dimerizing with SorCS2. The represented functional dimerization of fluorophore tagged SorCS2 validates functionality of the leucine rich domains adjacent to the inserted tags in the established fluorophore tagged SorCS subfamily proteins.

Excitingly, cells expressing either tagged Vps10p-D receptor except SorCS1b revealed a TrkB-independent co-transport of GFP labelled BDNF in live imaging experiments and an internalization of biotin labelled mBDNF. In fluorophore tagged SorCS1b expressing cells BDNF-GFP or mBDNF-biotin accumulated at the plasma membrane where SorCS1b is localized. These findings are in line with the demonstrated lack of endocytic trafficking of SorCS1b and suggest an interaction of all Vps10p-D receptors with BDNF. The TrkB independency was demonstrated by immunoblotting lysates of the used cell lines using an antibody against a TrkB. BDNF is a neurotrophin (NT) that is expressed in nearly all brain regions (Hofer et al., 1990; Yan et al., 1997). In the Golgi complex BDNF is found as a progenitor form containing a propeptide that, like the propeptide of the Vps10p-D receptors, can be cleaved off by furin in the TGN, by regulated convertases in secretory vesicles or even extracellularly to form mature BDNF (Kowiański et al., 2018). In neurons BDNF secretion is highly activity dependent and depending on the secreted isoform it binds varying neurotrophic receptors that activate specific signal cascades with opposed final effects (Conner et al., 1997; Dieni et al., 2012; Yang et al., 2009). The functional signalling pathways of neurotrophic factors are of major importance and its disruptions have been linked to several disorders like Huntington's disease

(Simmons, 2017), PD, AD (Allen et al., 2013; Lübke et al., 2021) and depression (Castrén and Monteggia, 2021; Levy et al., 2018). Secreted mBDNF binds to dimerized TrkB, which promotes cell survival, neuronal plasticity, synaptogenesis, proliferation, cell growth and LTP (Khalin et al., 2015). Interaction of TrkB with $p75^{NTR}$ increases mBDNF affinity, which increases cell survival (Hempstead et al., 1991). On the other hand, $p75^{NTR}$ also forms a trimeric complex with pro-BDNF and Sortilin or SorCS2 to promote apoptotic signalling (Glerup et al., 2014; Leloup et al., 2018; Nykjaer et al., 2004; Teng et al., 2005). Leloup et al. demonstrated that SorCS2 interacts with NTs as well as with $p75^{NTR}$ through its Vps10p-D (Leloup et al., 2018). Sortilin, SorCS2 and SorCS3 additionally have been shown to bind the NTs pro-NGF and mNGF (Deinhardt et al., 2011; Glerup et al., 2014; Leloup et al., 2018; Nykjaer et al., 2004; Teng et al., 2005; Westergaard et al., 2005). Therefore, all Vps10p-D receptors have been suspected to generally interact with NTs, but experimental examination remained absent. The results of my experiments, therefore, do not only show the functionality of the Vps10p-D in the fluorophore tagged receptors, but also indicate for the first time an interaction of all Vps10p-D receptors with BDNF independent of TrkB. Specifically, the interaction of mBDNF is shown, because mBDNF-biotin was internalized by all cells expressing tagged Vps10p-D receptors and accumulated at the surface of tagged SorCS1b expressing cells. In the live imaging experiments, the co-cultured cells expressed full length BDNF-GFP and therefore, it cannot be excluded whether the observed internalization included also secreted unprocessed pro-BDNF. In the performed experiments with mBDNF-Biotin, however, saturating amounts of BDNF were applied. Thus, no statement about the affinity of the proposed interactions can be made. For such affinity estimations and the question, whether all Vps10p-D receptors also interact with pro-BDNF further experimental validation is required.

Overall, the here established fluorophore tagged Vps10p-D receptors show functional protein folding and domain properties. They can be used for further analysis of Vps10p-D receptor dependent protein trafficking pathways by live imaging. We also demonstrate that they can be applied in FRET-FLIM based interaction studies. The fluorophore tagged Vps10p-D receptors can further be introduced by gene editing methods to overcome overexpression effects. Moreover, the fluorophore tags can also be exchanged by other tags like pH-sensitive fluorophores to observe their localizations in more acidic compartments or by protein purification tags.

7. Conclusions

In the here presented work I demonstrate that an ablation of either CLN3 or Pen2 result in similar deficits of the autophagy-lysosome system. This includes deficits in lysosomal degradation, a reduced number of lysosomes and an increased autophagy induction with a functioning autophagic flux. The further comparison of the different NCL subtypes with AD revealed surprising links underlying intracellular protein trafficking deficits in neurons especially in the autophagy-lysosome system. These findings support the hypothesis that the primary cause underlying AD is not the toxicity of amyloid plaques but rather previous intracellular impairments in protein trafficking and degeneration that cause excessive amyloid generation, a defective cellular energy metabolism and amyloid exposure to the extracellular space by neuronal disruption. The Vps10p-D receptor and AD risk factor SorLA is shown to interact through the last three amino acids of its cytoplasmic tail with the PDZ protein PICK1. This suggests that the endocytosis and trafficking of SorLA is at least partially regulated by PICK1 and that they maybe in concert regulate trafficking of other PICK1 interactors. SorLA is part of the Vps10p-D receptor family which facilitate various neuronal protein sorting mechanisms. Dysregulations in these mechanisms have been shown to be highly involved in impaired functionalities of the brain. Thus, as Vps10p-D receptors are genetic risk factors in several neurological and psychiatric diseases their investigation is of major importance. Therefore, I established functional internally tagged versions of all Vps10p-D receptors as a powerful tool to investigate their involvement in protein trafficking in live assays. I demonstrate their precise subcellular localizations to different endosomal compartments and investigate their trafficking in live cell experiments. I demonstrate the localization and trafficking of all Vps10p-D receptors through the Golgi-complex and early endosomes and high localization of Sortilin, SorLA and SorCS1c-α in late endosomes. I further demonstrate functional dimerization of the fluorophore tagged SorCS2 receptors and show for the first time that all Vps10p-D receptors interact with BDNF. This interaction with BDNF suggests the involvement of all Vps10p-D receptors in trophic and apoptotic signalling which yet has only been proposed for Sortilin and SorCS2.

8. Appendix

8.1. References

Adams, J., Feuerborn, M., Molina, J. A., Wilden, A. R., Adhikari, B., Budden, T. and Lee, S. Y. (2019). Autophagy–lysosome pathway alterations and alpha-synuclein up-regulation in the subtype of neuronal ceroid lipofuscinosis, CLN5 disease. *Sci Rep* **9**, 151.

Ahtiainen, L., van Diggelen, O. P., Jalanko, A. and Kopra, O. (2003). Palmitoyl protein thioesterase 1 is targeted to the axons in neurons. *Journal of Comparative Neurology* **455**, 368–377.

Ahtiainen, L., Luiro, K., Kauppi, M., Tyynelä, J., Kopra, O. and Jalanko, A. (2006). Palmitoyl protein thioesterase 1 (PPT1) deficiency causes endocytic defects connected to abnormal saposin processing. *Exp Cell Res* **312**, 1540–1553.

Al-Akhrass, H., Naves, T., Vincent, F., Magnaudeix, A., Durand, K., Bertin, F., Melloni, B., Jauberteau, M.-O. and Lalloué, F. (2017). Sortilin limits EGFR signaling by promoting its internalization in lung cancer. *Nat Commun* **8**, 1182.

Allen, S. J., Watson, J. J., Shoemark, D. K., Barua, N. U. and Patel, N. K. (2013). GDNF, NGF and BDNF as therapeutic options for neurodegeneration. *Pharmacol Ther* **138**, 155–175.

Alzheimer, A. (1907). Uber eine eigenartige Erkrankung der Hirnrinde. *Zentralbl. Nervenh. Psych* **18**, 177–179.

Andersen, O. M., Reiche, J., Schmidt, V., Gotthardt, M., Spoelgen, R., Behlke, J., von Arnim, C. A. F., Breiderhoff, T., Jansen, P., Wu, X., et al. (2005). Neuronal sorting protein-related receptor sorLA/LR11 regulates processing of the amyloid precursor protein. *Proc Natl Acad Sci U S A* **102**, 13461–13466.

Andersen, O. M., Schmidt, V., Spoelgen, R., Gliemann, J., Behlke, J., Galatis, D., McKinstry, W. J., Parker, M. W., Masters, C. L., Hyman, B. T., et al. (2006). Molecular dissection of the interaction between amyloid precursor protein and its neuronal trafficking receptor SorLA/LR11. *Biochemistry* **45**, 2618–2628.

Andersen, O. M., Bøgh, N., Landau, A. M., Pløen, G. G., Jensen, A. M. G., Monti, G., Ulhøi, B. P., Nyengaard, J. R., Jacobsen, K. R., Jørgensen, M. M., et al. (2022). A genetically modified minipig model for Alzheimer's disease with SORL1 haploinsufficiency. *Cell Rep Med* **3**, 100740.

Andres-Alonso, M., Kreutz, M. R. and Karpova, A. (2021). Autophagy and the endolysosomal system in presynaptic function. *Cellular and Molecular Life Sciences* **78**, 2621–2639.

Andrew, R. J., de Rossi, P., Nguyen, P., Kowalski, H. R., Recupero, A. J., Guerbette, T., Krause, S. v., Rice, R. C., Laury-Kleintop, L., Wagner, S. L., et al. (2019). Reduction of the expression of the late-onset Alzheimer's disease (AD) risk-factor BIN1 does not affect amyloid pathology in an AD mouse model. *J Biol Chem* **294**, 4477–4487.

Anggono, V. and Huganir, R. L. (2012). Regulation of AMPA receptor trafficking and synaptic plasticity. *Curr Opin Neurobiol* **22**, 461–469.

Antoniou, A., Baptista, M., Carney, N. and Hanley, J. G. (2014). PICK1 links Argonaute 2 to endosomes in neuronal dendrites and regulates miRNA activity. *EMBO Rep* **15**, 548.

Arstikaitis, P. and Gauthier-Campbell, C. (2006). BARS at the Synapse: PICK-1 Lipid Binding Domain Regulates Targeting, Trafficking, and Synaptic Plasticity. *Journal of Neuroscience* **26**, 6909–6910.

Bae, E.-J., Yang, N. Y., Lee, C., Kim, S., Lee, H.-J. and Lee, S.-J. (2015). Haploinsufficiency of cathepsin D leads to lysosomal dysfunction and promotes cell-to-cell transmission of α-synuclein aggregates. *Cell Death Dis* **6**, e1901–e1901.

Bagh, M. B., Peng, S., Chandra, G., Zhang, Z., Singh, S. P., Pattabiraman, N., Liu, A. and Mukherjee, A. B. (2017). Misrouting of v-ATPase subunit V0a1 dysregulates lysosomal acidification in a neurodegenerative lysosomal storage disease model. *Nat Commun* **8**, 14612.

Bai, B., Vanderwall, D., Li, Y., Wang, X., Poudel, S., Wang, H., Dey, K. K., Chen, P.-C., Yang, K. and Peng, J. (2021). Proteomic landscape of Alzheimer's Disease: novel insights into pathogenesis and biomarker discovery. *Mol Neurodegener* **16**, 55.

Bajaj, L., Lotfi, P., Pal, R., Ronza, A. di, Sharma, J. and Sardiello, M. (2019). Lysosome biogenesis in health and disease. *J Neurochem* **148**, 573–589.

Bajaj, L., Sharma, J., di Ronza, A., Zhang, P., Eblimit, A., Pal, R., Roman, D., Collette, J. R., Booth, C., Chang, K. T., et al. (2020). A CLN6-CLN8 complex recruits lysosomal enzymes at the ER for Golgi transfer. *Journal of Clinical Investigation* **140**, 4118–4132.

Bammens, L., Chávez-Gutiérrez, L., Tolia, A., Zwijsen, A. and de Strooper, B. (2011). Functional and topological analysis of Pen-2, the fourth subunit of the gamma-secretase complex. *J Biol Chem* **286**, 12271–12282.

Barr, F. and Lambright, D. G. (2010). Rab GEFs and GAPs. *Curr Opin Cell Biol* **22**, 461–470.

Basak, I., Hansen, R. A., Ward, M. E. and Hughes, S. M. (2021). Deficiency of the Lysosomal Protein CLN5 Alters Lysosomal Function and Movement. *Biomolecules* **11**, 1412.

Bats, C., Groc, L. and Choquet, D. (2007). The Interaction between Stargazin and PSD-95 Regulates AMPA Receptor Surface Trafficking. *Neuron* **53**, 719–734.

Baum, A. E., Akula, N., Cabanero, M., Cardona, I., Corona, W., Klemens, B., Schulze, T. G., Cichon, S., Rietschel, M., Nöthen, M. M., et al. (2008). A genome-wide association study implicates diacylglycerol kinase eta (DGKH) and several other genes in the etiology of bipolar disorder. *Mol Psychiatry* **13**, 197–207.

Beecham, G. W., Martin, E. R., Li, Y. J., Slifer, M. A., Gilbert, J. R., Haines, J. L. and Pericak-Vance, M. A. (2009). Genome-wide Association Study Implicates a Chromosome 12 Risk Locus for Late-Onset Alzheimer Disease. *Am J Hum Genet* **84**, 35–43.

Bellenguez, C., Küçükali, F., Jansen, I. E., Kleineidam, L., Moreno-Grau, S., Amin, N., Naj, A. C., Campos-Martin, R., Grenier-Boley, B., Andrade, V., et al. (2022). New insights into the genetic etiology of Alzheimer's disease and related dementias. *Nat Genet* **54**, 412–436.

Benitez, B. A. and Sands, M. S. (2017). Primary fibroblasts from CSPα mutation carriers recapitulate hallmarks of the adult onset neuronal ceroid lipofuscinosis. *Sci Rep* **7**, 6332.

Berger, Z., Ravikumar, B., Menzies, F. M., Oroz, L. G., Underwood, B. R., Pangalos, M. N., Schmitt, I., Wullner, U., Evert, B. O., O'Kane, C. J., et al. (2006). Rapamycin alleviates toxicity of different aggregate-prone proteins. *Hum Mol Genet* **15**, 433–442.

Best, H. L., Neverman, N. J., Wicky, H. E., Mitchell, N. L., Leitch, B. and Hughes, S. M. (2017). Characterisation of early changes in ovine CLN5 and CLN6 Batten disease neural cultures for the rapid screening of therapeutics. *Neurobiol Dis* **100**, 62–74.

Binder, L. I., Frankfurter, A. and Rebhun, L. I. (1985). The distribution of tau in the mammalian central nervous system. *J Cell Biol* **101**, 1371–1378.

Binkle, L., Klein, M., Borgmeyer, U., Kuhl, D. and Hermey, G. (2022). The adaptor protein PICK1 targets the sorting receptor SorLA. *Mol Brain* **15**, 1–11.

Bloom, G. S. (2014). Amyloid-β and tau: the trigger and bullet in Alzheimer disease pathogenesis. *JAMA Neurol* **71**, 505–508.

Boggild, S., Molgaard, S., Glerup, S. and Nyengaard, J. R. (2016). Spatiotemporal patterns of sortilin and SorCS2 localization during organ development. *BMC Cell Biol* **17**, 8.

Boland, B., Kumar, A., Lee, S., Platt, F. M., Wegiel, J., Yu, W. H. and Nixon, R. A. (2008). Autophagy induction and autophagosome clearance in neurons: relationship to autophagic pathology in Alzheimer's disease. *J Neurosci* **28**, 6926–6937.

Bonifacino, J. S. and Glick, B. S. (2004). The Mechanisms of Vesicle Budding and Fusion. *Cell* **116**, 153–166.

Bonifacino, J. S. and Rojas, R. (2006). Retrograde transport from endosomes to the trans-Golgi network. *Nat Rev Mol Cell Biol* **7**, 568–579.

Bordi, M., Berg, M. J., Mohan, P. S., Peterhoff, C. M., Alldred, M. J., Che, S., Ginsberg, S. D. and Nixon, R. A. (2016). Autophagy flux in CA1 neurons of Alzheimer hippocampus: Increased induction overburdens failing lysosomes to propel neuritic dystrophy. *Autophagy* **12**, 2467–2483.

Bourdenx, M., Martín-Segura, A., Scrivo, A., Rodriguez-Navarro, J. A., Kaushik, S., Tasset, I., Diaz, A., Storm, N. J., Xin, Q., Juste, Y. R., et al. (2021). Chaperone-mediated autophagy prevents collapse of the neuronal metastable proteome. *Cell* **184**, 2696-2714.e25.

Braakman, I. and Hebert, D. N. (2013). Protein Folding in the Endoplasmic Reticulum. *Cold Spring Harb Perspect Biol* **5**, a013201–a013201.

Brandenstein, L., Schweizer, M., Sedlacik, J., Fiehler, J. and Storch, S. (2016). Lysosomal dysfunction and impaired autophagy in a novel mouse model deficient for the lysosomal membrane protein Cln7. *Hum Mol Genet* **25**, 777–791.

Bras, J., Djaldetti, R., Alves, A. M., Mead, S., Darwent, L., Lleo, A., Molinuevo, J. L., Blesa, R., Singleton, A., Hardy, J., et al. (2016). Exome sequencing in a consanguineous family clinically diagnosed with early-onset Alzheimer's disease identifies a homozygous CTSF mutation. *Neurobiol Aging* **46**, 236.e1-236.e6.

Braulke, T. and Bonifacino, J. S. (2009a). Sorting of lysosomal proteins. *Biochim Biophys Acta Mol Cell Res* **1793**, 605–614.

Braulke, T. and Bonifacino, J. S. (2009b). Sorting of lysosomal proteins. *Biochim Biophys Acta* **1793**, 605–614.

Breiderhoff, T., Christiansen, G. B., Pallesen, L. T., Vaegter, C., Nykjaer, A., Holm, M. M., Glerup, S. and Willnow, T. E. (2013). Sortilin-Related Receptor SORCS3 Is a Postsynaptic Modulator of Synaptic Depression and Fear Extinction. *PLoS One* **8**, e75006.

Breijyeh, Z. and Karaman, R. (2020). Comprehensive Review on Alzheimer's Disease: Causes and Treatment. *Molecules* **25**, 5789.

Brion, J., Passareiro, H., Nunez, J. and Durand, J. (1985). Mise en évidence immunologique de la protéine tau au niveau des lésions de dégénérescence neurofibrillaire de la maladie d'Alzheimer. *Arch. Biol. (Bruxelles)* **95**, 229–235.

Bunk, J., Prieto Huarcaya, S., Drobny, A., Dobert, J. P., Walther, L., Rose-John, S., Arnold, P. and Zunke, F. (2021). Cathepsin D Variants Associated With Neurodegenerative Diseases Show Dysregulated Functionality and Modified α-Synuclein Degradation Properties. *Front Cell Dev Biol* **9**, 581805.

Burgert, T., Schmidt, V., Caglayan, S., Lin, F., Füchtbauer, A., Füchtbauer, E.-M., Nykjaer, A., Carlo, A.-S. and Willnow, T. E. (2013). SORLA-Dependent and -Independent Functions for PACS1 in Control of Amyloidogenic Processes. *Mol Cell Biol* **33**, 4308–4320.

Burgos, P. v., Mardones, G. A., Rojas, A. L., daSilva, L. L. P., Prabhu, Y., Hurley, J. H. and Bonifacino, J. S. (2010). Sorting of the Alzheimer's Disease Amyloid Precursor Protein Mediated by the AP-4 Complex. *Dev Cell* **18**, 425.

Butz, E. S., Chandrachud, U., Mole, S. E. and Cotman, S. L. (2020). Moving towards a new era of genomics in the neuronal ceroid lipofuscinoses. *Biochimica et Biophysica Acta (BBA) - Molecular Basis of Disease* **1866**, 165571.

Caballero, B., Bourdenx, M., Luengo, E., Diaz, A., Sohn, P. D., Chen, X., Wang, C., Juste, Y. R., Wegmann, S., Patel, B., et al. (2021). Acetylated tau inhibits chaperone-mediated autophagy and promotes tau pathology propagation in mice. *Nature Communications 2021 12:1* **12**, 1–18.

Caccamo, A., Majumder, S., Richardson, A., Strong, R. and Oddo, S. (2010). Molecular interplay between mammalian target of rapamycin (mTOR), amyloid-beta, and Tau: effects on cognitive impairments. *J Biol Chem* **285**, 13107–13120.

Caccamo, A., Magrì, A., Medina, D. X., Wisely, E. v., López-Aranda, M. F., Silva, A. J. and Oddo, S. (2013). mTOR regulates tau phosphorylation and degradation: implications for Alzheimer's disease and other tauopathies. *Aging Cell* **12**, 370–380.

Cadieux-Dion, M., Andermann, E., Lachance-Touchette, P., Ansorge, O., Meloche, C., Barnabé, A., Kuzniecky, R. I., Andermann, F., Faught, E., Leonberg, S., et al. (2013). Recurrent mutations in DNAJC5 cause autosomal dominant Kufs disease. *Clin Genet* **83**, 571–575.

Caglayan, S., Takagi-Niidome, S., Liao, F., Carlo, A.-S., Schmidt, V., Burgert, T., Kitago, Y., Füchtbauer, E.-M., Füchtbauer, A., Holtzman, D. M., et al. (2014). Lysosomal sorting of amyloid-β by the SORLA receptor is impaired by a familial Alzheimer's disease mutation. *Sci Transl Med* **6**, 223ra20.

Camp, L. A. and Hofmann, S. L. (1993). Purification and properties of a palmitoyl-protein thioesterase that cleaves palmitate from H-Ras. *Journal of Biological Chemistry* **268**, 22566–22574.

Campbell, C. H., Fine, R. E., Squicciarini, J. and Rome, L. H. (1983). Coated vesicles from rat liver and calf brain contain cryptic mannose 6-phosphate receptors. *Journal of Biological Chemistry* **258**, 2628–2633.

Cannelli, N., Garavaglia, B., Simonati, A., Aiello, C., Barzaghi, C., Pezzini, F., Cilio, M. R., Biancheri, R., Morbin, M., Bernardina, B. D., et al. (2009). Variant late infantile ceroid lipofuscinoses associated with novel mutations in CLN6. *Biochem Biophys Res Commun* **379**, 892–897.

Canuel, M., Lefrancois, S., Zeng, J. and Morales, C. R. (2008a). AP-1 and retromer play opposite roles in the trafficking of sortilin between the Golgi apparatus and the lysosomes. *Biochem Biophys Res Commun* **366**, 724–730.

Canuel, M., Korkidakis, A., Konnyu, K. and Morales, C. R. (2008b). Sortilin mediates the lysosomal targeting of cathepsins D and H. *Biochem Biophys Res Commun* **373**, 292–297.

Cao, Y., Espinola, J. A., Fossale, E., Massey, A. C., Cuervo, A. M., MacDonald, M. E. and Cotman, S. L. (2006). Autophagy is disrupted in a knock-in mouse model of juvenile neuronal ceroid lipofuscinosis. *Journal of Biological Chemistry* **281**, 20483–20493.

Cao, Y., Staropoli, J. F., Biswas, S., Espinola, J. A., MacDonald, M. E., Lee, J.-M. and Cotman, S. L. (2011). Distinct early molecular responses to mutations causing vLINCL and JNCL presage ATP synthase subunit C accumulation in cerebellar cells. *PLoS One* **6**, e17118.

Caporaso, G. L., Takei, K., Gandy, S. E., Matteoli, M., Mundigi, O., Greengard, P. and de Camilli, P. (1994). Morphologic and biochemical analysis of the intracellular trafficking of the Alzheimer beta/A4 amyloid precursor protein. *Journal of Neuroscience* **14**, 3122–3138.

Carlo, A.-S. (2013). Sortilin, a novel APOE receptor implicated in Alzheimer disease. *Prion* **7**, 378–82.

Castrén, E. and Monteggia, L. M. (2021). Brain-Derived Neurotrophic Factor Signaling in Depression and Antidepressant Action. *Biol Psychiatry* **90**, 128–136.

Cataldo, A. M., Paskevich, P. A., Kominami, E. and Nixon, R. A. (1991). Lysosomal hydrolases of different classes are abnormally distributed in brains of patients with Alzheimer disease. *Proc Natl Acad Sci U S A* **88**, 10998–11002.

Cataldo, A. M., Hamilton, D. J. and Nixon, R. A. (1994). Lysosomal abnormalities in degenerating neurons link neuronal compromise to senile plaque development in Alzheimer disease. *Brain Res* **640**, 68–80.

Cataldo, A. M., Barnett, J. L., Berman, S. A., Li, J., Quarless, S., Bursztajn, S., Lippa, C. and Nixon, R. A. (1995). Gene expression and cellular content of cathepsin D in Alzheimer's disease brain: evidence for early up-regulation of the endosomal-lysosomal system. *Neuron* **14**, 671–680.

Cataldo, A. M., Hamilton, D. J., Barnett, J. L., Paskevich, P. A. and Nixon, R. A. (1996). Properties of the endosomal-lysosomal system in the human central nervous system: disturbances mark most neurons in populations at risk to degenerate in Alzheimer's disease. *J Neurosci* **16**, 186–199.

Cataldo, A. M., Barnett, J. L., Pieroni, C. and Nixon, R. A. (1997). Increased neuronal endocytosis and protease delivery to early endosomes in sporadic Alzheimer's disease: neuropathologic evidence for a mechanism of increased beta-amyloidogenesis. *J Neurosci* **17**, 6142–6151.

Cataldo, A. M., Mathews, P. M., Boiteau, A. B., Hassinger, L. C., Peterhoff, C. M., Jiang, Y., Mullaney, K., Neve, R. L., Gruenberg, J. and Nixon, R. A. (2008). Down syndrome fibroblast model of Alzheimer-related endosome pathology: accelerated endocytosis promotes late endocytic defects. *Am J Pathol* **173**, 370–384.

Chandra, S., Gallardo, G., Fernández-Chacón, R., Schlüter, O. M. and Südhof, T. C. (2005). Alpha-synuclein cooperates with CSPalpha in preventing neurodegeneration. *Cell* **123**, 383–396.

Chandrachud, U., Walker, M. W., Simas, A. M., Heetveld, S., Petcherski, A., Klein, M., Oh, H., Wolf, P., Zhao, W. N., Norton, S., et al. (2015). Unbiased Cell-based Screening in a Neuronal Cell Model of Batten Disease Highlights an Interaction between Ca2+ Homeostasis, Autophagy, and CLN3 Protein Function. *J Biol Chem* **290**, 14361–14380.

Chasseigneaux, S. and Allinquant, B. (2012). Functions of Aβ, sAPPα and sAPPβ : similarities and differences. *J Neurochem* **120 Suppl 1**, 99–108.

Chaves, G., Stanley, J. and Pourmand, N. (2019). Mutant Huntingtin Affects Diabetes and Alzheimer's Markers in Human and Cell Models of Huntington's Disease. *Cells* **8**, 962.

Chavez, R. A., Miller, S. G. and Moore, H. P. H. (1996). A biosynthetic regulated secretory pathway in constitutive secretory cells. *Journal of Cell Biology* **133**, 1177–1191.

Chen, L., Chetkovich, D. M., Petralia, R. S., Sweeney, N. T., Kawasaki, Y., Wenthold, R. J., Bredt, D. S. and Nicoll, R. A. (2000). Stargazin regulates synaptic targeting of AMPA receptors by two distinct mechanisms. *Nature 2000 408:6815* **408**, 936–943.

Chen, Z. Y., Ieraci, A., Teng, H., Dall, H., Meng, C. X., Herrera, D. G., Nykjaer, A., Hempstead, B. L. and Lee, F. S. (2005). Sortilin controls intracellular sorting of brain-derived neurotrophic factor to the regulated secretory pathway. *Journal of Neuroscience* **25**, 6156–6166.

Chen, Y., Li, Q., Li, Q., Xing, S., Liu, Y., Liu, Y., Chen, Y., Liu, W., Feng, F. and Sun, H. (2020a). p62/SQSTM1, a Central but Unexploited Target: Advances in Its Physiological/Pathogenic Functions and Small Molecular Modulators. *J Med Chem* **63**, 10135–10157.

Chen, Q., Zhong, L., Zhou, C., Feng, Y., Liu, Q., Zhou, D., Lu, X., Du, G.-S., Jian, D., Luo, H., et al. (2020b). Knockdown of Parkinson's disease-related gene ATP13A2 reduces tumorigenesis via blocking autophagic flux in colon cancer. *Cell Biosci* **10**, 144.

Cheng, X. T., Zhou, B., Lin, M. Y., Cai, Q. and Sheng, Z. H. (2015). Axonal autophagosomes recruit dynein for retrograde transport through fusion with late endosomes. *J Cell Biol* **209**, 377–386.

Cheng, R., Tang, M., Martinez, I., Ayodele, T., Baez, P., Reyes-Dumeyer, D., Lantigua, R., Medrano, M., Jimenez-Velazquez, I., Lee, J. H., et al. (2018). Linkage analysis of multiplex Caribbean Hispanic families loaded for unexplained early-onset cases identifies novel Alzheimer's disease loci. *Alzheimers Dement (Amst)* **10**, 554–562.

Cho, S. and Dawson, G. (2000). Palmitoyl protein thioesterase 1 protects against apoptosis mediated by Ras-Akt-caspase pathway in neuroblastoma cells. *J Neurochem* **74**, 1478–1488.

Cho, J.-H., Huang, B. S. and Gray, J. M. (2016). RNA sequencing from neural ensembles activated during fear conditioning in the mouse temporal association cortex. *Sci Rep* **6**, 31753.

Christiansen, G. B., Andersen, K. H., Riis, S., Nykjaer, A., Bolcho, U., Jensen, M. S. and Holm, M. M. (2017). The sorting receptor SorCS3 is a stronger regulator of glutamate receptor functions compared to GABAergic mechanisms in the hippocampus. *Hippocampus* **27**, 235–248.

Christoforou, A., McGhee, K. A., Morris, S. W., Thomson, P. A., Anderson, S., McLean, A., Torrance, H. S., le Hellard, S., Pickard, B. S., Stclair, D., et al. (2011). Convergence of linkage, association and GWAS findings for a candidate region for bipolar disorder and schizophrenia on chromosome 4p. *Mol Psychiatry* **16**, 240–242.

Chung, K. M., Hernández, N., Sproul, A. A. and Yu, W. H. (2019). Alzheimer's disease and the autophagic-lysosomal system. *Neurosci Lett* **697**, 49–58.

Clee, S. M., Yandell, B. S., Schueler, K. M., Rabaglia, M. E., Richards, O. C., Raines, S. M., Kabara, E. A., Klass, D. M., Mui, E. T.-K., Stapleton, D. S., et al. (2006). Positional cloning of Sorcs1, a type 2 diabetes quantitative trait locus. *Nat Genet* **38**, 688–693.

Collingridge, G. L., Isaac, J. T. R. and Yu, T. W. (2004). Receptor trafficking and synaptic plasticity. *Nature Reviews Neuroscience 2004 5:12* **5**, 952–962.

Conner, J. M., Lauterborn, J. C., Yan, Q., Gall, C. M. and Varon, S. (1997). Distribution of brain-derived neurotrophic factor (BDNF) protein and mRNA in the normal adult rat CNS: evidence for anterograde axonal transport. *J Neurosci* **17**, 2295–2313.

Connolly, K. J., O'Hare, M. B., Mohammed, A., Aitchison, K. M., Anthoney, N. C., Taylor, M. J., Stewart, B. A., Tuxworth, R. I. and Tear, G. (2019). The neuronal ceroid lipofuscinosis protein Cln7 functions in the postsynaptic cell to regulate synapse development. *Sci Rep* **9**, 15592.

Corder, E. H., Saunders, A. M., Strittmatter, W. J., Schmechel, D. E., Gaskell, P. C., Small, G. W., Roses, A. D., Haines, J. L. and Pericak-Vance, M. A. (1993). Gene dose of apolipoprotein E type 4 allele and the risk of Alzheimer's disease in late onset families. *Science* **261**, 921–923.

Cormont, M., Metón, I., Mari, M., Monzo, P., Keslair, F., Gaskin, C., McGraw, T. E. and le Marchand-Brustel, Y. (2003). CD2AP/CMS regulates endosome morphology and traffic to the degradative pathway through its interaction with Rab4 and c-Cbl. *Traffic* **4**, 97–112.

Cotman, S. L. and Lefrancois, S. (2021). CLN3, at the crossroads of endocytic trafficking. *Neurosci Lett* **762**, 136117.

Cotman, S. L. and Staropoli, J. F. (2012). The juvenile Batten disease protein, CLN3, and its role in regulating anterograde and retrograde post-Golgi trafficking. *Clin Lipidol* **7**, 79–91.

Coulson, E. J. and Andersen, O. M. (2015). The A-B-C for SORting APP. *J Neurochem* **135**, 1–3.

Cramer, J. F., Gustafsen, C., Behrens, M. A., Oliveira, C. L. P., Pedersen, J. S., Madsen, P., Petersen, C. M. and Thirup, S. S. (2010). GGA autoinhibition revisited. *Traffic* **11**, 259–273.

Cremona, O., di Paolo, G., Wenk, M. R., Lüthi, A., Kim, W. T., Takei, K., Daniell, L., Nemoto, Y., Shears, S. B., Flavell, R. A., et al. (1999). Essential role of phosphoinositide metabolism in synaptic vesicle recycling. *Cell* **99**, 179–188.

Criollo, A., Maiuri, M. C., Tasdemir, E., Vitale, I., Fiebig, A. A., Andrews, D., Molgó, J., Díaz, J., Lavandero, S., Harper, F., et al. (2007). Regulation of autophagy by the inositol trisphosphate receptor. *Cell Death Differ* **14**, 1029–1039.

Dale, H. (1935). Pharmacology and Nerve-endings (Walter Ernest Dixon Memorial Lecture): (Section of Therapeutics and Pharmacology). *Proc R Soc Med* **28**, 319.

Danyukova, T., Ariunbat, K., Thelen, M., Brocke-Ahmadinejad, N., Mole, S. E. and Storch, S. (2018). Loss of CLN7 results in depletion of soluble lysosomal proteins and impaired mTOR reactivation. *Hum Mol Genet* **27**, 1711–1722.

de Strooper, B. (2003). Aph-1, Pen-2, and Nicastrin with Presenilin generate an active γ-Secretase complex. *Neuron* **38**, 9–12.

Dehay, B., Martinez-Vicente, M., Ramirez, A., Perier, C., Klein, C., Vila, M. and Bezard, E. (2012a). Lysosomal dysfunction in Parkinson disease: ATP13A2 gets into the groove. *Autophagy* **8**, 1389–1391.

Dehay, B., Ramirez, A., Martinez-Vicente, M., Perier, C., Canron, M. H., Doudnikoff, E., Vital, A., Vila, M., Klein, C. and Bezard, E. (2012b). Loss of P-type ATPase ATP13A2/PARK9 function induces general lysosomal deficiency and leads to Parkinson disease neurodegeneration. *Proc Natl Acad Sci U S A* **109**, 9611–9616.

Deinhardt, K., Kim, T., Spellman, D. S., Mains, R. E., Eipper, B. A., Neubert, T. A., Chao, M. v. and Hempstead, B. L. (2011). Neuronal growth cone retraction relies upon proneurotrophin receptor signaling through Rac. *Sci Signal* **4**, ra82.

Deiters, Otto. (1865). *Untersuchungen über Gehirn und Rückenmark des Menschen und der Säugethiere*. Schulze Max. Braunschweig: Druck und Verlag von Friedrich Vieweg und Sohn.

del Río-Hortega, P. (1919). El tercer elemento de los centros nerviosos. I. La microglia en estado normal II. Intervencion de la microglia en los procesos patologicos. HI. Naturaleza probable de la microglia. *Boll Socieded Esp biol* **9**, 69–120.

del Río-Hortega, P. (1921). La glía de escasas radiaciones (oligodendroglía). *Bol. Real Soc. Esp. Hist. Nat.* **21**, 63–92.

del Río-Hortega, P. (1922). ¿Son homologables la glía de escasas radiaciones y las células de Schwann? *Trab. Lab. Histol. Patol. 1922* **16**, 25–28.

DeTure, M. A. and Dickson, D. W. (2019). The neuropathological diagnosis of Alzheimer's disease. *Mol Neurodegener* **14**, 32.

di Malta, C., Cinque, L. and Settembre, C. (2019). Transcriptional regulation of autophagy: Mechanisms and diseases. *Front Cell Dev Biol* **7**, 114.

di Ronza, A., Bajaj, L., Sharma, J., Sanagasetti, D., Lotfi, P., Adamski, C. J., Collette, J., Palmieri, M., Amawi, A., Popp, L., et al. (2018). CLN8 is an endoplasmic reticulum cargo receptor that regulates lysosome biogenesis. *Nat Cell Biol* **20**, 1370–1377.

Díaz-Alonso, J. and Nicoll, R. A. (2021). AMPA receptor trafficking and LTP: Carboxy-termini, amino-termini and TARPs. *Neuropharmacology* **197**, 108710.

Dieni, S., Matsumoto, T., Dekkers, M., Rauskolb, S., Ionescu, M. S., Deogracias, R., Gundelfinger, E. D., Kojima, M., Nestel, S., Frotscher, M., et al. (2012). BDNF and its pro-peptide are stored in presynaptic dense core vesicles in brain neurons. *J Cell Biol* **196**, 775–788.

Dixit, R., Ross, J. L., Goldman, Y. E. and Holzbaur, E. L. F. (2008). Differential Regulation of Dynein and Kinesin Motor Proteins by Tau. *Science (1979)* **319**, 1086–1089.

Dixon, R. M., Mellor, J. R. and Hanley, J. G. (2009). PICK1-mediated glutamate receptor subunit 2 (GluR2) trafficking contributes to cell death in oxygen/glucose-deprived hippocampal neurons. *J Biol Chem* **284**, 14230–14235.

Dodson, S. E., Andersen, O. M., Karmali, V., Fritz, J. J., Cheng, D., Peng, J., Levey, A. I., Willnow, T. E. and Lah, J. J. (2008). Loss of LR11/SORLA enhances early pathology in a mouse model of amyloidosis: Evidence for a proximal role in Alzheimer's disease. *Journal of Neuroscience* **28**, 12877–12886.

Dolzhanskaya, N., Gonzalez, M. A., Sperziani, F., Stefl, S., Messing, J., Wen, G. Y., Alexov, E., Zuchner, S. and Velinov, M. (2014). A novel p.Leu(381)Phe mutation in Presenilin 1 is associated with very early onset and unusually fast progressing dementia, and lysosomal inclusions typically seen in Kufs disease. *J Alzheimers Dis* **39**, 23.

Domowicz, M. S., Chan, W.-C., Claudio-Vázquez, P., Henry, J. G., Ware, C. B., Andrade, J., Dawson, G. and Schwartz, N. B. (2019). Global Brain Transcriptome Analysis of a Tpp1 Neuronal Ceroid Lipofuscinoses Mouse Model. *ASN Neuro* **11**, 1759091419843393.

Dong, H., O'Brien, R. J., Fung, E. T., Lanahan, A. A., Worley, P. F. and Huganir, R. L. (1997). GRIP: a synaptic PDZ domain-containing protein that interacts with AMPA receptors. *Nature* **386**, 279–284.

Du, Y., Wooten, M. C., Gearing, M. and Wooten, M. W. (2009). Age-associated oxidative damage to the p62 promoter: implications for Alzheimer disease. *Free Radic Biol Med* **46**, 492–501.

Dumanis, S. B., Burgert, T., Caglayan, S., Füchtbauer, A., Füchtbauer, E. M., Schmidt, V. and Willnow, T. E. (2015). Distinct Functions for Anterograde and Retrograde Sorting of SORLA in Amyloidogenic Processes in the Brain. *J Neurosci* **35**, 12703–12713.

Eccles, J. (1976). From electrical to chemical transmission in the central nervous system. *Notes Rec R Soc Lond* **30**, 219–230.

Edvardson, S., Cinnamon, Y., Ta-Shma, A., Shaag, A., Yim, Y.-I., Zenvirt, S., Jalas, C., Lesage, S., Brice, A., Taraboulos, A., et al. (2012). A Deleterious Mutation in DNAJC6 Encoding the Neuronal-Specific Clathrin-Uncoating Co-Chaperone Auxilin, Is Associated with Juvenile Parkinsonism. *PLoS One* **7**, e36458.

Eggert, S., Gonzalez, A. C., Thomas, C., Schilling, S., Schwarz, S. M., Tischer, C., Adam, V., Strecker, P., Schmidt, V., Willnow, T. E., et al. (2018). Dimerization leads to changes in APP (amyloid precursor protein) trafficking mediated by LRP1 and SorLA. *Cellular and Molecular Life Sciences* **75**, 301–322.

Ehling, R., Nosková, L., Stránecký, V., Hartmannová, H., Přistoupilová, A., Hodaňová, K., Benke, T., Kovacs, G. G., Ströbel, T., Niedermüller, U., et al. (2013). Cerebellar dysfunction in a family harboring the PSEN1 mutation co-segregating with a cathepsin D variant p.A58V. *J Neurol Sci* **326**, 75–82.

Elia, L. P., Mason, A. R., Alijagic, A. and Finkbeiner, S. (2019). Genetic Regulation of Neuronal Progranulin Reveals a Critical Role for the Autophagy-Lysosome Pathway. *J Neurosci* **39**, 3332–3344.

Fedeli, C., Filadi, R., Rossi, A., Mammucari, C. and Pizzo, P. (2019). PSEN2 (presenilin 2) mutants linked to familial Alzheimer disease impair autophagy by altering Ca2+ homeostasis. *Autophagy* **15**, 2044.

Fenoglio, C., Galimberti, D., Cortini, F., Kauwe, J. S. K., Cruchaga, C., Venturelli, E., Villa, C., Serpente, M., Scalabrini, D., Mayo, K., et al. (2009). Rs5848 variant influences GRN mRNA levels in brain and peripheral mononuclear cells in patients with Alzheimer's disease. *J Alzheimers Dis* **18**, 603–612.

Fjorback, A. W., Seaman, M., Gustafsen, C., Mehmedbasic, A., Gokool, S., Wu, C., Militz, D., Schmidt, V., Madsen, P., Nyengaard, J. R., et al. (2012). Retromer binds the FANSHY sorting motif in sorLA to regulate amyloid precursor protein sorting and processing. *Journal of Neuroscience* **32**, 1467–1480.

Fleischer, B. (1983). Mechanism of glycosylation in the Golgi apparatus. *Journal of Histochemistry & Cytochemistry* **31**, 1033–1040.

Fleming, A., Bourdenx, M., Fujimaki, M., Karabiyik, C., Krause, G. J., Lopez, A., Martín-Segura, A., Puri, C., Scrivo, A., Skidmore, J., et al. (2022). The different autophagy degradation pathways and neurodegeneration. *Neuron* **110**, 935–966.

Fontaine, S. N., Zheng, D., Sabbagh, J. J., Martin, M. D., Chaput, D., Darling, A., Trotter, J. H., Stothert, A. R., Nordhues, B. A., Lussier, A., et al. (2016). DnaJ/Hsc70 chaperone complexes control the extracellular release of neurodegenerative-associated proteins. *EMBO J* **35**, 1537–1549.

Fossale, E., Wolf, P., Espinola, J. A., Lubicz-Nawrocka, T., Teed, A. M., Gao, H., Rigamonti, D., Cattaneo, E., MacDonald, M. E. and Cotman, S. L. (2004). Membrane trafficking and mitochondrial abnormalities precede subunit c deposition in a cerebellar cell model of juvenile neuronal ceroid lipofuscinosis. *BMC Neurosci* **5**, 57.

Fouad, S., Wells, O. S., Hill, M. A. and D'Angiolella, V. (2019). Cullin Ring Ubiquitin Ligases (CRLs) in Cancer: Responses to Ionizing Radiation (IR) Treatment. *Front Physiol* **10**, 1144.

Fujita, H., Saeki, M., Yasunaga, K., Ueda, T., Imoto, T. and Himeno, M. (1999). In VitroBinding Study of Adaptor Protein Complex (AP-1) to Lysosomal Targeting Motif (LI-Motif). *Biochem Biophys Res Commun* **255**, 54–58.

Fujiwara, H., Hasegawa, M., Dohmae, N., Kawashima, A., Masliah, E., Goldberg, M. S., Shen, J., Takio, K. and Iwatsubo, T. (2002). alpha-Synuclein is phosphorylated in synucleinopathy lesions. *Nat Cell Biol* **4**, 160–164.

Fukata, Y., Tzingounis, A. v, Trinidad, J. C., Fukata, M., Burlingame, A. L., Nicoll, R. A. and Bredt, D. S. (2005). Molecular constituents of neuronal AMPA receptors. *J Cell Biol* **169**, 399–404.

Funderburk, S. F., Marcellino, B. K. and Yue, Z. (2010). Cell "Self-Eating" (Autophagy) Mechanism in Alzheimer's Disease. *Mount Sinai Journal of Medicine: A Journal of Translational and Personalized Medicine* **77**, 59–68.

Furusawa, K., Takasugi, T., Chiu, Y. W., Hori, Y., Tomita, T., Fukuda, M. and Hisanaga, S. ichi (2019). CD2-associated protein (CD2AP) overexpression accelerates amyloid precursor protein (APP) transfer from early endosomes to the lysosomal degradation pathway. *J Biol Chem* **294**, 10886–10899.

Gandy, S. (2005). The role of cerebral amyloid beta accumulation in common forms of Alzheimer disease. *J Clin Invest* **115**, 1121–1129.

Geier, E. G., Bourdenx, M., Storm, N. J., Cochran, J. N., Sirkis, D. W., Hwang, J. H., Bonham, L. W., Ramos, E. M., Diaz, A., van Berlo, V., et al. (2019). Rare variants in the neuronal ceroid lipofuscinosis gene MFSD8 are candidate risk factors for frontotemporal dementia. *Acta Neuropathol* **137**, 71–88.

Geisler, C., Dietrich, J., Nielsen, B. L., Kastrup, J., Lauritsen, J. P. H., Ødum, N. and Christensen, M. D. (1998). Leucine-based receptor sorting motifs are dependent on the spacing relative to the plasma membrane. *J Biol Chem* **273**, 21316–21323.

Gent, J. and Braakman, I. (2004). Low-density lipoprotein receptor structure and folding. *Cellular and Molecular Life Sciences* **61**, 2461–2470.

Ginsberg, S. D., Alldred, M. J., Counts, S. E., Cataldo, A. M., Neve, R. L., Jiang, Y., Wuu, J., Chao, M. v., Mufson, E. J., Nixon, R. A., et al. (2010). Microarray analysis of hippocampal CA1 neurons implicates early endosomal dysfunction during Alzheimer's disease progression. *Biol Psychiatry* **68**, 885–893.

Glatigny, M., Moriceau, S., Rivagorda, M., Ramos-Brossier, M., Nascimbeni, A. C., Lante, F., Shanley, M. R., Boudarene, N., Rousseaud, A., Friedman, A. K., et al. (2019). Autophagy Is Required for Memory Formation and Reverses Age-Related Memory Decline. *Current Biology* **29**, 435-448.e8.

Glenner, G. G. and Wong, C. W. (1984). Alzheimer's disease: initial report of the purification and characterization of a novel cerebrovascular amyloid protein. *Biochem Biophys Res Commun* **120**, 885–890.

Glerup, S., Olsen, D., Vaegter, C. B., Gustafsen, C., Sjoegaard, S. S., Hermey, G., Kjolby, M., Molgaard, S., Ulrichsen, M., Boggild, S., et al. (2014). SorCS2 regulates dopaminergic wiring and is processed into an apoptotic two-chain receptor in peripheral glia. *Neuron* **82**, 1074–1087.

Glerup, S., Bolcho, U., Mlgaard, S., Bggild, S., Vaegter, C. B., Smith, A. H., Nieto-Gonzalez, J. L., Ovesen, P. L., Pedersen, L. F., Fjorback, A. N., et al. (2016). SorCS2 is required for BDNF-dependent plasticity in the hippocampus. *Mol Psychiatry* **21**, 1740–1751.

Goate, A., Chartier-Harlin, M. C., Mullan, M., Brown, J., Crawford, F., Fidani, L., Giuffra, L., Haynes, A., Irving, N., James, L., et al. (1991). Segregation of a missense mutation in the amyloid precursor protein gene with familial Alzheimer's disease. *Nature* **349**, 704–706.

Goodarzi, M. O., Lehman, D. M., Taylor, K. D., Guo, X., Cui, J., Quiñones, M. J., Clee, S. M., Yandell, B. S., Blangero, J., Hsueh, W. A., et al. (2007). SORCS1: A Novel Human Type 2 Diabetes Susceptibility Gene Suggested by the Mouse. *Diabetes* **56**, 1922–1929.

Gowrishankar, S., Yuan, P., Wu, Y., Schrag, M., Paradise, S., Grutzendler, J., de Camilli, P. and Ferguson, S. M. (2015). Massive accumulation of luminal protease-deficient axonal lysosomes at Alzheimer's disease amyloid plaques. *Proc Natl Acad Sci U S A* **112**, E3699–E3708.

Grbovic, O. M., Mathews, P. M., Jiang, Y., Schmidt, S. D., Dinakar, R., Summers-Terio, N. B., Ceresa, B. P., Nixon, R. A. and Cataldo, A. M. (2003). Rab5-stimulated up-regulation of the endocytic pathway increases intracellular beta-cleaved amyloid precursor protein carboxyl-terminal fragment levels and Abeta production. *J Biol Chem* **278**, 31261–31268.

Griffin, J. W. and Watson, D. F. (1988). Axonal transport in neurological disease. *Ann Neurol* **23**, 3–13.

Grundke-Iqbal, I., Iqbal, K., Tung, Y. C., Quinlan, M., Wisniewski, H. M. and Binder, L. I. (1986a). Abnormal phosphorylation of the microtubule-associated protein tau (tau) in Alzheimer cytoskeletal pathology. *Proc Natl Acad Sci U S A* **83**, 4913.

Grundke-Iqbal, I., Iqbal, K., Quinlan, M., Tung, Y.-C., Zaidi, M. S. and Wisniewski, H. M. (1986b). Microtubule-associated protein tau. A component of Alzheimer paired helical filaments. *OF BIOLOGICAL CHEMISTRY* **261**, 6084–6089.

Gusdon, A. M., Zhu, J., van Houten, B. and Chu, C. T. (2012). ATP13A2 regulates mitochondrial bioenergetics through macroautophagy. *Neurobiol Dis* **45**, 962–972.

Gustafsen, C., Glerup, S., Pallesen, L. T., Olsen, D., Andersen, O. M., Nykjær, A., Madsen, P. and Petersen, C. M. (2013). Sortilin and SorLA display distinct roles in processing and trafficking of amyloid precursor protein. *Journal of Neuroscience* **33**, 64–71.

Habib, E., Cook, A., Mathavarajah, S. and Dellaire, G. (2021). Adding Some "Splice" to Stress Eating: Autophagy, ESCRT and Alternative Splicing Orchestrate the Cellular Stress Response. *Genes (Basel)* **12**, 1196.

Hah, Y. S., Noh, H. S., Ha, J. H., Ahn, J. S., Hahm, J. R., Cho, H. Y. and Kim, D. R. (2012). Cathepsin D inhibits oxidative stress-induced cell death via activation of autophagy in cancer cells. *Cancer Lett* **323**, 208–214.

Hamano, T., Gendron, T. F., Causevic, E., Yen, S. H., Lin, W. L., Isidoro, C., Deture, M. and Ko, L. W. (2008). Autophagic-lysosomal perturbation enhances tau aggregation in transfectants with induced wild-type tau expression. *Eur J Neurosci* **27**, 1119–1130.

Hanani, M. and Verkhratsky, A. (2021). Satellite Glial Cells and Astrocytes, a Comparative Review. *Neurochem Res* **46**, 2525–2537.

Hanley, J. G. (2008). PICK1: a multi-talented modulator of AMPA receptor trafficking. *Pharmacol Ther* **118**, 152–160.

Hanley, J. G. and Henley, J. M. (2005). PICK1 is a calcium-sensor for NMDA-induced AMPA receptor trafficking. *EMBO J* **24**, 3266–3278.

Haung Yu, W., Cuervo, A. M., Kumar, A., Peterhoff, C. M., Schmidt, S. D., Lee, J. H., Mohan, P. S., Mercken, M., Farmery, M. R., Tjernberg, L. O., et al. (2005). Macroautophagy--a novel Beta-amyloid peptide-generating pathway activated in Alzheimer's disease. *J Cell Biol* **171**, 87–98.

Heckmann, B. L. and Green, D. R. (2019). LC3-associated phagocytosis at a glance. *J Cell Sci* **132**, jcs222984.

Hempstead, B. L., Martin-Zanca, D., Kaplan, D. R., Parada, L. F. and Chao, M. v. (1991). High-affinity NGF binding requires coexpression of the trk proto-oncogene and the low-affinity NGF receptor. *Nature* **350**, 678–683.

Henry, A. G., Aghamohammadzadeh, S., Samaroo, H., Chen, Y., Mou, K., Needle, E. and Hirst, W. D. (2015). Pathogenic LRRK2 mutations, through increased kinase activity, produce enlarged lysosomes with reduced degradative capacity and increase ATP13A2 expression. *Hum Mol Genet* **24**, 6013–6028.

Hermans-Borgmeyer, I., Hampe, W., Schinke, B., Methner, A., Nykjaer, A., Süsens, U., Fenger, U., Herbarth, B. and Chica Schaller, H. (1998). Unique expression pattern of a novel mosaic receptor in the developing cerebral cortex. *Mech Dev* **70**, 65–76.

Hermans-Borgmeyer, I., Hermey, G., Nykjaer, A. and Schaller, C. (1999). Expression of the 100-kDa neurotensin receptor sortilin during mouse embryonal development. *Molecular Brain Research* **65**, 216–219.

Hermey, G. (2009). The Vps10p-domain receptor family. *Cellular and Molecular Life Sciences* **66**, 2677–2689.

Hermey, G., Riedel, I. B., Hampe, W., Schaller, H. C. and Hermans-Borgmeyer, I. (1999). Identification and characterization of SorCS, a third member of a novel receptor family. *Biochem Biophys Res Commun* **266**, 347–351.

Hermey, G., Schaller, H. C. and Hermans-Borgmeyer, I. (2001a). Transient expression of SorCS in developing telencephalic and mesencephalic structures of the mouse. *Neuroreport* **12**, 29–32.

Hermey, G., Riedel, I. B., Rezgaoui, M., Westergaard, U. B., Schaller, C. and Hermans-Borgmeyer, I. (2001b). SorCS1, a member of the novel sorting receptor family, is localized in somata and dendrites of neurons throughout the murine brain. *Neurosci Lett* **313**, 83–87.

Hermey, G., Keat, S. J., Madsen, P., Jacobsen, C., Petersen, C. M. and Gliemann, J. (2003). Characterization of sorCS1, an Alternatively Spliced Receptor with Completely Different Cytoplasmic Domains That Mediate Different Trafficking in Cells. *Journal of Biological Chemistry* **278**, 7390–7396.

Hermey, G., Plath, N., Hübner, C. A., Kuhl, D., Schaller, H. C. and Hermans-Borgmeyer, I. (2004). The three sorCS genes are differentially expressed and regulated by synaptic activity. *J Neurochem* **88**, 1470–6.

Hermey, G., Sjøgaard, S. S., Petersen, C. M., Nykjaer, A. and Gliemann, J. (2006). Tumour necrosis factor α-converting enzyme mediates ectodomain shedding of Vps10p-domain receptor family members. *Biochem. J* **395**, 285–293.

Hermey, G., Schmidt, N., Bluhm, B., Mensching, D., Ostermann, K., Rupp, C., Kuhl, D. and Kins, S. (2015). SorCS1 variants and amyloid precursor protein (APP) are co-transported in neurons but only SorCS1c modulates anterograde APP transport. *J Neurochem* **135**, 60–75.

Hermey, G., Hoffmeister-Ullerich, S. A., Merz, B., Groß, D., Kuhl, D. and Kins, S. (2019). Amyloidosis causes downregulation of SorLA, SorCS1 and SorCS3 expression in mice. *Biol. Chem* **400**, 1181–1189.

Hernandez, D., Torres, C. A., Setlik, W., Cebrián, C., Mosharov, E. v., Tang, G., Cheng, H. C., Kholodilov, N., Yarygina, O., Burke, R. E., et al. (2012). Regulation of presynaptic neurotransmission by macroautophagy. *Neuron* **74**, 277–284.

Herrup, K. and Yang, Y. (2007). Cell cycle regulation in the postmitotic neuron: oxymoron or new biology? *Nature Reviews Neuroscience 2007 8:5* **8**, 368–378.

Herva, R., Tyynelä, J., Hirvasniemi, A., Syrjäkallio-Ylitalo, M. and Haltia, M. (2000). Northern epilepsy: a novel form of neuronal ceroid-lipofuscinosis. *Brain Pathol* **10**, 215–222.

Hofer, M., Pagliusi, S. R., Hohn, A., Leibrock, J. and Barde, Y. A. (1990). Regional distribution of brain-derived neurotrophic factor mRNA in the adult mouse brain. *EMBO J* **9**, 2459.

Holler, C. J., Davis, P. R., Beckett, T. L., Platt, T. L., Webb, R. L., Head, E. and Murphy, M. P. (2014). Bridging integrator 1 (BIN1) protein expression increases in the Alzheimer's disease brain and correlates with neurofibrillary tangle pathology. *J Alzheimers Dis* **42**, 1221–1227.

Honing, S. (1998). A di-leucine-based motif in the cytoplasmic tail of LIMP-II and tyrosinase mediates selective binding of AP-3. *EMBO J* **17**, 1304–1314.

Hu, F., Padukkavidana, T., Vægter, C. B., Brady, O. A., Zheng, Y., Mackenzie, I. R., Feldman, H. H., Nykjaer, A. and Strittmatter, S. M. (2010). Sortilin-mediated endocytosis determines levels of the frontotemporal dementia protein, progranulin. *Neuron* **68**, 654–667.

Hu, Y. B., Dammer, E. B., Ren, R. J. and Wang, G. (2015). The endosomal-lysosomal system: from acidification and cargo sorting to neurodegeneration. *Transl Neurodegener* **4**,.

Huang, T. Y., Zhao, Y., Li, X., Wang, X., Tseng, I.-C., Thompson, R., Tu, S., Willnow, T. E., Zhang, Y. and Xu, H. (2016). SNX27 and SORLA Interact to Reduce Amyloidogenic Subcellular Distribution and Processing of Amyloid Precursor Protein. *The Journal of Neuroscience* **36**, 7996–8011.

Huang, M., Modeste, E., Dammer, E., Merino, P., Taylor, G., Duong, D. M., Deng, Q., Holler, C. J., Gearing, M., Dickson, D., et al. (2020). Network analysis of the progranulin-deficient mouse brain proteome reveals pathogenic mechanisms shared in human frontotemporal dementia caused by GRN mutations. *Acta Neuropathol Commun* **8**, 163.

Hung, C. O. Y. and Livesey, F. J. (2018). Altered γ-Secretase Processing of APP Disrupts Lysosome and Autophagosome Function in Monogenic Alzheimer's Disease. *Cell Rep* **25**, 3647-3660.e2.

Hung, S. Y., Huang, W. P., Liou, H. C. and Fu, W. M. (2009). Autophagy protects neuron from Abeta-induced cytotoxicity. *Autophagy* **5**, 502–510.

Hung, C., Tuck, E., Stubbs, V., van der Lee, S. J., Aalfs, C., van Spaendonk, R., Scheltens, P., Hardy, J., Holstege, H. and Livesey, F. J. (2021). SORL1 deficiency in human excitatory neurons causes APP-dependent defects in the endolysosome-autophagy network. *Cell Rep* **35**, 109259.

Inoue, K., Rispoli, J., Kaphzan, H., Klann, E., Chen, E. I., Kim, J., Komatsu, M. and Abeliovich, A. (2012). Macroautophagy deficiency mediates age-dependent neurodegeneration through a phospho-tau pathway. *Mol Neurodegener* **7**, 48.

Jacobsen, K. T. and Iverfeldt, K. (2011). O-GlcNAcylation increases non-amyloidogenic processing of the amyloid-β precursor protein (APP). *Biochem Biophys Res Commun* **404**, 882–886.

Jacobsen, L., Madsen, P., Moestrup, S. K., Lund, A. H., Tommerup, N., Nykjær, A., Sottrup-Jensen, L., Gliemann, J. and Petersen, C. M. (1996). Molecular characterization of a novel human hybrid-type receptor that binds the alpha2-macroglobulin receptor-associated protein. *J Biol Chem* **271**, 31379–31383.

Jacobsen, L., Madsen, P., Jacobsen, C., Nielsen, M. S., Gliemann, J. and Petersen, C. M. (2001). Activation and functional characterization of the mosaic receptor SorLA/LR11. *J Biol Chem* **276**, 22788–22796.

Jacobsen, L., Madsen, P., Nielsen, M. S., Geraerts, W. P. M., Gliemann, J., Smit, A. B. and Petersen, C. M. (2002). The sorLA cytoplasmic domain interacts with GGA1 and -2 and defines minimum requirements for GGA binding. *FEBS Lett* **511**, 155–158.

Jansen, P., Giehl, K., Nyengaard, J. R., Teng, K., Lioubinski, O., Sjoegaard, S. S., Breiderhoff, T., Gotthardt, M., Lin, F., Eilers, A., et al. (2007). Roles for the pro-neurotrophin receptor sortilin in neuronal development, aging and brain injury. *Nat Neurosci* **10**, 1449–1457.

Januliene, D., Andersen, J. L., Nielsen, J. A., Quistgaard, E. M., Hansen, M., Strandbygaard, D., Moeller, A., Petersen, C. M., Madsen, P. and Thirup, S. S. (2017a). Acidic Environment Induces Dimerization and Ligand Binding Site Collapse in the Vps10p Domain of Sortilin. *Structure* **25**, 1809-1819.e3.

Januliene, D., Manavalan, A., Ovesen, P. L., Pedersen, K. M., Thirup, S., Nykjær, A. and Moeller, A. (2017b). Hidden Twins: SorCS Neuroreceptors Form Stable Dimers. *J Mol Biol* **429**, 2907–2917.

Jaulin-Bastard, F., Saito, H., le Bivic, A., Ollendorff, V., Marchetto, S., Birnbaum, D. and Borg, J. P. (2001). The ERBB2/HER2 receptor differentially interacts with ERBIN and PICK1 PSD-95/DLG/ZO-1 domain proteins. *J Biol Chem* **276**, 15256–15263.

Jerič, B., Dolenc, I., Mihelič, M., Klarić, M., Zavašnik-Bergant, T., Gunčar, G., Turk, B., Turk, V. and Stoka, V. (2013). N-terminally truncated forms of human cathepsin F accumulate in aggresome-like inclusions. *Biochimica et Biophysica Acta (BBA) - Molecular Cell Research* **1833**, 2254–2266.

Jiang, Y., Mullaney, K. A., Peterhoff, C. M., Che, S., Schmidt, S. D., Boyer-Boiteau, A., Ginsberg, S. D., Cataldo, A. M., Mathews, P. M. and Nixon, R. A. (2010). Alzheimer's-related endosome dysfunction in Down syndrome is Abeta-independent but requires APP and is reversed by BACE-1 inhibition. *Proc Natl Acad Sci U S A* **107**, 1630–1635.

Jin, W., Ge, W. P., Xu, J., Cao, M., Peng, L., Yung, W., Liao, D., Duan, S., Zhang, M. and Xia, J. (2006). Lipid binding regulates synaptic targeting of PICK1, AMPA receptor trafficking, and synaptic plasticity. *J Neurosci* **26**, 2380–2390.

Joch, M., Ase, A. R., Chen, C. X. Q., MacDonald, P. A., Kontogiannea, M., Corera, A. T., Brice, A., Séguéla, P. and Fon, E. A. (2007). Parkin-mediated Monoubiquitination of the PDZ Protein PICK1 Regulates the Activity of Acid-sensing Ion Channels. *Mol Biol Cell* **18**, 3105.

Jourdi, H., Iwakura, Y., Narisawa-Saito, M., Ibaraki, K., Xiong, H., Watanabe, M., Hayashi, Y., Takei, N. and Nawa, H. (2003). Brain-derived neurotrophic factor signal enhances and maintains the expression of AMPA receptor-associated PDZ proteins in developing cortical neurons. *Dev Biol* **263**, 216.

Jules, F., Sauvageau, E., Dumaresq-Doiron, K., Mazzaferri, J., Haug-Kröper, M., Fluhrer, R., Costantino, S. and Lefrancois, S. (2017). CLN5 is cleaved by members of the SPP/SPPL family to produce a mature soluble protein. *Exp Cell Res* **357**, 40–50.

Jumper, J., Evans, R., Pritzel, A., Green, T., Figurnov, M., Ronneberger, O., Tunyasuvunakool, K., Bates, R., Žídek, A., Potapenko, A., et al. (2021). Highly accurate protein structure prediction with AlphaFold. *Nature 2021 596:7873* **596**, 583–589.

Junaid, M. A., Wu, G. and Pullarkat, R. K. (2000). Purification and characterization of bovine brain lysosomal pepstatin-insensitive proteinase, the gene product deficient in the human late-infantile neuronal ceroid lipofuscinosis. *J Neurochem* **74**, 287–294.

Kaether, C., Scheuermann, J., Fassler, M., Zilow, S., Shirotani, K., Valkova, C., Novak, B., Kacmar, S., Steiner, H. and Haass, C. (2007). Endoplasmic reticulum retention of the γ-secretase complex component Pen2 by Rer1. *EMBO Rep* **8**, 743–748.

Kaleem, A. (2017). *Functional characterization of Ceroid Lipofuscinosis Neuronal 3 (CLN3) interactions*. Doctoral Thesis. Hamburg, Germany: University of Hamburg.

Kalyoncu, S., Keskin, O. and Gursoy, A. (2010). Interaction prediction and classification of PDZ domains. *BMC Bioinformatics* **11**, 357.

Kametani, F. and Hasegawa, M. (2018). Reconsideration of Amyloid Hypothesis and Tau Hypothesis in Alzheimer's Disease. *Front Neurosci* **12**, 25.

Kathiresan, S., Manning, A. K., Demissie, S., D'Agostino, R. B., Surti, A., Guiducci, C., Gianniny, L., Burtt, N. P., Melander, O., Orho-Melander, M., et al. (2007). A genome-wide association study for blood lipid phenotypes in the Framingham Heart Study. *BMC Med Genet* **8**, 1–10.

Kaushik, S. and Cuervo, A. M. (2018). The coming of age of chaperone-mediated autophagy. *Nature Reviews Molecular Cell Biology 2018 19:6* **19**, 365–381.

Kett, L. R., Stiller, B., Bernath, M. M., Tasset, I., Blesa, J., Jackson-Lewis, V., Chan, R. B., Zhou, B., di Paolo, G., Przedborski, S., et al. (2015). α-Synuclein-independent histopathological and motor deficits in mice lacking the endolysosomal Parkinsonism protein Atp13a2. *J Neurosci* **35**, 5724–5742.

Kettenmann, H., Hanisch, U.-K., Noda, M. and Verkhratsky, A. (2011). Physiology of Microglia. *Physiol Rev* **91**, 461–553.

Khalin, I., Alyautdin, R., Kocherga, G. and Bakar, M. A. (2015). Targeted delivery of brain-derived neurotrophic factor for the treatment of blindness and deafness. *Int J Nanomedicine* **10**, 3245–3267.

Kim, J. H. (2019). Genetics of Alzheimer's Disease. *Dement Neurocogn Disord* **17**, 131–136.

Kim, C. H., Hee Jung Chung, Lee, H. K. and Huganir, R. L. (2001). Interaction of the AMPA receptor subunit GluR2/3 with PDZ domains regulates hippocampal long-term depression. *Proc Natl Acad Sci U S A* **98**, 11725–11730.

Kim, S. J., Zhang, Z., Sarkar, C., Tsai, P. C., Lee, Y. C., Dye, L. and Mukherjee, A. B. (2008). Palmitoyl protein thioesterase-1 deficiency impairs synaptic vesicle recycling at nerve terminals, contributing to neuropathology in humans and mice. *J Clin Invest* **118**, 3075–3086.

Kim, E., Lee, Y., Lee, H. J., Kim, J. S., Song, B. S., Huh, J. W., Lee, S. R., Kim, S. U., Kim, S. H., Hong, Y., et al. (2010). Implication of mouse Vps26b-Vps29-Vps35 retromer complex in sortilin trafficking. *Biochem Biophys Res Commun* **403**, 167–171.

Kim, J., Kundu, M., Viollet, B. and Guan, K. L. (2011). AMPK and mTOR regulate autophagy through direct phosphorylation of Ulk1. *Nat Cell Biol* **13**, 132–141.

Kim, W. D., Wilson-Smillie, M. L. D. M., Thanabalasingam, A., Lefrancois, S., Cotman, S. L. and Huber, R. J. (2022). Autophagy in the Neuronal Ceroid Lipofuscinoses (Batten Disease). *Front Cell Dev Biol* **10**, 812728.

Kitago, Y., Nagae, M., Nakata, Z., Yagi-Utsumi, M., Takagi-Niidome, S., Mihara, E., Nogi, T., Kato, K. and Takagi, J. (2015). Structural basis for amyloidogenic peptide recognition by sorLA. *Nat Struct Mol Biol* **22**, 199–206.

Klein, M. (2019). *SorCS3 interactions and their implications for subcellular targeting*. Master Thesis. Bremen, Germany: University of Bremen.

Klein, M., Kaleem, A., Oetjen, S., Wünkhaus, D., Binkle, L., Schilling, S., Gjorgjieva, M., Scholz, R., Gruber-Schoffnegger, D., Storch, S., et al. (2022). Converging roles of PSENEN/PEN2 and CLN3 in the autophagy-lysosome system. *Autophagy* **18**, 2068–2085.

Klinger, S. C., Højland, A., Jain, S., Kjolby, M., Madsen, P., Svendsen, A. D., Olivecrona, G., Bonifacino, J. S. and Nielsen, M. S. (2016). Polarized trafficking of the sorting receptor SorLA in neurons and MDCK cells. *FEBS Journal* **283**, 2476–2493.

Klumperman, J., Kuliawat, R., Griffith, J. M., Geuze, H. J. and Arvan, P. (1998). Mannose 6–Phosphate Receptors Are Sorted from Immature Secretory Granules via Adaptor Protein AP-1, Clathrin, and Syntaxin 6–positive Vesicles. *J Cell Biol* **141**, 359.

Knight, E. M., Ruiz, H. H., Kim, S. H., Harte, J. C., Hsieh, W., Glabe, C., Klein, W. L., Attie, A. D., Buettner, C., Ehrlich, M. E., et al. (2016). Unexpected partial correction of metabolic and behavioral phenotypes of Alzheimer's APP/PSEN1 mice by gene targeting of diabetes/Alzheimer's-related Sorcs1. *Acta Neuropathol Commun* **4**, 16.

Knupp, A., Mishra, S., Martinez, R., Braggin, J. E., Szabo, M., Kinoshita, C., Hailey, D. W., Small, S. A., Jayadev, S. and Young, J. E. (2020). Depletion of the AD Risk Gene SORL1 Selectively Impairs Neuronal Endosomal Traffic Independent of Amyloidogenic APP Processing. *Cell Rep* **31**, 107719.

Koo, E. H., Squazzo, S. L., Selkoe, D. J. and Koo, C. H. (1996). Trafficking of cell-surface amyloid β-protein precursor I. Secretion, endocytosis and recycling as detected by labeled monoclonal antibody. *J Cell Sci* **109**, 991–998.

Kousi, M., Anttila, V., Schulz, A., Calafato, S., Jakkula, E., Riesch, E., Myllykangas, L., Kalimo, H., Topçu, M., Gökben, S., et al. (2012). Novel mutations consolidate KCTD7 as a progressive myoclonus epilepsy gene. *J Med Genet* **49**, 391–399.

Kowiański, P., Lietzau, G., Czuba, E., Waśkow, M., Steliga, A. and Moryś, J. (2018). BDNF: A Key Factor with Multipotent Impact on Brain Signaling and Synaptic Plasticity. *Cell Mol Neurobiol* **38**, 579–593.

Krabichler, B., Rostasy, K., Baumann, M., Karall, D., Scholl-Bürgi, S., Schwarzer, C., Gautsch, K., Spreiz, A., Kotzot, D., Zschocke, J., et al. (2012). Novel mutation in potassium channel related gene KCTD7 and progressive myoclonic epilepsy. *Ann Hum Genet* **76**, 326–331.

Krebs, C. E., Karkheiran, S., Powell, J. C., Cao, M., Makarov, V., Darvish, H., di Paolo, G., Walker, R. H., Shahidi, G. A., Buxbaum, J. D., et al. (2013). The Sac1 domain of SYNJ1 identified mutated in a family with early-onset progressive Parkinsonism with generalized seizures. *Hum Mutat* **34**, 1200–1207.

Kucera, A., Bakke, O. and Progida, C. (2016). The multiple roles of Rab9 in the endolysosomal system. *Commun Integr Biol* **9**, e1204498.

Kwart, D., Gregg, A., Scheckel, C., Murphy, E., Paquet, D., Duffield, M., Fak, J., Olsen, O., Darnell, R. and Tessier-Lavigne, M. (2019). A Large Panel of Isogenic APP and PSEN1 Mutant Human iPSC Neurons Reveals Shared Endosomal Abnormalities Mediated by APP β-CTFs, Not Aβ. *Neuron* **104**, 256-270.e5.

Lane, R. F., Raines, S. M., Steele, J. W., Ehrlich, M. E., Lah, J. A., Small, S. A., Tanzi, R. E., Attie, A. D. and Gandy, S. (2010). Diabetes-associated SorCS1 regulates Alzheimer's amyloid-β metabolism: Evidence for involvement of SorL1 and the retromer complex. *Journal of Neuroscience* **30**, 13110–13115.

Lau, C. G. and Zukin, R. S. (2007). NMDA receptor trafficking in synaptic plasticity and neuropsychiatric disorders. *Nature Reviews Neuroscience 2007 8:6* **8**, 413–426.

Lauritzen, I., Pardossi-Piquard, R., Bourgeois, A., Pagnotta, S., Biferi, M. G., Barkats, M., Lacor, P., Klein, W., Bauer, C. and Checler, F. (2016). Intraneuronal aggregation of the β-CTF fragment of APP (C99) induces Aβ-independent lysosomal-autophagic pathology. *Acta Neuropathol* **132**, 257–276.

Lee, H. J. and Zheng, J. J. (2010). PDZ domains and their binding partners: structure, specificity, and modification. *Cell Communication and Signaling 2010 8:1* **8**, 1–18.

Lee, J. H., Yu, W. H., Kumar, A., Lee, S., Mohan, P. S., Peterhoff, C. M., Wolfe, D. M., Martinez-Vicente, M., Massey, A. C., Sovak, G., et al. (2010). Lysosomal proteolysis and autophagy require presenilin 1 and are disrupted by Alzheimer-related PS1 mutations. *Cell* **141**, 1146–1158.

Lee, M. J., Chen, T. F., Cheng, T. W. and Chiu, M. J. (2011). rs5848 variant of progranulin gene is a risk of Alzheimer's disease in the Taiwanese population. *Neurodegener Dis* **8**, 216–220.

Lee, J. H., McBrayer, M. K., Wolfe, D. M., Haslett, L. J., Kumar, A., Sato, Y., Lie, P. P. Y., Mohan, P., Coffey, E. E., Kompella, U., et al. (2015). Presenilin 1 Maintains Lysosomal Ca(2+) Homeostasis via TRPML1 by Regulating vATPase-Mediated Lysosome Acidification. *Cell Rep* **12**, 1430–1444.

Lee, J. H., Wolfe, D. M., Darji, S., McBrayer, M. K., Colacurcio, D. J., Kumar, A., Stavrides, P., Mohan, P. S. and Nixon, R. A. (2020). β2-adrenergic Agonists Rescue Lysosome Acidification and Function in PSEN1 Deficiency by Reversing Defective ER-to-lysosome Delivery of ClC-7. *J Mol Biol* **432**, 2633–2650.

Lee, H. G., Wheeler, M. A. and Quintana, F. J. (2022a). Function and therapeutic value of astrocytes in neurological diseases. *Nat Rev Drug Discov* **21**, 339–358.

Lee, J., Xu, Y., Saidi, L., Xu, M., Zinsmaier, K. and Ye, Y. (2022b). Abnormal triaging of misfolded proteins by adult neuronal ceroid lipofuscinosis-associated DNAJC5/CSPα mutants causes lipofuscin accumulation. *Autophagy*.

Lee, J. H., Yang, D. S., Goulbourne, C. N., Im, E., Stavrides, P., Pensalfini, A., Chan, H., Bouchet-Marquis, C., Bleiwas, C., Berg, M. J., et al. (2022c). Faulty autolysosome acidification in Alzheimer's disease mouse models induces autophagic build-up of Aβ in neurons, yielding senile plaques. *Nature Neuroscience 2022 25:6* **25**, 688–701.

Leinonen, H., Keksa-Goldsteine, V., Ragauskas, S., Kohlmann, P., Singh, Y., Savchenko, E., Puranen, J., Malm, T., Kalesnykas, G., Koistinaho, J., et al. (2017). Retinal Degeneration In A Mouse Model Of CLN5 Disease Is Associated With Compromised Autophagy. *Sci Rep* **7**, 1597.

Leloup, N., Lössl, P., Meijer, D. H., Brennich, M., Heck, A. J. R., Thies-Weesie, D. M. E. and Janssen, B. J. C. (2017). Low pH-induced conformational change and dimerization of sortilin triggers endocytosed ligand release. *Nat Commun* **8**, 1–15.

Leloup, N., Chataigner, L. M. P. and Janssen, B. J. C. (2018). Structural insights into SorCS2–Nerve Growth Factor complex formation. *Nat Commun* **9**, 2979.

Lerma, J. and Marques, J. M. (2013). Kainate Receptors in Health and Disease. *Neuron* **80**, 292–311.

Levy, M. J. F., Boulle, F., Steinbusch, H. W., van den Hove, D. L. A., Kenis, G. and Lanfumey, L. (2018). Neurotrophic factors and neuroplasticity pathways in the pathophysiology and treatment of depression. *Psychopharmacology (Berl)* **235**, 2195.

Levy-Lahad, E., Wasco, W., Poorkaj, P., Romano, D. M., Oshima, J., Pettingell, W. H., Yu, C. E., Jondro, P. D., Schmidt, S. D., Wang, K., et al. (1995). Candidate Gene for the Chromosome 1 Familial Alzheimer's Disease Locus. *Science (1979)* **269**, 973–977.

Li, Y. H., Zhang, N., Wang, Y. N., Shen, Y. and Wang, Y. (2016). Multiple faces of protein interacting with C kinase 1 (PICK1): Structure, function, and diseases. *Neurochem Int* **98**, 115–121.

Lieberman, O. J. and Sulzer, D. (2020). The Synaptic Autophagy Cycle. *J Mol Biol* **432**, 2589–2604.

Lin, L., Sohar, I., Lackland, H. and Lobel, P. (2001). The human CLN2 protein/tripeptidyl-peptidase I is a serine protease that autoactivates at acidic pH. *J Biol Chem* **276**, 2249–2255.

Lin, Y.-C., Boone, M., Meuris, L., Lemmens, I., van Roy, N., Soete, A., Reumers, J., Moisse, M., Plaisance, S., Drmanac, R., et al. (2014). Genome dynamics of the human embryonic kidney 293 lineage in response to cell biology manipulations. *Nat Commun* **5**, 4767.

Ling, D., Song, H. J., Garza, D., Neufeld, T. P. and Salvaterra, P. M. (2009). Abeta42-Induced Neurodegeneration via an Age-Dependent Autophagic-Lysosomal Injury in Drosophila. *PLoS One* **4**, e4201.

Lionel, A. C., Crosbie, J., Barbosa, N., Goodale, T., Thiruvahindrapuram, B., Rickaby, J., Gazzellone, M., Carson, A. R., Howe, J. L., Wang, Z., et al. (2011). Rare copy number variation discovery and cross-disorder comparisons identify risk genes for ADHD. *Sci Transl Med* **3**, 95ra75.

Liu, J. and Li, L. (2019). Targeting Autophagy for the Treatment of Alzheimer's Disease: Challenges and Opportunities. *Front Mol Neurosci* **12**, 203.

Liu, J., Li, H., Zhou, B., Xu, L., Kang, X., Yang, W., Wu, S. and Sun, H. (2015). PGRN induces impaired insulin sensitivity and defective autophagy in hepatic insulin resistance. *Mol Endocrinol* **29**, 528–541.

Liu, L., Patnana, P. K. and Nimmagadda, S. C. (2022). Low-dose metformin and PEN2-dependent lysosomal AMPK activation: benefits outnumber side effects. *Signal Transduct Target Ther* **7**, 178.

Lojewski, X., Staropoli, J. F., Biswas-legrand, S., Simas, A. M., Haliw, L., Selig, M. K., Coppel, S. H., Goss, K. A., Petcherski, A., Chandrachud, U., et al. (2014). Human iPSC models of neuronal ceroid lipofuscinosis capture distinct effects of TPP1 and CLN3 mutations on the endocytic pathway. *Hum Mol Genet* **23**, 2005–2022.

Lonka, L., Kyttälä, A., Ranta, S., Jalanko, A. and Lehesjoki, A. E. (2000). The neuronal ceroid lipofuscinosis CLN8 membrane protein is a resident of the endoplasmic reticulum. *Hum Mol Genet* **9**, 1691–1697.

Lübke, J. H., Idoon, F., Mohasel-Roodi, M., Alipour, F., Hami, J., Ehteshampour, A., Mostafaee, H. and Sadeghi, A. (2021). Neurotrophic factors in Alzheimer's disease: pathogenesis and therapy. *Acta Neurobiol Exp (Wars)* **81**, 314–327.

Luebben, A. v., Bender, D., Becker, S., Crowther, L. M., Erven, I., Hofmann, K., Söding, J., Klemp, H., Bellotti, C., Stäuble, A., et al. (2022). Cln5 represents a new type of cysteine-based S-depalmitoylase linked to neurodegeneration. *Sci Adv* **8**, 8633.

Lyly, A., Marjavaara, S. K., Kyttälä, A., Uusi-Rauva, K., Luiro, K., Kopra, O., Martinez, L. O., Tanhuanpää, K., Kalkkinen, N., Suomalainen, A., et al. (2008). Deficiency of the INCL protein Ppt1 results in changes in ectopic F1-ATP synthase and altered cholesterol metabolism. *Hum Mol Genet* **17**, 1406–1417.

Ma, Q., Yang, J., Milner, T. A., Vonsattel, J.-P. G., Palko, M. E., Tessarollo, L. and Hempstead, B. L. (2017). SorCS2-mediated NR2A trafficking regulates motor deficits in Huntington's disease. *JCI Insight* **2**, e88995.

Ma, T., Tian, X., Zhang, B., Li, M., Wang, Y., Yang, C., Wu, J., Wei, X., Qu, Q., Yu, Y., et al. (2022). Low-dose metformin targets the lysosomal AMPK pathway through PEN2. *Nature 2022 603:7899* **603**, 159–165.

Maag, J. L. v, Panja, D., Sporild, I., Patil, S., Kaczorowski, D. C., Bramham, C. R., Dinger, M. E. and Wibrand, K. (2015). Dynamic expression of long noncoding RNAs and repeat elements in synaptic plasticity. *Front Neurosci* **9**, 351.

Maday, S., Wallace, K. E. and Holzbaur, E. L. F. (2012). Autophagosomes initiate distally and mature during transport toward the cell soma in primary neurons. *J Cell Biol* **196**, 407.

Majumder, S., Richardson, A., Strong, R. and Oddo, S. (2011). Inducing autophagy by rapamycin before, but not after, the formation of plaques and tangles ameliorates cognitive deficits. *PLoS One* **6**, e25416.

Malampati, S., Song, J.-X., Chun-Kit Tong, B., Nalluri, A., Yang, C.-B., Wang, Z., Gopalkrishnashetty Sreenivasmurthy, S., Zhu, Z., Liu, J., Su, C., et al. (2020). Targeting Aggrephagy for the Treatment of Alzheimer's Disease. *Cells* **9**, 311.

Malik, A. R. and Willnow, T. E. (2020). VPS10P Domain Receptors: Sorting Out Brain Health and Disease. *Trends Neurosci* **43**, 870–885.

Malik, A. R., Szydlowska, K., Nizinska, K., Asaro, A., van Vliet, E. A., Popp, O., Dittmar, G., Fritsche-Guenther, R., Kirwan, J. A., Nykjaer, A., et al. (2019). SorCS2 Controls Functional Expression of Amino Acid Transporter EAAT3 and Protects Neurons from Oxidative Stress and Epilepsy-Induced Pathology. *Cell Rep* **26**, 2792-2804.e6.

Mamo, A., Jules, F., Dumaresq-Doiron, K., Costantino, S. and Lefrancois, S. (2012). The Role of Ceroid Lipofuscinosis Neuronal Protein 5 (CLN5) in Endosomal Sorting. *Mol Cell Biol* **32**, 1855.

Marcusson, E. G., Horazdovsky, B. F., Cereghino, J. L., Gharakhanian, E. and Emr, S. D. (1994). The sorting receptor for yeast vacuolar carboxypeptidase Y is encoded by the VPS10 gene. *Cell* **77**, 579–586.

Marques, A. R. A., di Spiezio, A., Thießen, N., Schmidt, L., Grötzinger, J., Lüllmann-Rauch, R., Damme, M., Storck, S. E., Pietrzik, C. U., Fogh, J., et al. (2020). Enzyme replacement therapy with recombinant pro-CTSD (cathepsin D) corrects defective proteolysis and autophagy in neuronal ceroid lipofuscinosis. *Autophagy* **16**, 811–825.

Martinez, O. and Goud, B. (1998). Rab proteins. *Biochimica et Biophysica Acta (BBA) - Molecular Cell Research* **1404**, 101–112.

Matsui, H., Sato, F., Sato, S., Koike, M., Taruno, Y., Saiki, S., Funayama, M., Ito, H., Taniguchi, Y., Uemura, N., et al. (2013). ATP13A2 deficiency induces a decrease in cathepsin D activity, fingerprint-like inclusion body formation, and selective degeneration of dopaminergic neurons. *FEBS Lett* **587**, 1316–1325.

Mazella, J., Zsürger, N., Navarro, V., Chabry, J., Kaghad, M., Caput, D., Ferrara, P., Vita, N., Gully, D., Maffrand, J. P., et al. (1998). The 100-kDa neurotensin receptor is gp95/sortilin, a non-G-protein- coupled receptor. *Journal of Biological Chemistry* **273**, 26273–26276.

Mazzoni, F., Safa, H. and Finnemann, S. C. (2014). Understanding photoreceptor outer segment phagocytosis: use and utility of RPE cells in culture. *Exp Eye Res* **126**, 51–60.

Meckler, X. and Checler, F. (2016). Presenilin 1 and presenilin 2 target γ-secretase complexes to distinct cellular compartments. *Journal of Biological Chemistry* **291**, 12821–12837.

Meldrum, B. S., Akbar, M. T. and Chapman, A. G. (1999). Glutamate receptors and transporters in genetic and acquired models of epilepsy. *Epilepsy Res* **36**, 189–204.

Mikhaylova, M., Bera, S., Kobler, O., Frischknecht, R. and Kreutz, M. R. (2016). A Dendritic Golgi Satellite between ERGIC and Retromer. *CellReports* **14**, 189–199.

Mishra, S., Knupp, A., Szabo, M. P., Williams, C. A., Kinoshita, C., Hailey, D. W., Wang, Y., Andersen, O. M. and Young, J. E. (2022). The Alzheimer's gene SORL1 is a regulator of endosomal traffic and recycling in human neurons. *Cell Mol Life Sci* **79**, 162.

Mitok, K. A., Keller, M. P. and Attie, A. D. (2022). Sorting through the extensive and confusing roles of sortilin in metabolic disease. *J Lipid Res* **63**, 100243.

Mizushima, N., Yamamoto, A., Matsui, M., Yoshimori, T. and Ohsumi, Y. (2004). In vivo analysis of autophagy in response to nutrient starvation using transgenic mice expressing a fluorescent autophagosome marker. *Mol Biol Cell* **15**, 1101–1111.

Mole, S. E. and Cotman, S. L. (2015). Genetics of the neuronal ceroid lipofuscinoses (Batten disease). *Biochim Biophys Acta* **1852**, 2237–2241.

Mueller-Steiner, S., Zhou, Y., Arai, H., Roberson, E. D., Sun, B., Chen, J., Wang, X., Yu, G., Esposito, L., Mucke, L., et al. (2006). Antiamyloidogenic and neuroprotective functions of cathepsin B: implications for Alzheimer's disease. *Neuron* **51**, 703–714.

Nakamura, N. and Kurosaka, A. (2019). Mucin-type glycosylation as a regulatory factor of amyloid precursor protein processing. *J Biochem* **165**, 205–208.

Nakamura, S. and Yoshimori, T. (2017). New insights into autophagosome-lysosome fusion. *J Cell Sci* **130**, 1209–1216.

Narayan, P., Sienski, G., Bonner, J. M., Lin, Y.-T., Seo, J., Baru, V., Haque, A., Milo, B., Akay, L. A., Graziosi, A., et al. (2020). PICALM Rescues Endocytic Defects Caused by the Alzheimer's Disease Risk Factor APOE4. *Cell Rep* **33**, 108224.

Neely, K. M., Green, K. N. and LaFerla, F. M. (2011). Presenilin is necessary for efficient proteolysis through the autophagy-lysosome system in a γ-secretase-independent manner. *Journal of Neuroscience* **31**, 2781–2791.

Newell-Liwa, K., Seong, E., Burmeister, M. and Faundez, V. (2007). Neuronal and non-neuronal functions of the AP-3 sorting machinery. *J Cell Sci* **120**, 531–541.

Nicolas, G., Charbonnier, C., Wallon, D., Quenez, O., Bellenguez, C., Grenier-Boley, B., Rousseau, S., Richard, A. C., Rovelet-Lecrux, A., le Guennec, K., et al. (2015). SORL1 rare variants: a major risk factor for familial early-onset Alzheimer's disease. *Molecular Psychiatry 2016 21:6* **21**, 831–836.

Nielsen, M. S., Jacobsen, C., Olivecrona, G., Gliemann, J. and Petersen, C. M. (1999). Sortilin/neurotensin receptor-3 binds and mediates degradation of lipoprotein lipase. *J Biol Chem* **274**, 8832–8836.

Nielsen, M. S., Madsen, P., Christensen, E. I., Nykjær, A., Gliemann, J., Kasper, D., Pohlmann, R. and Petersen, C. M. (2001). The sortilin cytoplasmic tail conveys Golgi-endosome transport and binds the VHS domain of the GGA2 sorting protein. *EMBO Journal* **20**, 2180–2190.

Nielsen, M. S., Gustafsen, C., Madsen, P., Nyengaard, J. R., Hermey, G., Bakke, O., Mari, M., Schu, P., Pohlmann, R., Dennes, A., et al. (2007). Sorting by the Cytoplasmic Domain of the Amyloid Precursor Protein Binding Receptor SorLA. *Mol Cell Biol* **27**, 6842–6851.

Nielsen, M. S., Keat, S. J., Hamati, J. W., Madsen, P., Gutzmann, J. J., Engelsberg, A., Pedersen, K. M., Gustafsen, C., Nykjær, A., Gliemann, J., et al. (2008). Different motifs regulate trafficking of SorCS1 isoforms. *Traffic* **9**, 980–994.

Nikoletopoulou, V. and Tavernarakis, N. (2018). Regulation and Roles of Autophagy at Synapses. *Trends Cell Biol* **28**, 646–661.

Nilsson, I. M. and von Heijne, G. (1993). Determination of the distance between the oligosaccharyltransferase active site and the endoplasmic reticulum membrane. *J Biol Chem* **268**, 5798–801.

Nilsson, P., Sekiguchi, M., Akagi, T., Izumi, S., Komori, T., Hui, K., Sörgjerd, K., Tanaka, M., Saito, T., Iwata, N., et al. (2015). Autophagy-related protein 7 deficiency in amyloid β (Aβ) precursor protein transgenic mice decreases Aβ in the multivesicular bodies and induces Aβ accumulation in the Golgi. *Am J Pathol* **185**, 305–313.

Nixon, R. A. (2004). Niemann-Pick Type C disease and Alzheimer's disease: the APP-endosome connection fattens up. *Am J Pathol* **164**, 757–61.

Nixon, R. A. (2017). Amyloid precursor protein and endosomal-lysosomal dysfunction in Alzheimer's disease: inseparable partners in a multifactorial disease. *FASEB J* **31**, 2729–2743.

Nixon, R. A. and Cataldo, A. M. (2006). Lysosomal system pathways: genes to neurodegeneration in Alzheimer's disease. *J Alzheimers Dis* **9**, 277–289.

Nixon, R. A. and Yang, D. S. (2011). Autophagy Failure in Alzheimer's Disease – Locating the Primary Defect. *Neurobiol Dis* **43**, 38.

Nixon, R. A., Wegiel, J., Kumar, A., Yu, W. H., Peterhoff, C., Cataldo, A. and Cuervo, A. M. (2005). Extensive involvement of autophagy in Alzheimer disease: an immuno-electron microscopy study. *J Neuropathol Exp Neurol* **64**, 113–122.

Nixon, R. A., Yang, D. S. and Lee, J. H. (2008). Neurodegenerative lysosomal disorders: a continuum from development to late age. *Autophagy* **4**, 590–599.

Nomura, J., Jaaro-Peled, H., Lewis, E., Nuñez-Abades, P., Huppe-Gourgues, F., Cash-Padgett, T., Emiliani, F., Kondo, M. A., Furuya, A., Landek-Salgado, M. A., et al. (2016). Role for neonatal D-

serine signaling: prevention of physiological and behavioral deficits in adult Pick1 knockout mice. *Mol Psychiatry* **21**, 386–93.

Nordstedt, C., Caporaso, G. L., Thyberg, J., Gandy, S. E. and Greengard, P. (1993). Identification of the Alzheimer beta/A4 amyloid precursor protein in clathrin-coated vesicles purified from PC12 cells. *Journal of Biological Chemistry* **268**, 608–612.

Nukina, N. and Ihara, Y. (1986). One of the antigenic determinants of paired helical filaments is related to tau protein. *J Biochem* **99**, 1541–1544.

Nykjaer, A. and Willnow, T. E. (2012). Sortilin: A receptor to regulate neuronal viability and function. *Trends Neurosci* **35**, 261–270.

Nykjaer, A., Lee, R., Teng, K. K., Jansen, P., Madsen, P., Nielsen, M. S., Jacobsen, C., Kliemannel, M., Schwarz, E., Willnow, T. E., et al. (2004). Sortilin is essential for proNGF-induced neuronal cell death. *Nature* **427**, 843–848.

Nyuzuki, H., Ito, S., Nagasaki, K., Nitta, Y., Matsui, N., Saitoh, A. and Matsui, H. (2020). Degeneration of dopaminergic neurons and impaired intracellular trafficking in Atp13a2 deficient zebrafish. *IBRO Rep* **9**, 1–8.

Oetjen, S., Mahlke, C., Hermans-Borgmeyer, I. and Hermey, G. (2014). Spatiotemporal expression analysis of the growth factor receptor SorCS3. *Journal of Comparative Neurology* **522**, 3386–3402.

Oetjen, S., Kuhl, D. and Hermey, G. (2016). Revisiting the neuronal localization and trafficking of CLN3 in juvenile neuronal ceroid lipofuscinosis. *J Neurochem* **139**, 456–470.

Offe, K., Dodson, S. E., Shoemaker, J. T., Fritz, J. J., Gearing, M., Levey, A. I. and Lah, J. J. (2006). The lipoprotein receptor LR11 regulates amyloid β production and amyloid precursor protein traffic in endosomal compartments. *Journal of Neuroscience* **26**, 1596–1603.

Ohmi, K., Kudo, L. C., Ryazantsev, S., Zhao, H. Z., Karsten, S. L. and Neufeld, E. F. (2009). Sanfilippo syndrome type B, a lysosomal storage disease, is also a tauopathy. *Proc Natl Acad Sci U S A* **106**, 8332–8337.

Olsen, D., Kaas, M., Lundhede, J., Molgaard, S., Nykjær, A., Kjolby, M., Østergaard, S. D. and Glerup, S. (2019). Reduced Alcohol Seeking and Withdrawal Symptoms in Mice Lacking the BDNF Receptor SorCS2. *Front Pharmacol* **10**, 1–9.

Opazo, P., Labrecque, S., Tigaret, C. M., Frouin, A., Wiseman, P. W., de Koninck, P. and Choquet, D. (2010). CaMKII Triggers the Diffusional Trapping of Surface AMPARs through Phosphorylation of Stargazin. *Neuron* **67**, 239–252.

Palade, G. E. (1958). Microsomes and Ribonucleoprotein Particles. In *Microsomal particles and protein synthesis* (ed. Roberts, R. B.), pp. 36–62. New York, Published on behalf of the Washington Academy of Sciences, Washington, D.C., by Pergamon Press.

Pallesen, L. T., Gustafsen, C., Cramer, J. F., Petersen, S. V., Thirup, S. S., Madsen, P. and Petersen, C. M. (2020). PAK Kinases Target Sortilin and Modulate Its Sorting. *Mol Cell Biol* **40**, e00411-19.

Pan, X., Zaarur, N., Singh, M., Morin, P. and Kandror, K. v. (2017). Sortilin and retromer mediate retrograde transport of Glut4 in 3T3-L1 adipocytes. *Mol Biol Cell* **28**, 1667–1675.

Pardee, A. B. (1954). NUCLEIC ACID PRECURSORS AND PROTEIN SYNTHESIS. *Proceedings of the National Academy of Sciences* **40**, 263–270.

Parks, B. W., Nam, E., Org, E., Kostem, E., Norheim, F., Hui, S. T., Pan, C., Civelek, M., Rau, C. D., Bennett, B. J., et al. (2013). Genetic Control of Obesity and Gut Microbiota Composition in Response to High-Fat, High-Sucrose Diet in Mice. *Cell Metab* **17**, 141–152.

Passantino, R., Cascio, C., Deidda, I., Galizzi, G., Russo, D., Spedale, G. and Guarneri, P. (2013). Identifying protein partners of CLN8, an ER-resident protein involved in neuronal ceroid lipofuscinosis. *Biochim Biophys Acta* **1833**, 529–540.

Pasternak, S. H., Bagshaw, R. D., Guiral, M., Zhang, S., Ackerleyll, C. A., Pak, B. J., Callahan, J. W. and Mahuran, D. J. (2003). Presenilin-1, nicastrin, amyloid precursor protein, and gamma-secretase activity are co-localized in the lysosomal membrane. *J Biol Chem* **278**, 26687–26694.

Paterson, A. D., Waggott, D., Boright, A. P., Hosseini, S. M., Shen, E., Sylvestre, M. P., Wong, I., Bharaj, B., Cleary, P. A., Lachin, J. M., et al. (2010). A genome-wide association study identifies a novel major locus for glycemic control in type 1 diabetes, as measured by both A1C and glucose. *Diabetes* **59**, 539–549.

Pearse, B. M., Smith, C. J. and Owen, D. J. (2000). Clathrin coat construction in endocytosis. *Curr Opin Struct Biol* **10**, 220–228.

Peng, C., Trojanowski, J. Q. and Lee, V. M. Y. (2020). Protein transmission in neurodegenerative disease. *Nat Rev Neurol* **16**, 199.

Peter, B. J., Kent, H. M., Mills, I. G., Vallis, Y., Butler, P. J. G., Evans, P. R. and McMahon, H. T. (2004). BAR Domains as Sensors of Membrane Curvature: The Amphiphysin BAR Structure. *Science (1979)* **303**, 495–499.

Petersen, C. M., Nielsent, M. S., Nykjaer, A., Jacobsen, L., Tommerup, N., Rasmussen, H. H., Røigaard, H., Gliemann, J., Madsen, P. and Moestrup, S. K. (1997). Molecular identification of a novel candidate sorting receptor purified from human brain by receptor-associated protein affinity chromatography. *J Biol Chem* **272**, 3599–3605.

Petersen, C. M., Nielsen, M. S., Jacobsen, C., Tauris, J., Jacobsen, L., Gliemann, J., Moestrup, S. K. and Madsen, P. (1999). Propeptide cleavage conditions sortilin/neurotensin receptor-3 for ligand binding. *EMBO Journal* **18**, 595–604.

Philtjens, S., van Mossevelde, S., van der Zee, J., Wauters, E., Dillen, L., Vandenbulcke, M., Vandenberghe, R., Ivanoiu, A., Sieben, A., Willems, C., et al. (2018). Rare nonsynonymous variants in SORT1 are associated with increased risk for frontotemporal dementia. *Neurobiol Aging* **66**, 181.e3-181.e10.

Pickford, F., Masliah, E., Britschgi, M., Lucin, K., Narasimhan, R., Jaeger, P. A., Small, S., Spencer, B., Rockenstein, E., Levine, B., et al. (2008). The autophagy-related protein beclin 1 shows reduced

expression in early Alzheimer disease and regulates amyloid beta accumulation in mice. *J Clin Invest* **118**, 2190–2199.

Pierce, J. P., Mayer, T. and McCarthy, J. B. (2001). Evidence for a satellite secretory pathway in neuronal dendritic spines. *Curr Biol* **11**, 351–355.

Pietilä, M., Sahgal, P., Peuhu, E., Jäntti, N. Z., Paatero, I., Närvä, E., Al-Akhrass, H., Lilja, J., Georgiadou, M., Andersen, O. M., et al. (2019). SORLA regulates endosomal trafficking and oncogenic fitness of HER2. *Nat Commun* **10**, 2340.

Polito, V. A., Li, H., Martini-Stoica, H., Wang, B., Yang, L., Xu, Y., Swartzlander, D. B., Palmieri, M., Ronza, A., Lee, V. M., et al. (2014). Selective clearance of aberrant tau proteins and rescue of neurotoxicity by transcription factor EB. *EMBO Mol Med* **6**, 1142–1160.

Poulsen, E. T., Larsen, A., Zollo, A., Jørgensen, A. L., Sanggaard, K. W., Enghild, J. J. and Matrone, C. (2015). New Insights to Clathrin and Adaptor Protein 2 for the Design and Development of Therapeutic Strategies. *Int J Mol Sci* **16**, 29446–29453.

Progida, C., Nielsen, M. S., Koster, G., Bucci, C. and Bakke, O. (2012). Dynamics of Rab7b-Dependent Transport of Sorting Receptors. *Traffic* **13**, 1273–1285.

Prokop, S., Haass, C. and Steiner, H. (2005). Length and overall sequence of the PEN-2 C-terminal domain determines its function in the stabilization of presenilin fragments. *J Neurochem* **94**, 57–62.

Quadri, M., Fang, M., Picillo, M., Olgiati, S., Breedveld, G. J., Graafland, J., Wu, B., Xu, F., Erro, R., Amboni, M., et al. (2013). Mutation in the SYNJ1 gene associated with autosomal recessive, early-onset Parkinsonism. *Hum Mutat* **34**, 1208–1215.

Quistgaard, E. M., Madsen, P., Grøftehauge, M. K., Nissen, P., Petersen, C. M. and Thirup, S. S. (2009). Ligands bind to Sortilin in the tunnel of a ten-bladed β-propeller domain. *Nature Structural & Molecular Biology 2008 16:1* **16**, 96–98.

Qureshi, Y. H., Patel, V. M., Berman, D. E., Kothiya, M. J., Neufeld, J. L., Vardarajan, B., Tang, M., Reyes-Dumeyer, D., Lantigua, R., Medrano, M., et al. (2018). An Alzheimer's Disease-Linked Loss-of-Function CLN5 Variant Impairs Cathepsin D Maturation, Consistent with a Retromer Trafficking Defect. *Mol Cell Biol* **38**, e00011-18.

Rajagopalan, S., Rane, A., Chinta, S. J. and Andersen, J. K. (2016). Regulation of ATP13A2 via PHD2-HIF1α Signaling Is Critical for Cellular Iron Homeostasis: Implications for Parkinson's Disease. *J Neurosci* **36**, 1086–1095.

Ramirez-Montealegre, D. and Pearce, D. A. (2005). Defective lysosomal arginine transport in juvenile Batten disease. *Hum Mol Genet* **14**, 3759–3773.

Ramón y Cajal, S. (1906). The structure and connexions of neurons. *Nobel Lecture* **1901–1921**, 220–253.

Ramonet, D., Podhajska, A., Stafa, K., Sonnay, S., Trancikova, A., Tsika, E., Pletnikova, O., Troncoso, J. C., Glauser, L. and Moore, D. J. (2012). PARK9-associated ATP13A2 localizes to intracellular

acidic vesicles and regulates cation homeostasis and neuronal integrity. *Hum Mol Genet* **21**, 1725–1743.

Rao, R. v and Bredesen, D. E. (2004). Misfolded proteins, endoplasmic reticulum stress and neurodegeneration. *Curr Opin Cell Biol* **16**, 653–662.

Rao-Ruiz, P., Couey, J. J., Marcelo, I. M., Bouwkamp, C. G., Slump, D. E., Matos, M. R., van der Loo, R. J., Martins, G. J., van den Hout, M., van IJcken, W. F., et al. (2019). Engram-specific transcriptome profiling of contextual memory consolidation. *Nat Commun* **10**, 2232.

Rapoport, T. A. (2007). Protein translocation across the eukaryotic endoplasmic reticulum and bacterial plasma membranes. *Nature 2007 450:7170* **450**, 663–669.

Rebecca, V. W., Nicastri, M. C., Fennelly, C., Chude, C. I., Barber-Rotenberg, J. S., Ronghe, A., McAfee, Q., McLaughlin, N. P., Zhang, G., Goldman, A. R., et al. (2019). PPT1 Promotes Tumor Growth and Is the Molecular Target of Chloroquine Derivatives in Cancer. *Cancer Discov* **9**, 220–229.

Reitz, C., Tokuhiro, S., Clark, L. N., Conrad, C., Vonsattel, J. P., Hazrati, L. N., Palotás, A., Lantigua, R., Medrano, M., Jiménez-Velázquez, I. Z., et al. (2011). SORCS1 alters amyloid precursor protein processing and variants may increase Alzheimer's disease risk. *Ann Neurol* **69**, 47–64.

Rezgaoui, M., Hermey, G., Riedel, I. B., Hampe, W., Schaller, H. C. and Hermans-Borgmeyer, I. (2001). Identification of SorCS2, a novel member of the VPS10 domain containing receptor family, prominently expressed in the developing mouse brain. *Mech Dev* **100**, 335–338.

Ribeiro, L. F., Verpoort, B., Nys, J., Vennekens, K. M., Wierda, K. D. and de Wit, J. (2019). SorCS1-mediated sorting in dendrites maintains neurexin axonal surface polarization required for synaptic function. *PLoS Biol* **17**, e3000466.

Riemenschneider, M., Blennow, K., Wagenpfeil, S., Andreasen, N., Prince, J. A., Laws, S. M., Förstl, H. and Kurz, A. (2006). The cathepsin D rs17571 polymorphism: effects on CSF tau concentrations in Alzheimer disease. *Hum Mutat* **27**, 532–537.

Rocca, D. L. and Hanley, J. G. (2015). PICK1 links AMPA receptor stimulation to Cdc42. *Neurosci Lett* **585**, 155–159.

Rogaeva, E., Meng, Y., Lee, J. H., Gu, Y., Kawarai, T., Zou, F., Katayama, T., Baldwin, C. T., Cheng, R., Hasegawa, H., et al. (2007). The neuronal sortilin-related receptor SORL1 is genetically associated with Alzheimer disease. *Nat Genet* **39**, 168–177.

Rohe, M., Synowitz, M., Glass, R., Paul, S. M., Nykjaer, A. and Willnow, T. E. (2009). Brain-derived neurotrophic factor reduces amyloidogenic processing through control of SORLA gene expression. *Journal of Neuroscience* **29**, 15472–15478.

Rohe, M., Hartl, D., Fjorback, A. N., Klose, J. and Willnow, T. E. (2013). SORLA-Mediated Trafficking of TrkB Enhances the Response of Neurons to BDNF. *PLoS One* **8**, e72164.

Rozas, J. L., Gómez-Sánchez, L., Mircheski, J., Linares-Clemente, P., Nieto-González, J. L., Vázquez, E. M., Luján, R. and Fernández-Chacón, R. (2012). Motorneurons require cysteine string

protein-α to maintain the readily releasable vesicular pool and synaptic vesicle recycling. *Neuron* **74**, 151–165.

Rumbaugh, G., Sia, G. M., Garner, C. C. and Huganir, R. L. (2003). Synapse-Associated Protein-97 Isoform-Specific Regulation of Surface AMPA Receptors and Synaptic Function in Cultured Neurons. *Journal of Neuroscience* **23**, 4567–4576.

Sahu, R., Kaushik, S., Clement, C. C., Cannizzo, E. S., Scharf, B., Follenzi, A., Potolicchio, I., Nieves, E., Cuervo, A. M. and Santambrogio, L. (2011). Microautophagy of cytosolic proteins by late endosomes. *Dev Cell* **20**, 131–139.

Sakamoto, K. and Jessen, N. (2022). PEN2: Metformin's new partner at lysosome. *Cell Research 2022 32:6* **32**, 507–508.

Sannerud, R., Esselens, C., Ejsmont, P., Mattera, R., Rochin, L., Tharkeshwar, A. K., De Baets, G., De Wever, V., Habets, R., Baert, V., et al. (2016). Restricted Location of PSEN2/γ-Secretase Determines Substrate Specificity and Generates an Intracellular Aβ Pool. *Cell* **166**, 193–208.

Sarkar, C., Sadhukhan, T., Bagh, M. B., Appu, A. P., Chandra, G., Mondal, A., Saha, A. and Mukherjee, A. B. (2020). Cln1-mutations suppress Rab7-RILP interaction and impair autophagy contributing to neuropathology in a mouse model of infantile neuronal ceroid lipofuscinosis. *J Inherit Metab Dis* **43**, 1082–1101.

Sarret, P., Krzywkowski, P., Segal, L., Nielsen, M. S., Petersen, C. M., Mazella, J., Stroh, T. and Beaudet, A. (2003). Distribution of NTS3 receptor/sortilin mRNA and protein in the rat central nervous system. *Journal of Comparative Neurology* **461**, 483–505.

Savas, J. N., Ribeiro, L. F., Wierda, K. D., Wright, R., DeNardo-Wilke, L. A., Rice, H. C., Chamma, I., Wang, Y.-Z., Zemla, R., Lavallée-Adam, M., et al. (2015). The Sorting Receptor SorCS1 Regulates Trafficking of Neurexin and AMPA Receptors. *Neuron* **87**, 764–780.

Schmidt, V., Sporbert, A., Rohe, M., Reimer, T., Rehm, A., Andersen, O. M. and Willnow, T. E. (2007). SorLA/LR11 regulates processing of amyloid precursor protein via interaction with adaptors GGA and PACS-1. *J Biol Chem* **282**, 32956–32964.

Schmidtke, C., Tiede, S., Thelen, M., Käkelä, R., Jabs, S., Makrypidi, G., Sylvester, M., Schweizer, M., Braren, I., Brocke-Ahmadinejad, N., et al. (2019). Lysosomal proteome analysis reveals that CLN3-defective cells have multiple enzyme deficiencies associated with changes in intracellular trafficking. *J Biol Chem* **294**, 9592–9604.

Schmiedt, M. L., Bessa, C., Heine, C., Ribeiro, M. G., Jalanko, A. and Kyttälä, A. (2010). The neuronal ceroid lipofuscinosis protein CLN5: new insights into cellular maturation, transport, and consequences of mutations. *Hum Mutat* **31**, 356–365.

Schreij, A. M. A., Fon, E. A. and McPherson, P. S. (2016). Endocytic membrane trafficking and neurodegenerative disease. *Cellular and Molecular Life Sciences* **73**, 1529–1545.

Schuck, S. (2020). Microautophagy - distinct molecular mechanisms handle cargoes of many sizes. *J Cell Sci* **133**, jcs246322.

Schulz, A., Kohlschütter, A., Mink, J., Simonati, A. and Williams, R. (2013). NCL diseases — clinical perspectives. *Biochimica et Biophysica Acta (BBA) - Molecular Basis of Disease* **1832**, 1801–1806.

Seaman, M. N. J. (2012). The retromer complex-endosomal protein recycling and beyond. *J Cell Sci* **125**, 4693–4702.

Shade, L. M. P., Katsumata, Y., Hohman, T. J., Nho, K., Saykin, A. J., Mukherjee, S., Boehme, K. L., Kauwe, J. S. K., Farrer, L. A., Schellenberg, G. D., et al. (2022). Genome-wide association study of brain arteriolosclerosis. *J Cereb Blood Flow Metab* **42**, 1437–1450.

Sharma, M., Burré, J., Bronk, P., Zhang, Y., Xu, W. and Südhof, T. C. (2012). CSPα knockout causes neurodegeneration by impairing SNAP-25 function. *EMBO J* **31**, 829–841.

Shaw, G., Morse, S., Ararat, M. and Graham, F. L. (2002). Preferential transformation of human neuronal cells by human adenoviruses and the origin of HEK 293 cells. *The FASEB Journal* **16**, 869–871.

Sheng, J., Su, L., Xu, Z. and Chen, G. (2014). Progranulin polymorphism rs5848 is associated with increased risk of Alzheimer's disease. *Gene* **542**, 141–145.

Sherrington, R., Rogaev, E. I., Liang, Y., Rogaeva, E. A., Levesque, G., Ikeda, M., Chi, H., Lin, C., Li, G., Holman, K., et al. (1995). Cloning of a gene bearing missense mutations in early-onset familial Alzheimer's disease. *Nature* **375**, 754–760.

Shih, A. Z. L., Chen, Y.-C., Speckmann, T., Søndergaard, E., Schürmann, A., Verchere, C. B. and Willnow, T. E. (2022). SORLA mediates endocytic uptake of proIAPP and protects against islet amyloid deposition. *Mol Metab* **65**, 101585.

Silva, M. C., Nandi, G. A., Tentarelli, S., Gurrell, I. K., Jamier, T., Lucente, D., Dickerson, B. C., Brown, D. G., Brandon, N. J. and Haggarty, S. J. (2020). Prolonged tau clearance and stress vulnerability rescue by pharmacological activation of autophagy in tauopathy neurons. *Nature Communications 2020 11:1* **11**, 1–18.

Simmons, D. A. (2017). Modulating Neurotrophin Receptor Signaling as a Therapeutic Strategy for Huntington's Disease. *J Huntingtons Dis* **6**, 303–325.

Sisodia, S. S. (1992). Beta-amyloid precursor protein cleavage by a membrane-bound protease. *Proc Natl Acad Sci U S A* **89**, 6075–6079.

Sleat, D. E., Maita, I., Banach-Petrosky, W., Larrimore, K. E., Liu, T., Cruz, D., Baker, L., Maxfield, F. R., Samuels, B. and Lobel, P. (2022). Elevated levels of tripeptidyl peptidase 1 do not ameliorate pathogenesis in a mouse model of Alzheimer disease. *Neurobiol Aging* **118**, 106–107.

Smith, K. R., Damiano, J., Franceschetti, S., Carpenter, S., Canafoglia, L., Morbin, M., Rossi, G., Pareyson, D., Mole, S. E., Staropoli, J. F., et al. (2012). Strikingly different clinicopathological phenotypes determined by progranulin-mutation dosage. *Am J Hum Genet* **90**, 1102–1107.

Smith, A. H., Ovesen, P. L., Skeldal, S., Yeo, S., Jensen, K. P., Olsen, D., Diazgranados, N., Zhao, H., Farrer, L. A., Goldman, D., et al. (2018). Risk Locus Identification Ties Alcohol Withdrawal Symptoms to SORCS2. *Alcohol Clin Exp Res* **42**, 2337–2348.

Smith, P. K., Sen, M. G., Fisher, P. R. and Annesley, S. J. (2019). Modelling of Neuronal Ceroid Lipofuscinosis Type 2 in Dictyostelium discoideum Suggests That Cytopathological Outcomes Result from Altered TOR Signalling. *Cells* **8**, 469.

Solé-Domènech, S., Rojas, A. v., Maisuradze, G. G., Scheraga, H. A., Lobel, P. and Maxfield, F. R. (2018). Lysosomal enzyme tripeptidyl peptidase 1 destabilizes fibrillar Aβ by multiple endoproteolytic cleavages within the β-sheet domain. *Proc Natl Acad Sci U S A* **115**, 1493–1498.

Sørensen, A. T., Rombach, J., Gether, U. and Madsen, K. L. (2022). The Scaffold Protein PICK1 as a Target in Chronic Pain. *Cells* **11**, 1255.

Sottejeau, Y., Bretteville, A., Cantrelle, F.-X., Malmanche, N., Demiaute, F., Mendes, T., Delay, C., Alves Dos Alves, H., Flaig, A., Davies, P., et al. (2015). Tau phosphorylation regulates the interaction between BIN1's SH3 domain and Tau's proline-rich domain. *Acta Neuropathol Commun* **3**, 58.

Stadelmann, C., Timmler, S., Barrantes-Freer, A. and Simons, M. (2019). Myelin in the central nervous system: Structure, function, and pathology. *Physiol Rev* **99**, 1381–1431.

Stanley, P. (2011). Golgi Glycosylation. *Cold Spring Harb Perspect Biol* **3**, a005199–a005199.

Staropoli, J. F., Karaa, A., Lim, E. T., Kirby, A., Elbalalesy, N., Romansky, S. G., Leydiker, K. B., Coppel, S. H., Barone, R., Xin, W., et al. (2012). A homozygous mutation in KCTD7 links neuronal ceroid lipofuscinosis to the ubiquitin-proteasome system. *Am J Hum Genet* **91**, 202–208.

Steinberg, J. P., Takamiya, K., Shen, Y., Xia, J., Rubio, M. E., Yu, S., Jin, W., Thomas, G. M., Linden, D. J. and Huganir, R. L. (2006). Targeted in vivo mutations of the AMPA receptor subunit GluR2 and its interacting protein PICK1 eliminate cerebellar long-term depression. *Neuron* **49**, 845–860.

Storch, S., Pohl, S. and Braulke, T. (2004). A dileucine motif and a cluster of acidic amino acids in the second cytoplasmic domain of the batten disease-related CLN3 protein are required for efficient lysosomal targeting. *J Biol Chem* **279**, 53625–53634.

Strittmatter, W. J., Saunders, A. M., Schmechel, D., Pericak-Vance, M., Enghild, J., Salvesen, G. S. and Roses, A. D. (1993). Apolipoprotein E: high-avidity binding to beta-amyloid and increased frequency of type 4 allele in late-onset familial Alzheimer disease. *Proc Natl Acad Sci U S A* **90**, 1977–1981.

Subkhangulova, A., Malik, A. R., Hermey, G., Popp, O., Dittmar, G., Rathjen, T., Poy, M. N., Stumpf, A., Beed, P. S., Schmitz, D., et al. (2018). SORCS 1 and SORCS 3 control energy balance and orexigenic peptide production. *EMBO Rep* **19**, e44810.

Sweitzer, S. M. and Hinshaw, J. E. (1998). Dynamin undergoes a GTP-dependent conformational change causing vesiculation. *Cell* **93**, 1021–1029.

Szabo, M. P., Mishra, S., Knupp, A. and Young, J. E. (2022). The role of Alzheimer's disease risk genes in endolysosomal pathways. *Neurobiol Dis* **162**, 105576.

Takami, M., Nagashima, Y., Sano, Y., Ishihara, S., Morishima-Kawashima, M., Funamoto, S. and Ihara, Y. (2009). gamma-Secretase: successive tripeptide and tetrapeptide release from the transmembrane domain of beta-carboxyl terminal fragment. *J Neurosci* **29**, 13042–13052.

Takasugi, N., Tomita, T., Hayashi, I., Tsuruoka, M., Niimura, M., Takahashi, Y., Thinakaran, G. and Iwatsubo, T. (2003). The role of presenilin cofactors in the γ-secretase complex. *Nature 2003 422:6930* **422**, 438–441.

Tam, J. H. K., Cobb, M. R., Seah, C. and Pasternak, S. H. (2016). Tyrosine Binding Protein Sites Regulate the Intracellular Trafficking and Processing of Amyloid Precursor Protein through a Novel Lysosome-Directed Pathway. *PLoS One* **11**, e0161445.

Tan, J. Z. A. and Gleeson, P. A. (2019). Cargo Sorting at the trans-Golgi Network for Shunting into Specific Transport Routes: Role of Arf Small G Proteins and Adaptor Complexes. *Cells 2019, Vol. 8, Page 531* **8**, 531.

Tanaka, Y., Chambers, J. K., Matsuwaki, T., Yamanouchi, K. and Nishihara, M. (2014). Possible involvement of lysosomal dysfunction in pathological changes of the brain in aged progranulin-deficient mice. *Acta Neuropathol Commun* **2**, 78.

Tauris, J., Gustafsen, C., Christensen, E. I., Jansen, P., Nykjaer, A., Nyengaard, J. R., Teng, K. K., Schwarz, E., Ovesen, T., Madsen, P., et al. (2011). Proneurotrophin-3 may induce Sortilin-dependent death in inner ear neurons. *European Journal of Neuroscience* **33**, 622–631.

Tebar, F., Bohlander, S. K. and Sorkin, A. (1999). Clathrin assembly lymphoid myeloid leukemia (CALM) protein: localization in endocytic-coated pits, interactions with clathrin, and the impact of overexpression on clathrin-mediated traffic. *Mol Biol Cell* **10**, 2687–2702.

Teng, H. K., Teng, K. K., Lee, R., Wright, S., Tevar, S., Almeida, R. D., Kermani, P., Torkin, R., Chen, Z. Y., Lee, F. S., et al. (2005). ProBDNF induces neuronal apoptosis via activation of a receptor complex of p75 NTR and sortilin. *Journal of Neuroscience* **25**, 5455–5463.

Terashima, A., Pelkey, K. A., Rah, J.-C., Suh, Y. H., Roche, K. W., Collingridge, G. L., McBain, C. J. and Isaac, J. T. R. (2008). An essential role for PICK1 in NMDA receptor-dependent bidirectional synaptic plasticity. *Neuron* **57**, 872–82.

Thelen, M., Damme, M., Schweizer, M., Hagel, C., Wong, A. M. S., Cooper, J. D., Braulke, T. and Galliciotti, G. (2012). Disruption of the autophagy-lysosome pathway is involved in neuropathology of the nclf mouse model of neuronal ceroid lipofuscinosis. *PLoS One* **7**, e35493.

Thomas, G. M., Hayashi, T., Huganir, R. L. and Linden, D. J. (2013). DHHC8-dependent PICK1 palmitoylation is required for induction of cerebellar long-term synaptic depression. *J Neurosci* **33**, 15401–15407.

Tian, Y., Bustos, V., Flajolet, M. and Greengard, P. (2011). A small-molecule enhancer of autophagy decreases levels of Abeta and APP-CTF via Atg5-dependent autophagy pathway. *FASEB J* **25**, 1934–42.

Tobaben, S., Thakur, P., Fernández-Chacón, R., Südhof, T. C., Rettig, J. and Stahl, B. (2001). A trimeric protein complex functions as a synaptic chaperone machine. *Neuron* **31**, 987–999.

Tobaben, S., Varoqueaux, F., Brose, N., Stahl, B. and Meyer, G. (2003). A brain-specific isoform of small glutamine-rich tetratricopeptide repeat-containing protein binds to Hsc70 and the cysteine string protein. *J Biol Chem* **278**, 38376–38383.

Topp, J. D., Gray, N. W., Gerard, R. D. and Horazdovsky, B. F. (2004). Alsin is a Rab5 and Rac1 guanine nucleotide exchange factor. *J Biol Chem* **279**, 24612–24623.

Torres, G. E., Yao, W. D., Mohn, A. R., Quan, H., Kim, K. M., Levey, A. I., Staudinger, J. and Caron, M. G. (2001). Functional interaction between monoamine plasma membrane transporters and the synaptic PDZ domain-containing protein PICK1. *Neuron* **30**, 121–134.

Tsunemi, T., Hamada, K. and Krainc, D. (2014). ATP13A2/PARK9 regulates secretion of exosomes and α-synuclein. *J Neurosci* **34**, 15281–15287.

Ubelmann, F., Burrinha, T., Salavessa, L., Gomes, R., Ferreira, C., Moreno, N. and Guimas Almeida, C. (2017). Bin1 and CD2AP polarise the endocytic generation of beta-amyloid. *EMBO Rep* **18**, 102–122.

Uddin, M. S., Stachowiak, A., Mamun, A. al, Tzvetkov, N. T., Takeda, S., Atanasov, A. G., Bergantin, L. B., Abdel-Daim, M. M. and Stankiewicz, A. M. (2018). Autophagy and Alzheimer's Disease: From Molecular Mechanisms to Therapeutic Implications. *Front Aging Neurosci* **10**, 04.

Usenovic, M., Tresse, E., Mazzulli, J. R., Taylor, J. P. and Krainc, D. (2012). Deficiency of ATP13A2 leads to lysosomal dysfunction, α-synuclein accumulation, and neurotoxicity. *J Neurosci* **32**, 4240–4246.

Uusi-Rauva, K., Kyttälä, A., van der Kant, R., Vesa, J., Tanhuanpää, K., Neefjes, J., Olkkonen, V. M. and Jalanko, A. (2012). Neuronal ceroid lipofuscinosis protein CLN3 interacts with motor proteins and modifies location of late endosomal compartments. *Cell Mol Life Sci* **69**, 2075–2089.

Vaegter, C. B., Jansen, P., Fjorback, A. W., Glerup, S., Skeldal, S., Kjolby, M., Richner, M., Erdmann, B., Nyengaard, J. R., Tessarollo, L., et al. (2011). Sortilin associates with Trk receptors to enhance anterograde transport and neurotrophin signaling. *Nat Neurosci* **14**, 54–61.

van Bogaert, P., Azizieh, R., Désir, J., Aeby, A., de Meirleir, L., Laes, J. F., Christiaens, F. and Abramowicz, M. J. (2007). Mutation of a potassium channel-related gene in progressive myoclonic epilepsy. *Ann Neurol* **61**, 579–586.

Vance, J. E., Stone, S. J. and Faust, J. R. (1997). Abnormalities in mitochondria-associated membranes and phospholipid biosynthetic enzymes in the mnd/mnd mouse model of neuronal ceroid lipofuscinosis. *Biochim Biophys Acta* **1344**, 286–299.

Varadi, M., Anyango, S., Deshpande, M., Nair, S., Natassia, C., Yordanova, G., Yuan, D., Stroe, O., Wood, G., Laydon, A., et al. (2022). AlphaFold Protein Structure Database: massively expanding the structural coverage of protein-sequence space with high-accuracy models. *Nucleic Acids Res* **50**, D439–D444.

Vesa, J., Hellsten, E., Verkruyse, L. A., Camp, L. A., Rapola, J., Santavuori, P., Hofmann, S. L. and Peltonen, L. (1995). Mutations in the palmitoyl protein thioesterase gene causing infantile neuronal ceroid lipofuscinosis. *Nature* **376**, 584–587.

Vidal-Donet, J. M., Cárcel-Trullols, J., Casanova, B., Aguado, C. and Knecht, E. (2013). Alterations in ROS activity and lysosomal pH account for distinct patterns of macroautophagy in LINCL and JNCL fibroblasts. *PLoS One* **8**, e55526.

Vieira, S. I., Rebelo, S., Esselmann, H., Wiltfang, J., Lah, J., Lane, R., Small, S. A., Gandy, S., da Cruz E Silva, E. F. and da Cruz E Silva, O. A. B. (2010). Retrieval of the Alzheimer's amyloid precursor protein from the endosome to the TGN is S655 phosphorylation state-dependent and retromer-mediated. *Mol Neurodegener* **5**, 40.

Vilariño-Güell, C., Wider, C., Ross, O. A., Dachsel, J. C., Kachergus, J. M., Lincoln, S. J., Soto-Ortolaza, A. I., Cobb, S. A., Wilhoite, G. J., Bacon, J. A., et al. (2011). VPS35 mutations in Parkinson disease. *Am J Hum Genet* **89**, 162–167.

Vines, D. and Warburton, M. J. (1998). Purification and characterisation of a tripeptidyl aminopeptidase I from rat spleen. *Biochim Biophys Acta* **1384**, 233–242.

Viswanathan, J., Mäkinen, P., Helisalmi, S., Haapasalo, A., Soininen, H. and Hiltunen, M. (2009). An association study between granulin gene polymorphisms and Alzheimer's disease in Finnish population. *Am J Med Genet B Neuropsychiatr Genet* **150B**, 747–750.

von Eisenhart-Rothe, P., Grubman, A., Greferath, U., Fothergill, L. J., Jobling, A. I., Phipps, J. A., White, A. R., Fletcher, E. L. and Vessey, K. A. (2018). Failure of Autophagy-Lysosomal Pathways in Rod Photoreceptors Causes the Early Retinal Degeneration Phenotype Observed in Cln6nclf Mice. *Invest Ophthalmol Vis Sci* **59**, 5082–5097.

von Waldeyer, W. (1891). Ueber einige neuere Forschungen im Ge- biete derAnatomie des Centralnerven systems. *DEUTSCHE MEDICINISCHE WOCHENSCHRIFT* **45**, 1244–1246.

Wang, B., Shi, G. P., Yao, P. M., Li, Z., Chapman, H. A. and Brömme, D. (1998). Human cathepsin F. Molecular cloning, functional expression, tissue localization, and enzymatic characterization. *J Biol Chem* **273**, 32000–32008.

Wang, S. H., Shih, Y. L., Ko, W. C., Wei, Y. H. and Shih, C. M. (2008). Cadmium-induced autophagy and apoptosis are mediated by a calcium signaling pathway. *Cell Mol Life Sci* **65**, 3640–3652.

Wang, Y., Martinez-Vicente, M., Krüger, U., Kaushik, S., Wong, E., Mandelkow, E. M., Cuervo, A. M. and Mandelkow, E. (2009). Tau fragmentation, aggregation and clearance: the dual role of lysosomal processing. *Hum Mol Genet* **18**, 4153–4170.

Wang, H. F., Yu, J. T., Zhang, W., Wang, W., Liu, Q. Y., Ma, X. Y., Ding, H. M. and Tan, L. (2012). SORCS1 and APOE polymorphisms interact to confer risk for late-onset Alzheimer's disease in a Northern Han Chinese population. *Brain Res* **1448**, 111–116.

Wang, Y. N., Zhou, L., Li, Y. H., Wang, Z., Li, Y. C., Zhang, Y. W., Wang, Y., Liu, G. and Shen, Y. (2015). Protein Interacting with C-Kinase 1 Deficiency Impairs Glutathione Synthesis and Increases

Oxidative Stress via Reduction of Surface Excitatory Amino Acid Carrier 1. *J Neurosci* **35**, 6429–6443.

Wang, H., Wang, R., Carrera, I., Xu, S. and Lakshmana, M. K. (2016). TFEB Overexpression in the P301S Model of Tauopathy Mitigates Increased PHF1 Levels and Lipofuscin Puncta and Rescues Memory Deficits. *eNeuro* **3**, 9340–9351.

Wang, B., Stanford, K. R. and Kundu, M. (2020). ER-to-Golgi Trafficking and Its Implication in Neurological Diseases. *Cells* **9**, 408.

Wang, Y., Zeng, W., Lin, B., Yao, Y., Li, C., Hu, W., Wu, H., Huang, J., Zhang, M., Xue, T., et al. (2021). CLN7 is an organellar chloride channel regulating lysosomal function. *Sci Adv* **7**, eabj9608.

Wang, Y., Cao, X., Liu, P., Zeng, W., Peng, R., Shi, Q., Feng, K., Zhang, P., Sun, H., Wang, C., et al. (2022). KCTD7 mutations impair the trafficking of lysosomal enzymes through CLN5 accumulation to cause neuronal ceroid lipofuscinoses. *Sci Adv* **8**, eabm5578.

Westergaard, U. B., Kirkegaard, K., Sørensen, E. S., Jacobsen, C., Nielsen, M. S., Petersen, C. M. and Madsen, P. (2005). SorCS3 does not require propeptide cleavage to bind nerve growth factor. *FEBS Lett* **579**, 1172–1176.

Whyte, L. S., Lau, A. A., Hemsley, K. M., Hopwood, J. J. and Sargeant, T. J. (2017). Endo-lysosomal and autophagic dysfunction: a driving factor in Alzheimer's disease? *J Neurochem* **140**, 703–717.

Wilson, C. A., Murphy, D. D., Giasson, B. I., Zhang, B., Trojanowski, J. Q. and Lee, V. M. Y. (2004). Degradative organelles containing mislocalized alpha-and beta-synuclein proliferate in presenilin-1 null neurons. *J Cell Biol* **165**, 335–346.

Wirtschafter, J. D., Slagel, D. E., Foxx, W. J. and Rizzo, F. J. (1977). Intraocular axonal swelling produced by partial, immediately retrobulbar ligature of optic nerve. *Invest Ophthalmol Vis Sci* **16**, 537–41.

Wisniewski, K. E., Maslinska, D., Kitaguchi, T., Kim, K. S., Goebel, H. H. and Haltia, M. (1990a). Topographic heterogeneity of amyloid B-protein epitopes in brains with various forms of neuronal ceroid lipofuscinoses suggesting defective processing of amyloid precursor protein. *Acta Neuropathol* **80**, 26–34.

Wisniewski, K. E., Kida, E., Gordon-Majszak, W. and Saitoh, T. (1990b). Altered amyloid beta-protein precursor processing in brains of patients with neuronal ceroid lipofuscinosis. *Neurosci Lett* **120**, 94–96.

Wolfe, M. S. (2020). Unraveling the complexity of γ-secretase. *Semin Cell Dev Biol* **105**, 3–11.

Wolfe, D. M., Lee, J. hyun, Kumar, A., Lee, S., Orenstein, S. J. and Nixon, R. A. (2013). Autophagy failure in Alzheimer's disease and the role of defective lysosomal acidification. *Eur J Neurosci* **37**, 1949–1961.

Won, S., Levy, J. M., Nicoll, R. A. and Roche, K. W. (2017). MAGUKs: multifaceted synaptic organizers. *Curr Opin Neurobiol* **43**, 94–101.

Wu, H., Nash, J. E., Zamorano, P. and Garner, C. C. (2002). Interaction of SAP97 with Minus-end-directed Actin Motor Myosin VI. *Journal of Biological Chemistry* **277**, 30928–30934.

Wu, Y., Cao, H., Baranova, A., Huang, H., Li, S., Cai, L., Rao, S., Dai, M., Xie, M., Dou, Y., et al. (2020). Multi-trait analysis for genome-wide association study of five psychiatric disorders. *Transl Psychiatry* **10**, 209.

Xia, W. (2000). Role of presenilin in gamma-secretase cleavage of amyloid precursor protein. *Exp Gerontol* **35**, 453–460.

Xia, J., Chung, H. J., Wihler, C., Huganir, R. L. and Linden, D. J. (2000). Cerebellar long-term depression requires PKC-regulated interactions between GluR2/3 and PDZ domain-containing proteins. *Neuron* **28**, 499–510.

Xing, Y., Böcking, T., Wolf, M., Grigorieff, N., Kirchhausen, T. and Harrison, S. C. (2010). Structure of clathrin coat with bound Hsc70 and auxilin: mechanism of Hsc70-facilitated disassembly. *EMBO J* **29**, 655–65.

Xing, J., Li, Y. and Zhao, H. (2021). Knockdown of CLN5 inhibits the tumorigenic properties of glioblastoma cells via the Akt/mTOR signaling pathway. *Oncol Lett* **21**, 387.

Xu, J. and Xia, J. (2006). Structure and function of PICK1. *Neurosignals* **15**, 190–201.

Xu, W., Xu, J., Wang, Y., Tang, H. and Deng, Y. (2013). The Genetic Variation of SORCS1 Is Associated with Late-Onset Alzheimer's Disease in Chinese Han Population. *PLoS One* **8**, 63621.

Xu, J., Xu, J., Kam, C., Luo, J. H. and Xia, J. (2014). PICK1 Mediates Synaptic Recruitment of AMPA Receptors at Neurexin-Induced Postsynaptic Sites. *The Journal of Neuroscience* **34**, 15415.

Xu, H. M., Tan, L., Wan, Y., Tan, M. S., Zhang, W., Zheng, Z. J., Kong, L. L., Wang, Z. X., Jiang, T., Tan, L., et al. (2017). PGRN Is Associated with Late-Onset Alzheimer's Disease: a Case-Control Replication Study and Meta-analysis. *Mol Neurobiol* **54**, 1187–1195.

Yagishita, S., Murayama, M., Ebihara, T., Maruyama, K. and Takashima, A. (2015). Glycogen Synthase Kinase 3β-mediated Phosphorylation in the Most C-terminal Region of Protein Interacting with C Kinase 1 (PICK1) Regulates the Binding of PICK1 to Glutamate Receptor Subunit GluA2. *J Biol Chem* **290**, 29438–29448.

Yamazaki, H., Bujo, H., Kusunoki, J., Seimiya, K., Kanaki, T., Morisaki, N., Schneider, W. J. and Saito, Y. (1996). Elements of Neural Adhesion Molecules and a Yeast Vacuolar Protein Sorting Receptor Are Present in a Novel Mammalian Low Density Lipoprotein Receptor Family Member. *Journal of Biological Chemistry* **271**, 24761–24768.

Yan, Q., Rosenfeld, R. D., Matheson, C. R., Hawkins, N., Lopez, O. T., Bennett, L. and Welcher, A. A. (1997). Expression of brain-derived neurotrophic factor protein in the adult rat central nervous system. *Neuroscience* **78**, 431–448.

Yang, J., Siao, C. J., Nagappan, G., Marinic, T., Jing, D., McGrath, K., Chen, Z. Y., Mark, W., Tessarollo, L., Lee, F. S., et al. (2009). Neuronal release of proBDNF. *Nat Neurosci* **12**, 113–115.

Yang, J., Ma, Q., Dincheva, I., Giza, J., Jing, D., Marinic, T., Milner, T. A., Rajadhyaksha, A., Lee, F. S. and Hempstead, B. L. (2021). SorCS2 is required for social memory and trafficking of the NMDA receptor. *Mol Psychiatry* **26**, 927–940.

Yasa, S., Modica, G., Sauvageau, E., Kaleem, A., Hermey, G. and Lefrancois, S. (2020). CLN3 regulates endosomal function by modulating Rab7A-effector interactions. *J Cell Sci* **133**, jcs234047.

Yasa, S., Sauvageau, E., Modica, G. and Lefrancois, S. (2021). CLN5 and CLN3 function as a complex to regulate endolysosome function. *Biochem J* **478**, 2339–2357.

Yong, X. L. H., Cousin, M. A. and Anggono, V. (2020). PICK1 Controls Activity-Dependent Synaptic Vesicle Cargo Retrieval. *Cell Rep* **33**, 108312.

Yu, W. H., Kumar, A., Peterhoff, C., Shapiro Kulnane, L., Uchiyama, Y., Lamb, B. T., Cuervo, A. M. and Nixon, R. A. (2004). Autophagic vacuoles are enriched in amyloid precursor protein-secretase activities: Implications for β-amyloid peptide over-production and localization in Alzheimer's disease. *International Journal of Biochemistry and Cell Biology* **36**, 2531–2540.

Yuksel, M. and Tacal, O. (2019). Trafficking and proteolytic processing of amyloid precursor protein and secretases in Alzheimer's disease development: An up-to-date review. *Eur J Pharmacol* **856**, 172415.

Yun, H. R., Jo, Y. H., Kim, J., Nguyen, N. N. Y., Shin, Y., Kim, S. S. and Choi, T. G. (2020). Palmitoyl Protein Thioesterase 1 Is Essential for Myogenic Autophagy of C2C12 Skeletal Myoblast. *Front Physiol* **11**, 569221.

Zare-Shahabadi, A., Masliah, E., Johnson, G. V. W. and Rezaei, N. (2015). Autophagy in Alzheimer's disease. *Rev Neurosci* **26**, 385–95.

Zeng, Z., Miao, N. and Sun, T. (2018). Revealing cellular and molecular complexity of the central nervous system using single cell sequencing. *Stem Cell Res Ther* **9**, 234.

Zhang, Y. Q., Henderson, M. X., Colangelo, C. M., Ginsberg, S. D., Bruce, C., Wu, T. and Chandra, S. S. (2012). Identification of CSPα clients reveals a role in dynamin 1 regulation. *Neuron* **74**, 136–150.

Zhang, Z., Yang, X., Song, Y. Q. and Tu, J. (2021). Autophagy in Alzheimer's disease pathogenesis: Therapeutic potential and future perspectives. *Ageing Res Rev* **72**, 101464.

Zhao, X., Liberti, R., Jian, J., Fu, W., Hettinghouse, A., Sun, Y. and Liu, C. ju (2021). Progranulin associates with Rab2 and is involved in autophagosome-lysosome fusion in Gaucher disease. *J Mol Med (Berl)* **99**, 1639–1654.

Zheng, W., Chen, Q., Wang, C., Yao, D., Zhu, L., Pan, Y., Zhang, J., Bai, Y. and Shao, C. (2020). Inhibition of Cathepsin D (CTSD) enhances radiosensitivity of glioblastoma cells by attenuating autophagy. *Mol Carcinog* **59**, 651–660.

Zhong, Y., Mohan, K., Liu, J., Al-Attar, A., Lin, P., Flight, R. M., Sun, Q., Warmoes, M. O., Deshpande, R. R., Liu, H., et al. (2020). Loss of CLN3, the gene mutated in juvenile neuronal ceroid

lipofuscinosis, leads to metabolic impairment and autophagy induction in retina pigment epithelium. *Biochim Biophys Acta Mol Basis Dis* **1866**, 165883.

Zhou, D., Zhou, M., Wang, Z., Fu, Y., Jia, M., Wang, X., Liu, M., Zhang, Y., Sun, Y., Zhou, Y., et al. (2019). Progranulin alleviates podocyte injury via regulating CAMKK/AMPK-mediated autophagy under diabetic conditions. *J Mol Med (Berl)* **97**, 1507–1520.

Zimprich, A., Benet-Pagès, A., Struhal, W., Graf, E., Eck, S. H., Offman, M. N., Haubenberger, D., Spielberger, S., Schulte, E. C., Lichtner, P., et al. (2011). A mutation in VPS35, encoding a subunit of the retromer complex, causes late-onset Parkinson disease. *Am J Hum Genet* **89**, 168–175.

8.2. Acknowledgements

First, I would like to express my deep gratitude to my supervisor PD Dr. Guido Hermey. Working with him is always very enriching and joyful. By carrying interesting conversations, in which he would share his wide knowledge he made me grow personally and as a scientist. I am grateful that he was always very supportive, involved me always in the development and planning of new projects, and that he gave me the freedom and flexibility to investigate in what I was curious about with the methods I am most interested in. I thank him also for his high ambition to prepare me for a scientific career by involving me in all kinds of scientific processes. I thank him very much for the opportunity to work with him in the last years, which I enjoyed very much.

I also thank Prof. Dr. Christian Lohr for reviewing this dissertation and for sending me out into the scientific world by being my very first supervisor during earlier projects. I thank him for his encouragement and for the support in the last years.

I would like to thank Prof. Dr. Dietmar Kuhl for letting me perform my research work in his institute.

I am grateful for the support and valuable discussions with PD Dr. Sabine Hoffmeister-Ullerich and Dr. Frank Heisler when presenting my work progress.

I thank Dr. Lars Binkle for his collaboration and scientific expertise during discussions.

I would like to thank Dr. Antonio Virgilio Failla for the collaboration opportunity and that he educated me in several microscopy techniques.

I thank all former and current members of the Institute for Molecular and Cellular Cognition during work for a wonderful working environment with very fun and talented people that never hesitate to help and support wherever they can. I thank Barbara Merz, Ute Süsens and Andrea Zaisser for their technical and theoretical support in various experiments. I thank Dagmar Boshold for keeping our bureaucratic back and always creating a positive atmosphere. Special thanks go to Daniela Ballesteros, Abdurahman Kuku and Xiaoyu Yang for a lot of moral and scientific support and for the wonderful times we spent. I further want to thank and acknowledge Dr. Ora Ohana, Dr. Xiaoyan Gao, Dr. Ralf Scholz, Dr. Tiemo Marquarding, Milena Gjorgjeva, Christina Stanke, Iris Pfeffer, Bele Geertz and Frederic Beba for their kind help, nice discussions, and the good times.

Lastly, I want to thank my family and friends. Without them I would never have come this far. My special thanks go to my husband Sid Brammer who always supports me emotionally and covers my back so I can follow my scientific goals. The love and support I got from my family and friends over the years made me the strong, balanced, and confident person I am today.

Eidesstattliche Versicherung

Hiermit erkläre ich an Eides statt, dass ich die vorliegende Dissertationsschrift selbst verfasst und keine anderen als die angegebenen Quellen und Hilfsmittel benutzt habe.

21.12.2022, Hamburg 

Datum und Ort | Unterschrift

Marcel Klein